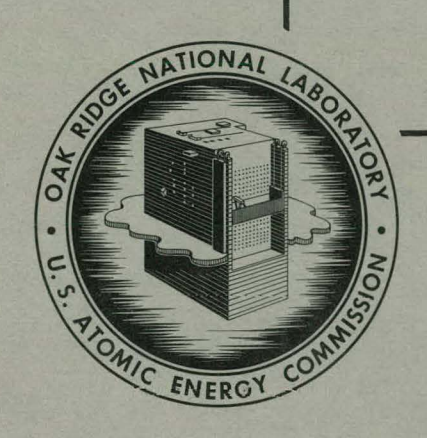
ORNL-3347 UC-41 — Health and Safety TID-4500 (18th ed.)

MASTER

HEALTH PHYSICS DIVISION

ANNUAL PROGRESS REPORT

FOR PERIOD ENDING JULY 31, 1962



### OAK RIDGE NATIONAL LABORATORY

operated by
UNION CARBIDE CORPORATION
for the
U.S. ATOMIC ENERGY COMMISSION

#### **DISCLAIMER**

This report was prepared as an account of work sponsored by an agency of the United States Government. Neither the United States Government nor any agency Thereof, nor any of their employees, makes any warranty, express or implied, or assumes any legal liability or responsibility for the accuracy, completeness, or usefulness of any information, apparatus, product, or process disclosed, or represents that its use would not infringe privately owned rights. Reference herein to any specific commercial product, process, or service by trade name, trademark, manufacturer, or otherwise does not necessarily constitute or imply its endorsement, recommendation, or favoring by the United States Government or any agency thereof. The views and opinions of authors expressed herein do not necessarily state or reflect those of the United States Government or any agency thereof.

## **DISCLAIMER**

Portions of this document may be illegible in electronic image products. Images are produced from the best available original document.

Printed in USA. Price: \$2.75 Available from the Office of Technical Services
U. S. Department of Commerce
Washington 25, D. C.

#### - LEGAL NOTICE -

This report was prepared as an account of Government sponsored work. Neither the United States, nor the Commission, nor any person acting on behalf of the Commission:

- A. Makes any warranty or representation, expressed or implied, with respect to the accuracy, completeness, or usefulness of the information contained in this report, or that the use of any information, apparatus, method, or process disclosed in this report may not infringe privately owned rights; or
- B. Assumes any liabilities with respect to the use of, or for damages resulting from the use of any information, apparatus, method, or process disclosed in this report.

As used in the above, "person acting on behalf of the Commission" includes any employee or contractor of the Commission, or employee of such contractor, to the extent that such employee or contractor of the Commission, or employee of such contractor prepares, disseminates, or provides access to, any information pursuant to his employment or contract with the Commission, or his employment with such contractor.

Contract No. W-7405-eng-26

#### HEALTH PHYSICS DIVISION ANNUAL PROGRESS REPORT

For Period Ending July 31, 1962

K. Z. Morgan, Director

DATE ISSUED

NOV 12 1962

OAK RIDGE NATIONAL LABORATORY
Oak Ridge, Tennessee
operated by
UNION CARBIDE CORPORATION
for the
U. S. ATOMIC ENERGY COMMISSION

# THIS PAGE WAS INTENTIONALLY LEFT BLANK

## Summary

#### 1. RADIOACTIVE WASTE DISPOSAL

#### Liquid Injection into Deep Permeable Formations

The low-level wastes presently being considered for disposal by deep-well injection require containment for about 200 yr. Intermediate-level wastes, requiring containment for 450 yr, may be considered for disposal by this method if low-level wastes can be handled satisfactorily. It is unlikely that high-level wastes resulting from chemical processing of spent reactor fuel elements will be released to the ground without first immobilizing the fission products.

Strontium-90, the major contributor to the hazard of the waste, will move only 1 to 10% as fast as the transporting water because of ion exchange. Precipitation reactions will provide additional restrictions to radiostrontium movement. Cesium-137 will be expected to move much more slowly than Sr<sup>90</sup> because of highly selective exchange reactions. Ruthenium-106 movement is not likely to be hazard-controlling.

#### Disposal by Hydraulic Fracturing

Completion of the test drilling and a survey of the test holes at the site of the second fracturing experiment have shown that the rock structure in this area is simpler than reported last year, but has confirmed that the fractures themselves are essentially parallel to the bedding planes. A test well at the site of the proposed disposal plant, about 3000 ft southwest of the site of the fracturing experiment, was drilled to a depth of 3263 ft. It penetrated the lower half of the Conasauga formation, all of the Rome sandstone, all of the Chickamauga limestone, and about 150 ft into the top of the Knox dolomite. Besides the shales in the lower Conasauga, 400 ft of well-bedded shale was found in the Chickamauga in the interval

between about 1650 and 2850 ft. The next step in this program will be to test these shales as a possible disposal site.

Waste, cement, and additives can be mixed to give slurries with characteristics favorable for hydrofracturing operations. A preliminary mix formulation with usable pumping time of 8½ hr and a measurable compressive strength after 24-hr curing has been developed. The fluid loss tests showed that less than 5% of the fluid will be lost in 30 min.

#### Disposal in Salt Formations

Current emphasis on the treatment of aqueous high-level wastes by converting them into solids has made it necessary to intensify studies related to the disposal of solids in salt.

A computer code has been programmed and run to determine the space requirements for solid-waste containers of various sizes containing waste of different ages, based on the assumption that the disposal operation will consist in storing the containers in holes drilled in the mine floor. Further studies on the thermal properties of salt have shown that thermal properties calculated from the results of the liquid-waste experiment are within 10 to 20% of the values obtained for single crystals.

In order to obtain data necessary for the design of mine rooms to contain radioactive solids, a network of 11 new extensometer stations has been installed in the Kansas mines to measure room closure at various overburden pressures, percent extractions, and room ages. Calculations have been made of the gamma dose to the salt surrounding solids containers buried in the mine floor. Results indicate that the gamma dose will exceed  $1 \times 10^8$  r (dose at which some structural damage will occur) only in local areas near the containers.

Laboratory studies on the effect of high temperatures (higher than 100°C) on the thermal stability of rock salt have been performed and indicate that at temperatures in excess of 200°C shattering of the salt near the holes may occur. Field tests to determine what effect this localized shattering will have on the temperature rise near the hole are being conducted.

#### Clinch River Studies

Analyses of flows in the Clinch River and White Oak Creek for the last 10 yr showed a mean annual dilution of 450, but also showed that a 30-day dilution factor of 78 would on the average occur once in 10 yr. Two dispersion tests at 8000 and 20,000 cfs with Au<sup>198</sup> showed time of travel to the Emory River of 31 hr and 9.3 hr respectively. This is in good agreement with calculated values.

Results of water sampling and analyses indicate that no  ${\rm Ru}^{106}$  and very little  ${\rm Sr}^{90}$  are removed from the river water between the mouth of White Oak Creek and Centers Ferry (16 miles). Some losses of  ${\rm Co}^{60}$  and  ${\rm Cs}^{137}$  may occur, but further analyses will be necessary to determine exactly how much.

Sorption of Sr<sup>90</sup> and Cs<sup>137</sup> by the bottom sediments in tap water (similar to river water) was 5 and 93% respectively.

#### Study of White Oak Creek Drainage Basin

The Process Waste Water Treatment Plant is the largest single contributor of radioactive waste to White Oak Creek in Bethel Valley; however, significant quantities of radionuclides enter the creek from the sanitary sewage, laundry, and other sources within the valley. The amount of strontium detected at temporary water-sampling stations, located along White Oak Creek and its tributaries, was found to vary with stream discharge. Also, a relation exists between the concentration of suspended solids in the creek water and cesium transport and the amount of strontium sorbed. Thus, during periods of high stream discharge and/or high suspended solid load, there is an increase in the amount of strontium and/or cesium transported in the creek. The amount of activity contributed to the creek as a result of local and general fallout is insignificant in comparison with that contributed by other sources of contamination.

A series of soil samples was taken within the bed of former White Oak Lake and radiochemically analyzed to determine the distribution and total amount of Ru<sup>106</sup> in the soil. The activity flows onto the bed from two streams that drain the intermediate-level waste pit area. Results of the investigation show that (1) as of February 1962 there was approximately 1200 curies of Ru<sup>106</sup> along two tracts in the bed of former White Oak Lake, (2) the highest concentrations of Ru<sup>106</sup> are found in the uppermost 2 in, of soil, (3) about 75% of the activity found in the lake bed is associated with the first 2 ft of soil, and (4) although Ru<sup>106</sup> is being transported by ground water through the lake bed soil, a relatively small amount of it is reaching the creek in this manner.

#### Ion Exchange Studies of Minerals

The cesium exchange properties of vermiculite were improved by collapsing the vermiculite lattice with ammonium ions or with one of the heavy alkali-metal cations. Pretreatment of the vermiculite with potassium increased the number of exchange sites at the edges of collapsed basal spacings, where cesium can be incorporated into the lattice by "edge fixation." This increased the cesium  $K_d$  in 0.5 M NaNO<sub>3</sub> by a factor of 2.7. Addition of NH<sub>4</sub>+, Cs+, Rb+, or K+ to the influent resulted in "interlayer fixation" of cesium, as a result of collapse of the lattice to physically entrap the cesium sorbed at the basal surface exchange sites. In this case the cesium  $K_d$  was increased by a factor of about 4.4.

Column studies with rock phosphate showed excellent removals of strontium by this material. The main advantage of this material over calcite is the elimination of phosphate addition; its cheap cost and ready availability make it more appealing than resins.

A highly selective sorbent for strontium has been prepared by heating gibbsite  $[Al(OH)_3]$  above its decomposition temperature of  $150^{\circ}$ C. The heating resulted in the formation of aluminum oxides with high surface area (>200 m²/g), in contrast to the low surface area ( $\sim 0.3$  m²/g) for gibbsite. Distribution coefficients ( $K_d$ ) ranged from 4000 to 40,000 when the solid/solution ratio was increased from 0.001 g per 50 ml to 0.05 g per 50 ml. A raw aluminum ore (bauxite from Arkansas)

strontium sorbing properties when the gibbsite component was decomposed by heating.

#### Evaluation of Engineering, Economics, and Hazards

Shipping of calcined wastes in vessels of 6-, 12-, and 24-in. diameters in 5-ft-diam carriers of lead, iron, and depleted uranium was evaluated. Shipping in lead was cheaper than in iron or depleted uranium, but for long distances shipping in uranium carriers was almost as cheap as shipping in lead.

Study of storage of calcined solids in salt showed that acidic Purex waste generated the most heat and, therefore, required the largest spacing. For a 15,000-Mw (electrical) nuclear economy this would require 2 to 20 acres/yr, depending upon the type of waste calcined. Cost of storage in salt ranged from  $6 \times 10^{-3}$  to  $30 \times 10^{-3}$  mill/kwhr (electrical). Sixty to eighty-five percent of the total cost was due to salt removal.

#### 2. RADIATION ECOLOGY

#### White Oak Lake Bed Studies

Samples taken in 1961 from White Oak Lake bed showed that concentrations of radionuclides in plants and herbivorous insects were essentially unchanged since 1958. Values for Sr<sup>90</sup> and Cs<sup>137</sup> in predaceous insects were lower in 1961 than in 1958, but the difference results from more reliable sampling in 1961 rather than an actual decrease in concentrations of radionuclides. Estimates in 1961 for predaceous insects agree with theoretical expectations for transfer of radionuclides between insect representatives of the trophic levels of this ecosystem.

Significant concentrations of ten radionuclides were detected in the carcasses of 26 wild small mammals from upper White Oak Lake bed. Ruthenium-106 in rice rats averaged highest and ranged from  $5\times10^2$  to  $8\times10^3$   $\mu\mu c$  per g of dry carcass. The radioanalyses indicated that rice rats fed in the vicinity of the radioactive surface seeps, which are contaminated with predominately Ru<sup>106</sup>.

Metaphosphate glass rods (fluorods) were adopted as in vivo dosimeters for estimation of dose accumulated by wild mammals on the lake bed. Experiments were performed to determine the response of the fluorods to the radiation energy spectrum from mixed radionuclides in the soil. A combination of measurements with shielded and unshielded pocket ionization chambers and film, and high-Z and low-Z fluorods, indicated that unshielded Toshiba low-Z glass rods could be used to obtain satisfactory dose estimates.

Fourteen cotton rats were tagged with  $100-\mu c$   $Ta^{182}$  wires and released into enclosures delimiting the uncontaminated natural habitat. The use of the tags permitted evaluation of the enclosures (designed for confining animals on White Oak Lake bed) for retaining cotton rats and also permitted quick detection of animals which had died presumably from a combination of cold weather and parasitic infestation.

Hematological measurements are being used as a possible indication of radiation effects in wild mammals on White Oak Lake bed. Because of the paucity of hematological information on wild mammals, basic blood studies were undertaken on some of the wild mammals from uncontaminated These measurements included total erythrocyte count, total leukocyte count, differential count, and hematocrit. Within the rodent family Cricetidae, an inverse relation was found between erythrocyte number and body weight for the six species studied. A comparison of total leukocyte counts for a small sample of rice rats from uncontaminated areas and the lake bed indicated a lower number of cells for the lake-bed animals  $(4.2 \times 10^3 / \text{mm}^3 \text{ vs } 6.0 \times 10^3 / \text{mm}^3)$ .

Breeding pairs of known-history cotton rats were released during mid-June 1962 into pens on the upper lake bed for the first phase of an experiment to test for radiation effects on blood and food chain transfer of radionuclides. The animals were sampled for blood, weighed, and tagged subcutaneously with glass rod dosimeters prior to release. The first resampling was carried out two weeks postrelease and showed for both groups a general drop in red blood cell number and an increase in white blood cell number. This change in blood picture was considered to be the result of adaptive physiologic mechanisms, since it was explicit in both groups.

#### Forest Studies

Analog computer methods were used to simulate changes in the succession and Cs<sup>137</sup> redistribution in a herbaceous ecosystem. A combination of

positive and negative feedback loops regulated the rapid buildup to maximum oscillations in biomass Rapid buildup typifies plant per unit area. succession on moist bare areas like the sediments exposed following drainage of White Oak Lake in 1955. Other studies of this lake bed previously showed that only a few percent of the Cs137 incorporated in sediments is readily "available," and a small fraction of this percentage becomes circulated through plant-animal food chains each year. However, the rapid turnover by herbaceous plants and insects implies prompt attainment of maximum levels of biological contamination. Contamination levels would decrease only slowly, mainly owing to radioactive decay in soils, unless favorable successional changes in species composition or remedial steps of land treatment were introduced.

Litter-bag techniques are providing data on the functional nature of arthropod communities inhabiting decaying leaf litter, whereas radioactive tracer techniques are providing a means of quantifying the role of these organisms. velopment of arthropod communities in freshly fallen litter is analogous to ecological succession. Differences in forest substrate produced greater effects on the type of arthropod community than did differences between the leaf species. The accumulation of Sr85, Co60, and Cs134 by forestfloor millipedes (Dixidesmus erasus) was measured in both field and laboratory experiments. Strontium-85 accumulation was constant throughout a 40-day period in the laboratory; Co<sup>60</sup> concentrations in millipedes equilibrated with concentrations in food during this period, and Cs<sup>134</sup> body burdens peaked after 3 days and then declined at a rate which reflected loss of cesium from leaf litter due to leaching. Field experimentation showed similar patterns of accumulation for these isotopes, but results were less conclusive owing to low levels of activity and the influence of environmental factors. Effects of arthropods and of microflora on rates of litter breakdown were studied by comparing loss of weight and Cs134 from oak leaves decomposing in the presence and in the absence of arthropods. Naphthalene was chosen over other insecticides because it excluded arthropods from the litter without affecting the microflora. Over a 35-week period, 100 g of naphthalene on 1 m<sup>2</sup> of oak litter reduced the arthropod numbers by 2 orders of magnitude, increased microbial plate counts two to three times,

had no effect on direct counts of soil microflora and soil and litter respiration, reduced litter weight loss by 15%, and reduced loss of Cs<sup>134</sup> by 50%.

Periodic quantitative estimates of the microflora in various environments and subsequently of corresponding amounts of microbial tissue are essential for prediction of microbial accumulation and turnover of minerals, including radioisotopes, under various ecological conditions. Results of such microbial counts show a positive correlation between microflora and rate of litter breakdown, temperature, and moisture. Litter-leaf species influenced composition as well as abundance of the microflora. Microbial immobilization of radionuclides in decomposing leaf litter may surpass 50% of the initial mineral content. The amount of mineral immobilized depends on the isotope, leaf species, microbial development, weather, subsoil, and arthropod activity. In contrast to other leaf species, the microbial decomposition of mulberry leaves resulted in mobilization of minerals.

6)

The second year of a tracer study of Cs134 in white oak trees was completed. In 1961, as in 1960, an average of 40% of the 2 mc injected in the tree trunk was transferred to plants. Of this, approximately one-half returned to woody tissue, one-third fell with leaves, and one-sixth rained out. Horizontal and vertical distribution in understory, litter, and mineral soil was studied around three trees on each of four soils (upland and lowland types derived from cherty dolomite and Conasauga shale). A 20  $\times$  25 m ( $\frac{1}{8}$  acre) plot dominated by tulip poplar was tagged with Cs<sup>137</sup>. Except for a short delay due to drought, translocation to tree crowns approached seasonal maximum values in 2 to 4 weeks. Soon after rain began leaching Cs<sup>137</sup> from the canopy, to the litter and soil, mushrooms showed a steady accumulation.

#### Clinch River Studies

Aquatic ecology studies continue to emphasize the fate and effects of radionuclides released to the Clinch River. A study under way suggests that fish populations may be tagged with radionuclides deposited in the bony tissues (scales). The biological half-lives of radionuclides in fish are being measured in connection with population tagging studies and with investigations pertaining to the role of fish in the dispersal of radioactive

contamination of the environment. Preliminary results indicate a 40-day half-life for radiocesium in bluegills (*Lepomis macrochirus*), and a 1-day half-life for radiostrontium in soft tissues of white crappie (*Pomoxis annularis*). The stable strontium content of white crappie flesh and bone is being determined to test the possibility of predicting concentrations of Sr<sup>90</sup> in fish on the basis of the stable strontium content of fish tissue and water. Preliminary results from strontium and Sr<sup>90</sup> analyses of bone are in good agreement with values expected from laboratory releases of Sr<sup>90</sup>.

The study of the effect of radiation from low-level radioactive waste releases on a natural population of *Chironomus tentans* is continuing. In October 1961, there was a significantly greater number of heterozygous inversions in the irradiated population than in a nearby nonirradiated population. Additional control areas were established along the Clinch River upstream from White Oak Creek in order to verify the observed difference in heterozygous inversions. A seasonal trend in chromosomal polymorphism has not been demonstrated in the irradiated population.

The comparative strontium concentrations of contemporary and prehistoric clam shells were used to determine the biogeochemical strontium cycle in the environment. Current studies showed that there is a nonhomogeneous distribution of strontium within fresh-water clam (Unionidae) The strontium content of annual inner shell layers usually increases with age, whereas it is relatively constant in the outer shell layers. The outer layers contain an average of 77% as much strontium as do the inner layers. Barium concentrations are correlated with strontium, whereas the correlation of manganese, magnesium, and sodium concentrations in the shell layers is not consistent and appears to depend upon the species.

#### 3. RADIATION PHYSICS AND DOSIMETRY

#### Theoretical Physics of Dosimetry

Calculations of the dose due to high-energy radiations are in progress. A code has been partially completed to determine the depth dose in a tissue slab due to incident neutrons and protons of energies up to 400 Mev. The relationship has been established between the Vavilov-Cherenkov effect and the longitudinal and hybrid instabilities

in plasma-beam interactions. An electron beamplasma interaction in the presence of a magnetic field was analyzed, and it has been found that for a wave aligned in the direction of the magnetic field the instability has a frequency which is always below the gyrofrequency of stationary ions. The role of physical quantities in radiation dosimeters has been studied in conjunction with the generalized principle of dosimetry. A new model for spontaneous and radiation carcinogenesis has been investigated. A study of positron annihilation in free-electron gas has been made in which one assumes a static interaction between a given electron pair, and the annihilation has been expressed in terms of ladder Feynman diagrams. Absorption of photons in metals due to electron-electron collisions has been investigated. A study has been made of "distant ionization" produced by heavy ions in tissue elements beyond the adiabatic limit.

#### Experimental Physics of Dosimetry

Experimental work on the amount of ionization produced by alpha particles in mixtures of argon with various atomic and molecular gases has continued. It has been shown that the data fit a model in which two excited states in argon transfer sufficient energy to the added gas to ionize the latter. Studies of the interaction of low-energy (less than 1 ev) electrons in H2O show that the drift velocity in mixtures of H2O with gases like C2H4, CH4, and CO2 is appreciably decreased due to the addition of a few percent of II,O. The results have been interpreted in terms of longduration collision and have been generalized to other gases having permanent electrical dipole moments. A new time-of-flight method for the investigation of properties of electron swarms has been developed. The distribution of the flight times for individual electrons is interpretable in terms of the diffusion coefficient, the drift velocity, and the attachment coefficient.

The electron slowing-down spectra in copper of positrons and negatrons from Cu<sup>64</sup> were measured, the former with an anthracene coincidence spectrometer and the latter with the Keplertron, or spherical electrostatic analyzer. The primary slowing-down flux in the former was in excellent agreement with the continuous slowing-down model; the secondary electron spectrum in the latter was of a preliminary nature but nonetheless

showed a pronounced buildup of secondary electrons, the number of which doubled each time the energy was halved from about 40 kev to 1 ev. Studies of the emission spectra of metal foils irradiated by energetic electrons (25 to 120 kev) were continued with considerably increased accuracy due to the design, construction, and use of a grating calibrator for concave diffraction gratings, and to refinements in foil preparation and thickness measuring techniques. Spectra are in agreement with the transition radiation theory of Ritchie and Eldridge except for foils of high atomic number, where, in addition, visible bremsstrahlung is found. A new irradiation chamber has been built which permits observation of light from 0 to 153° from the electron beam direction under ultrahigh vacuum conditions.

#### Dosimetry Methods and Applications

Specific accomplishments this year include the development of a sensitive gamma-ray dosimeter having a negligible response to neutrons, the completion and testing of the Health Physics Research Reactor, and extensive experiments in Operation BREN. BREN was the major effort relative to the Ichiban Program, the objective of which is the determination of the radiation exposure of the survivors of the nuclear bombings of Hiroshima and Nagasaki, Japan.

#### Physics of Tissue Damage

The emission spectra of x-irradiated trypsin, tyrosine, phenylalanine, and tryptophan in a helium atmosphere have been obtained at 77°K with an interference filter spectrograph, both during irradiation (immediate luminescence) and after irradiation during warmup (thermoluminescence). Calibration of the spectrometer against an NBS standard light source has made possible measurements of the total light yield, which varied from 0.17% of total energy absorbed for trypsin to 3.8% for tryptophan. The ratio of energy emitted in thermoluminescence to that in immediate luminescence varies from 0.0004 to 0.008 for these materials. The intensity of thermoluminescence was found to be strongly dependent on the presence of a gas both during irradiation and during warmup; that is, with a vacuum of the order of 10<sup>-5</sup> mm Hg, the light intensity decreased by at least a factor of 50. Spectra varied from material to material but did not depend on the particular gas present (He, Ar, O<sub>2</sub>). Similar experiments on NaCl showed a linear increase of thermoluminescent light intensity with crystalline surface area, indicating that electron trapping by adsorbed gas at the surfaces of crystals may play an important role.

#### 4. INTERNAL DOSIMETRY

#### Estimation of Internal Dose

A computer code written to estimate the body burden of Pu<sup>239</sup> (exclusive of lung burden) has been adapted to estimate the total intake of Pu<sup>239</sup> to blood from urinalysis data on excreted Pu<sup>239</sup>. This makes it possible to check the accuracy of the model and method by using data on hospital patients who received Pu<sup>239</sup> intravenously. By fitting an excretion rate curve to each individual's data and by using all the urinalysis data, the intake is estimated within an accuracy of ±30% in all cases tested. Under practical conditions of sampling of employees, the error may be considerably larger.

#### Stable-Element Metabolism by Man

The dose rates and annual doses of individuals continuously exposed to radioactive material in the environment will be approximately proportional to the concentration of the radionuclide in the various tissues of these individuals. A stable isotope of the same element should have a similar distribution in these tissues, and thus the form of the distribution of the annual dose or dose rate may be inferred from studies of the distribution of concentrations of stable isotopes in human tissues. Statistical methods given by Brunk and Massey have been applied to data for normal isotope distribution in human tissue as reported by Tipton et al., Bryant et al., and Kulp et al. The method by Brunk determines a band such that at each concentration value one may assert with 95% confidence that the true distribution function lies below (above) the upper (lower) boundary of the band. The method by Massey has been applied to obtain a 95% confidence band for the entire cumulative distribution curve. In the majority of cases studied, one may assert with 95% confidence that not more than 5% of the population groups

sampled have concentration values above three times the sample mean, thus providing some quantitative interpretation of the assumption used in the reports of the Federal Radiation Council.

Average values are given for 23 trace elements in 967 tissue samples from San Francisco, Atlanta, and New York. The ORNL spectrographic data agree with those from the University of Tennessee, and with wet-chemical results. A method is described for the determination of trace elements in bone ash. Experiments designed to test for losses of trace elements during dry ashing are described.

The use of the IBM 1620 and 7090 data processing machines for treatment of the data from the program for trace elements in human tissue makes it possible to achieve a much more complete and accurate statistical study. Since the highly skewed data from this program cannot be treated in the ordinary manner, Kendall's method for calculating the rank correlation coefficient is used.

Rank correlation coefficients between elements in a single tissue and between tissues with regard to a single element have been calculated for 24 elements and 19 tissues. The results for the nonessential elements Al, Ba, Cd, Cr, Pb, and Sn and the essential element Mn are reported here. Aluminum is correlated for the most part with nonessential elements. Barium shows interesting correlations with essential elements which should be studied further. Cadmium is highly correlated with zinc. Chromium, lead, and tin show no consistent pattern. Manganese is highly correlated with magnesium in all tissues, with most essential elements in the brain and with nonessential elements in the lung.

Further statistical studies are under way.

#### Microscopic and Autoradiographic Studies of Distribution of Uranium in the Rat Kidney

The concentration ratio of uranium in the rat kidney, which is the ratio of the average number of disintegrations per field of the cortex to the average number of disintegrations per unit field for the entire organ, is now expressed as  $R_b$ , and is estimated by autoradiographic measurements to be 1.3 and by the radiochemical estimation to be 1.2.

In converting from counts to disintegrations per minute per gram, evidence points to the conclusion that the photographic emulsion penetrates the tissue, and so essentially all tracks are visible under the microscope.

A comparison has been made between the activity in the autoradiograms and that found by radiochemical analysis. Although the difficulties of technique may increase the variance, giving considerable spread in individual values, there was a gross check between the two methods.

The fractions of injected dose retained in kidney show some nonlinearity with the dose level and, in general, increase with increasing dose level.

In general, the tracks are found in the proximal convoluted tubules. The track count in the distal tubules tends to increase with increasing postinjection time. In one rat sacrificed at 84 days, the higher number of counts was in the distal tubules.

Pathological conditions become apparent in tissues two days after injection with 1000 and 100 μg of uranium per kg of body weight. At four and seven days after injection, at the high level, there is extensive cellular degeneration of the hyaline droplet type in the proximal convoluted tubules, and in the intermediate level mildly nephrotic conditions are found. At 28 days no abnormalities are observed except at the level of 1000  $\mu g/kg$ , where atrophy and regeneration are present.

#### 5. HEALTH PHYSICS TECHNOLOGY

Methods of measurement and redispersion of particulates are being evaluated as a function of The likelihood of resurface characteristics. dispersing particulate contamination by air blowing over the surface is essentially the same for a wide range of surface roughness. The apparent hazard as indicated by smear and adhesive-paper measurements decreases for the rougher surfaces. Surfaces covered with an oily film show little redispersion due to air currents, whereas the apparent hazard as indicated by smears and adhesive-paper samples is the same as that for clean surfaces of the same material.

Submicron aerosols have been produced with the exploding-wire aerosol generator by the explosion of 18 different metals in air and in argon. The aerosol yield, color of deposit collected on membrane filters, and chemical composition are

tabulated. The composition of aerosols generated by wire explosions in air is found to vary with the voltage used. Gas pressure in the explosion chamber at the instant of explosion affects the yield and may influence particle size. Particlesize analysis is reported for an aluminum aerosol.

During the year the IVGS facility has been improved by the addition of a transistorized 512-channel analyzer, three thin crystals for low-energy photon analyses, and development work which is expected to provide a counting geometry that is less dependent on body shape, size, and location of deposit. A computer program for rapid processing of counting data is being prepared. This method of data processing will allow expansion of the counting program to include many additional routine examinations. A total of 102 people have been counted, and of these, 13 have shown measurable amounts of gamma-ray activity other than the normal K<sup>40</sup> and Cs<sup>137</sup>.

In support of the NS "Savannah" medical program, shipboard procedures have been established for detecting significant exposures to internal radioactive contamination and for estimating radionuclide deposition in the body organs. Direct gamma-ray spectrometry of raw urine samples provides adequate sensitivity for detecting significant exposures to gross mixtures of radioactive corrosion products or fission products. The employment of a collimated  $3 \times 3$  in. NaI(Tl) crystal to scan selected portions of the body offers sufficient sensitivity to estimate organ burdens of gamma-emitting radionuclides.

Special studies carried out during this year include human thyroid uptake of protein-bound I<sup>131</sup> in milk and a comparison of cattle thyroid uptake with I<sup>131</sup> content of milk. The application of the IVGS facility for the detection and measurement of internal deposits of transuranic elements is being investigated.

A procedure has been developed for the analysis of milk for  $I^{131}$  which is sensitive to <10  $\mu\mu$ c/liter. It is based on the extraction of  $I^{131}$  directly from liquid milk onto a strong-base anion exchange resin. The  $I^{131}$  activity is counted directly on the resin by summing the counts within the 0.364-Mev gamma photopeak, using a 4 × 2 in. NaI(T1) crystal with a gamma spectrometer. The recovery of  $I^{131}$  from 3 liters of milk is about 90%.

Detailed interpretation of the  $Sr^{90}$  excretion data resulting from an accidental human exposure indicates that the total excreted during the first 22 days represents about 71.6% of the initial intake. In this period the amount excreted via urine is approximately three and one-half times that eliminated in the feces. These data have been fitted by using a variety of functions and a number of commonly used side conditions. A tabulation of the parameter estimates illustrates one potentially major source of disagreement between investigators fitting their data with power functions of the form  $At^{-B}$ .

## 6. EDUCATION, TRAINING, AND CONSULTATION

The need for trained health physicists, both in this country and abroad, continues. The AEC Fellowship students and several foreign students completed the program at Vanderbilt University and Oak Ridge, and the Fellowship group for the 1962-63 program has been selected. Lectures and laboratory courses were provided for Laboratory, division, and civic programs.

It is anticipated that in the future more training in health physics will be provided for ORNL personnel and for foreign students on an individual basis.

## Contents

SU	IMMARY	iii
ı.	RADIOACTIVE WASTE DISPOSAL	1
	Liquid Injection into Deep Permeable Formations  Nature of the Wastes Considered for Deep-Well Disposal  Ion Exchange of Radionuclides.  Movement of Radionuclides in Relation to the Movement of Water  Conclusions.	1 1 1 3
	Disposal by Hydraulic Fracturing	5 5 7
	Thermal Studies Plastic Flow Studies Thermal Stability of Rock Salt High-Temperature Experiments	10 11 13 15 19 20
	Hydrology Water Sampling and Analysis	20 20 21 22
	Sources of Contamination and Movement of Radionuclides in the Creek	27 27 30 34
	Behavior of Cesium in Vermiculite Systems	34 34 37 40
	Shipping of Calcined Solids	42 43 43
	Geologic and Hydrologic Studies by U.S. Geological Survey  Cooperation of Other Agencies in ORNL Studies.  Visiting Investigators from Abroad.  Nuclear Safety Review	44 45 45 45 45 46

2.	RADIATION ECOLOGY	47
	Transfer of Fission Products Through Plant to Insect Food Chains  Bioaccumulation of Radionuclides by Mammals Resident on Upper White  Oak Lake Bed  In Vivo Dosimetry with Miniature Glass Rods  Field Studies of Mammals Labeled with Radioactive Tags	47 47 48 49 51 52
		54
	Analog Computer Model for Biomass and Cs 137 in a Herbaceous Ecosystem	56 56
	Radioactive Tracer Studies with Millipedes	59 61 62 64 64 65
	Mobility of Cs <sup>137</sup> Tracer in a Forest of Tulip Poplar	66
	Strontium in White Crappie (Pomoxis annularis) Flesh and Bone  Biological Half-Life of Strontium and Cesium in Fish  Fish Marking and Population Studies  Radiation Effects on Chironomus tentans  Strontium in Fresh-Water Clam Shells	67 67 68 68 70 70
3.	RADIATION PHYSICS AND DOSIMETRY	73
	Electromagnetic Properties of a Plasma-Beam System Vavilov-Cherenkov Effect and "Bohr Radiation" Produced by a Beam of Charged Particles in a Dispersive Medium. "Distant Ionization" Produced by Heavy Ions in Tissue.  Dosimetry of High-Energy Radiations Role of Physical Quantities in Radiation Dosimetry.  Model for Spontaneous and Radiation Carcinogenesis.  Positron Annihilation in a Free Electron Gas Absorption of Photons in Metals Due to Electron-Electron Collisions.  Surface Absorption of Photons in Metals.  Optical Bremsstrahlung in a Dielectric Medium.	73 73 74 74 75 76 77 78 78
	Ionization of Gas Mixtures	79 79 80 81 81 82 84
	Radiation Measurements over Simulated Plane Sources	85 85
	Energy Response of G-M Tubes	85

	Fast-Neutron Spectrometer	87 88
	Health Physics Research Reactor (HPRR)	88 88 93
	Physics of Tissue Damage  Emission Spectra of the Low-Temperature Thermoluminescence from  X-Irradiated Biochemicals	99 99
4.	INTERNAL DOSIMETRY	101
	Estimation of Internal Dose	101 101
	Stable-Element Metabolism by Man Statistical Evaluation of Dose Resulting from a Constant Level of Contamination in the Environment Tissue Analysis Laboratory Progress Report Further Statistical Interpretations of Trace Element Concentration in Human Tissue	104 104 109
	Microscopic and Autoradiographic Studies of Uranium Distribution in the Rat Kidney	128
5.	HEALTH PHYSICS TECHNOLOGY	142
	Aerosol Project	142 142 145 147
	ORNL In Vivo Gamma-Ray Spectrometer Facility  Analysis of Milk for I 131 by Anion Exchange Resin: The Effect of Protein-Bound I 131  N S. "Savannah" Bioassay Development Program.  Excretion of Sr 90 by Man	147 149 152 153
6.	EDUCATION, TRAINING, AND INFORMATION	155
Pί	JBLICATIONS	156
PA	PERS	159
LE	ECTURES	163

## Radioactive Waste Disposal

E. G. Struxness

R. J. Morton

F. L. Parker

# LIQUID INJECTION INTO DEEP PERMEABLE FORMATIONS

D. G. Jacobs

O. M. Sealand

# Nature of the Wastes Considered for Deep-Well Disposal

Early considerations of disposal of radioactive waste into deep wells by the American Petroleum Institute Subcommittee on Disposal of Radioactive Waste dealt with the possible disposal of the highest levels of radioactive waste, the reactorfuel reprocessing wastes. These wastes are so highly radioactive that thermal cooling is required, and their handling poses severe problems in protection of operating personnel from overexposure to radiation. The volumes of these wastes are low. (Over the past few years techniques have been implemented to drastically reduce the volume from 800 to about 60 gal of waste generated by the reprocessing of a ton of reactor fuel.) Their intense hazard justifies expenditure of a substantial sum of money per unit volume to ensure their safe handling. Because of their extreme hazard, it is unlikely that such wastes will purposely be discharged directly to the ground without some pretreatment to reduce the mobility of the more hazardous radionuclides.

It now seems likely that initial application of deep-well techniques will be in the disposal of the high-volume, low-level process waste-water streams. The stable-chemical composition of ORNL low-level waste is essentially the same as that of local tap water, and only Sr<sup>90</sup> is consistently above the permissible concentration for drinking water. The 200 yr required for Sr<sup>90</sup>

If deep-well disposal proves satisfactory for low-level wastes, it is possible that disposal of intermediate-level wastes will follow. Oak Ridge National Laboratory intermediate-level waste is a high-salt-content waste (~0.5 N Na<sup>+</sup>) to which excess caustic (NaOH) is added to precipitate most of the calcium, Sr<sup>90</sup>, and rare earths. Although most of the Sr<sup>90</sup> is removed during neutralization, it remains the hazard-controlling radionuclide in the supernate, being at approximately 100,000 times the permissible drinking-water concentration. Cesium-137 and ruthenium-106 are also above the permissible concentration levels in this waste stream.

#### Ion Exchange of Radionuclides

When radioactive liquids are discharged into the ground, the primary means of transport of the activity is by the movement of water through the The radionuclides follow the same paths of movement as the transporting water but move at a slower velocity due to the sorptive properties of minerals, primarily the clay minerals, present in the formation. Although the sands constituting good aquifiers are fairly "clean," there is a sufficient quantity of clays present to give them a significant exchange capacity. Kaufman et al. 2 measured the exchange capacities of several California oil sands and obtained values ranging from 0.48 to 20 meq/100 g with a mean value of  $\sim 5$  meq/100 g. Movement of the radionuclides can be predicted by describing the

to decay to the permissible drinking-water concentration gives an idea of the containment time required for safe disposal of this waste stream.

<sup>&</sup>lt;sup>1</sup>T. V. Moore et al., Problems in the Disposal of Radioactive Waste in Deep Wells, American Petroleum Institute, Dallas, Texas, October 1958.

<sup>&</sup>lt;sup>2</sup>W. J. Kaufman, R. G. Orcutt, and G. Klein, *Underground Movement of Radioactive Wastes*, Sanitary Engineering Research Laboratory, University of California, Berkeley, Aug. 1, 1955.

movement of water in the formation and correcting for sorptive processes.

The exchange capacity of Richfield sand, a typical deep-well formation, was determined by saturating with calcium, leaching with sodium acetate, and titrating the effluent calcium with EDTA. An average exchange capacity of 2.96 meg/100 g was obtained.

To determine the effects of ionic competition on the sorption of radiostrontium, multicomponent exchange systems were investigated. In the study of sodium-calcium-strontium exchange, the columns were presaturated with 0.005 M Ca(NO<sub>3</sub>)<sub>2</sub> solution containing various concentrations of NaNO, . The columns were then saturated with chloride solutions of the same cationic composition to which was added  $Sr^{85}$  ( $\sim 2 \times 10^{-8}$  M SrCl<sub>2</sub>). The effluent was sampled at 25-ml intervals and counted for Sr<sup>85</sup>. After saturation, the calcium and strontium were removed by leaching the column with neutral 1 M sodium acetate. Aliquots of the eluate were counted for Sr85, and samples were analyzed for calcium by EDTA titration. Leaching continued until the columns were depleted of calcium and strontium. In these experiments the exchange capacity of the Richfield sand had risen to an average of 4.27 meq/100 g, and the selectivity of exchange for strontium compared with calcium was found to be  $\sim 1.1$ .

A second series of sodium-calcium-strontium exchange studies was run with the same columns in order to describe more adequately the exchange between calcium and sodium and its influence on strontium sorption. The results of these studies (series II) are shown in Table 1.1. The exchange capacity of the sand showed a further increase with continued cycles of saturation and leaching. The selectivity coefficient for sorption of calcium compared with sodium is 25.0 g/ml, while it appears that the selectivity for strontium over calcium increases when a smaller percentage of the total exchange sites is occupied by calcium. In the absence of calcium at pH 7, the Richfield sand is very selective in the uptake of strontium compared with sodium.

The selective sorption of strontium over calcium on Richfield sand agrees with observation of strontium-calcium exchange on reference clay minerals (Table 1.2). Divalent-exchange studies, made with Conasauga shale, indicated that the preference of the cation-exchange surface for strontium over other alkaline-earth cations decreases with decreasing size of the hydrated ion.

Cesium Exchange. — The basal surface of the platelike layer lattice clay minerals is composed of open hexagonal networks of oxygen atoms. The openings in this basal surface are of such a size that potassium, rubidium, or cesium ions, which are all easily dehydrated, can partially penetrate the surface and come much closer to the seat of the lattice charge than the more completely hydrated alkali-metal and alkaline-earth cations. Thus, cesium is ordinarily very strongly sorbed by most clay minerals from waste solutions

Table 1.1. Calcium-Sodium-Strontium Exchange Properties of Richfield Sand (Series II)

Ca <sup>2+</sup> (meq/ml)	Na <sup>†</sup> (meq/ml)	1	Exchange Capacity acq/100 g)	K <sup>Sr</sup> Ca	K <sup>Ca</sup> (g/ml)	K <sup>Sr</sup> (g/ml)
0.00	0.50		6.87			326.0
0.01	0.00		6.59	1.06		*
0.01	0.10		6.64	1.10	25.6	28.2
0.01	0.20		7.22	1.32	21.2	27.7
0.01	0.30		6.86	1.32	26.1	34.5
0.01	0.40		7.04	1.39	23.4	32.6
0.01	0.50		6.77	1.29	28.6	36.9
		Av	6.86	1.25	25.0	

Table 1.2. Strontium Exchange Properties of Various Clay Minerals

Mineral	K <sup>Sr</sup> <sub>Mg</sub>	K <sup>Sr</sup> Ca	K <sup>Sr</sup> Ba
Vermiculite		1.31 ± 0.16	
Fithian illite		1.19 ± 0.17	
Kaolinite		1.21 ± 0.19	
Wyoming bentonite		1.33 ± 0.29	
Arizona bentonite		1.26 ± 0.15	
Conasauga shale	1.44 ± 0.14	1.24 ± 0.06	1.00 ± 0.26

composed primarily of sodium or calcium salts and will usually move much more slowly than strontium in the ground, especially when illitic clays are predominant.

Ruthenium Behavior. - The behavior of ruthenium in the ground is more complicated than that of either strontium or cesium, due to its tendency to form complex ions and to the effect of pH and oxidation-reduction potentials on its behavior. Much of the ruthenium in the ORNL low-level waste stream probably exists in noncomplexed forms and would be deterred from movement in the soil by ion exchange of cationic species and by a combination of surface precipitation and filtration of the oxides and hydroxides of ruthenium in oxidation states 3 and 4. However, in the intermediate-level wastes, which originate as nitric acid, the tendency for formation of nitrosonitrato complexes is much more pronounced. These complexes resist changes in oxidation state and are removed slowly in the ground.

The behavior of ruthenium in the ground is difficult to predict. However, in the ground disposal of ORNL intermediate-level wastes, ruthenium is the first radionuclide to reach monitoring wells, but most of the ruthenium (80 to 90%) is removed from solution while it passes through less than 100 ft of shale. Only about 50% of the remaining radioruthenium is removed before the water reaches the surface.

Movement of ruthenium in the ground from the disposal of low-level waste would pose no problem, as the  $\mathrm{Ru}^{106}$  concentration of this waste

 $(1.4 \times 10^{-5}~\mu c/ml)$  is initially below the MPC $_{\rm w}$ . In the disposal of intermediate-level wastes (2  $\mu c$  of Ru $^{106}$  per ml), it would be necessary to contain the ruthenium for only about 12 yr to allow decay to the MPC $_{\rm w}$ .

## Movement of Radionuclides in Relation to the Movement of Water

Cations do not move through the ground as rapidly as the transporting water, because a portion of the cations is exchanged onto the solid phase. The effect of sorption on the velocity of migration of a radionuclide can be expressed quantitatively by:<sup>3</sup>

$$\frac{\overline{v}_R}{\overline{v}_{\rm H_2O}} = \frac{1}{1 + (K_d)_R \rho_b/f},$$

where  $\rho_b$  is the bulk density of the formation, f is the fraction pore space,  $\overline{v}_R/\overline{v}_{\rm H_2O}$  is the ratio of the mean velocity of the radionuclide to the mean velocity of the transporting water, and  $(K_d)_R$  is the ratio of the amount of a radionuclide sorbed per unit weight of exchanger to the amount of unsorbed radionuclides per unit volume of solution.

A solution does not move through porous media with uniform velocity, but becomes dispersed. Because anions are not actively sorbed by cation exchangers, they can be used to measure the dispersion of the solution front. In the columns described under "Ion Exchange of Radionuclides," above, chloride was determined in the effluent as nitrate solution was displaced by chloride solution in order to determine the velocity distribution of the water.

An equation useful for describing the concentration history of the effluent from an ion-exchange column operated under conditions of linear flow has been derived by Glueckauf<sup>4</sup> by use of the concept of the "theoretical plate":

$$c/c^0 = \frac{1}{2} + Ae \left[ \sqrt{N} \left( \frac{V - \overline{V}}{\sqrt{V \overline{V}}} \right) \right],$$

<sup>&</sup>lt;sup>3</sup>M. N. E. Rifai, W. J. Kaufman, and D. K. Todd, Dispersion Phenomena in Laminar Flow Through Porous Media, Sanitary Engineering Research Laboratory, University of California, Berkeley, July 1, 1956.

<sup>&</sup>lt;sup>4</sup>E. Glueckauf, Trans. Faraday Soc. 51, 1540 (1955).

#### where

c = concentration of the exchanging species in the effluent,

c<sup>0</sup> = concentration of the exchanging species in the influent,

$$Ae[y] = \frac{1}{\sqrt{2\pi}} \int_0^y \exp\left(\frac{-y^2}{2}\right) dy ,$$

N = number of theoretical plates in the column,

V =throughput volume,

 $\vec{V}$  = throughput volume at the inflection point of the curve, where  $c/c^0 = \frac{1}{2}$ .

It is seen that the strontium breakthrough curve can be predicted on the basis of dispersion of the solution in the column (Fig. 1.1). This implies that radionuclide breakthrough at a particular point in the environment can be predicted by observing the breakthrough of a water tracer and correcting for the sorptive properties of the formation for the radionuclide in question.

Calculations based on the exchange properties of Richfield sand (Table 1.1) and the chemical characteristics of the ORNL low- and intermediate-level waste streams indicate that Sr<sup>90</sup> will move about 1% as fast as the low-level waste solution and about 10% as fast as the intermediate-level

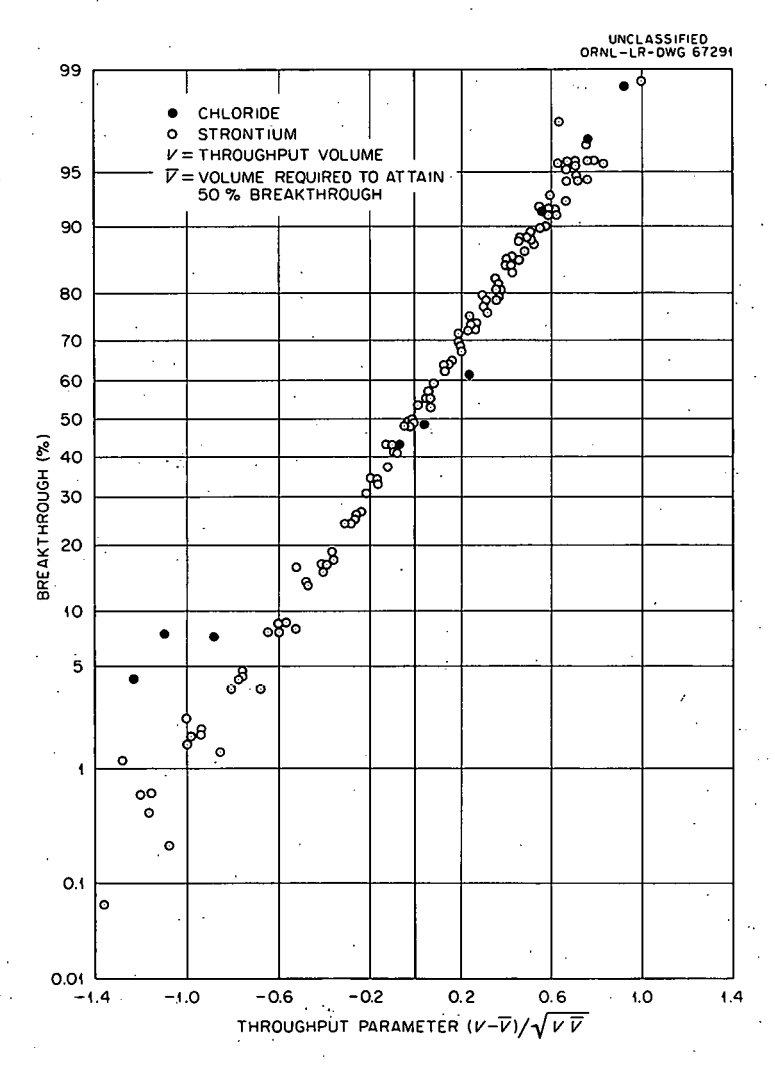


Fig. 1.1. Comparison of Chloride and Strontium Breakthrough Curves.

waste solution, at pH 7. However, in a high-pH system the precipitation of slightly soluble calcium-strontium salts is likely, and it would result in much slower movement of the strontium than predicted from simple ion exchange in a neutral-pH system.

Cesium is held more strongly by the clay mineral exchangers than strontium and is present in the waste streams in relatively less hazardous quantities. Therefore, its movement would contribute much less to the total hazard than would the movement of strontium. Ruthenium movement would become hazard-controlling in intermediate-level waste disposal only if its movement were unrestricted and the movement of strontium were slowed by an additional factor of 5 by precipitation reactions.

#### Conclusions

The wastes presently being considered for disposal by deep-well injection are high-volume, low-level wastes; the ORNL low-level waste stream would require containment for about 200 yr. ORNL intermediate-level wastes, requiring 465-yr containment, may be considered later for disposal by this method. It seems unlikely that the high-level wastes, which result from chemical processing of spent fuel elements, will be released to the ground without first immobilizing the fission products.

Velocities of fission-product movement in the ground will be less than that of the transporting water, due to ion exchange of radiocations by clay minerals. Precipitation reactions and filtration will provide additional restrictions on radionuclide migration. The restricted movement of radionuclides compared to water would make it possible to use a deep aquifier as a large ionexchange bed, rather than just as a storage basin. Such a system might employ an injection well and a series of producing pressure-relief wells. A volume of waste several times the storage volume of the formation could be decontaminated by passing through the formation before permissible concentrations of radioactivity were exceeded at the producing wells.

ું હતું

#### DISPOSAL BY HYDRAULIC FRACTURING

W. de Laguna T. Tamura
B. L. Houser E. G. Struxness
H. O. Weeren<sup>5</sup>

The purpose of this investigation is to determine the feasibility of disposing of liquid radioactive waste by mixing it with cement, or some other hardening agent, and then injecting the slurry deep into bedded rock through a specially constructed well. The pressure developed at the bottom of the well forces the rock to fracture, along the bedding planes under favorable circumstances, so that the waste-cement mixture flows out into the rock in a thin horizontal sheet and then hardens.

#### Field Tests

Three years ago (October 1959) a preliminary field experiment was conducted by pumping 27,000 gal of cement grout into a local formation at a depth of 300 ft. Subsequent test drilling showed that this had formed a cement-filled fracture parallel to the bedding extending out from the injection well for distances up to 400 ft, largely updip. In a second experiment a year ago, about 91,500 gal of grout was injected into the shale at a depth of 934 ft, and, a week later, 132,770 gal was injected into the same well at a depth of 694 ft.

Test drilling at this site was still in progress when last year's annual progress report was prepared. At that time incomplete data suggested that the injection well had, by chance, been drilled into a narrow down-faulted or down-folded block of rock. Further drilling cast serious doubt on this interpretation, and a survey of the deviation of the drill holes from vertical disproved it Except for the original stratigraphic test hole and the injection well, all of the test holes were found to have deviations of from 20 to 30°; it is apparent that both the subsurface structure and the structure and shape of the grout sheets are much simpler than at first believed. Detailed stratigraphic mapping in oil fields has, on occasion, been similarly complicated by test wells that deviated by as much as 60° from the vertical.

<sup>&</sup>lt;sup>5</sup>Member of Chemical Technology Division.

While both grout sheets are now known to be essentially parallel to the bedding of the shale, it is also clear that both worked their way upward a little stratigraphically as they moved out. In the case of the upper sheet, which extended out to a maximum of about 500 ft to the northeast, this upward cross-fracturing amounted to about 50 ft. Although there is no reason to believe that there are any major folds or faults in the area, both the surface outcrops and the rock cores show narrow zones of drag folds with an amplitude of a few inches to a few feet. The data available are consistent with the explanation that the fractures were deflected upward by a foot or two where they crossed one of these zones, but it would almost be necessary to mine out the area to determine just what did happen. The general impression, however, is that the fracture pattern developed is favorable for the proposed method of waste disposal; even though the fractures were deflected upward slightly as they moved out, they quickly returned in each case to an orientation conformable to the bedding and showed no tendency to send up spurs of any length toward the surface.

The cores also showed that the upper grout sheet consisted of four or five separate sheets, locally in contact with one another in the same fracture, but in other areas separated by from a few inches to a few feet of shale. Apparently the grout sheet moved out until its leading edge had lost enough water to the shale to materially increase its viscosity and so impede the advance of the fracture. A second fracture then formed at or near the well and moved out along the same or nearly the same level as the first, until it, in turn, lost water and halted, when it was followed by a third, a fourth, and even a fifth sheet. This mechanism, although somewhat speculative, suggests that fluid loss additives may be used to influence the maximum extent of the fractures. Such additives are used routinely in the petroleum industry for the same purpose.

Completion of test drilling confirmed that the grout sheets did not extend out as far from the injection well as the surface uplift, nor were they as symmetrically arranged around the injection well; therefore, surface measurements cannot be used directly to map the extent of the grout sheets. The correlation between the amount of surface uplift and the thickness of the grout sheet was, however, somewhat better than at first believed; further measurements of the thickness of the

grout and allowance for the deviation of the wells will be required before a final comparison can be made.

The volume of the uplift measured at the surface is greater than the volume of grout injected, and the injection pressures were considerably higher than the static weight of the overburden. These data can only be explained if the thinly bedded shale and limestone overlying the fractures had sufficient tensile and shear strength to act as a beam. This is not generally believed to be the case with rock when such large spans are involved (the area uplifted had a maximum diameter of over 1500 ft), but the conditions were unusual in that seldom are such relatively impermeable and wellbedded rocks subjected to hydraulic fracturing, nor are such detailed measurements of uplift usually obtained. The ultimate strength of the beam, when subjected to repeated increments of uplift, has a bearing on the problem of how many successive waste-filled fractures can be developed from a single well. It is probable that this can be determined only through experience.

In the summer of 1961 a test well (Joy No. 1) was drilled to a depth of 3263 ft, about 3000 ft southwest on strike from the injection well of the second fracturing experiment. All of this test well was cored. The hard Rome sandstone was encountered at a depth of 1002 ft, almost exactly the same as the depth in the injection well used for the second fracturing experiment, and the bottom of the Rome formation was reached at 1360 ft, where it was found to be cut off by one of the main thrust faults of this area. It had been anticipated that the thrust fault would be found at a greater depth; that is, that the fault plane dipped more steeply than it does and that the Rome formation would be somewhat thicker in depth than was found to be the case. Consideration had even been given to the possibility that these deeper Rome beds might be sandstones of very low but significant permeability and porosity, which would have made them of interest as a potential disposal zone. It is now apparent that no beds of significant permeability or porosity exist in the stratigraphic column below the Laboratory.

The first hundred feet of the 358 ft of Rome formation was very hard compact sandstone; the balance consisted of interbedded sandstone and sandy shale, very much the same as the beds exposed in surface outcrops. The bottom hundred

feet of the interbedded sandstone and shale, however, is distorted, folded, and crushed, but it has been thoroughly recemented. This folding and crushing is presumed to date from the period of overthrust faulting at the close of the Paleozoic. The actual fault plane, between 1357 and 1360 ft, consisted of sheared, soft, very fine-grained shaly gouge, of apparently very low permeability. This material was not cemented, which suggests that it may be due to geologically somewhat more recent movement along the old fault plane. The fault appears to provide a marked structural discontinuity between the overlying and underlying formations.

Below the Rome formation, and after passing through the fault zone, the well penetrated 1766 ft of the Chickamauga limestone. This formation is dominantly a hard, fine- to medium-grained limestone, most of it in thin well-defined beds, and it is probable that a large part of it could be used for disposal by hydraulic fracturing. 1628 or 1700 and 1847 ft, and also between 2648 and 2852 ft, the formation consists of very thin-bedded argillaceous limestone or calcareous shale. These beds are somewhat harder and more brittle than the red shale in the lower Conasauga, but break cleanly and easily along the bedding, and appear to provide the best possibility for waste disposal in the Chickamauga. Except for a few tens of feet of rock immediately below the fault zone, the Chickamauga limestone, including the calcareous shales, is not deformed by smallscale folding or faulting, as are the shales in the Conasauga. The apparent dip of the Chickamauga is about 10°, but, due to deviation of the test well from vertical, the true dip is probably about 20°. (All the test wells deviated updip.)

Plans for the coming year include first some more relatively shallow testing in the shells between 700 and 1000 ft, and then drilling a larger-diameter well to a depth of 2900 ft near the site of the deep test hole to determine the pressures required to fracture the calcareous shales in the zone between 2648 and 2852 ft, and also to determine the fluid containment properties of these beds. Measurements of permeability and porosity on core samples suggest that the fluid will be very largely contained in the fracture. As many as three observation wells may be drilled around this injection well, but no elaborate fracturing or drilling program at this depth is contemplated.

This group of wells will, however, be so constructed that they can, later, be used for tests with actual disposal of waste. Plans for the mixing and pumping plant for these tests are being prepared, but little real progress will be possible until the operating pressures required have been determined by the deep field test mentioned above, until more is known about the wastecement mixtures that will be used, and until provision has been made for the consulting services of one of the major companies experienced in the hydraulic fracturing of oil wells.

#### Hydrofracture Mix Development

The primary requirements for the mix are that it shall (1) remain sufficiently fluid for mixing, pumping, and injection, and for a long enough duration to assure the completion of these operations, and (2) then set up sufficiently through hydration so that the mix will be confined in the fracture. These requirements are not difficult to satisfy for water-cement slurries, but waste solutions with significant and varying amounts of dissolved ions complicate the system. In order to take advantage of the knowledge, experience, and talents of those who are engaged in hydrofracturing operations, a subcontract was awarded to Westco Research of Dallas, Texas.

Preliminary Testing and Evaluation of Cement-Waste Compatibility. — The first objective in the development of the mix was to gain a general understanding of the properties of waste-cement slurries, including their pumpability. Some of the properties measured, in most cases by techniques recommended by the American Petroleum Institute, were consistency, setting time, fluid loss, and compression strength.

The basic composition of the simulated waste used was:

$0.317 \text{ M NaNO}_3$ ,	$0.025 M NH_4NO_3$ ,
0.219 M NaOH,	$0.022 \text{ M AI(NO}_3)_3$ ,
0.037 M Na <sub>2</sub> SO <sub>4</sub> ,	0.006 M NaCl.

After the slurry was mixed in a Waring blender, it was visually inspected for evidence of flash setting, initial gel strength, and viscosity. Flash

<sup>&</sup>lt;sup>6</sup>API Recommended Practice for Testing Oil-Well Cements and Cement Additives, API RP 10B, American Petroleum Institute, New York, March 1961.

setting and high initial gel strength are dependent on the chemical composition of the cement and the waste solution. Viscosity is affected by the waste solution-to-cement ratio. Slurries had a high initial gel strength when prepared with Volunteer type I Portland cement, 208 cc of waste solution per pound, but not when the proportions of waste solution to cement were larger. Apparently, close attention will have to be given to the chemical composition of the waste and the ratio of waste to cement in designing the ultimate mix.

Permissible pumping time, defined as the time during which the viscosity of the slurry is less than 100 poises, is one of the most important properties of the waste-cement slurry. Actually, 100 poises is far too high for pumping; in most cases, the viscosity is held below 20 to 25 poises. Pumping time was measured on the Pan American thickening-time tester<sup>6</sup> which simulates conditions of temperature and pressure for various well depths; that is, for a depth of 2000 ft, a bottom-hole temperature of 91°C, and a bottomhole pressure of 1540 psi. It was found that increasing the volume of waste from 208 to 245 cc increased the pumping time from approximately  $2\frac{3}{4}$  to  $3\frac{3}{4}$  hr, or the same as when 208 cc of distilled water was used. When the sodium nitrate concentration in the synthetic waste solution was increased from 0.3 to 3 M, the pumping time increased to 8 hr, 20 min.

Compressive strength tests were made to determine the effect of changing waste concentration on the setting properties. It remained relatively constant over a side range of compositions when the grout was cured at 80°F, even when the waste solution contained ten times the salt concentra-The compressive strength was much more sensitive to waste composition when the grout was cured at a higher temperature (Fig. 1.2). These mixes contained only waste solution and cement; they contained no additives. Additives, such as bentonite, fly ash, and Pozmix, are often used to keep the cement particles suspended in the mix during setting; such additives tend to decrease the compressive strength of the set grout.

These initial tests show that waste solution and cement are compatible and will form a slurry which is pumpable. Ideally, one might require the mix to be of very low viscosity, for optimum pumpability; to remain pumpable only as long as neces-

sary to complete the operation, thereby minimizing the wait for cement to set up; and to start setting immediately after being pumped into the fracture, reducing settling of the suspended cement. However, for practical reasons, these ideal requirements must be modified and a compromise reached as to what will be expected in the way of viscosity, pumping time, and setting characteristics. For operating purposes, the viscosity of the mix was required to be less than 30 poises, and the usable pumping time was to be greater than 8 hr. No minimum compressive strength was imposed on the mix, since triaxial loading of the grout will not require support of the overburden by the grout sheet; the requirement that the slurry will set was imposed, however.

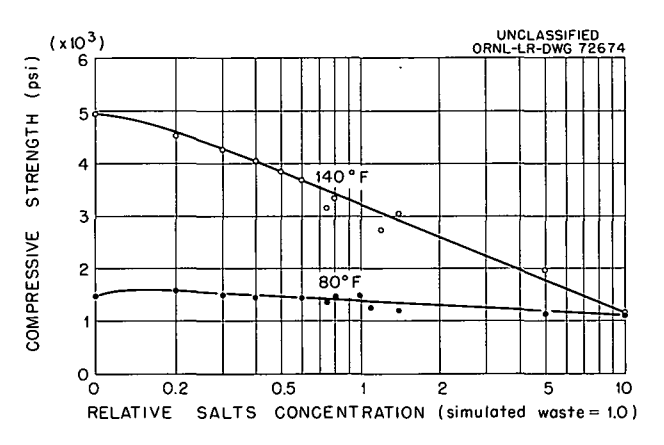


Fig. 1.2. Effect of Changing the Waste Salt Content on the Compressive Strength After 24-hr Curing at 80 and 140°F.

Preliminary Mixes Containing Additives. - Because waste composition can vary, concentrations of salts ten times the original concentration were also considered for testing purposes. It was also deemed desirable that the slurry retain as much of the fluid as possible. The fluid loss test defined by API measures the tendency of the slurry to dehydrate by filtration of the liquid through pores in the formation in contact with the grout. Results for two proprietary fluid loss additives, Cemad-1 and ET-181-6, are given in Table 1.3. The use of these additives is based on their ability to prevent dehydration of the slurry. A reduction in the fluid loss is observed as concentration of additives is increased. It is encouraging to note that, with concentrated wastes, very low fluid losses can be obtained.

Table 1.3. Effect of Fluid Loss Additives on Fluid Retention by Waste-Cement Slurries

Additive	Concentration	Slurry (cc of Wa	ste per lb of cement)	Fluid Loss	
Additive	of Additive (%)	Normal Waste	10 × Normal Waste	(cc/30 min)	(%)
ET-181-6	0	208		69 <sup>a</sup>	
	. 1.0	208		91	44
	1.3	208		51.3	25
	1.5	208		46.0	22
	1.3 .		268	113	42
	1.3 <sup>b</sup>		. 450	298	66
Cemad•1	1.0		268	65.7	24
	1.5		268	52	19
	1.5		298	64	21
	2.0		298	49	16
	3.0		298	37	12
	4.0		298	28	9.4
	5.0		298	20	6.7
	7.0		298	11	3.7

<sup>&</sup>lt;sup>a</sup>In 30 sec the slurry was dehydrated, and blowout occurred; the recorded volume is the actual volume lost during the 30 sec.

Numerous combinations of waste-cement additives were prepared, and various properties were measured, including fluid loss, thickening time, and compressive strength. The results from selected samples are shown in Table 1.4.

The addition of bentonite is based on the following considerations: (1) it allows more waste to be used per given weight of the more costly cement; (2) it retards the setting time of the mix; (3) it reduces the dehydration or fluid-loss characteristics of the mix; and (4) it helps to keep the cement particles in suspension. The lastnamed property is extremely important, since the long pumping time required will be favorable for settling of the cement particles. Settling, which can occur before the cement sets, not only results in a grout of uneven properties, but can cause bleeding or separation of liquid from the solid phase.

The calcium lignosulfonate (CLS) was added primarily as a dispersant and retarder. Note that a change from 0.7 to 1.0% CLS more than doubled

the thickening time when tested at 3000-ft bottomhole conditions (Table 1.4). The use of this agent is highly desirable, since a small amount will extend the pumping time to meet the requirements and will reduce the viscosity of suspensions with high solids content.

Calcium chloride is used to accelerate and control the setting time of a grout. When long pumpability times are required, it is desirable to control the setting time with CaCl<sub>2</sub>, as slight changes in conditions (i.e., lower temperature, excess CLS) may prevent setting for an extremely long time if CaCl<sub>2</sub> is omitted.

Although the short-term (24 hr) compressive strengths shown in Table 1.4 are low after a 24-hr curing period, it should be remembered that longer curing time will increase the strength. Initial set is important, since this is the changeover from the fluid state to the solid, and causes immobilization of the grout.

Studies conducted thus far have shown that waste solutions, cement, and additives normally

<sup>&</sup>lt;sup>b</sup>Plus 6% bentonite.

Table 1.4.	Fluid Loss, Thickening Time, and Compressive Strengths of Selected Mixes, All Containing
	332 cc of Waste per Ib of Cement and Containing 6% Bentonite

Cemad-1	Calcium Lignosulfonate (%)	CaCl <sub>2</sub> (%)	Fluid Loss (cc/30 min)	Thickening Time <sup>a</sup> (hr:min)		Compressive Strength
(%)				1000 ft	3000 ft	(psi after 24 hr)
1.0	0.7	0.5	59			
1.5	0.7	0.5	34			
2.0	0.7	0.5	13	10:25	6:35	76
2.0	0.7	0.5	13	10:25	6:35	76
2.0	0.9	0.5	35			i.s. <i>b</i>
2.0	1.0	0.5	22		15:00	i.s. <sup>c</sup>
2.0	0.7	0	39	8:35		22
2.0	0.7	0.5	13	10:25	6:35	76
2.0	0.7	1.0	16	8:40	4:40	80
2.0	0.7	3.0	9	3:55		142

<sup>&</sup>lt;sup>a</sup>Thickening time determined for 1000 and 3000 ft bottom-hole conditions.

used in the petroleum industry are compatible, and the slurry properties can be changed as well as controlled. One mix with promising characteristics is composed of the following materials:

454 g (1 lb) Volunteer type 1 Portland cement

332 cc Simulated waste

6% (27.2 g) Bentonite

2% (9.08 g) Cemad-1

0.7% (3.17 g) Calcium lignosulfonate

0.5% (2.27 g) Calcium chloride

This mix has been subjected to a larger number of tests than other mix formulations. The measured thickening time for this slurry composition is 10 hr and 25 min for bottom-hole conditions at 1000 ft. The slurry viscosity was 10 poises for 6½ hr and less than 30 poises for 8½ hr. After curing at 80°F for 24 hr, the mix had a compressive strength of 76 psi. A mix of very similar composition showed 80 psi after 24 hr and 1265 psi after 3 days, which suggests that the proposed mix will also have a much higher compressive strength after 3 days' curing.

After curing for 5 days at 80°F, the selected mix was divided into three sections, and the following values for specific gravity were obtained: top,

1.4807 g/cc; middle, 1.4969 g/cc; bottom, 1.5356 g/cc. The difference in specific gravities from the top to bottom sections is about 4%. In these tests bleeding was not observed. The measured fluid loss was 13 cc in 30 min, compared with 160 cc loss in a mix of similar composition but with no fluid-loss additive.

Further tests are being conducted, not only to verify these results and to evaluate the effect of changing waste composition on slurry properties, but to develop a mix which will have even better properties, particularly of reduced settling, and which will be cheaper to formulate.

#### DISPOSAL IN SALT FORMATIONS

W. J. Boegly, Jr. F. M. Empson R. L. Bradshaw H. Kubota<sup>7</sup> T. W. Hodge F. L. Parker

E. G. Struxness

Current philosophy on the disposal of aqueous high-level wastes (that is, solidification of liquid wastes into solids followed by storage in some dry location) has intensified the studies related

bi.s. = Initial set.

CInitial set observed after 1 days.

<sup>&</sup>lt;sup>7</sup>Member of Analytical Chemistry Division.

to storage of solid wastes in salt. Storage of solids will result in salt temperatures higher than those produced in previous liquid-waste studies. It is necessary to learn the effect on the salt formation of raising large volumes of salt to temperatures higher than 100°C and of raising small volumes of salt to temperatures higher than 200°C.

Mine disposal of solid wastes is now visualized as being performed by inserting the canned wastes into holes drilled in the mine floor. Thus, in the salt surrounding the holes high temperatures will be reached, and the effect of these temperatures on the creep and thermal expansion of salt and the possibility of localized shattering of the salt surrounding the holes must be investigated. The major emphasis during the past year has been on laboratory and field studies of these problems.

During the latter part of the year, a feasibility study on a demonstration of disposal operations in salt with radioactive heat sources was completed. This experiment would use 14 canned ETR fuel assemblies to simulate the solidified wastes in heat generation and radioactivity. The reason for using the fuel assemblies is that pilot production of solid wastes is not expected before 1965.

#### Thermal Studies

Arrays of Cylindrical Sources. — The infiniteslab calculation reported last year gives conservative estimates of mine space requirements for an evenly distributed heat source. However, if discrete sources are used, it is necessary to ascertain the temperature perturbations around the sources.

In the joint Health Physics-Chemical Technology economic study (see the section, "Evaluation of Engineering, Economics, and Hazards," this chapter), the waste packages to be disposed of are cylinders 6, 12, or 24 in. in diameter by 10 ft long.

As a part of this study an equation has been developed based on the following considerations: (1) With cylinders equally spaced on triangular centers, each will be in the middle of a hexagonal area which is peculiar to itself. (2) If there are a large number of cylinders, all containing identical heat sources and all placed in the mine simultaneously, it may be assumed that no heat flows across the vertical boundaries of the hexagonal area. (3) If the hexagonal boundary is approximated by a circle, the problem is reduced to that of a single finite-length cylindrical heat source in the center of an infinitely long cylinder whose sides are perfectly insulated. (4) For temperatures outside the heat-generating cylinder, an insignificant error is introduced if the heat source is assumed to be a line in the center of the cylinder.

An equation for the temperature rise in an infinitely long cylinder due to an instantaneous point source of heat is given by Carslaw and Jaeger<sup>9</sup>. This equation was integrated on the axial dimension to obtain an expression for an instantaneous line source. Since the fission product heat-generation rate is made up of decaying exponentials, the solution for the case of exponential heat-generation decay was obtained from the solution for the instantaneous line source by a superposition or convolution integral. The following equation for temperature rise in an infinite cylinder due to a finite line source resulted:

$$V = \sum_{i=1}^{m} \frac{Q_{i}}{\pi \rho c a^{2}} e^{-\lambda_{i} t} \left\{ \frac{1}{\lambda_{i}} \left[ e^{\lambda_{i} t} \operatorname{erf} \frac{b}{\sqrt{4\kappa t}} - 1 + e^{(\lambda_{i} t - b^{2}/4\kappa t)} \operatorname{Rw} \left( \sqrt{\lambda_{i} t} + \frac{ib}{\sqrt{4\kappa t}} \right) \right] + \sum_{n=1}^{\infty} \frac{J_{0}(\alpha_{n} r)}{(\lambda_{i} - \kappa \alpha_{n}^{2}) J_{0}^{2}(\alpha_{n} a)} \left[ e^{(\lambda_{i} - \kappa \alpha_{n}^{2})t} \operatorname{erf} \frac{b}{\sqrt{4\kappa t}} - 1 + \cosh \left( b \sqrt{\frac{|\lambda_{i} - \kappa \alpha_{n}^{2}|}{\kappa}} \right) + \frac{1}{2} e^{-b\sqrt{|\lambda_{i} - \kappa \alpha_{n}^{2}|/\kappa}} \operatorname{erf} \left( \sqrt{\frac{|\lambda_{i} - \kappa \alpha_{n}^{2}|}{\sqrt{4\kappa t}}} - \frac{b}{\sqrt{4\kappa t}} \right) - \frac{1}{2} e^{b\sqrt{|\lambda_{i} - \kappa \alpha_{n}^{2}|/\kappa}} \operatorname{erf} \left( \sqrt{\frac{|\lambda_{i} - \kappa \alpha_{n}^{2}|}{\sqrt{4\kappa t}}} \right) \right\}, \quad (1)$$

<sup>&</sup>lt;sup>8</sup>E. G. Struxness et al., Health Phys. Div. Ann. Progr. Rept. July 31, 1961, ORNL-3189, p 58.

<sup>9</sup> II. S. Carslaw and J. C. Jaeger, Conduction of Heat in Solids, 2d ed., p 378, Oxford Press, London, 1959.

where

V = temperature rise in infinite cylinder at a radial distance r from the center of the continuous line source, °F,

 $Q_i$  = heat generation of *i*th nuclide at time of burial of waste, Btu hr<sup>-1</sup> ft<sup>-1</sup>,

 $\rho c$  = volume heat capacity of medium, Btu  $ft^{-3} (^{\circ}F)^{-1}$ ,

a = radius of infinite cylinder, ft,

 $\lambda_i = \text{decay constant of } i \text{th nuclide, hr}^{-1}$ ,

t = time after burial of waste, hr,

2b = length of line source, ft,

 $\kappa$  = thermal diffusivity of medium, ft<sup>2</sup>/hr,

Rw() = real part of complex error function w(z), dimensionless,

 $i = \sqrt{-1}$ ,

 $a_n a = \text{positive roots} \cdot \text{of } J_1(\alpha a), \text{ excluding}$   $a_n = 0,$ 

r = radial distance from center of infinite cylinder, ft.

Equation (1) was programmed in FORTRAN code for the IBM 7090 computer, and space requirements for storage of pot calciner cylinders in the floor were calculated. The validity of the results was checked by comparison with isolated line source results for times short enough that no appreciable heat had penetrated to the insulated wall of the infinite cylinder, and with slab code results for times long enough that there was little radial temperature dependence in the infinite cylinder.

Thermal Properties of Salt. — Birch and Clark 10 have measured the temperature dependence of the conductivity and diffusivity of single natural halite (NaCl) crystals. Later, Schneider, Hughes, and Robertson, 11 with rock-salt aggregates from the Carey mine at Hutchinson, Kansas, obtained a conductivity curve of the same shape but showing about 25% greater conductivity than the Birch values.

The conductivity and diffusivity obtained in the field tests with cylindrical sources and with the  $7\frac{1}{2}$ -ft cubes  $^{12}$  were only 10 to 20% lower than those for the single crystal. In addition, laboratory tests at 28°C of both irradiated and unirradiated aggregate samples indicated approximately 25% lower conductivity than that of the single natural crystal.  $^{13}$  This relatively close agreement lends confidence to theoretical calculations of temperature rise based on single-crystal values.

Although both conductivity and diffusivity decrease rather sharply with increasing temperature, the theoretical equations developed to date assume constant thermal properties. To be conservative, the theoretical calculations must be made with values for the thermal properties at the highest temperatures which may be reached in a particular case. It has been felt that this may impose an unduly severe restriction, since only the salt in contact with the waste or waste container will ever reach this peak temperature, while salt at greater distances may be at much The results obtained with lower temperatures. the infinite-slab equation indicate that this need not be a concern for the slab geometry, since the peak temperature rise is not a strong function of the conductivity and diffusivity. For example, the peak temperature rise in the slab calculated with the 100°C salt conductivity and diffusivity was only 18% less than that calculated with the 300°C salt thermal properties, even though the conductivity was 70% greater and the diffusivity 90% greater than at 300°C. A similar relationship was found for most cases with the infinite array of line sources.

It has been found that unrestrained rock-salt aggregates shatter rather violently when heated to temperatures of 200 to 300°C, due to the presence of small quantities of water trapped in negative crystals. If this shattering occurs in salt in situ, it may result in poorer thermal conductivity and consequently increased waste temperature rise in the localized area near the heat source.

<sup>&</sup>lt;sup>10</sup>F. Birch and H. Clark, "The Thermal Conductivity of Rocks and Its Dependence on Temperature and Composition," Am. J. Sci. 238, 529-58, 1940.

<sup>11</sup>W. A. Schneider, H. Hughes, and E. C. Robertson, "Thermal Conductivity to 300°C of Natural Salt," Technical Letter: Special Project 2, U.S. Department of the Interior, Geological Survey, Washington, D.C., Apr. 20, 1962.

<sup>&</sup>lt;sup>12</sup>E. G. Struxness et al., Health Phys. Div. Ann. Progr. Rept. July 31, 1961, ORNL-3189, p 57.

<sup>&</sup>lt;sup>13</sup>Letter from F. Birch, Harvard University, to F. L. Parker, June 6, 1959.

#### **Plastic Flow Studies**

Field Studies. — In order to obtain field data on the effects of mine depth, percent salt extraction, and age of mine opening on the plastic flow occurring in existing salt mines, an expanded program of field measurements has been initiated. This information will be used to verify or implement theoretical calculations of room closure under various conditions of stress.

Eleven new stations have been installed during the past year (seven in the Hutchinson mine and four in the Lyons mine). In addition to these new stations, the existing station installed by ORNL and the two stations installed by the University of Texas in the Hutchinson mine will be used. All of the new stations installed in the Hutchinson mine consist of "Reidometer"-type gages, measuring floor movement, ceiling movement, or column movement, and extensometers, measuring the total movement between the floor and the ceiling.

Stations have been located in the Hutchinson mine to show: (1) for a constant percent salt extraction, the effect of mine age from 3 months to 9 yr (four stations); (2) for a different percent extraction, the effect of age from 10 to 14 yr (two stations); (3) for a room and panel mining method, the effect of ages from 30 to 39 yr (three stations); and (4) movement in an airway of 30-ft width adjacent to the high-temperature array (39-yr-old station). Figure 1.3 shows the approximate location of these stations in the Hutchinson mine.

Four stations were installed in the Lyons mine to measure flow in a mine at a greater depth (1000 ft vs 650 ft). Two of these stations are located in the last rooms mined prior to termination of the mining operation, in rooms which show no visual evidence of floor "buckling" or ceiling "sag." The purpose of these stations is to obtain information on flow at greater depths, both for comparison and as background information on the possible use of this area for tests with high-level solids. The other stations are located in an older section of the mine to measure flow in the floor and ceiling of rooms of the same dimensions. The basic difference between these stations is that the gages in the first room are attached between the salt roof and the salt floor, whereas the ends of the gages in the second room are installed in the shale and salt layers located about 1 ft above the ceiling and in the shale about

1 ft below the existing floor. It is hoped that data will be obtained to show that the relatively thin layers of salt above the roof and below the floor are moving, or being squeezed, at a faster rate than the overlying shales. This assumption is based on observations in other parts of the mine, in which the upper 1 ft of salt above the ceiling of the room has "sagged," and the relatively thin layer of salt above the shale parting in the floor has "buckled" due to the pressure transmitted to the salt by the pillars. Not enough measurements have yet been made to predict the rate of movement or expected maximum closure, but the few measurements made thus far indicate that the amount and rate of deformation are much less than those observed in Hutchinson; however, it is a much older mine, and the flow would be expected to be very small.

Cumulative Gamma-Radiation Dose in Salt-Mine Disposal of Pot-Calcined Solid Wastes. — Previous studies  $^{14}$  on the effect of gamma radiation on the structural properties of rock salt have shown that gamma dosages to  $1\times10^8$  r produce negligible changes in creep rate and compressive strength, but that dosages above this value may produce significant changes (decrease in compressive strength, slight decrease in creep rate). Since the salt in rooms containing radioactive waste will be exposed to radiation for long periods of time, it is possible that the  $1\times10^8$  r dose will be exceeded at the surface of the walls.

The MIT Engineering Practice School developed a computer program for the IBM 7090 and with it estimated the gamma dose in salt and in the room for pot-calcined solids stored in the floor of a salt mine. <sup>15</sup> The variables in the computer program are: room height and width, depth of pot burial, rectangular pot spacing, pot diameter, number of energy groups considered, activity vs time for each energy group, properties of the material, and distance of the first row of pots from the wall. The output from the program gives: (1) the gamma dose in salt for each energy level per time increment and sum of increments, (2) the accumulated gamma dose in salt for each energy level at each time increment, and (3) the sum of

<sup>&</sup>lt;sup>14</sup>B. D. Gunter and F. L. Parker, The Physical Properties of Rock Salt as Influenced by Gamma Rays, ORNL-3027 (Mar. 6, 1961).

<sup>&</sup>lt;sup>15</sup>M. H. Cornillaud, E. P. Demetri, and R. A. Loring, Waste Disposal in Salt Mines: Computer Code for the Determination of Dose, KT-581 (Nov. 8, 1961).

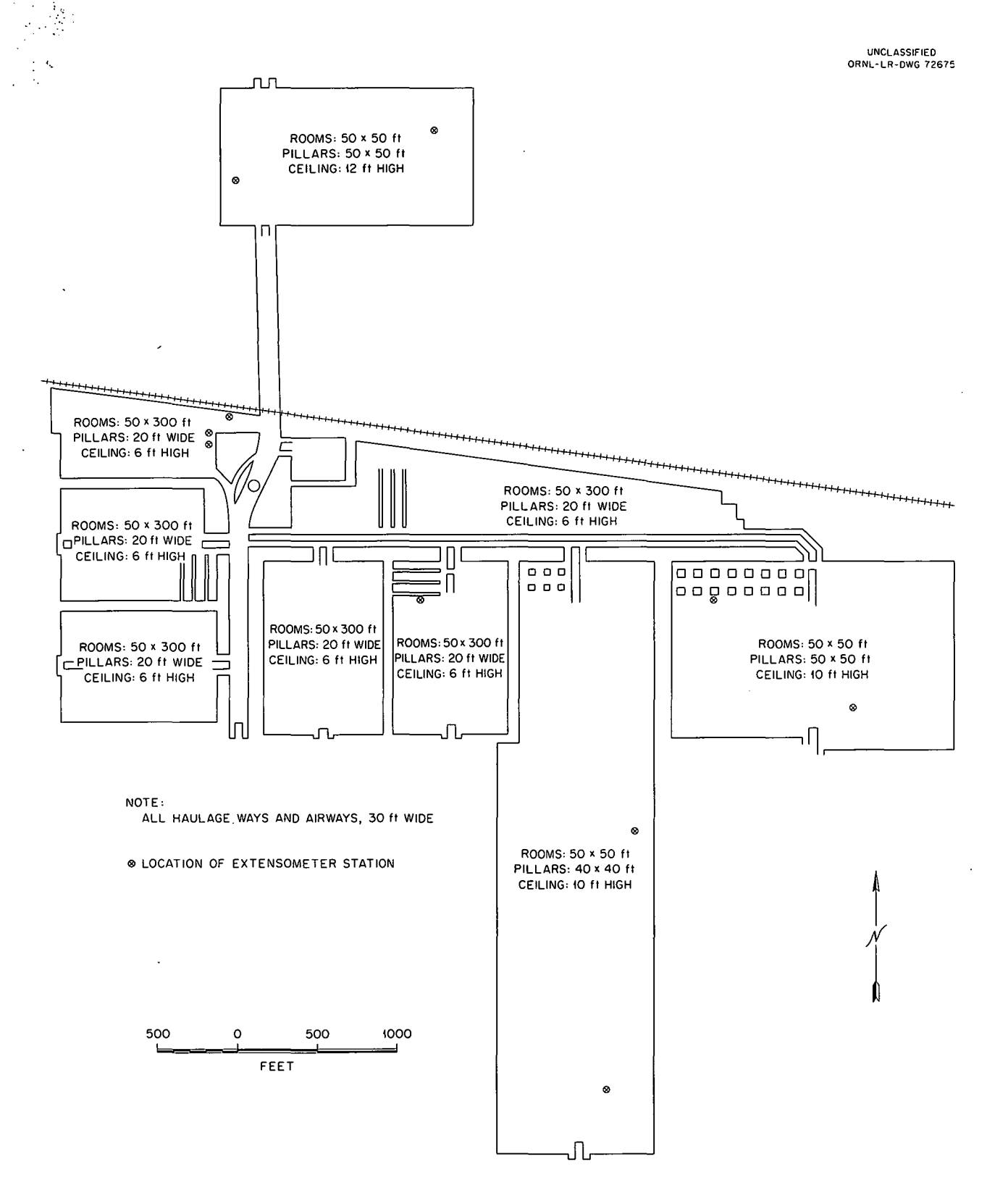


Fig. 1.3. Plan of Hutchinson Mine, Showing Locations of Plastic Flow Stations.

these or the total accumulated gamma dose from time of storage to time t. For the air dose in the room above the buried pots, the dose rate in milliroentgens per hour can be obtained at any desired time.

Limitations of the computer program as written are that the pot spacing must be rectangular in plan view, that the dose cannot be calculated for gamma rays passing through more than two media, and, finally, that the pots are considered as line sources and the dose close to the pots cannot be computed accurately. However, for the purpose intended, the results are satisfactory.

As an example, calcined acidic Purex waste in 6-in.-diam pots buried 7 ft beneath the floor of a 15-ft-high, 50-ft-wide, very long room was considered. The pot spacing was assumed to be 5 ft. Figure 1.4 shows the variation of total dose (for storage times from 2 to 10<sup>6</sup> yr) with distance from the wall for points on the ceiling and floor of the room, and points between the pots. Results indicate that the gamma dose in the ceiling is less than that in the floor, and that the dose between pots is nearly constant across the room. The only sources that contribute significantly to the dose at a point are the two pots on either side of it. Figure 1.5 shows the variation of the total gamma dose between pots as a function of wastecooling time. If cooling time before storage is increased from 2 to 14 yr, the dose is reduced more than half.

Results of this study indicate that gamma dose at the center line between pots will not exceed  $3 \times 10^6$  rad for 2-yr-cooled waste and thus that the irradiation of the bulk of the salt surrounding the room will not exceed the dose at which structural damage will occur. In local areas near the pots the dose may exceed  $1 \times 10^8$  r; however, the volume of salt will be small and the corresponding effect of a decrease in compressive strength will also be small. These calculations are being extended to cover spacings of cans that are not rectangular and the effect of cylindrical vs line sources. When the extent of salt having a dose greater than  $1 \times 10^8$  r is known, calculations will be made on the effect of this factor on the structural integrity of the room.

Effect of Salt Extraction and Depth on Stability of Mine Openings. — In order to conceptually design a disposal operation in salt, it is necessary

to be able to predict the allowable percent salt extraction as a function of depth for various conditions of structural stability. Until equations have been developed to express these relationships, it is desirable to attempt to relate observed conditions to percent extraction and depth and develop an empirical approach to this problem. This is shown in Fig. 1.6 as a function of the calculated pillar load, assuming 1 psi per foot of overburden. The boundaries of the various conditions of stability in the figure are derived from observations reported on mine conditions. By use of these boundaries, the desired relationships between depth of the mine, percent salt extraction, and stability conditions have been calculated. For example, if a negligible amount of structural flow can be tolerated, then the maximum allowable pillar load is 2000 psi, and operation to the left of curve A of Fig. 1.6 must be maintained. On the other hand, if some spalling and a few percent closure of the rooms can be tolerated, then the pillar load can be increased to 3000 psi, and operation can be anywhere to the left of curve C. In the first case (negligible flow) it may be seen from Fig. 1.6 that the stability criterion cannot be met at depths greater than 2000 ft. It may also be seen that any extraction of salt at depths greater than 3500 ft will produce large structural flows.

The time factor involved in structural flow has not been included in this study, and it may take several years for such things as roof falls and floor heaves to occur. In general, the greater the pillar load, the faster the flow occurs. In Germany some mines are operated with pillar loads much greater than those in this country, and the rooms are either allowed to collapse or backfilled soon after excavation to prevent collapse.

#### Thermal Stability of Rock Salt

In order to determine the effect of temperature on salt, 1- to 2-lb salt samples have been heated to elevated temperatures. Salt samples removed from the mine are not comparable to salt in place, because the stresses are altered on mining. However, the results of the laboratory study are expected to give an insight into the possible phenomena that might be expected in actual disposal operations.

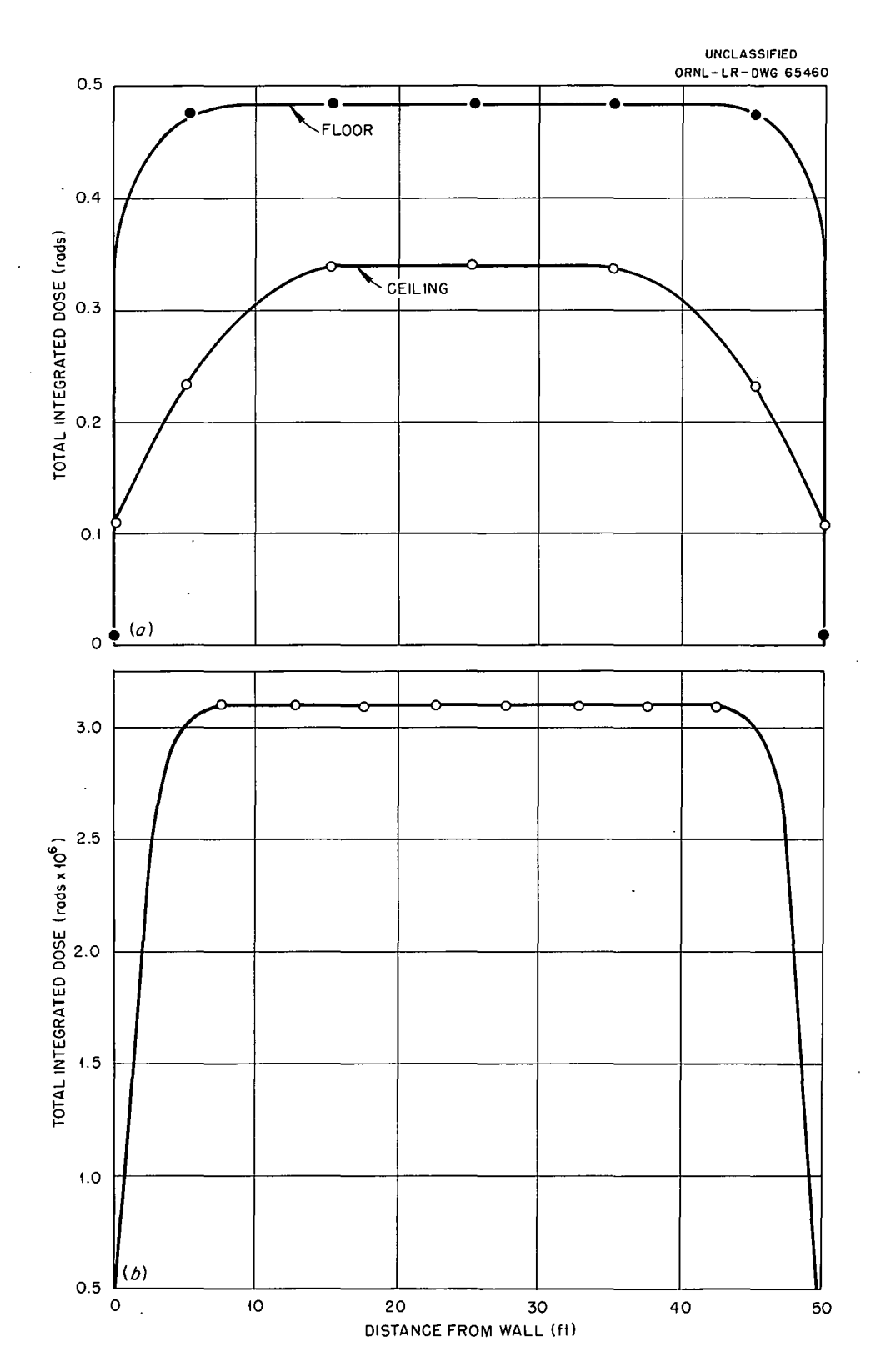


Fig. 1.4. Gamma Dose (a) to Ceiling and Floor and (b) in Floor Between Pots, as a Function of Distance from Wall.

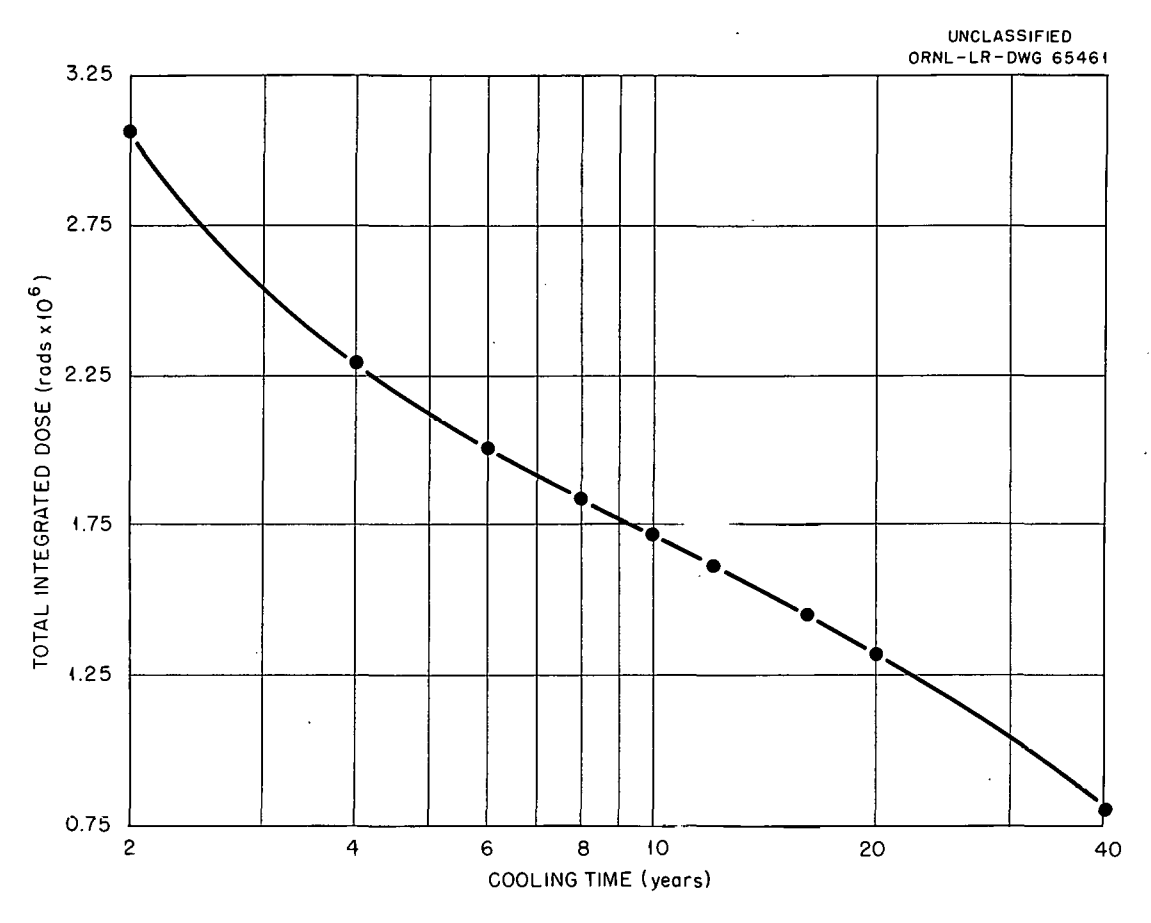


Fig. 1.5. Gamma Dose Between Pots as a Function of Cooling Time.

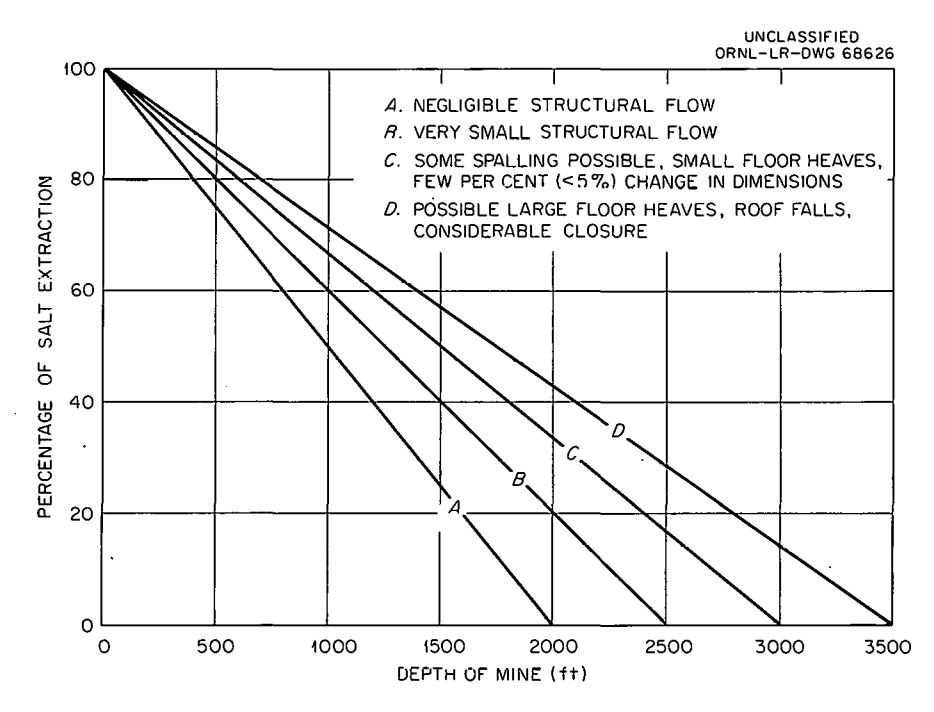


Fig. 1.6. Effect of Percent Salt Extraction and Depth on Structural Stability of a Mine Opening.

Salt from the Hutchinson mine was used in the initial study. It was found that the salt mass fractured with considerable violence when heated to about 250 to 280°C. The explosion was violent enough to lift the door of the muffle furnace, as well as to rupture the wire basket which was used to contain the sample. Each explosion was associated with the release of a cloud of steam, and took place in about the same temperature range regardless of the rate of heating.

Quantitative measurement of the amount of water released and more detailed observations of the effect of temperature on the salt are being carried out by heating the salt in a "bomb." The moisture released is swept into a tared absorption bottle and weighed. Heating is terminated at 350°C, since the glass equipment begins to soften above that temperature.

When the salt is heated, there is initially a large disintegration at a temperature above 200°C, followed by lesser events at random temperature increases up to the upper limit of heating. Nearly all of the water is released during the initial large fracture, and all is released before the temperature exceeds 300°C. The heating process reduces the original salt mass into particles which vary in size from fine powder to centimeter-size crystals.

The results thus far are shown in Table 1.5. There is a significant difference in the disintegration temperature between the samples from the Hutchinson and Lyons mines. The sample showing the greatest moisture content was a clear crystal from the Hutchinson mine containing several visible inclusions of water. The variation in the water content is apparently due to the random distribution and size of these inclusions throughout the salt. There is, however, a significant difference in the range of moisture yields from the two locales. Salt samples from mines in other parts of the country will be tested in a similar manner for comparative purposes.

Three possible mechanisms for the fracturing have been advanced: (1) unequal thermal expansion along the crystal axis, (2) chemical reactions such as the combustion of organics, and (3) the pressure effects of superheated steam. The salt from a given site "explodes" at nearly the same temperature regardless of the rate of heating. Even a very slow rate of heating, which could have the effect of annealing some of the strains in the crystals, does not alter the temperature at

which the first disintegration occurs. Analysis of the gas produced shows a trace of carbon dioxide which is of a magnitude far below that which would be produced by a reaction capable of causing the observed phenomenon. The vapor pressure of water rises sharply from 1 atm at 100°C to 15 atm at 200°C, 38 atm at 250°C, and 84 atm at 300°C. These considerations, along with the observed release of steam, lead to the conclusion that the greatest single cause of the disintegration process is the pressure of the heated water. It seems likely that unequal expansion or similar thermal effects are responsible for the minor splittings observed at temperatures over 300℃.

Table 1.5. Thermal Analysis of Salt from the Hutchinson and Lyons Mines

Source	Weight of Sample (g)	Disintegrating Temperature (°C)	Water Released <sup>©</sup> (%)
Hutchinson	702	245	0.127
	763	245	0.182
	467	220	0.293
	530	265	0.150
a	153		1.08
Lyons	1327	215	0.090
٠	667	220	0.048
	714	215	0.100
	- 709	. 215	0.082

aClear crystal.

Another problem to be considered is the combined effect of temperature and gamma radiation on the salt. Previous tests have shown that the radiolytic process in a confined saturated salt solution will attain a steady-state pressure of about 10 atm, a pressure that is well within the limits of stability of the salt. The effect of temperature upon the radiolytic steady-state pressure is not known, and tests are planned to determine what effects the combined forces of temperature and radiation have upon salt stability.

#### **High-Temperature Experiments**

A large-diameter electric heat source to investigate the physical changes of salt in situ due to temperatures greater than 80°C has been run (experiment I). Power was applied to the heater at a rate of 3 kw for 70 hr before inspection of the interior of the hole. At that time water (or brine) and recrystallized salt had filled the annulus to about 6 in. below the top of the heater. After 84 hr the annulus was completely filled with salt, and the experiment was terminated.

The highest salt temperature measured was 127°C (106°C rise) at 9.6 in. from the center of the heater (Fig. 1.7). The maximum salt temperature (4 in. from the heater center) is estimated from the computed curves of Fig. 1.7 to be approximately 200°C. These are theoretical curves with thermal conductivity and diffusivity adjusted so that the 9.2-in. curve coincides with the experimental points for a temperature rise from 50 to 105°C. This procedure gives a thermal conductivity of 2.7 Btu hr<sup>-1</sup> ft<sup>-1</sup> (°F)<sup>-1</sup> (single

crystal value for 70°C) and a diffusivity of 0.08 ft<sup>2</sup>/hr (130°C value).

It was thought that the water which had caused the termination of experiment I had entered the formation due to the use of brine as drilling fluid in preparation for the experiment. It was, therefore, decided that additional tests should be carried out in a different area of the mine with air as the drilling fluid. Subsequent examination of shale samples from holes drilled with air revealed that the shale contained approximately 10% moisture, which could have been evaporated from the shale and condensed in the hole to supply the moisture found.

Experiment II is in the floor of the mine, and experiment III in the wall of the column east of the previous experiments. Operation of these tests will differ from experiment I in that higher power inputs will be used, so that the peak temperature can be increased from about 200 to 300°C. In addition, instrumentation is provided for measuring floor rise around the heater in the floor and column expansion about the wall installation,

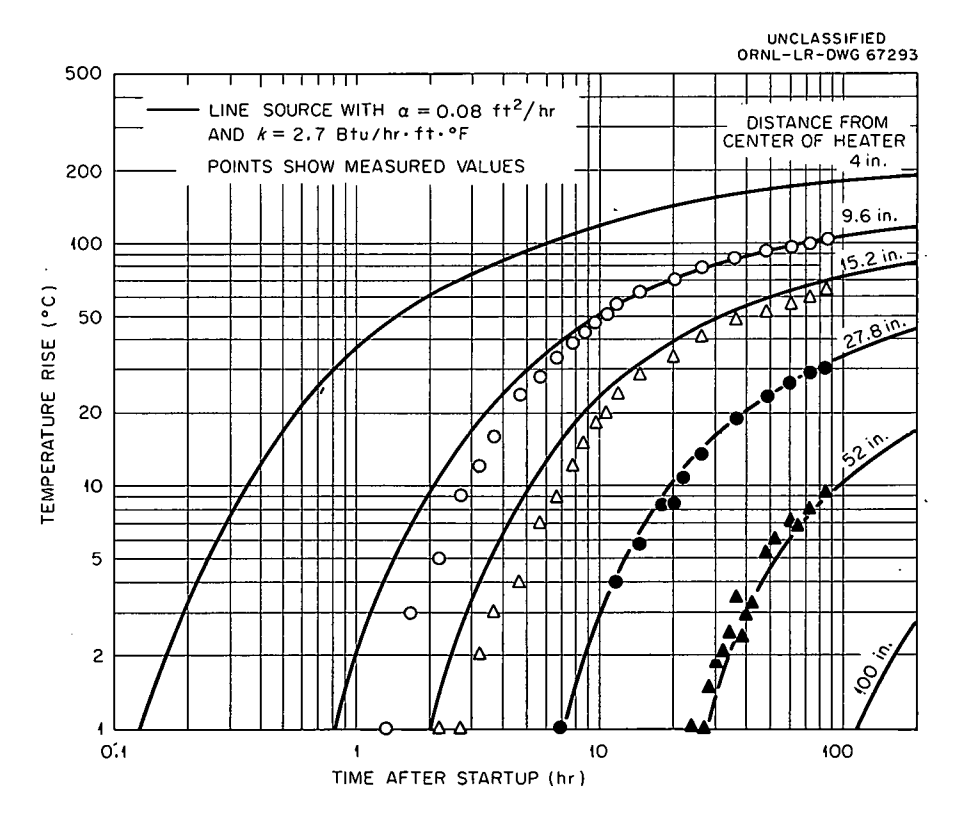


Fig. 1.7. Comparison of Temperature Rise in High-Temperature Cylinder Test I with Theoretical for Line Source. Heater was  $6\frac{5}{8}$  in. diam by 4 ft; power input 3100 w.

and a vapor purge system will be installed in the hole to remove any moisture from the shales.

### Direct Liquid Disposal in Crushed Salt

The major problem in the direct disposal of high-level liquid radioactive waste is the off-gas which results from radiolytic decomposition of water and of water vapor. It has been found that if liquid waste is dispersed through crushed rock salt, the radioactivity will be present in a film of liquid on the surface of the granules, and radiolysis will be reduced. The mine area required to store the wastes from a given weight of fuel is the same regardless of the volume and is a function of the total heat-radiating property of the solution. It can be shown that if a salt mine were being excavated for the purpose of waste storage, it would be economically advantageous to stow at least part of the salt extracted into another excavation.

By assuming a waste volume of 60 gal/ton, which has a cooling time (approximately 3 yr) that requires 200 ft<sup>2</sup> of mine area for adequate heat removal, the liquid depth per square foot would be 0.5 in. If this solution is poured over 6 ft of crushed salt, most of the liquid will be retained as a surface film on salt particles, and very little free solution will be found.

Laboratory studies with gamma radiation from Co<sup>60</sup> indicate that the water in such a system, when subjected to temperatures about 60°C or more above ambient, tends to be moved upward, eventually collecting as a layer of liquid water on top of the salt. Very little pressure buildup associated with radiolytic gas production is observed until the free liquid layer begins to form, at which point there is a pronounced increase in the rate of buildup. This pressure buildup can be inhibited by absorbing the water layer that is formed on an absorbent material like vermiculite.

#### **CLINCH RIVER STUDIES**

P. H. Carrigan 16	R. J. Morton
B. J. Frederick 16	F. L. Parker
R. J. Pickering <sup>16</sup>	E. G. Struxness
W. E. Parker <sup>17</sup>	
· - · · · · · · · · · · · · · · · · · ·	T. Tamura
B. P. Glass <sup>17</sup>	E. E. Eastwood
S. H	lelf <sup>18</sup>

The Clinch River Studies have been continued in cooperation with the U.S. Atomic Energy Commission, the U.S. Public Health Service, the U.S. Geological Survey, the Tennessee Valley Authority, the Tennessee Game and Fish Commission, and the Tennessee Stream Pollution Control Board. In these studies the fate of radioactive releases to the river, the diluting capacity of the river system, and the long-term effects of radioactive contamination on the fluvial environment are being investigated.

The Clinch River Study Steering Committee held meetings on October 26 and 27, 1961, and on April 25 and 26, 1962. During these meetings progress on the Studies has been reported, future plans discussed, and reports issued. 19-21 Subcommittees (of the Steering Committee) on Water Sampling and Analyses, Bottom Sediments, Aquatic Biology, and Safety Evaluation have been appointed and are guiding work in specific fields of the Studies.

#### Hydrology

**Dilution Factors.** – For the period October 1, 1950, to September 30, 1960, the dilution by flows in the Clinch River of releases from White Oak Creek has been computed. <sup>21</sup> Based on the mean annual discharges observed in the Clinch River and White Oak Creek, the mean annual dilution factor is about 450, and the median daily dilution factor is 570. The range in extremes of the daily dilution factor is from 5.1 to 4330.

Minimum dilution factors for periods of 1, 7, 15, and 30 days have been determined for recurrence intervals of 1 to 11 yr. Results of this frequency study indicate that the minimum 30-day dilution factor is 78 for a recurrence interval of 10 yr, or that once in 10 yr the average dilution factor for an entire month will be only 78.

**Dispersion Tests.** – Dispersion tests with Au<sup>198</sup> were conducted on August 30–31, 1961,<sup>21</sup> and February 1, 1962. The tracer was injected at

<sup>16</sup> U.S. Geological Survey.

<sup>&</sup>lt;sup>17</sup>Temporary summer employee.

<sup>&</sup>lt;sup>18</sup>U.S. Army, Picatinny Arsenal.

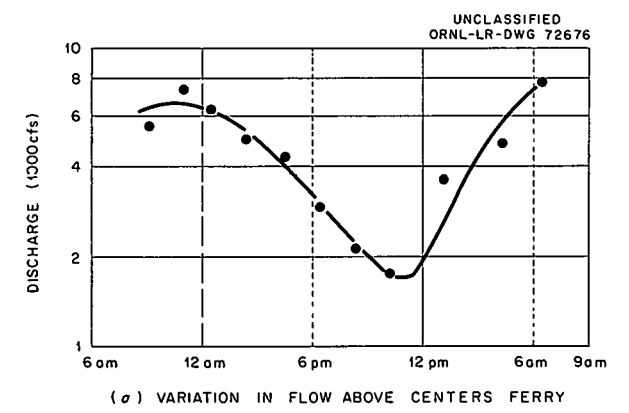
<sup>&</sup>lt;sup>19</sup>R. J. Morton (ed.), Status Report No. 1 on Clinch River Study, ORNL-3119 (July 27, 1961).

<sup>&</sup>lt;sup>20</sup>R. J. Morton (ed.), Status Report No. 2 on Clinch River Study, ORNL-3202 (Mar. 30, 1962).

<sup>&</sup>lt;sup>21</sup>R. J. Morton (ed.), Status Report No. 3 on Clinch River Study (in press).

the mouth of White Oak Creek. Time for the tracer to reach the Oak Ridge Gaseous Diffusion Plant, 6.3 miles downstream, and the mouth of the Emory River, 16.3 miles downstream, were 8 and 31 hr for a flow of 8000 cfs in the Clinch River and 2.8 and 9.3 hr for a flow of 20,000 cfs. The time of travel of water in the study reach which has been measured in these tests has verified computations of the time of travel by TVA. These tests also indicated that water discharged from White Oak Creek is dispersed uniformly across the river channel within 4 to 6 miles downstream.

During a 24-hr period on August 17-19, 1961, when the release of radioactivity from White Oak Creek was relatively constant, the variations in radionuclide concentration and in flow in the Clinch River with time were observed at the water quality station above Centers Ferry. The variation in flow of the Clinch River was the result of hydroelectric operations at Norris Dam. As shown in Fig. 1.8, the variation in radionuclide concentration was negligible in comparison with the variation in flow.



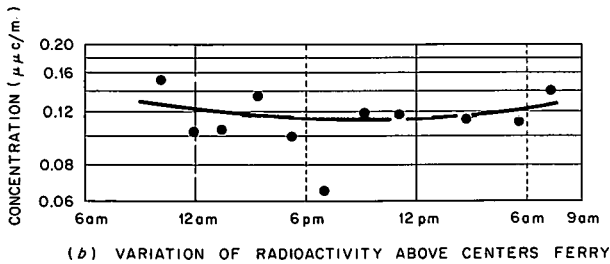


Fig. 1.8. Effect of Power Releases from Norris Lake on Flow and Radioactivity in Clinch River above Centers Ferry, near Kingston, Tennessee.

Melton Hill Dam Construction. — The diversion canal around the Melton Hill Dam site closed about July 31, 1962. Water is now flowing over the spillway. The first generating unit is scheduled to begin operation in July, 1963, and due to its operation as a peak load plant, changes in the river regime will occur.

#### **Water Sampling and Analysis**

Sampling Stations. - The network of water sampling stations was described in the 1961 Annual Progress Report. 22 Locations of these stations are shown in Fig. 1.9. Water samples from the stations during the past year have been analyzed for concentrations of suspended sediments, stable chemical constituents, and long-lived radioactive constituents. Weekly and monthly composites which are proportional to the flow are prepared. Samples are shipped to the U.S. Public Health Service for radiochemical analyses and to the Tennessee Stream Pollution Control Board for stable chemical analyses of major constituents. The network was established on November 1, 1960. Prior to February, 1962, the composite of samples collected at the water plant of ORGDP was not proportional to the flow.

Stable Chemical Analyses. - A summary of the results of stable chemical analyses is given in Table 1.6. The data indicates that the river water is of intermediate hardness and of low organic content.

Radiochemical Analyses. — Radionuclide loads passing the water sampling stations at the Oak Ridge Water Plant, at White Oak Dam, and above Centers Ferry have been computed for the first half of 1961 by use of analyses reported by Morton. The radionuclide load is the product of radionuclide concentration, streamflow, and time interval, and represents the quantity of radionuclide passing the sampling point during the stated period. The loads passing the stations at the water plant and at the dam have been combined and compared with the load passing the station above Centers Ferry.

Results indicate that essentially no Ru<sup>106</sup> and only a small amount of Sr<sup>90</sup> were lost from the river water between the mouth of White Oak Creek and the Centers Ferry sampling station. Because

<sup>&</sup>lt;sup>22</sup>K. Z. Morgan et al., Health Phys. Div. Ann. Progr. Rept. July 31, 1961, ORNL-3189.

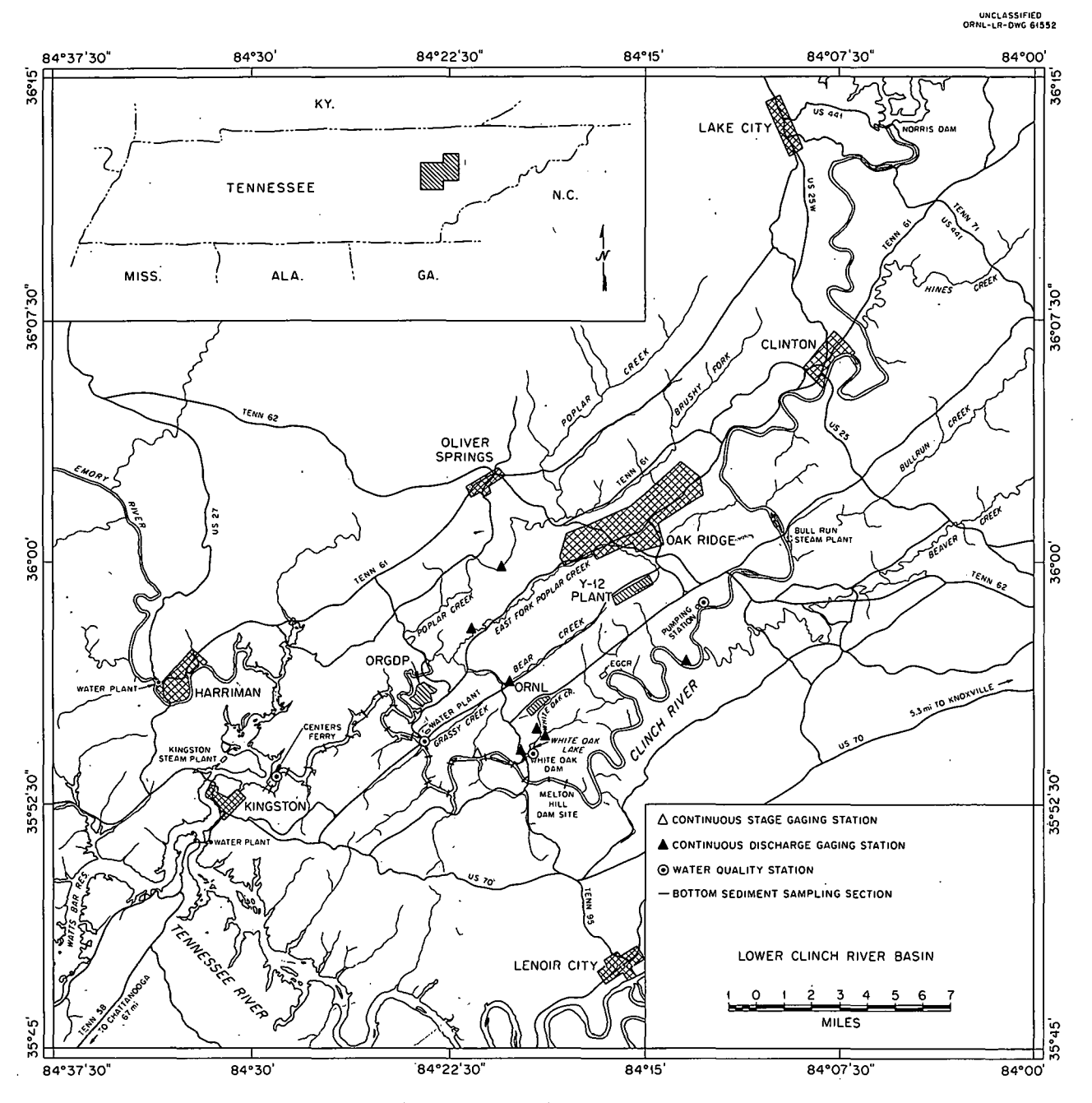


Fig. 1.9. Map of Clinch River Basin, Showing Locations of Sampling Stations.

of very low sample concentrations, analytical results indicate only that losses of Co<sup>60</sup> and Co<sup>137</sup> may occur, and the exact loss cannot be computed at this time. Further investigations of the material balances for these latter two nuclides are being undertaken.

#### **Bottom Sediment Studies**

Core Samplers. — Results of work in 1960<sup>20</sup> have indicated that deeper penetration of the bottom sediments by a core sampler is necessary. Many core samplers have been tested for penetration

Table 1.6a. Summary of Stable-Chemical Analyses of Water Samples from ORGDP Water Plant, CRM 14.5, Weekly Analyses

		Concentrat	tion (ppm) <sup>a</sup>	
Constituent	Average	Standard Deviation	Maximum	Minimum
	Nov. 2,	1960, to Sept. 10, 196	1	
Ca	21.3	3.0	30	17
Mg	6.97	2.33	10	<2.0
Na	2.46	0.54	4.7	1.8
K	1.37	0.15	2.3	1.1
NO <sub>3</sub>	6.01		40	0.59
Suspended solids	23.5	19.9	104	0.75
Total solids	154	23	231	127
Loss on ignition	28.7	18.0	. 95	10.5
	Nov. 28	, 1960, to Sept. 10, 196	51	
CI	1.65	0.54	4.51	1.1
SO <sub>4</sub>	10.9	4.5	27	0.8
PO <sub>4</sub>	0.238	0.174	<1	< 0.003
нсо <sub>3</sub>	112	12	134	87
рН	7.67	0.35	8.4	6.5
Conductivity	215	14	282	190
	Feb. 6,	1961, to Sept. 10, 196		
Cs	<0.01			
Sr	0.068	0.0094	0.08	0.04
Со	<0.02			
Ru	< 0.1	•		

<sup>&</sup>lt;sup>a</sup>Conductivity is in μmho/cm; pH is dimensionless.

capabilities, compaction effects on samples, and retention of sample during recovery. No single device was found to be satisfactory throughout the study reach. In material finer than gravel, the best sampling device for long cores has proved to be the "Swedish foil sampler." For short sample runs in very flocculent material, some samples can be obtained by using a split-spoon sampler with a flap valve or a basket shoe with collapsible Mylar flap. For sampling sand, the TVA volumetric silt sampler is useful. An oceanographic-type piston core sampler with a basket

shoe has proved satisfactory for sampling fine sediment up to 5-ft thick. In material coarser than gravel, core samples cannot be obtained and small clamshell dredges appear to be the only recourse.

Determination of Radioactivity in Sediments. — From measurements of radioactivity in core samples collected in the study reach during 1962, the depth of the radioactive zone is being determined, the variation of fission product concentration with depth of sediment is being described, and the total fission product activity is being computed. The study reach extends from the

vicinity of White Oak Creek to the mouth of the Clinch River. Core sampling by Sprague and Henwood, Inc., Scranton, Pennsylvania, was begun on June 25, 1962. Seventeen sections in the reach, selected on the bases of core sampling

Table 1.6b. Summary of Stable-Chemical Analyses of Water Samples from ORGDP Water Plant,
CRM 14.5, Triweekly Analyses

Constituent	Cond	entration (ppr	n)
Constituent	Average	Maximum	Minimum
Fe	b. 6, 1961, to S	Sept. 10, 1961	
Cu	0.028	0.10	<0.01
Rb	< 0.005		
NH <sub>4</sub>		. 1	0.02
Zn	0.139 <sup>a</sup>	19	0.059
Ba	0.3-<0.05		
Al	0.117	0.34	0.01
Fe	0.081	0.37	0.003
Mn	0.01		
Si	1.73	2.4	0.24
Τί	0.030	0.06	0.01
Zr	0.032	0.06	0.01
· Ni	0.01		
F	0.20	0.33	0.05

<sup>&</sup>lt;sup>a</sup>Maximum observed concentration is questionable and was not included in computing the average of nine observations.

done in 1960; measurements of sediment deposition by TVA, and gamma counting of sediments in situ, are being cored. In addition, cores are being obtained in two sections of the Emory River and two sections of Poplar Creek.

Physico-Chemical Characteristics of Bottom Sediments in Clinch River. - Surveys of radioactivity in the bottom sediments have indicated that the highest levels of activity occur at the mouth of and about 9 miles below White Oak Core samples of fine sediments which were obtained at five sections in the study reach during 1961 were analyzed to determine particlesize distribution, mineral content, and exchange Core samples which were collected capacity. at more closely spaced sections were analyzed to determine sorption capacity. These analyses were undertaken to ascertain whether the level of radioactivity in the sediments was influenced by some bulk physico-chemical characteristic.

The sediments are a well-graded silty loam with fairly constant clay content. The minimum median particle size of 20  $\mu$  was found at a section 8.9 miles downstream from White Oak Creek. The sand and silt fractions of the sediment were almost entirely quartz. The mineral content of the clay fraction is given in Table 1.7.

The determined exchange capacity for the five composited sections was relatively constant,  $11.3 \pm 0.2 \text{ meq}/100 \text{ g}$ . In all cases the determined exchange capacity was exceeded by the exchangeable cation concentration,  $22.0 \pm 3.7 \text{ meq}/100 \text{ g}$ .

In demineralized water the mean strontium sorption was  $(49.3 \pm 1.7)\%$  for all samples analyzed. In Oak Ridge tap water, obtained from the Clinch

Table 1.7. Mineral Contents (Parts per Ten) of Clay-Size Particles of Clinch River Bottom Sediment<sup>a</sup>

Clinch River Mile	Quartz	Vermiculite	Mica	Kaolinite	Randomly Interstratified Vermiculite-Mica
4.7	4	. 2	2	1	1
7.6	3	2 .	2	2	1
11.9	3	2	2	2	1
15.3	4	2	1	2	. 1
19.2	. 4	. 2	1	2	1

<sup>&</sup>lt;sup>a</sup>Mineral analyses by U.S. Geological Survey.

Table 1.8. Strontium Sorption by Clinch River Sediments

											•	Clinch R	iver Mile							<u>.</u>			
Time			4.7	5	.8	6	5.9		8.0	9	.0	1	0.0	1	1.0		12.0	1	3.0	1	4.6	1	16.0
(hr)		Тар	Demin.a	Tap	Demin.	Тар	Demin.	Тар	Demin.	Тар	Demin.	Тар	Demin.	Тар	Demin.	Tap	Demin.	Тар	Demin.	Тар	Demin.	Тар	Demin.
1 .	%	3.39	39.46	3.65	57.67	2.24	54.10	4.55	42.10	3.63	48.23	2.90	45.24	4.75	39.20	4.22	35.27	3.49	52.97	2.64	45.28	4.72	36.07
	$K_{d}$	70	1300	76	2700	47	2400	95	1500	75	1900	60	880	100	1300	88	1100	72	2300	54	1700	99	1100
	рH	7.29	7.37	7.75	7.65	7.15	7.16	7.32	7.45	7.17	7.21	7.12	7.21	7.82	8.05	7.38	7.52	7.81	7.74	7.15	7.19	7.39	7.44
4	%	1.98	41.89	6.02	60.74	2.88	50.92	3.92	44.41	4.66	47.05	3.56	45.45	5.93	37.20	2.22	38.12	6.68	54.28	3.09	46.63	3.15	45.52
	$K_{d}$	40	1400	130	3100	59	2100	82	1600	98	1800	74	1700	125	1200	45	1200	145	2400	64	1700	65	1700
٠	pН	7.39	7.50	7.82	7.61	7.30	7.40	7.48	7.49	7.38	7.45	7.35	7.42	7.81	8.20	7.50	7.50	7.90	7.72	7.34	7.40	7.50	7.50
24	%	3.38	44.30	5.73	62.52	3.06	51.69	5.43	46.30	3.83	48.41	3.57	46.57	4.72	37.85	4.85	43.10	6.71	57.22	3.00	50.29	4.89	49.40
	Kd	70	1600	120	3300	63	2100	115	1700	80	1900	74	1700	99	1200	100	1500	145	2700	62	2000	105	2000
	pН	7.61	7.51	7.59	7.55	7.51	7.45	7.69	7.52	7.51	7.48	7.61	7.43	7.64	8.25	7.78	7.69	7.55	7.69	7.59	7.55	7.78	7.65
168	%	3.52	44.66	5.93 <sup>b</sup>	57.14 <sup>b</sup>	4.86 <sup>c</sup>	50.19 <sup>c</sup>	4.93	52.49	4.74 <sup>c</sup>	49.17 <sup>c</sup>	4.53 <sup>c</sup>	46.28 <sup>c</sup>	5.22 <sup>b</sup>	36.91 <sup>b</sup>	5.10	46.60	7.14 <sup>b</sup>	53.20 <sup>b</sup>	4.79 <sup>c</sup>	54.31 <sup>c</sup>	5.00	50.92
	$K_d$	73	1600	125	2700	100	2000	105	2200	100	1900	95	1700	110	1200	105	1700	155	2300	100	2400	105	2100
	pН	7.79	7.82	8.20	7.69	8.01	7.55	7.63	7.89	7.81	7.80	8.10	7.58	8.15	7.90	7.91	7.91	8.11	7.75	7.69	7.81	8.18	7.80

<sup>&</sup>lt;sup>a</sup>Demineralized.

<sup>b</sup>Time, 192 hr.

<sup>c</sup>Time, 216 hr.

Table 1.9. Cesium Sorption by Clinch River Sediments

Tap water:  $X = (93.10 \pm 1.94)\%$ 

Demineralized water:  $X = (97.58 \pm 0.25)\%$ 

											Clinch Riv	er Mile											
Time (hr)			4.7	5.	8	6	.9	8.0	0	9	.0	10	0.0	1	1.0	1	2.0	13.	0	1	4.6	10	6.0
(,		Тар	Demin.a	Тар	Demin.	Tap	Demin.	Tap	Demin.	Тар	Demin.	Tap	Demin.	Тар	Demin.	Tap	Demin.	Тар	Demin.	Тар	Demin.	Тар	Demin.
1	%	59.24	82.59	72.03	89.82	64.61	90.13	67.16	8 9.17	59.58	88.55	54.57	43.42	62.36	88.50	55.30	83.00	72.98	88.02	54.94	85.95	46.90	72.09
	$K_{d}$	2900	9500	5100	17,600	3700	18,300	4100	16,500	2900	15,500	2400	10,800	3300	15,400	2500	9800	5400	14,700	2400	12,200	1800	5200
	pН	7.24	7.26	7.08	7.20	7.30	7.40	7.30	7.35	7.21	7.51	7.20	7.46	7.11	7.31	7.30	7.37	7.15	7.20	7.24	7.40	7.27	7.32
4	%	69.64	84.04	77.41	93.39	73.97	91.32	81.72	92.78	69.89	91.76	62.38	89.16	70.24	90.49	70.38	89.76	81.00	91.26	64.82	90.79	59.22	83.88
	$K_{d}$	4600	14,700	6900	28,300	5700	21,000	8900	25,700	4600	22,700	3300	16,400	4700	19,000	4800	17,500	8500	20,900	3700	19,700	2900	10,400
	pН	7.53	7.50	7.26	7.29	7.40	7.48	7.50	7.60	7.39	7.55	7.43	7.50	7.29	7.60	7.60	7.60	7.30	7.40	7.40	7.51	7.55	7.60
24	%	80.27	93.51	87.82	95.56	85.81	94.95	89.80	96.52	84.02	94.91	76.75	94.17	83.17	95.21	83.23	92.63	91.04	94.81	80.79	93.97	76.97	93.04
	$\kappa_{d}$	8100	28,800	14,400	43,100	12,100	37,600	17,600	55,400	10,500	37,300	6600	32,300	9900	39,800	9900	25,100	20,300	36,500	8400	31,200	6700	26,700
	pН	7.81	7.61	7.55	7.48	7.71	7.60	7.89	7.70	7.77	7.64	7.80	7.68	7.59	7.69	7.93	7.75	7.56	7.50	7.80	7.61	7.90	7.70
168	%	90.90	97.18	94.56	98.06	94.37 <sup>b</sup>	97.58 <sup>b</sup>	96.01	98.55	93.73 <sup>b</sup>	97.78 <sup>b</sup>	91.16 <sup>b</sup>	97.25 <sup>b</sup>	92.01	97.48	93.41	97.82	94.96	97.59	91.88 <sup>b</sup>	97.58 <sup>b</sup>	91.06	96.50
	$K_{d}$	20,000	68,900	34,800	101,000	33,500	80,800	48,100	136,000	29,900	88,100	20,600	70,700	23,000	77,300	28,400	89,800	36,700	81,100	22,600	80,500	20,400	55,200
	pН	8.00	7.75	7.91	7.59	8.20	7.78	8.00	7.89	8.20	7.80	8.30	7.83	7.90	7.76	8.30	7.79	7.92	7.71	8.30	7.80	8.00	7.80

<sup>&</sup>lt;sup>a</sup>Demineralized.

<sup>b</sup>Time, 192 hr.

River, the strontium sorption decreased to  $(5.07 \pm 0.27)\%$ , apparently because of the high calcium concentration in the tap water. Results of these sorption analyses are listed in Table 1.8. The mean cesium sorption is  $(93.10 \pm 1.94)\%$  in tap water and  $(97.58 \pm 0.25)\%$  in demineralized water. These results, shown in Table 1.9, suggest that the mineralogy of the fine sediments is fairly uniform throughout the study reach.

# STUDY OF WHITE OAK CREEK DRAINAGE BASIN

T. F. Lomenick R. M. Richardson<sup>23</sup>
H. J. Wyrick W. M. McMasters<sup>23</sup>
T. W. Hodge, Jr.

# Sources of Contamination and Movement of Radionuclides in the Creek

All ORNL facilities that contribute significant quantities of fission products to the environment are located in the White Oak Creek drainage basin. There are 23 known sources of contamination in the basin. The creek receives directly the discharges of partially treated process waste water, laundry water, sanitary sewage, reactor cooling water effluents, and eventually seepage from the intermediate-level waste seepage pits and five solid-waste burial grounds. Runoff from land surfaces subjected to local and general fallout also contributes some activity to the creek. In addition, some radionuclides enter the creek from the beds of former White Oak Lake and the intermediate pond.

Techniques and Equipment Employed in Assessing Sources. — Temporary water sampling stations were installed at White Oak Creek miles (WOCM) 2.6 and 3.9 and along the tributary stream draining the northwest portion of the Bethel Valley area to assess the amount and type of activity associated with fallout, burial grounds, and other sources that could not be monitored directly (see Fig. 1.10). In addition, representative samples were taken of the effluent from the laundry and

<sup>&</sup>lt;sup>23</sup>U.S. Geological Survey.

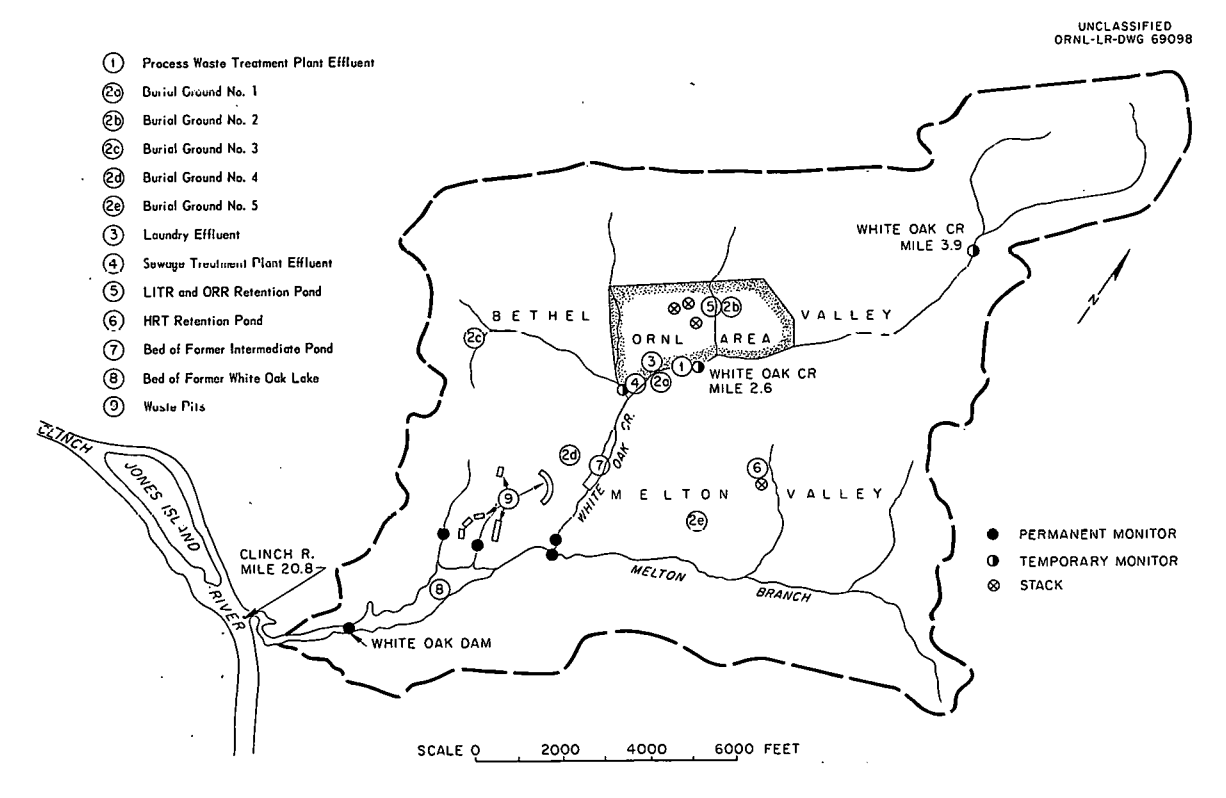


Fig. 1.10. Map of White Oak Creek Basin, Showing Sources of Radioactive Contamination and Stream Monitoring Stations.

the sewage treatment plant. The sampling devices used at the stations have been described previously. 24

Findings at Monitoring Stations. — The Process Waste Water Treatment Plant (PWWTP) is the major source of contamination to White Oak Creek within Bethel Valley (ORNL plant site). However, significant quantities of radionuclides enter the creek from other facilities in the valley. A summary of the activity detected at the laundry, the sewage treatment plant, stream sampling stations, and the PWWTP for the period May-October 1961 is shown in Table 1.10. It is of interest to note that during the six-month sampling period, the sewage treatment plant contributed approximately 150 mc of Sr<sup>90</sup>, 100 mc of TRE<sup>3+</sup> (exclusive of  $Y^{90}$ ), 32 mc of Cs<sup>137</sup>, 7 mc of Co<sup>60</sup>, and 7 mc of Ru 106. Although the amount detected is small in comparison to that released from the PWWTP, it is rather large for a facility that should be relatively free from contamination. concentration of Sr<sup>90</sup> in the sewage water effluent was  $1.7 \times 10^{-6} \,\mu\text{c/cc}$  or about 40% of the MPC... The weekly contribution of Sr<sup>90</sup> to the creek from this facility was fairly constant, but for the remaining radionuclides the releases were somewhat sporadic.

The amounts of activity detected in weekly samples at the stream stations vary over a wide range. For the northwest tributary station and

<sup>24</sup>E. G. Struxness et al., Health Phys. Div. Ann. Progr. Rept. July 31, 1961, ORNL-3189, pp 6-7.

the monitor at WOCM 3.9, the total amount of strontium detected appears to vary with stream discharge (Figs. 1.11 and 1.12). This suggests that most of the strontium enters the streams to the surface and ground water leaching and not to sporadic releases or spills, etc. Also, an increase in the suspended solid load in the streams at these stations is generally followed by a corresponding increase in cesium transport (Fig. 1.13) and an increase in the amount of Thus during periods of high strontium sorbed. stream discharge and/or high suspended solid load, the transport of strontium and/or cesium is high. In Figs. 1.11, 1.12, and 1.13 it is noted that cesium and strontium transport in weeks in which suspended solids and/or stream discharge is high exceeded that in several weeks when suspended solids and/or stream discharge was low. For the water sampling station at WOCM 2.6 the correlations mentioned above are not as pronounced. At this station there is some indication that radionuclides enter the creek within the ORNL plant site from intermittent and/or accidental releases. For the six-month sample period it is noted that during most periods the transport of radionuclides past the stream sampling stations is relatively small compared with the amount discharged to the creek from the PWWTP, but for short times substantial amounts are transported.

The drainage area of the sampling station at WOCM 3.9 does not contain any Laboratory facilities or waste disposal areas. Thus, the activity detected at this station is the result of rainout and of rainfall and surface runoff leaching and

Table 1.10. Principal Radionuclides Discharged to White Oak Creek from Sources in Bethel Valley,

May-October 1961

<b>.</b>	Sr <sup>89,90</sup>		$TRE^{3+(a)}$		C	Cs <sup>137</sup>		co <sup>60</sup>	R	u <sup>106</sup>	Totals
Station	(mc)	(%)	(mc)	(%)	(mc)	(%)	(mc)	(%)	(mc)	(%)	(mc)
Northwest tributary stream	33	0.85	34	1.38	30	2.98	1	0.23	7	1.98	105
White Oak Creek Mile 2.6	. 123	3.17	83	3.28	153	15.21	89	20.41	43	12.15	491
Sanitary sewage	150	3.87	100	3.95	32	3.18	7	1.61	7	1.98	296
Laundry	9	0.24	· 11	0.44	11	1.09	6	1.37	1	0.28	38
Process Waste Water Treatment Plant	3560	91.87	2300	90.95.	780	77.54	333	76.38	296	83.61	7269
Totals	3875	100.00	2528	100.00	1006	100.00	436	100.00	354	100.00	8199

aExclusive of Y 90.

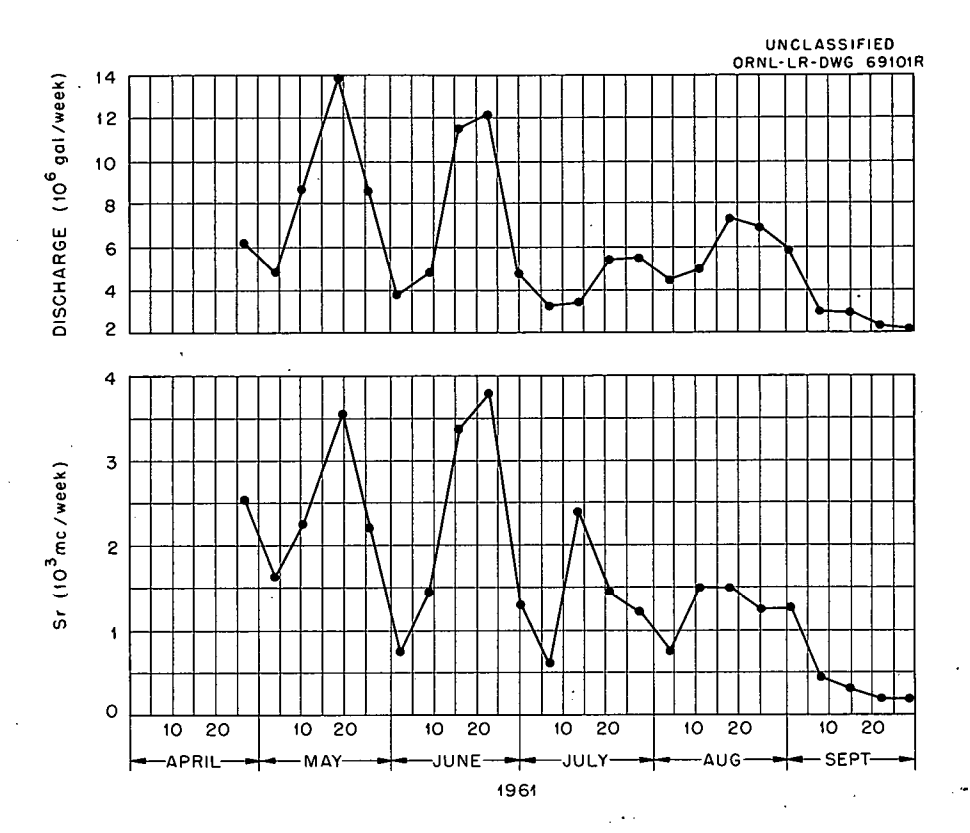


Fig. 1.11. Stream Discharge and Strontium Transport at Northwest Tributary.

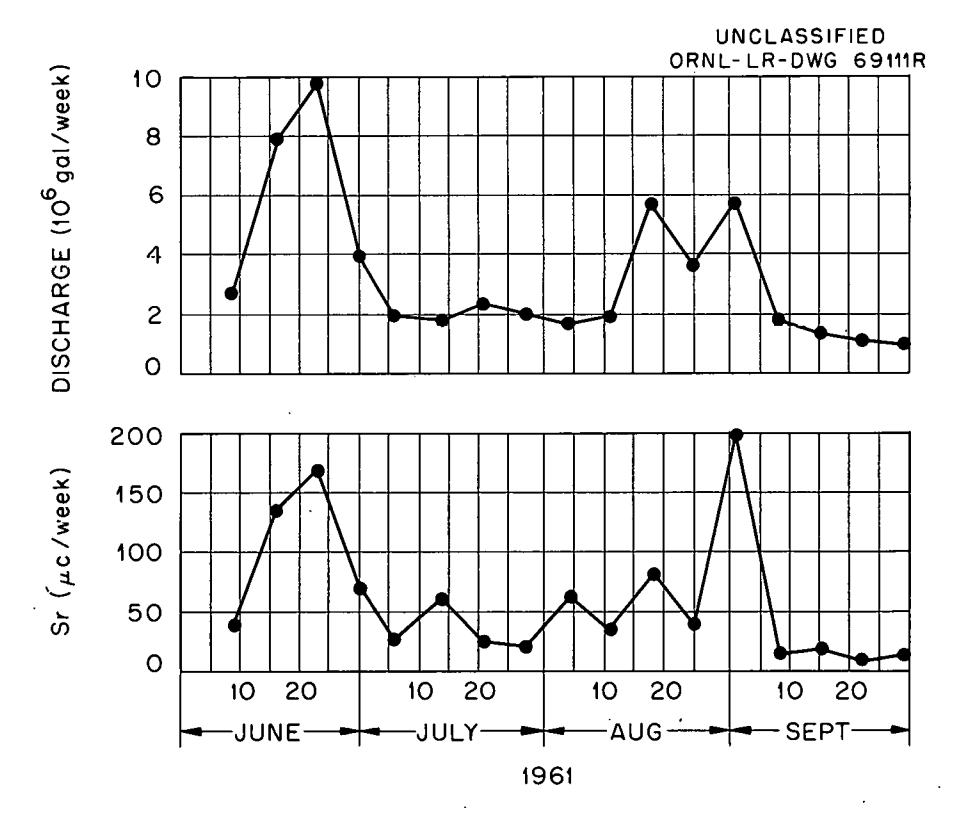


Fig. 1.12. Stream Discharge and Strontium Transport at WOCM 3.9 Station.

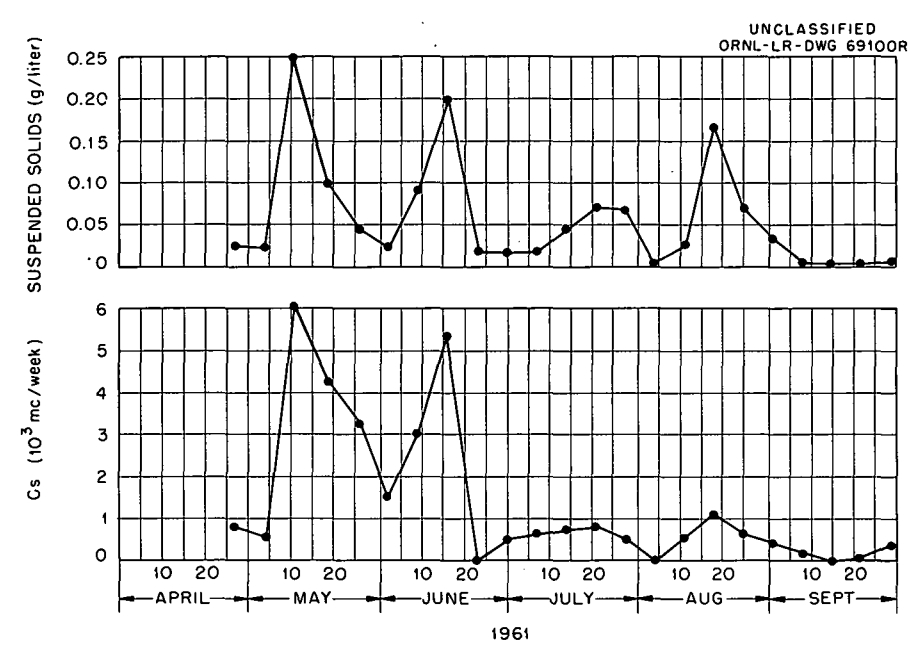


Fig. 1.13. Suspended Solids Concentration and Cesium Transport at Northwest Tributary Station.

transporting soils contaminated by Laboratory and general fallout. For the sample period May 31, 1961 to October 6, 1961, approximately 1010  $\mu$ c of Sr<sup>90</sup>, 2120  $\mu$ c of TRE<sup>3+</sup> (exclusive of Y<sup>90</sup>), 1970  $\mu$ c of Cs<sup>137</sup>, and 1450  $\mu$ c of Ru<sup>106</sup> were detected. Although the watershed above this station is roughly comparable in size to that above the northwest tributary station, the amount of activity detected for the same period at this station, WOCM 3.9, was less than 5% of that detected at the northwest tributary station. For the station at WOCM 2.6, which has a drainage area about three times that above WOCM 3.9, the same general comparison can be made.

Thus, assuming that the activity detected at the WOCM 3.9 station is representative of the quantity and type of radionuclides entering surface streams over the entire drainage system due to Laboratory and general fallout, it is concluded that in comparison with other sources of contamination, local and general fallout contribute an insignificant amount of activity to White Oak Creek.

#### White Oak Lake Bed

White Oak Lake was created in the fall of 1943 by damming White Oak Creek at mile 0.6. The lake, covering some 44 acres, served as a final settling basin for low-level radioactive wastes discharged from ORNL. It was drained in 1955, leaving approximately 1,000,000 ft<sup>3</sup> of contaminated sediments. The dry lake bed is now being further contaminated by seepage from the intermediate-level waste pits. An investigation is in progress to determine the quantity, distribution, and transport of radionuclides within the area.

Hydrology. — A series of shallow auger holes, 5-6 ft deep, was completed in the bed of former White Oak Lake to define the configuration of the water table and to determine the direction of ground-water movement. Water-level measurements in these wells, made about once each week for the period August 28, 1961, to January 5, 1962, indicated that the depth to ground water in the area generally varied from 3 to 5 ft below the land surface during the dry summer months and from <1 to 1.5 ft below the land surface during the wet winter months when transpiration and evaporation are lower.

Water-contour maps of the area show that the general direction of ground-water movement is normal to the flow of White Oak Creek in the lower portion of the site; in the upper bed the pattern is more complex. A water table contour map for September 22, 1961 (Fig. 1.14), indicates that the configuration of the water table in the upper part of the area is measurably affected by the

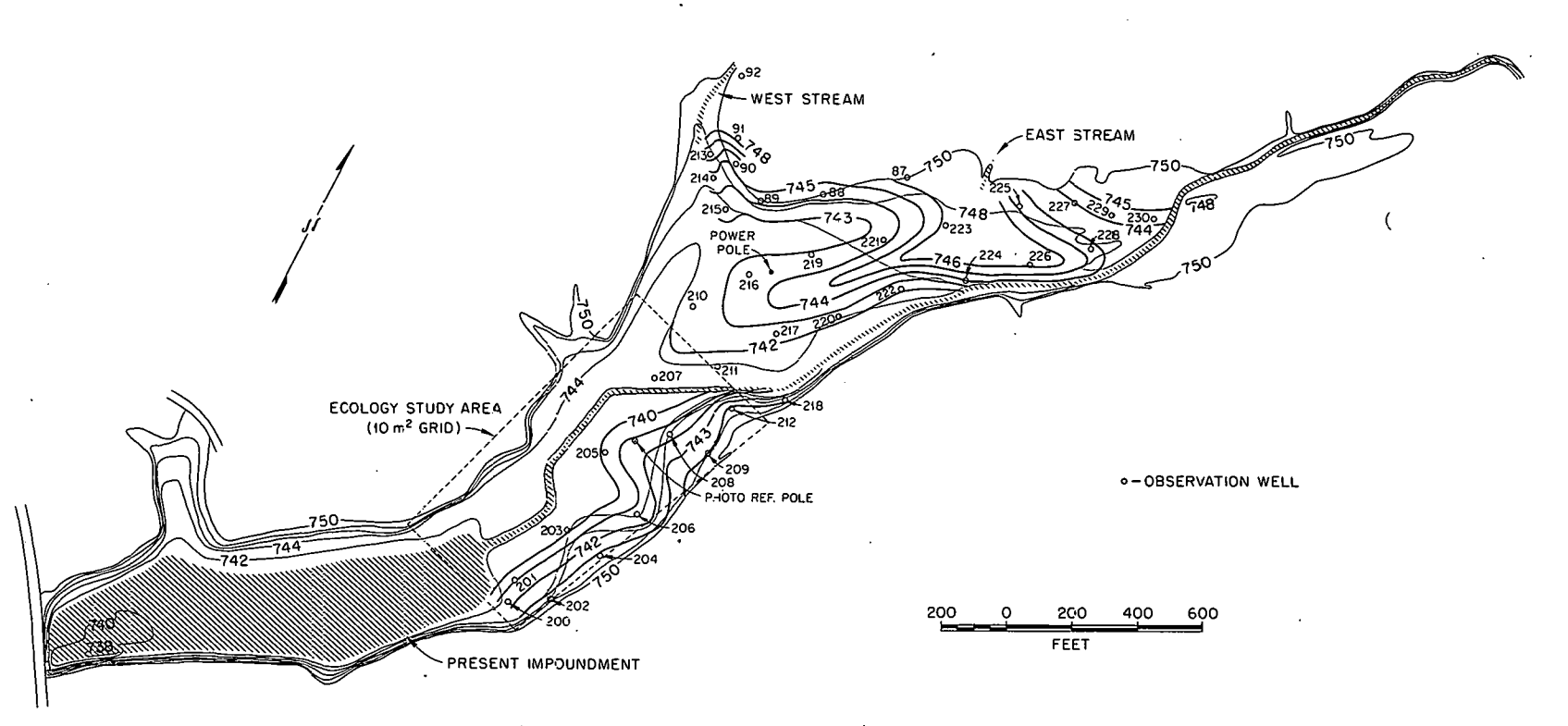


Fig. 1.14. Water Table Contours at White Oak Lake Bed, Sept. 22, 1961.

flow of surface water onto the lake bed from two streams that drain the waste pit area. During the dry summer months, these streams recharge the ground water in the lake bed, with little or no surface water flowing directly into the creek. However, in the wet winter months, when the ground water in the lake bed is close to the land surface, some of the water from these streams flows over the surface of the bed into White Oak Creek.

The rate of ground water movement in the upper 2 ft of soil varies from 0.2 to 1.0 ft/day, while movement in the material 3 to 5 ft below the surface ranges from 0.01 to 0.05 ft/day. Thus, the maximum rate of travel in the upper layer of soil is approximately 20 times that in the lower layer.

Distribution of Radionuclides. - The two streams that drain the waste pit area transport several thousand curies of Ru 106 per year onto the lake bed; however, less than half the ruthenium finds its way into White Oak Creek. During the dry months these streams, as mentioned above, recharge the ground water in the lake bed and thus allow little if any Ru<sup>106</sup> to travel over the land surface to White Oak Creek. However, in the wet winter months more of the ruthenium flows over the surface of the lake bed into the creek. Since the lake bed soil is more permeable near the land surface, the ruthenium moves more readily through the upper part of the soil column. Thus, it is concluded that most of the activity enters the upper few inches of the lake bed soil during the dry months when the water table is "low," but it is transported laterally and vertically through the soil during the winter months when the water table lies relatively near the surface.

A series of soil samples was taken during February 1962, within the lake bed and radiochemically analyzed to determine the distribution and total amount of Ru<sup>106</sup> in the soil. The cores, varying in depth from 24 to 60 in., were taken approximately 50 ft apart along lines at right angles to the surface flow of waste over the lake bed (see Fig. 1.15). Counting results from the samples were plotted on cross sections through the soil to indicate the vertical and lateral distribution of the activity. For cross section B-B' (see Fig. 1.16) it is noted that the highest con-

centrations of activity occur in the uppermost few inches of soil near boreholes 2 and 3. This condition is as expected, since the surface flow of waste at this cross section is largely confined to this zone. Although some of the highest concentrations of Ru 106 found in the lake bed were detected in this cross section, there was relatively little contamination of the soil below 2 ft. Near borehole 5 more activity was detected at depths of 0.5 and 2 ft than at the land surface. This indicates that ground water is transporting Ru106 through the soil to points of discharge in or near the creek. The same general pattern of Ru 106 distribution exists at other cross sections along the tract, except that there is a decrease in maximum concentrations of activity in the soil along cross sections further from the source of contamination. For tract 2, the distribution pattern of the ruthenium is similar; however, the contamination zone is not nearly as widespread.

The curies of Ru<sup>106</sup> in each cross section were calculated and the results summed to yield the total Ru<sup>106</sup> in each tract. As of February 1962, the lake bed contained approximately 1200 curies of Ru<sup>106</sup>. It is of interest that 85% of the Ru<sup>106</sup> was found along tract 1. This is due largely to the greater percentage of ruthenium transport onto the lake bed from the east stream (85% of the total in 1960 and 62% in 1961).

It is likely that the amount of Ru 106 in the lake bed will vary greatly throughout the year. Others 26 have shown that the amount of activity leaving the waste pits is largely dependent on the concentration and total volume of Ru 106 pumped to the system. Thus, large changes in the volume and concentration of waste transported to the waste pits will measurably, affect the amount of Ru 106 that flows onto the lake bed. In addition, less ruthenium is removed from the waste flow during the wet winter months, when most of the water flows over the surface of the bed into the creek, than during the dry summer months, when the waste streams recharge the ground water in the area. Finally, the short half-life of the isotope (1 yr) will cause the budget in the area to change measurably in a relatively short period of time.

<sup>&</sup>lt;sup>25</sup>D. Kirkham, Am. Geophys. Union Trans. **32**(4), 582-90 (August 1951).

<sup>&</sup>lt;sup>26</sup>K. E. Cowser, "Movement of Ruthenium in the ORNL Waste-Pit System," Ground Disposal of Radioactive Wastes, Second Conference Proceedings, Chalk River, Ontario, Canada, September 26-29, 1961, TID-7628, pp 513-31.

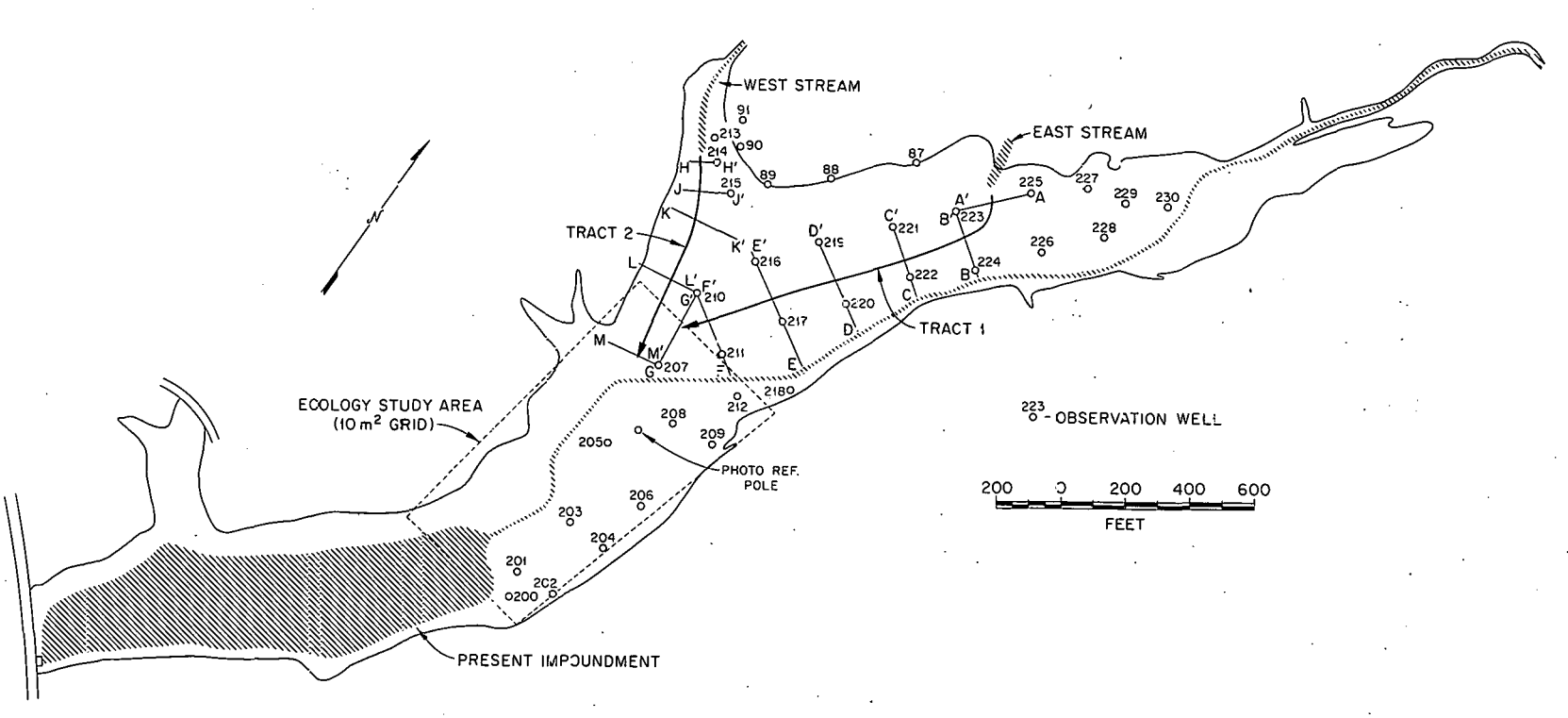


Fig. 1,15. Map of White Oak Lake Bed, Showing Transverse Lines of Boreholes.

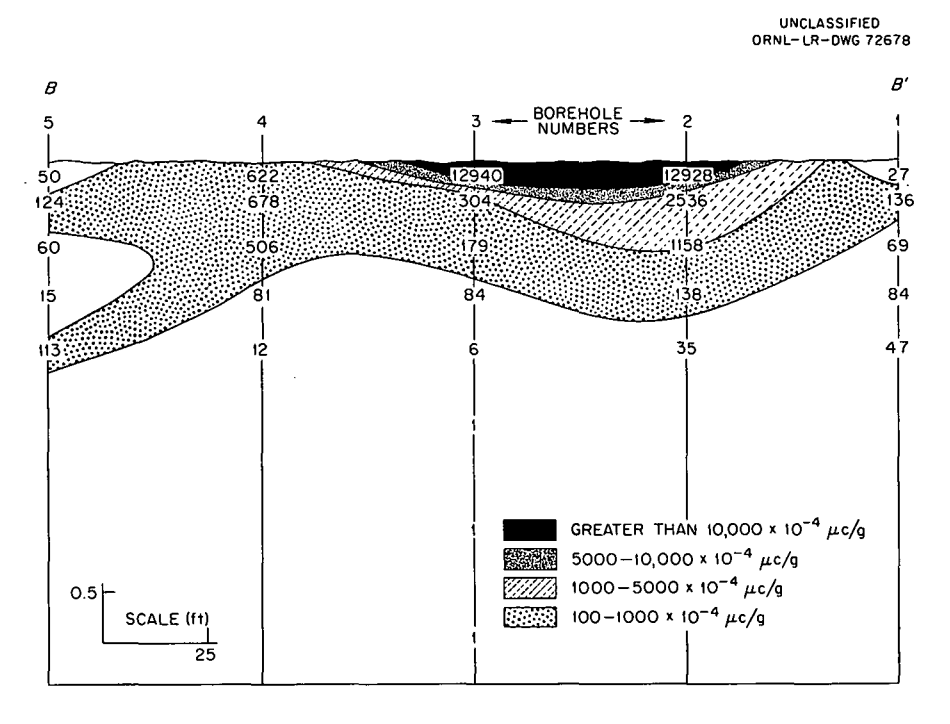


Fig. 1.16. Cross Section B-B' in White Oak Lake, Showing Ru<sup>106</sup> Concentration.

In summary, results of this investigation show that (1) as of February 1962, there was approximately 1200 curies of Ru<sup>106</sup> along the two measured tracts in the bed of former White Oak Lake, (2) the highest concentrations of Ru<sup>106</sup> are found in the uppermost 2 in. of soil, (3) about 75% of the ruthenium found in the lake bed is associated with the first 2 ft of soil, and (4) although ruthenium is being transported by ground water through the lake bed soil, a relatively small amount of it is reaching the creek in this manner.

#### Flow Time in White Oak Creek

To determine the minimum time of travel through White Oak Creek during high base flow periods, a 3-day study of time of travel was begun on May 1, with fluorescein dye and visual inspection. The study began at a point about 600 ft upstream from Building 6000 and ended at White Oak Dam. Discharge at the gaging station "White Oak Creek below ORNL" was 5.5 cfs. Minimum time of travel for the 15,190 ft of channel studied was 541 min and the average maximum velocity was 0.48 ft/sec. Velocities ranged from 0.11 ft/sec in White Oak Lake to 0.78 ft/sec below the Process Waste Water Treatment Plant effluent to White Oak Creek.

On May 16 a time-of-travel study was made in White Oak Creek, with 206 mc of Au<sup>198</sup> as a tracer. Discharge at the gaging station "White Oak Creek below ORNL" was 4.7 cfs. Although the background count was extremely high, stations in the pool below the old intermediate pond and at the gaging station "White Oak Creek below ORNL" were able to record passage of the tracer. The mean velocity of the tracer from the initial point to the gaging station, a distance of 3650 ft, was 0.45 ft/sec. The tracer had a duration of 2 hr, 13 min at the gaging station.

#### ION EXCHANGE STUDIES OF MINERALS

T. Tamura	D. G. Jacobs
W. P. Bonner	O. H. Meyers
F. S. Brinkley	C. J. Gailledreau <sup>27</sup>

#### Behavior of Cesium in Vermiculite Systems

The behavior of cesium in vermiculite systems is of interest for two reasons: (1) vermiculite is one of the few clay minerals with sufficiently

 $<sup>^{27}</sup>$ Exchange scientist from Centre D'Etudes Nucleaires de Saclay, France.

large particle size to be of practical use in waste decontamination by columns, and (2) when it is treated with one of the heavier alkali-metal cations, the lattice spacing changes measurably, producing steric effects which alter the exchange properties of the vermiculite.

Pretreatment of Vermiculite with Potassium. -Vermiculite (hydrobiotite obtained from the Zonolite Co., Traveler's Rest, S.C.) was pretreated with potassium, resulting in varying degrees of collapse of the interlayered biotite-vermiculite lattices. Lattice collapse was accompanied by a drop in the exchange capacity, because the exchange sites lying within the collapsed basal spacing are no longer freely accessible to the counterions. Seven and one-half liters of 0.5 M NaNO3 containing the mass equivalent of 2  $\mu$ c of Cs<sup>137</sup> per ml and tagged with Cs137 was passed through 10-g columns of the collapsed vermiculite at an average flow rate of 1.3 ml  $cm^{-2}$   $min^{-1}$ . After the columns were saturated with cesium, they were divided into four sections for determination of the final exchange capacity, by the calcium titration method of Jackson, 28 and the cessum

loading. Each solution used in determination of the exchange capacity was counted for cesium and the total cesium was computed. The  $K_d$  for cesium increased with a decrease in exchange capacity, because of the increased number of edge fixation sites made available by lattice collapse (Table 1.11). The leaching action of the sodium nitrate removed a portion of the potassium from interlayer fixation sites, causing expansion of part of the vermiculite lattice.

Addition of Potassium to the Influent. — As the potassium concentration is increased (Table 1.12), lattice collapse occurs and the cesium and potassium are entrapped by "interlayer fixation," as evidenced by a drop in the exchange capacity and a decrease in the percentage of cesium leached. Although the potassium is competitive with cesium for the interlayer fixation sites, the cesium  $K_d$  increases with increasing potassium concentration, passing through a maximum at  $0.04 \text{ M KNO}_3$ . Above this concentration the increased potassium concentration is not balanced by an increase in the number of interlayer fixation sites.

The percentage of cesium leached is more directly related to the exchange capacity than to the cesium  $K_d$ , decreasing as the exchange capacity decreases. This is due to a shift from

Table 1.11. Effect of Potassium Pretreatment of Vermiculite on Cesium Sorption from 0.5 M NaNO $_3$  Containing the Mass Equivalent of 2  $\mu c$  of Cs $^{137}$  per ml

	Cesium Excha	ange Capacity	o : "		37 D '111 . '	
Column No.	Initial Final (meq/100 g)		Cesium K <sub>d</sub> (ml/g)	Cesium Leached (%)	X-Ray Diffraction (before saturation)	
1 ,	55.7	74.9	108	16.3	No change from sodium vermiculite	
2	48.9	73.9	112	15.1	Random interlayering with lower spacings	
3	42.3	75.0	124	14.4	Equally intense maxima at 10 and 11 A	
4	38.0	73.7	133	16.1	Most intense maximum at 10 A; also peak at 11 A	
5	13.0	64.2	201	9.0	10-A peak with random interlayering with higher spacings	
6	5.9	45.9	272	7.0	Sharp 10-A peak	

<sup>&</sup>lt;sup>28</sup>M. L. Jackson, Soil Chemical Analysis, Prentice-Hall, New Jersey.

Table 1.12.	Effect of Addition of Potassium to the Influent on the Sorption of Cesium by Vermicu	lite
	from 0.5 M NaNO <sub>2</sub> Containing the Mass Equivalent of 2 $\mu$ c of Cs $^{137}$ per ml	

Potassium Concentration (M)	Cesium K <sub>d</sub> (ml/g)	Cesium Leached (%)	Final CEC (meq/100 g)	X-Ray Diffraction (after saturation)
0.0000	154	12.6	75.4	
0.0001	147	13.0	74.9	
0.001	137	15.2	70.2	
0.01	357	7.60	60.0	
0.02	483	5.83	38.1	First signs of increased interlayering with lower spacings
0.03	695	4.90	26.2	10-A peak with some random interlayering with higher spacings
0.04	727	4.63	17.9	
0.05	634	4.56	15.3	
0.08	373	4.10	9.1	Sharp 10-A peak
0.10	265	3.26	8.6	

edge fixation to interlayer fixation as the dominant sorption mechanism. As a greater fraction of the cesium occupies interlayer fixation sites, it is less readily leached.

Addition of Other Collapse-Inducing Cations to the Influent. — Other heavy alkali-metal cations and ammonium ions also cause collapse of the vermiculite lattice. Since they are more strongly held than potassium, a smaller concentration is required in  $0.5\,M$  NaNO $_3$  to initiate lattice collapse and to obtain optimum cesium removals (Table 1.13). The behavior of the ammonium-treated influent was somewhat different from that of the other systems; the  $K_d$  was higher but the percentage of cesium leached was also much greater than for the alkali-metal cations.

Step Increases in Influent Potassium Concentration. — Because collapse of all interlayer spacings does not occur at the minimal concentration for initiating lattice collapse, and because increases in the potassium concentration increase competition with cesium for fixation sites, it seemed that the optimum procedure would be to operate at the minimum  $(K^+)/(Na^+)$  until the easily

collapsed lattices are all in the collapsed state. This would be evident by an increase in the cesium activity of the effluent. Gradual increases of the  $(K^+)/(Na^+)$  would result in additional lattice collapse and increased cesium sorption, until finally a state would be reached where all possible collapse had been accomplished. Beyond this point, increases in potassium concentration would merely interfere with cesium sorption.

Two liters of the 0.5 M NaNO<sub>3</sub> solution was passed through a 10-g vermiculite column. Complete cesium breakthrough was observed. When this influent solution was brought to 0.01 M KNO<sub>3</sub>, the cesium activity of the effluent dropped to less than 15% of the influent activity after 200 ml of solution had passed through the column. A second breakthrough wave was observed when 2 liters of this solution had passed through the column, and cesium activity in the effluent was decreased to less than 1% of the influent activity by increasing the potassium concentration of the influent to 0.02 M. A third breakthrough wave occurred after passage of 2 liters of this solution. This was followed by 7.5 liters of 0.08 M, and

Cation	Cation Concentration (M)	Cesium K <sub>d</sub> (ml/g)	Cesium Leached (%)	Final CEC (meq/100 g
K <sup>+</sup>	0.040	727	4.63	17.9
NH <sub>4</sub> +	0.010	1851	13.1	42.8
Rb +	0.0015	556	4.22	41.0
Cs <sup>+</sup>	0.0004	557	3.38	47.7

Table 1.13. Optimum Concentrations of Collapse-Inducing Cations for Cesium Sorption by Vermiculite from 0.5 M NaNO $_3$  Containing the Mass Equivalent of 2  $\mu$ c of Cs  $^{137}$  per ml

0.35 liters of 0.10 M KNO $_3$ . After this last breakthrough wave, 0.25 liter of the 0.5 M NaNO $_3$  solution was passed through the column before the final breakthrough wave was obtained. A cesium  $K_d$  of 2255 ml/g was obtained, 4.49% of which was leached off during the determination of the exchange capacity. The final exchange capacity of the vermiculite was 18.3 meq/100 g.

The first breakthrough wave is obtained when the original cesium fixation sites are satisfied. Addition of potassium to the influent results in collapse of part of the lattices, which causes more cesium to be entrapped by interlayer fixation and to be held at the additional edge fixation sites of the newly collapsed lattices. Successive increases in the potassium concentration of the influent result in additional lattice collapse until all lattices are in a collapsed state. Since the partial cesium capacity is increased by each increase in potassium concentration, a reduction in the cesium activity of the effluent is observed. The final breakthrough wave is obtained after cesium satisfies the edge fixation sites in the absence of the highly competitive potassium.

Effect of Temperature. — As expected, increased temperatures resulted in faster rates of the exchange reactions, but the effect on cesium sorption is influenced by other exchange reactions occurring in the system. When 0.5~M NaNO<sub>3</sub> tagged with  $Cs^{137}$  was passed through columns of sodium- or potassium-treated vermiculite, a more rapid release of potassium from the collapsed layers was favored at higher temperatures and resulted in a greater degree of lattice expansion. This resulted in a higher exchange capacity and a lower cesium  $K_d$  (Table 1.14).

When the 0.5 M NaNO3 influent solution was brought to 0.04 M KNO3 the reverse reaction was favored and also proceeded at a faster rate. As a result, more complete lattice collapse and a reduced exchange capacity was favored by higher temperatures. However, at 81°C, 0.04 M KNO<sub>2</sub> provided too much competition for cesium (either the lattices were collapsed before the cesium could arrive at the exchange sites within the basal spacing or the elevated temperature reduced the hydration of the potassium ion, resulting in a higher affinity of the vermiculite surface for the potassium) and resulted in lower cesium sorption than at room temperature. In the cold system (0°C), collapse of the vermiculite lattices was not sufficiently complete, as evidenced by the higher exchange capacity, and by the fact that optimum cesium removal was not obtained.

## Rock Phosphate Columns for Strontium Decontamination

The mineral, apatite, is contained in the ore material, rock phosphate. This mineral has been shown to possess highly selective removal characteristics for strontium when used in basic media. The advantages of the use of rock phosphate in columns are its abundance, low cost, and availability in sized particles. The samples used in this study, mined at Mulberry, Florida, were donated by the International Minerals and Chemical Corporation.

Comparison of Efficiency with That of Calcite. — The primary objective of this experiment was to compare the efficiency of rock phosphate with

Temperature ( <sup>O</sup> C)	Solution	Cesium K <sub>d</sub> (ml/g)	CEC (meq/100 g)	Cesium Leached (%)
81	6 liters of 0.5 M NaNO3	95	84.7	22.0
25	·	109	67.3	23.0
0		115	63.4	22.4
81	8 liters of (0.5 M NaNO $_3$ + 0.04 M KNO $_3$ )	140	8.0	3.42
25		610	14.9	5.82
0		379	28.0	7.06
	81 25 0 81 25	81 6 liters of 0.5 M NaNO <sub>3</sub> 25 0 81 8 liters of (0.5 M NaNO <sub>3</sub> + 0.04 M KNO <sub>3</sub> ) 25	Temperature (°C)       Solution $K_d$ (ml/g)         81       6 liters of 0.5 M NaNO <sub>3</sub> 95         25       109         0       115         81       8 liters of (0.5 M NaNO <sub>3</sub> + 0.04 M KNO <sub>3</sub> )       140         25       610	Temperature (°C)       Solution $K_d$ (ml/g)       CEC (meq/100 g)         81       6 liters of 0.5 M NaNO <sub>3</sub> 95       84.7         25       109       67.3         0       115       63.4         81       8 liters of (0.5 M NaNO <sub>3</sub> + 0.04 M KNO <sub>3</sub> )       140       8.0         25       610       14.9

8 liters of 0.5 M NaNO3

Table 1.14. Influence of Temperature on the Sorption of Cesium by Vermiculite

that of calcite, a material previously reported to be effective for strontium decontamination under appropriate conditions. The simulated waste solution had the following composition:

81

25

0

K-Vermiculite

$NaNO_3$	0.53 M
NaOH	$6.12 \times 10^{-3} M$
Sr <sup>2+</sup>	0.01 ppm
Sr <sup>85</sup>	3014 counts min <sup>-1</sup> ml <sup>-1</sup> at 20% counting efficiency
PO <sub>4</sub> 3-	120 ppm

The basic nature of the solution and the addition of phosphate are known to be necessary for the calcite columns to be effective in removing strontium.

The calcite column, which had been studied at the French CEA installation at Saclay, exhibited a decontamination factor (influent activity/effluent activity = D.F.) starting at 1.0 and rising to a maximum value of 100 after 600 bed volumes (B.V.). The saturation capacity of 20.0 g of calcite was of the order of 10,000 B.V. The rock phosphate column exhibited the same D.F. at the start but the D.F. was over 100 after 80 B.V. and averaged 200 during 1320 B.V.

Since the effluent activity was too low to be conveniently monitored, a fresh 20-liter solution of waste was prepared; the activity of the Sr<sup>85</sup> was raised to 31,610 counts min<sup>-1</sup> ml<sup>-1</sup>. The D.F. was found to increase immediately, and during 72 B.V. it averaged 2000. Since the effluent activity was only 10% of the background, it is felt that the D.F. of the rock phosphate column is a minimal value. On the other hand the D.F. of 100 for calcite represents a more exact value, since the effluent activity was of the order of the background activity.

106

218

301

74.8

62.9

52.2

15.6

13.7

9.8

In order to induce breakthrough of the column, the simulated waste solution was adjusted to give a reduced PO<sub>4</sub> <sup>3-</sup> concentration of 50 ppm. However with the continued high D.F. of 1000-2000, no breakthrough was observed after 3075 B.V. Hence, it was found to be more efficient to count sections of the column. The results are shown in Fig. 1.17 as test column No. 1. Note that the abscissa is plotted as cumulative bed weight, which is directly proportional to bed depth. In the last section of the column there was no detectable Sr<sup>85</sup>. A "buildup" factor is reported in Table 1.15; this factor

$$\frac{q}{c_0} = \frac{\text{av activity per } g}{\text{av activity in the influent}}.$$

The maximum  $q/c_0$  is  $5 \times 10^3$ , and the nature of the curve at the intercept in Fig. 1.17 suggests that this may be the maximum value for this factor under these test conditions.

Table 1.15	Comparison of an le	on Exchange Resin	. Calcite, and Rock	Phosphate for Sr 90	Removal from Waste
1 4516 1.15.	Comparison of an in	on Exchange Negin	, culcito, and noce	. I mospilate for si	

	D.F.	pH Required	PO <sub>4</sub> Required	"Buildup" Factor	Cost	Effect of Ca <sup>2+</sup> in the Waste
Resin <sup>a</sup>	1000	12	None	1,000	\$50 per cubic ft	Slightly detrimental
Calcite	100	11-12	50-100 ppm	10,000	Mostly transportation	Highly detrimental
Rock phosphate	1000	10	None	5,000	Mostly transportation	Slightly detrimental

<sup>&</sup>lt;sup>a</sup>Phenolic-carboxylic cation exchange resin Duolite CS 100 studied by R. R. Holcomb and J. T. Roberts (ref 29). The column's condition was similar to that used in rock phosphate study.

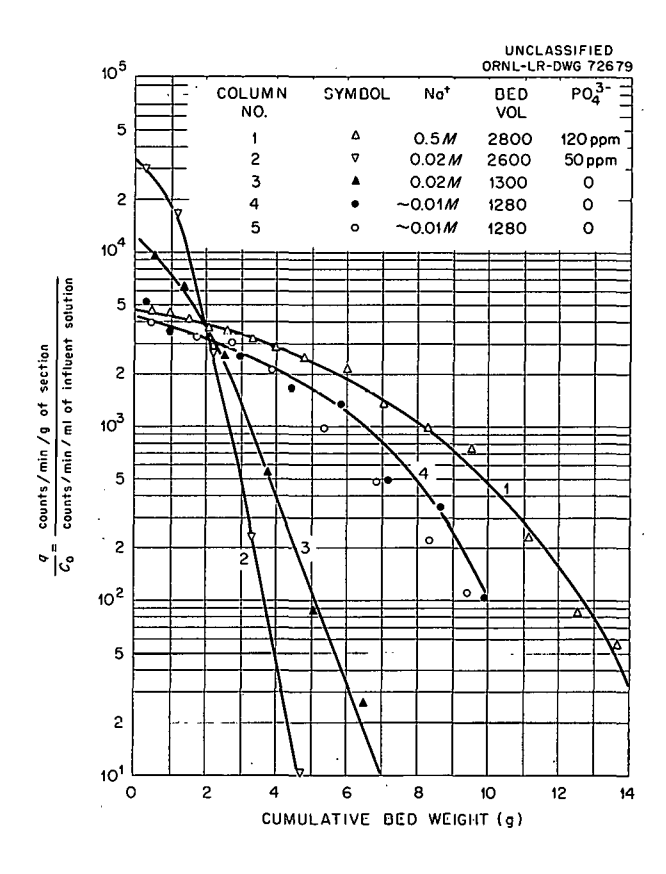


Fig. 1.17. Strontium Removal by Rock Phosphate Column Under Various Conditions.

Effect of Sodium Ion Concentrations. — The main purpose of column No. 2 was to test the effect of sodium ion concentration. A high sodium concentration had been found necessary for good performance in the calcite column; in this test the sodium ion concentration was reduced to 0.02 M and the phosphate ion concentration was 50 ppm. After 2582 B.V., the column was dismantled and

the sections counted for strontium retention. Results are also presented in Fig. 1.17. High sodium ion concentration is definitely detrimental for the rock phosphate column; a "buildup" factor of  $3\times10^4$  was determined after 2582 B.V. The activity in the column has not moved down as far as that observed for column No. 1. Thus, unlike the calcite column, high sodium concentration is detrimental for optimum performance for the rock phosphate column.

Effect of Phosphate Additions. - Test column No. 3 was run to test the need for adding 50 ppm of phosphate. The curve in Fig. 1.17 shows that the strontium activity had traveled farther down column No. 3 after 1340 B.V. as compared with column No. 2, which contained 50 ppm phosphate and had passed 2582 B.V. of waste. This behavior suggests that the phosphate was necessary. A possible explanation for the role of phosphate in this rock phosphate system is the mineral content of the rock phosphate ore. mineral content based on chemical analysis of the ore was calculated, it was found that the material contained 80% apatite. The remaining minerals are likely to be quartz (from the SiO, analysis) and calcite (from the excess CaO and from the assumed CO2 content of a deficit in the total analysis). If the material contained calcite. then the phosphate may be necessary to prevent the calcite from interfering, as well as to aid strontium removal by acting as a sorbent through the calcite-phosphate reaction.

<sup>&</sup>lt;sup>29</sup>R. R. Holcomb and J. T. Roberts, Low Level Waste Treatment by Ion Exchange II: Use of Weak Acid, Carboxylic-Phenolic Ion Exchange Resins, ORNL TM-5 (Sept. 25, 1961).

In column No. 4 operation, laboratory waste which had been clarified and filtered was used to test the performance of the rock phosphate The pH of the solution was about 12, the calcium content was  $1 \times 10^{-4}$  meg/ml. The sodium concentration was not known but was probably of the order of  $10^{-2}$  M. Column operation was maintained under a condition similar to that of column No. 3; the exception, of course, being the nature of the waste. The D.F. ranged in the order of 1000; the contamination traveled further down in column No. 4 than in No. 3 after 1300 B.V. (see Fig. 1.17). The "buildup" factor was approximately 5000; the reduction in "buildup" was likely due to the increase by about 400 times in the calcium-strontium concentration.

Comparison of Rock Phosphate with Other Sorbents. — In order to get a better idea of the performance of the rock phosphate column, a chart is included for comparing several potentially useful materials (Table 1.15). The resin data were obtained for columns of the same diameter but containing 25 cm of resin rather than 10 g of calcite or rock phosphate.

Calcite requires 50-100 ppm of phosphate ions in addition to the high pH. Both calcite and rock phosphate are relatively cheap materials compared with the resin (Duolite CS 100); calcite does show a high "buildup" factor. However, if one reduces the concentration of sodium ion, which is not required for the rock phosphate column, "buildup" factors greater than 10,000 can also be obtained for rock phosphate.

Tests with rock phosphate columns were also run in which the waste solution was treated with sufficient EDTA to reduce the calcium ion concentration from  $1 \times 10^{-4}$  to  $5 \times 10^{-6}$  meq/ml. The data, which are plotted in Fig. 1.17 as column No. 5, show that at this concentration level EDTA did not have a strong detrimental effect on strontium removal by the rock phosphate. This latter observation may be significant, since complexing agents are known to affect the efficiencies of removal of strontium in actual waste solutions.

#### Alumina as a Strontium Sorber

Earlier reports, 30,31 suggested the usefulness of alumina-type compounds for selective removal of strontium from waste solutions. These earlier studies dealt with reagent grade aluminum oxide

powder. In soils, hydrous aluminum oxides are commonly occurring minerals, and it was, therefore, felt desirable to compare the naturally occurring materials with reagent grade alumina.

Identification and Preparation of a Selective Strontium Sorbent. – An aluminum hydroxide (gibbsite) source material was obtained from Reynolds Metal Company, Louisville, Kentucky, and was labeled Arkansas bauxite. Based on the x-ray diffraction analysis and thermal data, there were 60% kaolin and 40% gibbsite in the sample. This material was tested and compared with reagent grade aluminum oxide (Table 1.16). The analysis showed that the Arkansas bauxite was not as effective as alumina for strontium removal prior to heating, but superior to it when heated to 350°C. Heating was used to decompose the gibbsite to the oxide in order to obtain a comparable product. The weight of heated bauxite was reduced proportionately, since heating results in a loss in weight. To confirm the role of the gibbsite in the bauxite, aluminum hydroxide from Fisher Chemical Company, identified as gibbsite, and kaolinite from Georgia were obtained and examined. The unheated aluminum hydroxide showed very low selectivity for strontium, but the material heated to 450°C was more selective for strontium. Kaolinite, a low-cation-capacity exchanger, showed a decrease in selectivity after being heated to 600°C. The kaolinite sample had been heated and prepared earlier for other purposes. These tests not only revealed the usefulness of heated bauxite but established the importance of alumina-type materials as strontium sorbers.

Heating Temperature Relationship for Gibbsite Conversion. — To establish the necessary heating temperature of gibbsite for improved removal of strontium, samples of gibbsite were heated at various temperatures until equilibrium weight-loss was attained. The temperature, time, surface-area, and weight-loss data are recorded in Table 1.17. Note that the material increased in surface area by 1000 times after heating to 200°C. The decomposition temperature of gibbsite is about 150-300°C, and the observed behavior of this material is in accordance with the results pub-

<sup>&</sup>lt;sup>30</sup>T. Tamura and E. G. Struxness, Removal of Strontium from Wastes, ORNL CF-60-10-43 (November 1960).

<sup>&</sup>lt;sup>31</sup>K. Z. Morgan et al., Health Phys. Div. Ann. Progr. Rept. July 31, 1961, ORNL-3189, pp 33-37.

Table 1.16.	Percentage Removal of Strontium by Several Materials at pH 10 After Several
	Solid-Waste Solution Contact Times

Contact	Aluminum	Arkansas Bauxite (40% Gibbsite)		Aluminum Hudanida		Kaolinite	
Time (hr)	Oxide 0.2500 g	Unheated 0.2500 g	350°C 0.1667 g	Unheated 0.2500 g	450°C 0.2500 g	Unheated 0.2500 g	600°C 0.2150 g
1	79.3	42.4	96.6	2.44	99.8	17.3	15.2
4	86.0	46.4	98.6	4.40	99.9	38.2	18.5
24	91.6	49.6	99.3	3.44	99.9	46.4	23.7

Table 1.17. Equilibrium Weight-Loss and Surface-Area Data for Aluminum Hydroxide Heated at Different Temperatures

Heating Temperature (°C)	Heating Duration (hr:min)	Weight Loss (%)	Surface Area (m <sup>2</sup> /g)
100	15:00	0.00	0.3
200	173:20	25.00	303
300	23:20	29.71	
400	17:25	31.33	280
500	6:35	33.37	202
800	25:50	34.22	74
$Al_2O_3^a$			6.6

<sup>&</sup>lt;sup>a</sup>Aluminum oxide ignited powder from Allied Chemical Co.

lished by Weiser.<sup>32</sup> The decomposition of gibbsite may be written as:

$$2 \text{ Al(OH)}_3 \xrightarrow{\text{heat}} \text{Al}_2 \text{O}_3 + 3 \text{ H}_2 \text{O}$$
,

and the weight loss should be 34.64% for the pure compound. The measured value for the 800°C-heated sample used in these tests is 34.22%. From the data in Table 1.17, it appears that for maximum development of surface area the minimum decomposition temperature is best. It is however, apparent that a long heating time is required.

Strontium-removal data by the materials heated as shown in Table 1.17 is given in Table 1.18. For comparison, the gibbsite sample which had been used and heated at 450°C for 3 hr is included and reported in the last column. The pH for these tests was adjusted initially to 10.0 and no further adjustments made. The decrease in strontium sorbed noted after the 24-hr contact is believed due to the gradual decrease in pH which must have occurred with longer contact time, since earlier tests with alumina had shown that the higher pH is better for strontium removal.

The best heating temperature for strontium removal by aluminum hydroxide is 400°C in these tests. It is interesting to note that heating at this temperature did not generate as much surface area as in the 200°C-heated sample but that the sample did lose more weight. These tests are exploratory in nature and not many conclusions can be drawn; however, these results do strongly indicate surface area as an important parameter in alumina's effectiveness as a strontium sorbent.

Efficiency of Heat-Treated Gibbsite for Strontium. — The removal of strontium by a sample of gibbsite heated at  $500^{\circ}$ C for 3 hr, with different amounts of the heat-treated material, is given in Table 1.19. In addition to the removal percentage, the distribution coefficient  $(K_d)$  was calculated and included in Table 1.19. The increasing  $K_d$  with increasing amount of material is interesting, since this type of behavior was noted for illitecesium reactions reported elsewhere. The interpretation for this observation assumed the presence of a small amount of sites very selective

<sup>&</sup>lt;sup>32</sup>H. B. Weiser, Textbook of Colloid Chemistry, p 313, Wiley, New York, 1949.

<sup>&</sup>lt;sup>33</sup>D. G. Jacobs and T. Tamura, 7th Intern. Congr. Soil Science 2, 206 (1960).

Table 1.18. Percentage Removal of Strontium by Heat-Treated Aluminum Hydroxide

Contact Time	_ I	Equilibrium Heating at Specified Temperature					
(hr)	100°C	200°C	400℃	500°C	800°C	3-hr Heating at 450°C	
1	0.13	67.5	78.8	73.9	42.0	73.5	
3	1.45	72.1	81.0	74.1	38.8	74.7	
24	1.86	72.1	78.5	66.0	37.4	71.6	
pH <sup>a</sup>	7.34	7.90	8.08	7.90	7.74	8.54	

<sup>&</sup>lt;sup>a</sup>The pH was initially adjusted to 10.0 and no further adjustments were made. The pH readings were taken after 50-hr contact.

Table 1.19. Percentage Strontium Removal and Distribution Coefficient  $(K_d)$  of Aluminum Oxide Prepared by Heating Al(OH)<sub>3</sub> to  $500^{\circ}$ C for 3 hr

Volume of waste: 50 ml in each case

Weight of Aluminum Oxide	Со	ntact Time	(hr)
(g)	1	4	24
0.001			
% Removal	8.17	7.25	8.33
K <sub>d</sub>	4450	3900	4550
0.005			
% Removal	28.75	32.49	34.47
K <sub>d</sub>	4030	4810	5260
0.010			
% Removal	52.42	59.20	60.74
$\kappa_{d}$	5500	7250	10,400
0.020			
% Removal	80.84	87.38	86.90
$\kappa_d^{}$	10,600	23,100	15,800
0.030			
% Removal	90.54	94.10	93.78
K <sub>d</sub>	16,000		25,200
0.050			
% Removal	94.53	97.29	97.50
K <sub>d</sub>	17,300	35,900	39,000

for the radionuclide. If highly selective sites are present in heated aluminum hydroxide, this suggests the use of this material as a "final scrubber" for strontium decontamination. Since activated alumina of high surface area is used widely and is available commercially, this makes the material even more attractive as a sorbent. Further work is being done on this material to obtain a better understanding of the reaction.

# EVALUATION OF ENGINEERING, ECONOMICS, AND HAZARDS

#### R. L. Bradshaw

A study has been undertaken in cooperation with the ORNL Chemical Technology Division to evaluate the economics and hazards associated with alternative methods for ultimate disposal of highly radioactive liquid and solid wastes. All steps between fuel processing and ultimate storage will be considered, and the study will define an optimum combination of operations for each disposal method and indicate the most promising methods for experimental study.

A 6-tonne/day (metric ton, 2200 lb) fuel processing plant is assumed, processing 1500 tonnes/yr of uranium converter fuel at a burnup of 10,000 Mwd/tonne and 270 tonnes/yr of thorium converter fuel at a burnup of 20,000 Mwd/tonne. This hypothetical plant would process all the fuel from a 15,000-Mwe nuclear economy, which may be in existence by 1975.

Cost studies on interim liquid storage and conversion of high-activity solutions to solids by

pot calcination were reported last year. Details are given in ORNL-3128<sup>34</sup> and ORNL-3129,<sup>35</sup> respectively.

reacidified Thorex in smaller cylinders at 3000 miles. Details of this study will be published in ORNL-3356.<sup>36</sup>

#### Shipping of Calcined Solids

Shipping costs of calcined solids were calculated assuming cylindrical carriers of iron, lead, and uranium with an inside diameter of 5 ft. Carriers would contain thirty-six 6-in.-diam vessels or four 24-in.-diam vessels of calcined solids.

A minimum age for each waste before shipping is necessary, because the temperature of the waste must not be allowed to rise above the maximum calcination temperatures and because the temperature of the lead carriers must not approach the melting point of lead. The carriers are aircooled and have no mechanical cooling equipment. Minimum ages for shipping 6-in.-diam and 24-in.-diam cylinders were 2.4 and 11 yr for acidic Purex, 1.0 and 3.0 yr for reacidified Purex, 0.66 and 3.4 yr for acidic Thorex, 0.33 and 0.82 yr for reacidified Thorex; minimum age for shipping acidic Thorex glass in 6-in.-diam cylinders was 0.33 yr.

Weights and costs for carriers at minimum ages were about 100 tons and \$50,000 for iron carriers, 80 tons and \$120,000 for lead carriers, and 65 tons and \$650,000 for uranium carriers. The total shipping costs calculated for round trip distances of 1000, 2000, and 3000 miles were the sums of carrier, rail freight, and handling charges. Shipping costs were lowest in all cases for lead carriers, but in some cases the use of lead carriers required higher minimum ages. At 1000 miles the use of iron carriers costs less than uranium carriers, but at 3000 miles the cost of uranium carriers is less than iron carriers and approaches the cost of lead carriers. Costs in lead carriers range from  $0.70 \times 10^{-3}$  mill/kwh<sub>e</sub> for four 24-in.-diam acidic Purex cylinders per carrier at 1000 miles to  $32.3 \times 10^{-3}$  mill/kwh for the shipment of

#### Storage of Calcined Solids in Salt

Tentative costs were calculated for the storage of cylinders of calcined waste buried in a vertical position in the floors of rooms in salt mines. The distance between cylinders is determined by the necessity for dissipating the heat of fission-product decay without exceeding the calcination temperature of the cylinders or an assumed maximum salt temperature of 200°C. Acidic Purex waste requires the largest spacing, from 20 ft at 2.3 yr to 11 ft at 30 yr for 6-in.-diam cylinders, from 36 ft at 5.5 yr to 23 ft at 30 yr for 12-in.-diam cylinders, and 56 ft at 30 yr for 24-in.-diam cylinders. Corresponding areas of mined space range from about 20 to 2 acres/yr.

In the conceptual design of the disposal operation, the waste container shipping cask will be removed from a rail car and carried into a hot cell which encloses the top of the waste shaft. Waste containers are then unloaded into a storage area, from which they are removed for lowering down the shaft into a motorized carrier at the working level of the mine. The carrier moves out to the current disposal area, lowers the container into a hole in the floor, and backfills the hole with fine crushed salt. Concurrently with this operation, salt is being mined in another corridor. A one-mile-square area is assumed to be served by a waste shaft. The operations will be conducted in one quadrant of the mine at such a time that the salt mining is completely isolated from the disposal operations. Disposal operations personnel and equipment will use the mining shaft for ingress and egress, however.

Ventilating air will come down a compartment in the mining shaft, with a portion being split off into the disposal tunnel. The disposal tunnel air will travel completely around the quadrant and exit up the waste shaft. The air will be drawn from the shaft, through the hot cell, through an absolute filter, and up a 200-ft stack. In order

<sup>&</sup>lt;sup>34</sup>R. L. Bradshaw et al., Evaluation of Ultimate Disposal Methods for Liquid and Solid Radioactive Wastes. I. Interim Liquid Storage, ORNL-3128 (Aug. 7, 1961).

<sup>&</sup>lt;sup>35</sup>J. J. Perona et al., Evaluation of Ultimate Disposal Methods for Liquid and Solid Radioactive Wastes. II. Conversion to Solid by Pot Calcination, ORNL-3192 (Sept. 27, 1961).

<sup>36</sup> J. J. Perona et al., Evaluation of Ultimate Disposal Methods for Liquid and Solid Radioactive Wastes. IV. Shipment of Calcined Solids, ORNL-3356 (in press).

that ventilating air never passes a filled storage area before it reaches the current working area, the disposal operations will start at the most remote point and work back toward the shaft. The criteria of isolation and ventilation require that a double tunnel be driven completely around the quadrant and the rooms on the outside of the peripheral tunnel be excavated before disposal operations start.

Cost figures were calculated for disposal at a depth of 1000 ft for two conditions of stability: one with very small structural flow and  $2\frac{1}{2}\%$  dimensional closure due to thermal flow, and one with considerable structural flow and 100% thermal closure of the rooms. These figures for typical waste combinations are shown in Table 1.20 for waste ages at burial of 1, 3, 10, and 30 yr. The costs of developing peripheral tunnels and storage space are based on an assumed cost of \$2 per ton for salt removal. Shafts and life-of-shaft items were amortized over the period of time required to fill the entire square mile  $(8\frac{1}{2})_2$  yr for 1-yr cooling and  $2\frac{1}{2}\%$  closure to 89 yr for 30-yr cooling and 100% closure).

Total costs ranged from  $6\times10^{-3}$  mill/kwh<sub>e</sub> for 100% room closure and 30-yr-cooled wastes to  $30\times10^{-3}$  mill/kwh<sub>e</sub> for 1-yr cooling and  $2\frac{1}{2}\%$  closure. Salt removal was 60 to 85% of the total cost.

Table 1.20. Costs of Ultimate Storage of Calcined Wastes in Salt at a Depth of 1000 ft

Waste		Costs, Mi	lls/kwh <sub>e</sub>
Age (yr)	Waste Combination	2.5% Closure	100% Closure
		× 10 <sup>-2</sup>	× 10 <sup>-2</sup>
1	Reacidified Purex, 6-indiam; acidic Thorex, 6-indiam	3.06	1.60
3	- Acidic Purex, 6-indiam; acidic Thorex, 12-indiam	1.54	0.84
10	Reacidified Purex filled twice, 12-indiam; acidic Thorex, 12-indiam	1.25	0.70
30	Acidic Purex, 12-indiam; acidic Thorex, 24-indiam	1.00	0.60

#### RELATED COOPERATIVE PROJECTS

### Geologic and Hydrologic Studies by U.S. Geological Survey

The U.S. Geological Survey continued to operate eight continuous-record gaging stations and a network of 24 partial-record, base-flow, and crest-stage stations. These stations are being used to obtain information on base-flow and flood characteristics of streams in the area and for quality-of-water sampling.

A generalized geologic map of the Oak Ridge Reservation and vicinity at a scale of 1:31,680 was prepared by the U.S. Geological Survey and the U.S. Army Map Service for the Research and Development Division of the U.S. Atomic Energy Commission. The map shows locations of major geologic contacts and faults on a topographic base of the Oak Ridge Area.

The detailed geologic mapping of White Oak Creek basin was begun in April 1962, with largescale aerial photographs as a mapping base.

As a part of the detailed investigation of the hydrology of the White Oak Creek basin, four additional continuous-record stream-gaging stations and three crest-stage gages have been installed on White Oak Creek.

To obtain information regarding ground-water conditions in the Knox Dolomite and the massive limestone unit of the Conasauga Shale underlying Melton Hill, a 610-ft-deep well was drilled in May Several cavities were penetrated, the 1962. largest of which was 6-ft thick. The groundsurface altitude of the well is about 1180 ft, and the well extends 170 ft below Clinch River level. At the time of completion of the well the water level stood at a depth of 185 ft. By July the water level had declined to 320 ft. No pumping test has been made on the well, but indications, based on response to bailing during and after drilling, are that the well has a yield of less than 100 gal/min.

The Knox Dolomite underlying Chestnut Ridge is the major water-bearing unit in White Oak Creek basin. Ground-water discharge from this belt of Knox sustains the flow of White Oak Creek throughout the year. Three wells were drilled on Chestnut Ridge in June 1962 — one at the base of the ridge, one at an intermediate elevation, and one at the crest — to obtain information on quantity and movement of ground water in this area.

### Cooperation of Other Agencies in ORNL Studies

The research and development program of the Radioactive Waste Disposal Section of this Division is of special interest to various public and private agencies. Several study projects provide an opportunity for others to participate, both to supplement the Laboratory's research effort and to gain information and experience of value to the other agency. The ways in which another agency may cooperate include assignment of on-loan personnel as temporary additions to the ORNL staff, performance of specific work under cooperative agreements to augment ORNL programs, work authorized under ORNL subcontracts and performed by the contracting agency, or coordination of related work projects with ORNL projects for mutual benefit.

Clinch River Study. - This is a cooperative study under the guidance of the Clinch River Study Steering Committee, which coordinates arrangements for participation of the agencies represented by membership on the Committee. These include, in addition to ORNL, the U.S. Geological Survey, the U.S. Public Health Service, the Tennessee Valley Authority, the Tennessee Department of Public Health and Stream Pollution Control Board, the Tennessee Game and Fish Commission, the Divisions of Reactor Development and Biology and Medicine of the U.S. Atomic Energy Commission, Washington, D.C., and the Biology Division of the U.S. Atomic Energy Commission, Oak Ridge Operations. The activities of the Steering Committee participation by the several agencies, and the results during the past year are presented in a preceding section (see "Clinch River Studies," this chapter).

Disposal in Salt Formations. — Agencies participating in this program during the past year have included the Geotechnical Corporation of Dallas, Texas, under an ORNL subcontract; the Department of Sanitary Engineering of the University of Texas, by cooperative agreement; and the Carey Salt Company of Hutchinson, Kansas, ORNL subcontractor. The results of this cooperative program are given in a preceding section (see "Disposal in Salt Formations," this chapter).

Disposal in Deep Wells. — The subcommittee of the Committee on Research of the American Association of Petroleum Geologists continued its study of the deep sedimentary basins of the United States to identify those best suited to radioactive waste disposal. Cooperation between this group, the U.S. Geological Survey, and the Oak Ridge National Laboratory has been active but informal. Somewhat more formal collaboration has been developed between the Laboratory, the U.S. Geological Survey, the U.S. Bureau of Mines, and the University of California for the planning and eventual operation of certain field experiments and demonstrations in the disposal of liquid wastes into permeable formations. The U.S. Geological Survey is at present searching for sites suitable for certain small-scale experiments on the injectivity of these wastes and on ion exchange phenomena under field conditions.

#### Visiting Investigators from Abroad

During the year, two "noncitizen guests," were on assignment as temporary members of the research staff of the Waste Disposal Section. A. L. Mohan of India and C. Gailledreau of France have completed their assignments. A. L. Mohan's studies on the removal of ruthenium from solutions by mineral sorption were reported last year. The C. Gailledreau's studies have been concerned with the mechanism and kinetics of strontium removal by mineral columns and with the use of ion exchange and paper chromatography in the study of ruthenium complexes in waste streams.

#### **Nuclear Safety Review**

One member of the Section served on the staff of Nuclear Safety as assistant editor. During the year, several individuals in the Section contributed review articles which were published under the category, "Consequences of Activity Release."

### Committee Work

American Standards Association. — As described in the report a year ago, <sup>38</sup> several members of the staff of the Radioactive Waste Disposal Section have continued to serve on ASA committees and

<sup>&</sup>lt;sup>37</sup>E. G. Struxness et al., Health Phys. Div. Ann. Progr. Rept. July. 31, 1961, ORNL-3189, pp 37-38.

<sup>&</sup>lt;sup>38</sup>E. G. Struxness et al., Health Phys. Div. Ann. Progr. Rept. July 31, 1961, ORNL-3189, p 79.

working groups. Two are members of ASA Sectional Committee N5, "Nuclear Fuel Cycle Engineering," as designated representatives of the American Society of Civil Engineers and of the Health Physics Society. These two and four others of the Section staff have participated in the work of ASA Subcommittee N5.2, "Radioactive Waste Disposal," and of Working Group N5.2.2 on "Site Selection Criteria."

International Commission on Radiological Protection - Committee V. - The Section leader served on Committee V - Handling of Radioisotopes and Waste Disposal with Special Tasks on Defining Site Criteria.

American Public Health Association Committee on Radiological Health. — One member of the Section has continued to serve on the APHA Program Area Committee on Radiological Health and has attended two meetings of the Committee. The purpose of the Committee is to assist public health departments to obtain and interpret information and to develop sound state and local programs of radiological health. This is done by means of information memoranda, program guides, reviews of existing or proposed laws and regulations pertaining to radiation control, and recommendations regarding training of public health personnel in radiological health.

AEC Advisory Committee on Deep-Well Disposal. — Two staff members have served on the AEC Advisory Committee on Deep-Well Disposal. This committee is advising the AEC in the coordination of effort in the Deep-Well Disposal Program and is reviewing plans for engineering-scale field tests.

ASCE - Committee on Sanitary Engineering Aspects of Nuclear Energy. - The Section leader served as a member of the Committee on Sanitary Engineering Aspects of Nuclear Energy of the American Society of Civil Engineers.

ORNL Committees and Special Working Groups. — One member of the staff has served on the "Laboratory Director's Ad Hoc Water Committee," This committee was organized to consider expansion of work at ORNL to cover saline water conversion and to make recommendations regarding the feasibility of setting up a National Water Laboratory at ORNL. During the past year an agreement has been signed with the Office of Saline Water, Department of the Interior, providing for ORNL

participation in the Saline Water Conversion Program.

Two sanitary engineers of the staff have been designated to provide advisory service to engineering design groups regarding protection of the potable water supply of the Laboratory against "crossover" contamination where it is necessary to lay water mains and waste pipes across one another or in close proximity. Upon request of the design engineers during the year, a number of designs have been reviewed and discussed in the preliminary stages, and final plans have been checked for approval of the methods of protection provided.

#### Participation in Educational Programs

The Section leader gave two 2-hr lectures in the AEC Fellowship Course in Radiological Physics, conducted by the Education and Training Section of the Division at Vanderbilt University in Nashville, Tennessee. Also during the ten weeks of field training in this course at ORNL, two students per week were assigned to work one week in the Waste Disposal Section under the supervision of two staff members.

In the Health Physics Course primarily for foreign students conducted by the Health Physics Division in the Oak Ridge School of Reactor Technology (ORSORT), four members of the Section gave six lectures and a field tour on radioactive waste problems and waste disposal studies at ORNL. Also, the course in physical geology conducted by ORSORT, given again by one member of the Waste Disposal staff, comprised approximately 30 lectures to the class of about 60 students, some American and some from other countries.

Four lectures and a field tour of the Laboratory's waste disposal facilities and ecological research activities were provided at ORNL by the staff of the Section as part of the course conducted by the U.S. Public Health Service on "Reactor Safety and Environmental Health Problems," in September 1961 and May 1962.

Two staff members gave lectures on "Radiation Problems Related to Public Health" for the College of Education, University of Tennessee, as part of the program in public health education for teachers.

### Radiation Ecology

S. I. Auerbach

#### WHITE OAK LAKE BED STUDIES

D. A. Crossley, Jr. C. L. Corley
P. B. Dunaway R. J. Pryor
S. V. Kaye H. E. Childs, Jr. 
L. L. Smith W. L. Tietjen 
W. K. Willard

Transfer of Fission Products Through Plant

D. A. Crossley, Jr. C. L. Corley W. L. Tietjen

to Insect Food Chains

The movement of fission products through natural ecological systems is being investigated through studies on the soil-plant-herbivorous insect-predaceous insect food chain. This work contributes to basic ecology through information on the flow of materials and energy in ecosystems, and also is of immediate practical value in understanding the environmental behavior of hazardous radionuclides. Work previously reported<sup>3</sup> has shown the extent to which insects accumulate Sr<sup>90</sup> and Cs<sup>137</sup>, estimated the amounts of these radionuclides which pass through insects in the food chain, and estimated the annual consumption of plants by insects. Work reported here, performed in the summer of 1961, involved further sampling of plants and insects on White Oak Lake bed to meet two objectives: (1) to obtain reliable data on the herbivore-predator transfer of radionuclides, and (2) to detect changes in radio-

Results of radioanalyses performed on 1961 collections are presented in Table 2.1, which compares 1961 results with those obtained from the 1958 samples. For both Sr<sup>90</sup> and Cs<sup>137</sup>, the plant and herbivorous insect samples indicate no significant change in radionuclide concentration over the 3-yr interval. Previous conclusions concerning feeding rates for the insect community and amounts of radionuclides transferred through plant-insect food chains thus remain unaltered. Coefficients of variation in radionuclide content are smaller for insects than for vegetation (14 vs 45 for  $Cs^{137}$ , 18 vs 32 for  $Sr^{90}$ ). This is indicative that herbivorous insects function as integrating samplers by feeding over a large area, so that local variation in radionuclide content in plants is minimized. Several samples of predaceous insects were taken, but all of them had to be composited for estimates of radionuclide concentration because of the small masses involved. Results (Table 2.1) show less Cs137 and Sr<sup>90</sup> in predaceous insects in 1961 than in 1958, but the discrepancy is probably due to less. reliable sampling in 1958. The 1961 results show a decrease in radionuclide concentration in transfer from herbivore to predator. This decrease is greater for Sr<sup>90</sup> than for Cs<sup>137</sup>. Previous findings for herbivorous insects were that they eliminate strontium more rapidly than cesium and thus reach lower equilibrium concentrations for strontium. Evidently similar phenomena occur in the herbivore to predator transfer of strontium and cesium. If the same model used for calculating food consumption by herbivores is indeed applicable, then it may be estimated that 4% of the radionuclides accumulated by herbivores pass

nuclide distribution in the ecosystem which might have occurred since the last major sampling in 1958.

ORINS research participant.

<sup>&</sup>lt;sup>2</sup>Temporary summer employee.

<sup>&</sup>lt;sup>3</sup>D. A. Crossley, Jr., and H. F. Howden, *Ecology* **42**, 302 (1961).

Table 2.1. Comparison of 1958 and 1961 Estimates of Cs <sup>137</sup> and Sr <sup>90</sup> Concentrations in the Plant-to-Insect Food Chain on White Oak Lake Bed

Mean ± standard error

	Сs <sup>137</sup> ( <i>µ</i> µ	per g of dry weight)	Sr <sup>90</sup> (μμο	per g of dry weight)
	1958	1961	1958	1961
Soil	7300 <sup>a</sup>	ь	450 <sup>a</sup>	ь
Plant (leaves)	110 ± 22 (4) <sup>c</sup>	160 ± 32 (5)	700 ± 188 (4)	690 ± 91 (6)
Herbivorous insects	87 (1)	78 ± 4.8 (5)	91 (1)	117 ± 9.5 (5)
Predaceous insects	97 (1)	73 (8 samples lumped)	81 (1)	55 (8 samples lumped

<sup>&</sup>lt;sup>a</sup>Soil values based on grand means from core samples.

through predaceous insects. By contrast, it was estimated that 6% of the radionuclides accumulated by plants pass through herbivorous insects.

Soils were not sampled in 1961, owing to the large number of samples and careful treatment that past experiences show would be necessary. Soil samples studies in 1956–1958 suggested a 50% loss of Sr<sup>90</sup> in 1.25 yr, <sup>4</sup> so that estimated soil concentrations of this radionuclide should be only about 20% of the 1958 values. The fact that no change occurred in Sr<sup>90</sup> concentration in vegetation does not necessarily suggest no change in concentration in soil, since ions competing with strontium will also have been lost. Probably the plants and animals now contain a greater fraction of the total radionuclides in the system than was estimated in 1958.

### Bioaccumulation of Radionuclides by Mammals Resident on Upper White Oak Lake Bed

S. V. Kaye H. E. Childs, Jr. P. B. Dunaway W. K. Willard

The upper White Oak Lake bed is an important area for radiation ecology research, because it is one of the few large areas available in the United States which is thickly vegetated and has radiation fields ranging as high as 2 to 5 rads per day from fission products in the soil. In the first large sample of wild mammals from this area (collected August 1961), significant concentrations of ten radionuclides were detected in the carcasses. Five species were represented in the sample, and the whole carcass (less GI tract) was prepared for radioassay for each specimen:

Number of Specimens Assayed
10
5
7
2
2
_
26

The nuclides Sr<sup>90</sup> and Co<sup>60</sup> were found in all animals; Ru<sup>106</sup> and Cs<sup>137</sup> were found in all animals except one. A distribution of the concentrations of these four radionuclides is shown in Fig. 2.1. The occurrence of Cs<sup>134</sup>, Zn<sup>65</sup>, Zr<sup>95</sup>-Nb<sup>95</sup>, and Ba<sup>140</sup>-La<sup>140</sup> was limited to a smaller number of the animals. All the isotopes mentioned except Ba<sup>140</sup>-La<sup>140</sup> have previously

<sup>&</sup>lt;sup>b</sup>No samples taken.

<sup>&</sup>lt;sup>C</sup>Numbers in parentheses indicate number of samples.

<sup>&</sup>lt;sup>4</sup>S. I. Auerbach et al., Health Phys. Div. Ann. Progr. Rept. July 31, 1960, ORNL-2994, p 156.

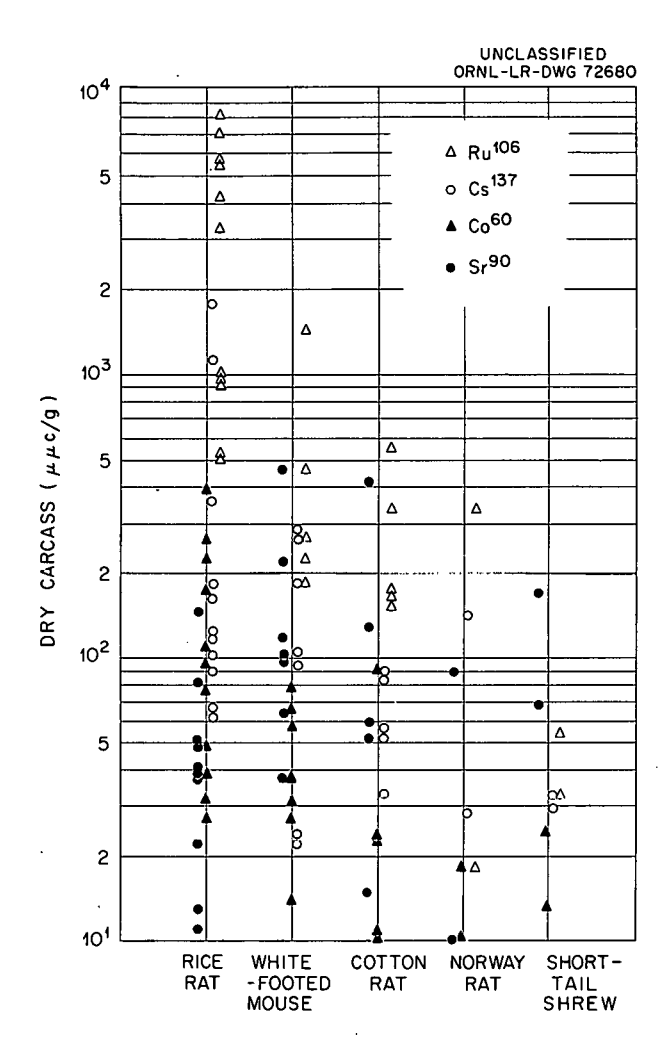


Fig. 2.1. Distribution of Concentrations of Radionuclides in WIId Small Mammals from Upper White Oak Lake Bed.

been found in mammals from the lake bed.<sup>5</sup> The presence of Ba<sup>140</sup>-La<sup>140</sup> can no doubt be attributed to waste released at ORNL and not to nuclear testing, because the sample collections antedate the recent atmospheric test series by Russia and the United States.

Ruthenium-106 concentrations in whole carcasses tended to be higher than the concentrations of the other isotopes and were highest in rice rats (5  $\times$  10<sup>2</sup> to 8  $\times$  10<sup>3</sup>  $\mu\mu$ c per g of dry carcass – Fig. 2.1). These concentrations of

Ru<sup>106</sup> in rice rats are explained on the basis of the environmental behavior of released ruthenium and the semiaquatic habitat requirements of rice rats. The Ru<sup>106</sup> seeps through the Conasauga shale formation underlying the liquidwaste pit system and reaches the lake bed in a highly mobile chemical state. This radioruthenium can be readily detected in surface seeps on the upper lake bed; these surface seeps constitute an ideal habitat for rice rats. The high Ru<sup>106</sup> in rice rats from White Oak Lake bed indicates that they confine most of their feeding to the seepage areas.

#### In Vivo Dosimetry with Miniature Glass Rods

S. V. Kaye R. J. Pryor

The measurement of external dose accumulated by wild mammals in radioactive areas is necessary in evaluating the effects of chronic exposure to ionizing radiation. This dose measurement is complicated by the heterogeneous radiation field on White Oak Lake bed and the movements of animals between high- and low-radiation areas. Silver metaphosphate glass rods (fluorods) appeared to be ideal dosimeters for this purpose, because they are only  $1 \times 6$  mm, they integrate doses from a few rads to thousands of rads, and they can be implanted in the mammals.

These dosimeters give accurate estimates of dose when the energy spectrum is above a certain threshold, but they have a peak energy-dependent response at ~50 kev. Unshielded glass dosimeters were exposed to the radiation field on the lake bed to determine whether the photon energies were high enough to produce a linear or nearlinear radiophotoluminescence response. A linear response would lend strong support to the hypothesis that unshielded fluorods can be used for accurate integration of in vivo dose in an area contaminated by mixed fission products. Several experiments were designed to test this hypothesis with Bausch and Lomb high-Z rods, Toshiba low-Z rods, pocket ionization chambers (PIC's), and the ORNL film badge dosimeter.

In one series of experiments, five high-Z and five low-Z glass rods were attached to the undersides of 0.125-in.-thick Plexiglas platforms placed about 1.2 in. above the soil surface in several different locations. The rods were contained separately in tiny nylon cylinders (wall thickness

<sup>&</sup>lt;sup>5</sup>S. V. Kaye and P. B. Dunaway, *Health Phys.* 7, 205-17 (1962).

was 0.047 in.) which were designed for in vivo One-hour dose readings were made with shielded and unshielded PIC's several times while the rods were being exposed. The shielding material was 0.040-in.-thick tin; this results in a PIC response which is linear and independent of photon energy down to  $\sim 25$  kev.<sup>6</sup> The cumulative doses from continuous exposure of fluorods during the days that 1-hr PIC readings were taken are shown in Table 2.2. Five rods each of Bausch and Lomb high-Z composition and Toshiba low-Z composition were exposed in seven different locations. In each case the high-Z rods recorded a higher dose than the low-Z rods, ranging from 15.0 to 51.4% higher. Obviously, the higher doses by the high-Z rods are due to energy dependence at low photon energies. Actually the high-Z rods are much more energy dependent than the unshielded PIC's and thus are even better indicators of the presence of low energies than the unshielded PIC's. The results of these experiments indicated that there are enough low energies on White Oak Lake bed to preclude the use of high-Z rods in favor of the less energy dependent low-Z rods for dosimetry.

In further studies the two kinds of fluorods were irradiated at three different dose levels with

gamma rays from an Ra<sup>226</sup> calibration source to test the relative sensitivities of the rods. These results are plotted in Fig. 2.2 and demonstrate a greater response (2.15) of Toshiba glass to a given dose than Bausch and Lomb glass. This finding is in good agreement with the factor of 2.3 determined experimentally by Auxier et al., <sup>7</sup>

<sup>&</sup>lt;sup>7</sup>J. A. Auxier et al., Health Phys. Div. Ann. Progr. Rept. July 31, 1961, ORNL-3189, p 175.

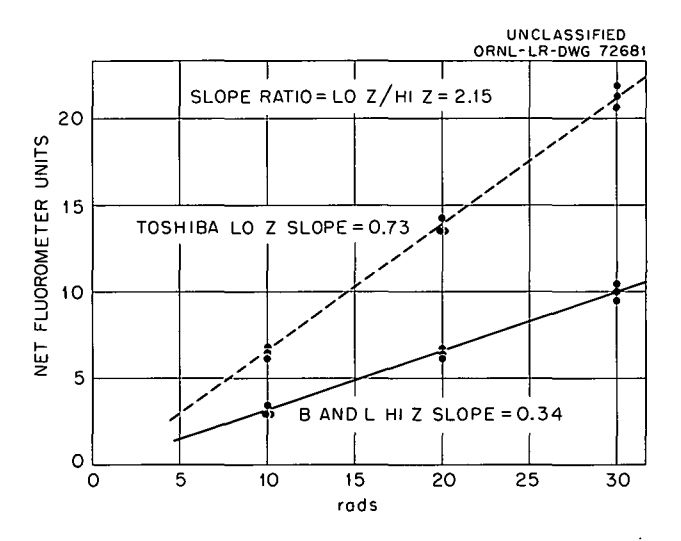


Fig. 2.2. Responses of Toshiba Low-Z Fluorods and Bausch & Lomb High-Z Fluorods to Known Doses of Gamma Rays from an Ra<sup>226</sup> Calibration Source.

٥ <sub>F</sub> .	w.	Sanders, J. A	١.	Auxier,	and	Ţ.	s.	Cheka,	Health
Phys.	2,	308-9 (1960)	).	•		•		•	

Table 2.2. Responses of Toshiba Low-Z Fluorods and Bausch & Lomb High-Z Fluorods to Mixed Radiations on Upper White Oak Lake Bed

Location	Low-Z Dose (rads ±standard deviation)	High-Z Dose (rads ±standard deviation)	Percent Difference $\left(\frac{\text{High-}Z - \text{Low-}Z}{\text{Low-}Z} \times 100\right)$		
1	13.3 ±0.47	16.0 ± 1.2	+20.3		
2	11.3 ±0.99	17.1 ± 2.7	+51.4		
3	$14.0 \pm 0.69$	16.1 ± 2.8	+15.0		
4	16.7 ±0.99	22.4 ±0.86	+34.2		
5	17.4 ± 1.5	25.6 ± 1.6	+47.2		
6	25.6 ± 1.4	32.3 ± 4.2	+30.1		
7	12.1 ±0.95	15.2 ± 2.1	+25.7		

and lends strong support for the use of Toshiba low-Z glass rod dosimeters over the use of Bausch and Lomb high-Z glass rods.

Standard ORNL filtered-film packets were paired with Toshiba low-Z fluorods and exposed on the upper lake bed. The doses estimated independently by the two types of dosimeters are shown in Table 2.3. The percent differences between film estimates and glass rod estimates range from -25.7 to +31.3 and signify the range of agreement by the two kinds of dosimeters. These results are considered good in view of the fact that they were conducted under field conditions, which included bright sunlight and darkness, daily temperature gradients of about 30°F, and one period of rain.

# Field Studies of Mammals Labeled with Radioactive Tags

S. V. Kaye G. E. Cosgrove P. B. Dunaway R. J. Pryor

Fourteen laboratory-reared cotton rats of wild parents were tagged with 100- $\mu$ c Ta<sup>182</sup> wires and released into the six 100-m<sup>2</sup> pens on Mammal Study Area No. 4 during January and February of

1962. A description of these pens and their intended use for radiation effects studies on mammals have been reported elsewhere. The objectives of this labeling experiment were to determine the effectiveness of the pens for retaining animals and to evaluate the intraspecific behavior of wild cotton rats released into the pens.

Tantalum-182 wires measuring  $1 \times 6$  mm were encapsulated in nylon cylinders of the same kind utilized in the glass rod experiments reported above. The method of insertion was similar to that reported by Kaye. Nylon cylinders containing the  $Ta^{182}$  wire were inserted subcutaneously by passing them through a hypodermic needle inserted between the scapulae. All of the released cotton rats were found dead in the pens from 4 to 14 days after release. Although the winter weather had been very severe during this period, complete mortality did not seem a likely result for animals which had been preconditioned to cold weather for six weeks in an unheated outdoor shed. Since the daily movements

Table 2.3. Comparison of Dose Estimates by Toshiba Low-Z Fluorods and ORNL Filtered-Film Packets Exposed on Upper White Oak Lake Bed

Location	Low-Z Glass Rod Dose (rads)	ORNL Filtered-Film Packet <sup>a</sup> (rads)	Percent Difference $\left(\frac{\text{Film - Low-}Z \text{ Glass}}{\text{Low-}Z \text{ Glass}} \times 100\right)$		
1	10.4	10.9	+ 4.8		
2	8.3	9.7	+16.9		
3	13.1	10.0	-23.8		
4	10.5	7.8	-25.7		
5	8.6	9.7	+12.8		
6	9.9	13.0	+31.3		
7	11.6	12.3	+10.6		
8 (control)	0	. 0	0		

 $<sup>^</sup>a$ E. D. Gupton of Applied Health Physics performed the film dosimetry.

<sup>&</sup>lt;sup>8</sup>S. I. Auerbach et al., *Health Phys. Div. Ann. Progr. Rept. July 31*, 1961, ORNL-3189, p 104.

<sup>9</sup>S. V. Kaye, Science 131, 824 (1960).

and activities of these animals in the pens were being studied by locating the Ta<sup>182</sup> wires, each of the animals was retrieved shortly after death. The livers of all 14 of these rats were found to be infested with cysts of larval tapeworms (Hydatigera taeniae formis), a species which requires a carnivorous intermediate host. The number of cysts per liver ranged from 4 to 67, and the cysts were 45-60 days old. Each cyst contained one larval worm.

Since the rats had not lived in the pens long enough to become infected by larval tapeworms which had developed to this size, it was felt that they must have become infected during their growth period in the animal colony. animals involved were offspring of three different mothers. One mother which had borne 11 of the infected rats was sacrificed, and no tapeworms were found. No tapeworm cysts were found in any other autopsied rats which had been reared in the laboratory. It was recalled that a feral cat had been discovered once in the animalconditioning shed. Ten cats from the adjacent area were trapped, sacrificed, and examined for parasites. Seven of the ten harbored adult Hydatigera taeniae/ormis in numbers ranging from 1 to 25. The conclusion reached was that the 14 cotton rats had ingested ova or segments of the tapeworm from a cat, or cats, with subsequent development of larval tapeworm cysts in the liver of the rats. If these animals had not been radiolabeled, it would not have been possible to have 100% retrieval of animals, nor would it have been possible to find the animals so soon after death. These two advantages of radiolabeling made possible the solution of what would have been a baffling biological problem. Although some of the animals survived as long as two weeks, none of them escaped from the pens. About 75 cotton rats subsequently have been stocked in the pens for various experiments. None of these animals has escaped, attesting to the efficiency of the pen structures for retaining animals.

# Hematology of Native Mammals on White Oak Laké Bed

P. B. Dunaway R. J. Pryor L. L. Smith S. V. Kaye

A study was initiated this year on the effects of chronic environmental radiation on the blood

of native small mammals living on White Oak Lake bed. Seasonal mean values for total erythrocytes (RBC) per cubic millimeter, total leukocytes (WBC) per cubic millimeter, differential counts, and hematocrits are being established. It is necessary to establish these counts because there is a paucity of hematological information for wild mammals, particularly for the small species.

Calibration and operating procedures for the Coulter electronic blood counter<sup>10</sup> were completed. Diluting solutions recommended for blood from humans and from laboratory rats and mice<sup>11-13</sup> were found to be unsatisfactory. A successful method was developed which consisted in initially diluting the blood sample with acetate-buffered saline. Subsequent treatment for erythrocyte or leukocyte counting utilized a gelatin or Triton X-100 (Rohm and Haas) solution. These solutions provided the required stability for determination of total counts and cell-size distribution.

Hematological measurements are shown in Table 2.4 for six species of the Cricetidae, the most important family of rodents in this area. important relationship was discovered for RBC number and volume in the Cricetidae. The number of erythrocytes per cubic millimeter is inversely related to the body weights of the species studied (Fig. 2.3). Mean erythrocyte volume is directly related to body weight (Table 2.4). Our incomplete results for other families of small mammals and a survey of the scanty data in the literature for other wild mammals indicate that this relationship is present in other taxa of mammals. This finding may be of great value to such fields as hematology, physiology, evolution, radiation biology, and radioecology.

Leukocyte numbers in the wild mammal populations exhibit wide variations, even within a species. Such variations are to be expected in mammals exposed to the stresses acting on a natural population. For instance, certain diseases can cause alterations in the WBC count. A cotton

<sup>&</sup>lt;sup>10</sup>Coulter Electronics, 590 West 20th Street, Hialeah, Fla.

<sup>&</sup>lt;sup>11</sup>G. Brecher, M. Schneiderman, and G. Z. Williams, Am. J. Clin. Pathol. 26, 1439-49 (1956).

<sup>&</sup>lt;sup>12</sup>W. J. Richar and E. S. Breakell, Am. J. Clin. Pathol. 31, 384-93 (1959).

<sup>&</sup>lt;sup>13</sup>C. F. T. Mattern, F. S. Brackett, and B. J. Olson, J. Appl. Physiol. 10, 56-70 (1957).

Table 2.4. Hematological Measurements for Six Species of Cricetid Rodents

	Mean Body Weight	Erythroc	ytes	T		
Species	(g) Mean Number (x 10 <sup>6</sup> /mm <sup>3</sup> )		Mean Volume (μ <sup>3</sup> )	Leukocytes (× 10 <sup>3</sup> /mm <sup>3</sup> )	Hematocrit (%)	
Eastern harvest mouse, Reithrodontomys humulis	$8.4 \pm 1.11 \ (4)^a$	12.36 ±0.689 (4)	39.5	4.5 (4)	51.0 (2)	
White-footed mouse,  Peromyscus leucopus	19.4 ±1.49 (30)	11.72 ±0.526 (29)	41.0	4.4 (29)	48.4 (24)	
Pine mouse, Microtus pinetorum	20.8 ± 2.40 (14)	10.22 ±0.709 (14)	42.5	7.6 (14)	42.9 (14)	
Rice rat, Oryzomys palustris	53.4 ± 5.98 (19)	8.04 + 0.345 (21)	60.7	4.5 (16)	48.8 (16)	
Cotton rat, Sigmodon hispidus	95.7 ±6.97 (76)	7.21 ±0.197 (76)	66.5	6.1 (72)	47.2 (72)	
Muskrat, Ondatra zibethicus	1283.6 ±150.59 (6)	5.79 ±0.415 (6)	74.0	18.5 (6)	42.8 (6)	

<sup>&</sup>lt;sup>a</sup>Number of variates in sample shown in parentheses.

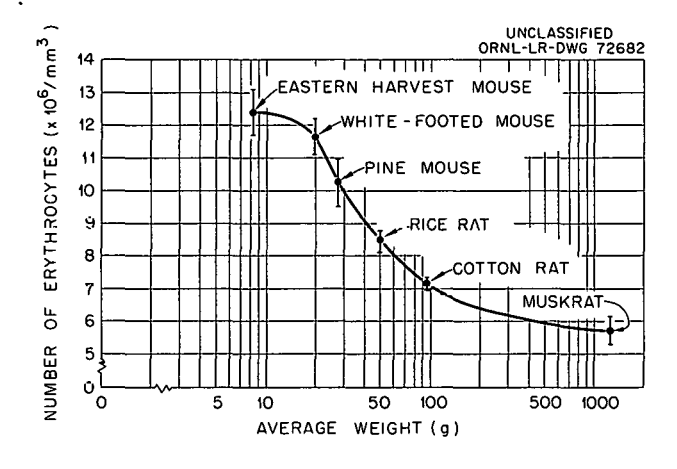


Fig. 2.3. Correlation Between Erythrocyte Number and Species Weight in Six Species of the Cricetidae.

rat with a squamous cell carcinoma had leukocytosis (19.3  $\times$  10<sup>3</sup> WBC), and a white-footed mouse infested with two parasitic bot-fly larvae also exhibited leukocytosis (13.7  $\times$  10<sup>3</sup> WBC). The average WBC number for the Cricetid rats and mice ranged from  $2.2 \times 10^3$  to  $7.6 \times 10^3$ , but the average count for muskrats was  $18.5 \times 10^3$ 

(Table 2.4). The muskrats may have been suffering from disease or some other stress, but they appeared to be in excellent condition. However, it may be that some larger mammals have higher Two woodchucks, Marmota monax WBC counts. (av wt, 4000 g), one opossum, Didelphis marsupialis (3003 g), five feral cats, Felis domesticus (2980 g), and one Norway rat, Rattus norvegicus (325.8 g) have been sampled. The WBC counts for these species were, respectively: 11.6, 16.0, 11.9, and 17.2 ( $\times$  10<sup>3</sup>). The reason for these relatively high WBC counts in these larger mammals may not be a simple size relationship. Larger species of mammals generally live longer than the smaller species and consequently have a longer time to develop diseases and parasite loads. The smallest species of mammals examined (least shrew, Cryptotis parva, av wt 4.9 g) had an average count of  $1.8 \times 10^3$  WBC.

Hematocrits ranged from 42.8 to 51.0% in the Cricetidae (Table 2.4). Hematocrits of the other species tested fell within this range except for the woodchucks and the opossum, which had hematocrits of 35.3 (av) and 38.0. The wood-

chucks are hibernators and had not been out of hibernation long (samples taken Mar. 14, 1962). Opossums belong to the primitive order Marsupialia.

Preliminary data for two species of lake bed mammals are shown in Table 2.5. The whitefooted mice from the lower lake bed were caught in areas with a radiation field of 15 mrads/hr or less. This species is found mainly in the relatively uncontaminated periphery of the lake bed. 14 The rice rats from the upper lake bed were taken from areas with radiation fields ranging from 50 to 500 mrads/hr. As pointed out in a previous section, the rice rats have the highest body burden of radionuclides and probably range into the most radioactive parts of the upper lake bed. Both the RBC and WBC counts of the white-footed mice from the uncontaminated and the lower lake bed were similar, but both the RBC and WBC counts of the rice rats from the upper lake bed were lower than the respective counts for the rice rats from uncontaminated areas. Although the results for the rice rats are suggestive, more species and greater numbers of mammals must be sampled.

#### Penned-Mammal Study

P.	в.	Dunaway	L.	L.	Smith
s.	٧.	Kaye	R.	J.	Pryor

This project encompasses studies of radiation effects on blood and supporting bioaccumulation and dose estimates for mammals penned on White Oak Lake bed. An important feature of this experiment is that animals of selected parentage, age, sex, size, and species can be introduced into a radioactive environment after preexposure blood sampling, marking, and implantation of glass rod dosimeters have been accomplished. The length of exposure time, as well as resampling and observation schedules, can be varied according to experimental design.

The first cotton rats for this project were released on June 13 and 15, 1962. About 1 yr of preparation was needed before stocking could be initiated. It was necessary to work out new techniques and procedures for electronic blood cell counting and glass rod dosimetry. A total of 21 pens were constructed, and a laboratory colony of known-history cotton rats was bred.

In the first phase of this project, one male and one female cotton rat from different parents were stocked in each of the seven pens on the upper White Oak Lake bed. Males and females from the same litters as the lake bed pairs were stocked in the six pens on Mammal Control Area No. 4, so that for each male or female on the lake bed, there was a littermate of the same sex on the control area. These pairs are allowed to reproduce in the pens so that the young are born to irradiated parents and receive in utero as well as postnatal irradiation. Blood samples are to be taken from the adults and young at monthly The glass rod dosimeters will be intervals. removed and the accumulated dose read when the animals are sacrificed at the end of the experiment. Tissues from the animals will be radioanalyzed so that bioaccumulation and dose rates can be estimated.

A soil core (1 in. in diam and 4 in. in depth) was taken at the intercepts of a 2.5-m grid within

Table 2.5. Erythrocyte and Leukocyte Total Counts for White-Footed Mice and Rice Rats on White Oak Lake Bed and Uncontaminated Areas

	RBC	$(\times 10^6/\mathrm{mm}^3)$		WBC ( $\times 10^3/\text{mm}^3$ )			
Species	Uncontaminated Areas	Lower Lake Bed	Upper Lake Bed	Uncontaminated Areas	Lower Lake Bed	Upper Lake Bed	
White-footed mouse	11.8 (19) <sup>a</sup>	11.8 (8)		3.9 (18)	3.8 (8)		
Rice rat	8.1 (11)		7.8 (12)	6.0 (5)		4.2 (12)	

aNumbers in parentheses indicate number of animals.

<sup>&</sup>lt;sup>14</sup>P. B. Dunaway and S. V. Kaye, Trans. 26th N. Amer. Wildl. Natl. Res. Conf., pp 167-85 (1961).

Table 2.6. Hematological Data for Penned Cotton Rats on White Oak Lake Bed and Control Area No. 4

		Weig	Weight (g)		RBC ( $\times 10^6/\text{mm}^3$ )		10 <sup>3</sup> /mm <sup>3</sup> )	Hematocrit (%)	
	Code Number	Prerelease	Two Weeks Postrelease	Prerelease	Two Weeks Postrelease	Prerelease	Two Weeks Postrelease	Prerelease	Two Week Postreleas
				White Oak Lal	ke Bed				
Males	63	112.9	91.6	6.84	6.57	4.5	8.1	43.5	47.5
	96	132.7	117.2	7.03	6.48	3.7	5.6	46.0	44.0
	. 137	131.2	130.3	7.81	6.99	8.2	10.8	50.0	45.0
	144	184.1	144.2	7.56	6.96	6.6	7.5	42.5	43.0
	151	139.4	128.4	7.85	7.64	3.5	6.1	51.5	52.0
	154	110.5	115.5	7.12	6.41	3.6	5.2	49.0	46.5
	Average	135.1	121.2	7.37	6.84	5.0	7.2	47.1	46.3
Females	98	121.0	127.8	6.59	5.31	5.9	9.1	42.0	34.5
	122	114.9	119.2	6.72	5.27	3.2	7.2		37.0
	125	121.0	112.6	6.84	6.40	3.5	7.1	44.0	40.5
	138	94.2	102.2	6.87	6.08	3.7	6.2	42.0	38.5
	142	102.7	114.0	6.51	6.00	3.5	5.6	41.5	40.5
	157	86.3	97.0	7.36	6.61	4.9	7.2	49.5	44.0
	160	92.6	89.6	6.51	5.88	2.6	6.0	43.5	41.0
	Average	104.7	108.9	6.77	5.94	3.9	6.9	43.8	39.8
	Average for both sexes	118.7	114.6	7.05	6.35	4.4	7.0	45.4	43.1
				Cantrol Area	No. 4			•	
Males	97	153.5	127.9	7.11	6.50	3.4	5.9	45.0	43.5
	139	115.5	106.7	8.49	7.04	3.5	2.3	50.0	39.5
	145	137.8	108.6	7.11	6.91	6.8	6.0	47.5	45.0
	152	139.1	119.8	7.72	7.07	4.8	7.7	51.0	43.5
	Average	136.5	115.8	7.61	6.88	4.6	5.5	48.4	42.9
Females	123	118.2	138.5	6.32	5.49	3.7	8.3	43.0	35.0
	128	97.9	•	6.77	6.15	3.5	3.6	44.0	39.0
	140	105.4		6.47	5.94	3.6	3.6	41.5	37.5
	141	100.3	107.2	6.84	6.31	2.2	7.4	44.5	41.5
	159	79.4	92.9	6.26	6.74	4.5	5.5	43.5	42.0
	161	97.8		6.51	5.75	3.2	12.3	41.5	36.0
	Average	99.3	112.9	6.53	6.06	3.4	6.8	43.0	38.5
	Average for both sexes	120.3	114.5	6.96	6.39	3.9	6.3	45.2	40.2

each pen on the lake bed. The top inch of each of the nine cores from each pen was removed, and these samples were composited, as were the nine bottom 3-in. samples from each pen. Vegetation cover maps were made for all pens, and samples of the dominant species from each cover type were taken. Radioanalytical data from the soil and vegetation samples will be utilized for investigation of soil-plant-animal transfer of radionuclides.

A flood on June 27 inundated six of the seven pens on the lake bed and necessitated removal of the animals. All 12 animals from the flooded pens were retrieved alive. Since it was necessary to remove the animals, it was decided to take blood samples at that time (two weeks postre-Accordingly, 13 individuals from the lease). lake bed and 10 from the control area were sampled and returned to the pens. Hematological data for these specimens are shown in Table 2.6. It is immediately obvious that the RBC decreased and the WBC increased in all lake bed animals. The RBC also decreased in all but one of the control animals, and the WBC increased in seven out of ten of the controls. The decrease in average hematocrit percentages reflects the decrease in RBC. The reasons for the decrease in erythrocytes and increase in leukocytes are not apparent at present, but these changes probably reflect responses of physiologic adaptive mechanisms to the environment.

The average weight decreased in both groups, with most of the weight loss occurring in the heaviest males. Weight loss was a common phenomenon in adult rats released into the pens during earlier experiments. Most of the females in the present experiment gained weight, which may be attributable to pregnancy.

Significant differences are not apparent in the results for the cotton rats on the radioactive lake bed and the nonradioactive control area. However, this experiment was designed to continue for several months in the expectation that effects of chronic radiation on the blood, if they occur, may not be manifested in a short time. If effects do appear, they may be detected during the monthly sampling schedule.

### FOREST STUDIES

J. S. Olson	C. L. Corley			
D. A. Crossley, Jr.	R. M. Anderson			
Martin Witkamp	G. J. Dodson			
H. D. Waller	W. C. Cate			
J. P. Witherspoon <sup>15</sup>				

### Analog Computer Model for Biomass and Cs <sup>137</sup> in a Herbaceous Ecosystem <sup>16</sup>

J. S. Olson

Analog computer models of ecological systems simulate the development of the system and the transfer of elements and isotopes within it. The accumulation of biomass and energy is important in the establishment or reestablishment of plants and animals on areas bared by natural or artificial disturbances, including erosion, flooding, sedimentation, fire, and perhaps blast or radiation from nuclear weapons. The transfer of elements within such a system is needed to attain and maintain its nutrient status. The pathways and rates of nutrient transfer also help regulate the redistribution of radioactive contaminants in the environment.

Methods described earlier<sup>17-19</sup> have been used to develop an analog "Ecological Computer, Organizer, and Simulator" (ECOS-A). Data from Auerbach et al.,<sup>20</sup> DeSelm and Shanks,<sup>21</sup> and Crossley and Howden,<sup>22</sup> based on studies of the

<sup>15</sup> ORINS Fellow.

<sup>16</sup> The aid of E. R. Mann and O. W. Burke of the Instruments and Controls Division in the use of the ORNL Analog Computer Facility is gratefully acknowledged.

<sup>&</sup>lt;sup>17</sup>R. B. Neel and J. S. Olson, Use of Analog Computers for Simulating the Movement of Isotopes in Ecological Systems, ORNL-3172 (1962).

<sup>18</sup> J. S. Olson, "Analog Computer Models for Movement of Nuclides Through Ecosystems," Radioecology. Proceedings of the First National Symposium on Radioecology, in press.

<sup>&</sup>lt;sup>19</sup>J. S. Olson et al., Health Phys. Div. Ann. Progr. Rept. July 31, 1961, ORNL-3189, pp 124-28.

<sup>&</sup>lt;sup>20</sup>S. I. Auerbach et al., Health Phys. Div. Ann. Progr. Rept. July 31, 1960, ORNL-2994, pp 147-56.

<sup>&</sup>lt;sup>21</sup>H. R. DeSelm and R. E. Shanks, "Accumulation and Cycling of Organic Matter and Chemical Constituents During Early Vegetational Succession on a Radioactive Waste Disposal Area," Radioecology. Proceedings of the First National Symposium on Radioecology, in press.

<sup>&</sup>lt;sup>22</sup>D. A. Crossley and H. F. Howden, *Ecology* **42**, 302-17 (1961).

drained bed of White Oak Lake, have suggested certain magnitudes for accumulation of biomass and transfer of Cs<sup>137</sup>. Simplifications have been made for illustrative purposes, so that correspondence between the model and detailed behavior of this or any other specific ecosystem is not to be expected. Relations typical of a large class of herbaceous systems in temperate climates can be seen, but differences among these systems would depend on changes in certain parameters and elaborations of the general model.

Figure 2.4a illustrates a delay in the production P of vegetation during its first year of establishment on a new bare area which is not preenriched with nutrients. (Actually, White Oak Lake bed was enriched with nitrates from fuel processing effluents prior to drainage of the lake, and showed high early production like that illustrated in an earlier report. <sup>23</sup>) A high positive feedback of production rate was assumed, proportional to vegetation and food energy already accumulated. This feedback accounts for the faster buildup in production in second and later growing seasons.

A maximum upper limit in productivity is assumed, which is 11 g m<sup>-2</sup> day<sup>-1</sup> "gross" pro-("Gross" production excludes any photosynthesis which is immediately counterbalanced by respiration rates that increase in direct proportion to photosynthetic rates.) The upper limit is self-imposed by the ecosystem's interception of all available light by different strata of species and leaves. Net production falls below "gross" photosynthetic rate due to an amount of respiration, R, which is represented in the model and computer circuit by a negative feedback. Here R is assumed directly proportional to total accumulated above-ground plant biomass, Accumulated "gross" and net production  $[\int_{t} P dt, \int_{t} (P - R) dt]$  over a series of growing seasons are represented by the ascending steps in Fig. 2.4b.

The earlier restriction to models with differential equations with constant coefficients has been relaxed. A servomultiplier was used to make the transfer rate from vegetation to litter fluctuate with season, as in the case of actual seasonal litter fall,

$$L_1 = k_{m16} M_1 (1.2 + \cos \omega t) / 1.2$$
, (1)

where

L<sub>1</sub> = instantaneous rate of litter fall and death of standing plant tissue,

M<sub>1</sub> = mass per unit area of above-ground vegetation,

 $k_{m16}$  = transfer rate of mass to compartment 6 as a fraction of  $M_1$ ,

 $(1.2 + \cos \omega t)/1.2 = \text{function varying from } \frac{1}{6} \text{ to}$  to  $\frac{11}{6}$  of the average rate.

As intended, in order to simulate the killing of vegetation by autumn frost, the maximum of  $L_1$ (Fig. 2.4c) falls between that of  $M_1$  (Fig. 2.4d) (late summer) and that of  $\cos \omega t$  (January 1). The amount of dead organic matter (M6) that accumulates before production approximately balances decay is governed by the rates of degradation by microorganisms,  $K_{m67}$ , and direct incorporation of organic matter into mineral soil,  $K_{m68}$ . These rates are here taken as 0.5 and 0 for simplicity. A seasonal oscillation around this steady state is maintained. Damped oscillations in root biomass  $M_2$  (Fig. 2.4d) result from the lag in food storage and the export of food from roots. to tops in the spring.

Results of Crossley and Howden<sup>24</sup> imply very rapid turnover of biomass as well as radioisotopes by herbivorous and predatory insects (M<sub>3</sub> and M<sub>4</sub>). If their biomass were regulated in proportion to the total vegetation biomass, they would show annual oscillations lagging slightly after those given for M<sub>1</sub>. Actually, insect biomass averaged 300 mg of dry weight per m<sup>2</sup> throughout the summer, which suggests that it may be regulated by production rates, and amounts of tender new growth and other factors besides total plant biomass.

On freshly deposited sediments, low in initial content of humus, an accumulation of both rapidly decomposing and slowly decomposing organic compounds would take place. Levels and rates of accumulation would be regulated by decomposition rates of microorganisms acting on both the unincorporated and incorporated organic debris. <sup>25</sup>

In areas previously contaminated by Cs<sup>137</sup> from radioactive waste, or contaminated suddenly as

<sup>&</sup>lt;sup>23</sup>R. B. Neel and J. S. Olson, op. cit., Fig. 19.

 $<sup>^{24}</sup>$ D. A. Crossley and H. F. Howden, op. cit., pp 310-12.

<sup>&</sup>lt;sup>25</sup>R. B. Neel and J. S. Olson, op. cit., Figs. 17-20.

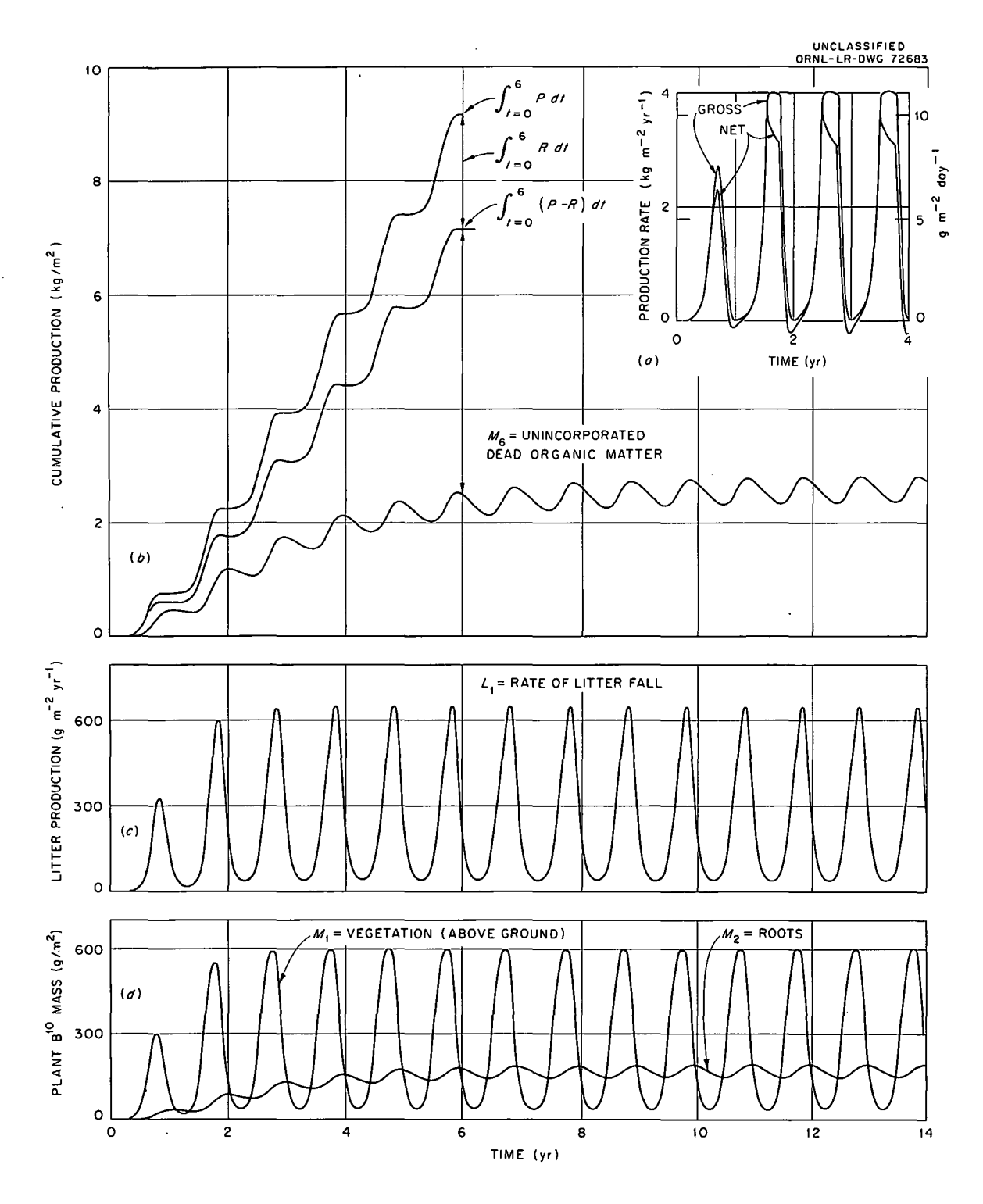


Fig. 2.4. Production in a Model Herbaceous Ecosystem. (a) Instantaneous rates of "gross" production P and net production (P-R) before and after approaching an upper limiting rate. (b) Cumulative production of P, R, and P-R.  $M_6$  is dead organic litter materials not yet decomposed or incorporated physically into mineral soil. (c) Instantaneous rate of litter fall,  $L_1$ . (d) Biomass of vegetation tops,  $M_1$ , and Roots,  $M_2$ .

in the area downwind from a surface burst of a thermonuclear bomb, Cs137 activity in soil would have maximum values at or near time t = 0. It would decrease at a rate controlled mainly by radioactive decay (Fig. 2.5a). Only a few percent of the total Cs137 (here about 2.5%) seems to be "available" for extraction with neutral ammonium acetate. The "available" fraction can probably be slowly replenished by loosely fixed Cs<sup>137</sup> on mineral lattice edges but only to a very slight extent from ions trapped between clay layers. 26 Some redistribution would take place into lower horizons of the soil.<sup>27</sup> However, complete removal of Cs<sup>137</sup> atoms from the profile normally would be slight, barring erosion of soil particles at the upper surface.

Lags in the promptness of maximum  $Cs^{137}$  concentration along the chain of transfer from soil to roots to foliage to herbivores and predators are shown in a normalized graph of radioactivity (Fig. 2.5b). The absolute levels of plant activity in  $\mu c$  per g of dry weight decrease by a factor of 0.1 to 0.3 in transfer from roots to tops, <sup>28</sup> and by a factor of about 0.5 in transfer to insects. <sup>29</sup>

The Cs<sup>137</sup> per unit area in biological components is the product of (isotope per g of material) and (g per m<sup>2</sup> of ground surface), and would show seasonal oscillations as well as slow radioactive decay (Fig. 2.6b). The fall of radioactive plant materials (Fig. 2.6a) to the ground surface would provide a potential reservoir of contaminated plant nutrients. These conceivably might be absorbed by surface roots in addition to the Cs<sup>137</sup> subsequently absorbed from mineral soil, but such recycling is not incorporated in the model illustrated here.

# Arthropod Populations Associated with Decaying Leaf Litter

D. A. Crossley, Jr. C. L. Corley

Arthropod populations which are instrumental in the breakdown of fallen-leaf litter are being studied with litter bag techniques. 30 Different types of leaf litter, enclosed in nylon net bags, can be placed in different forest types, and developing arthropod populations can be extracted from the bags with Berlese techniques. A previous report 31 dealt with gross numbers of arthropods and environmental factors affecting these numbers. More detailed analyses of arthropod populations are now nearing completion; these form the basis for conclusions concerning the relationships between arthropod population sizes, species, and rates of leaf-litter breakdown.

The experimental design involved three leaf species (pine, oak, and dogwood) in two forest stands (pine and oak). Each week a set of six litter bags (three leaf species in two stands) was brought into the laboratory, the arthropods were extracted, and the bags weighed, counted for radioactivity, and returned to the field. (Weight loss and radioisotope loss from these bags were discussed in a previous report. Eight such sets of bags were used, so that each litter bag was brought into the laboratory every eighth week. Analysis of the arthropod samples has included sorting by species, estimation of population sizes, and identification by microscopic examination.

The results of analyses of arthropod populations suggest that the development of animal communities in freshly fallen leaf litter is analogous to the more familiar phenomenon of ecological succession. The arthropod community which developed in freshly fallen leaf litter was composed of few species but many individuals. As litter decomposition proceeded, more arthropod species became established in litter bags, but these species were represented by few individuals. Whereas the development of the more complex community type was gradual, the major influx of species occurred in early summer. The most complex communities (i.e., the greatest number of species) were found in bags sampled in September and October, preceding additional leaf fall. Successional phenomena were exaggerated in the oak stand, and were evident in the pine

<sup>&</sup>lt;sup>26</sup>T. Tamura, personal communication.

<sup>27</sup> J. P. Witherspoon, S. I. Auerbach, and J. S. Olson, Cycling of Cesium-134 in White Oak Trees on Sites of Contrasting Soil Type and Moisture, ORNL-3328, in press.

<sup>&</sup>lt;sup>28</sup>I. V. Guliakin and E. V. Yudintseva, *Plant Uptake of Fission Products from an Aqueous Solution*, AEC-TR-2867 (translated from Russian, 1957).

<sup>&</sup>lt;sup>29</sup>D. A. Crossley and H. F. Howden, op. cit., pp 308-10.

<sup>&</sup>lt;sup>30</sup>D. A. Crossley and M. P. Hoglund, *Ecology*, in press.

<sup>31</sup> J. S. Olson et al., Health Phys. Div. Ann. Progr. Rept. July 31, 1961, ORNL-3189, pp 120-22.

<sup>&</sup>lt;sup>32</sup>J. S. Olson et al., Health Phys. Div. Ann. Progr. Rept. July 31, 1961, ORNL-3189, pp 115-18.

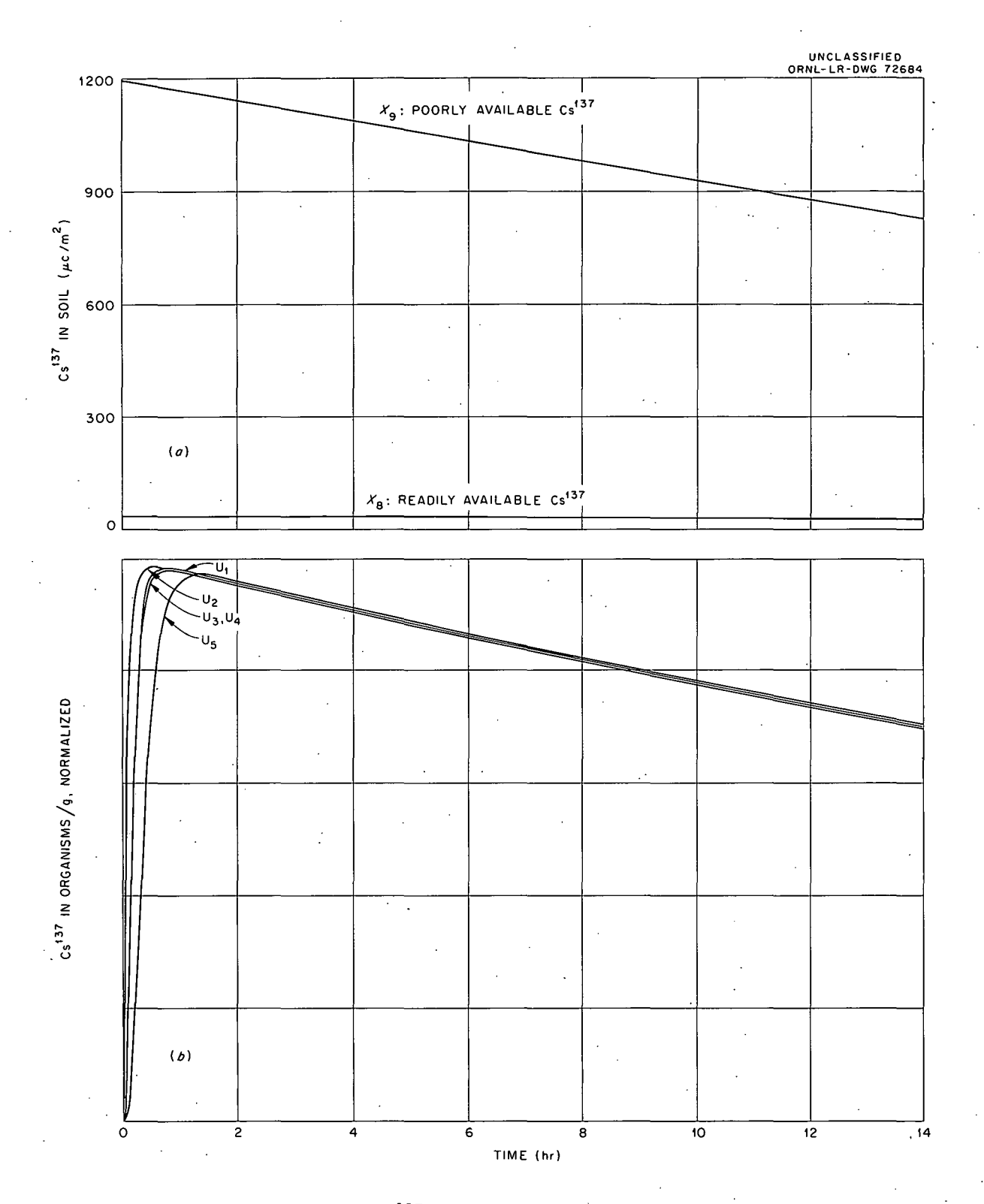


Fig. 2.5. Idealized Redistribution of  $\operatorname{Cs}^{137}$  in a Herbaceous Ecosystem. (a) Soil activity per unit area. (b) Plant activity per unit weight, normalized to transfer from roots  $U_2$  to tops  $U_1$ , insects  $U_3$  and  $U_4$ , and a vertebrate predator or omnivore.

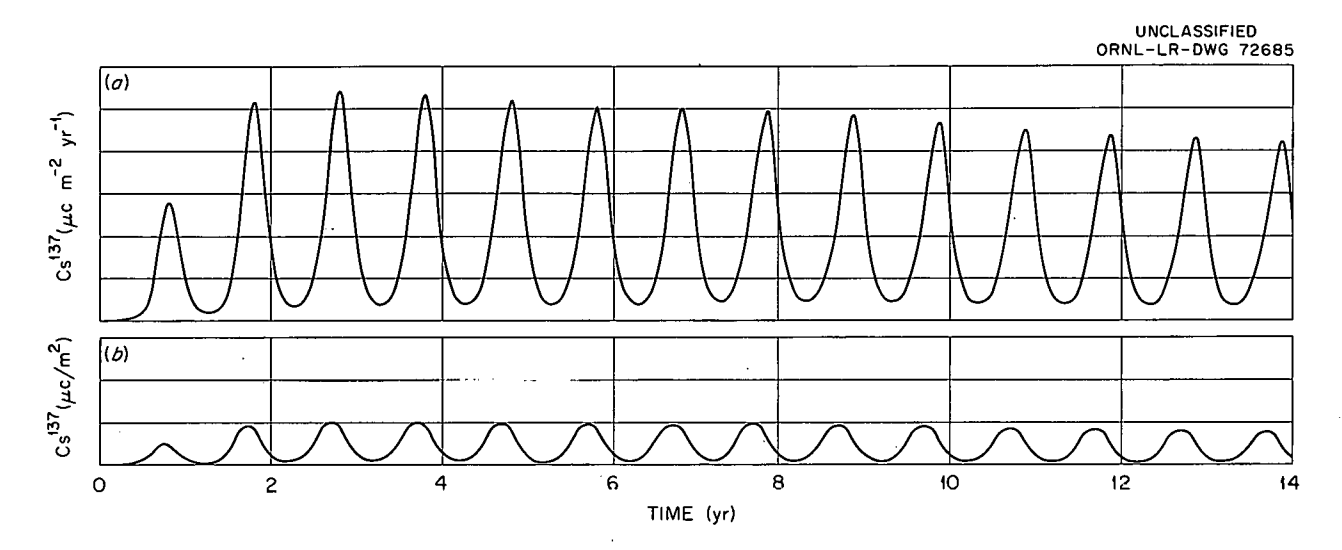


Fig. 2.6. Activity per Unit Area. (a) In litter fall. (b) In vegetation.

stand also. Probably the freshly fallen leaf litter forms a fairly homogeneous substrate which is being attacked by rapidly growing fungus colonies, and only later does a diversity of microhabitats become available for exploitation by microarthropods.

Type of forest stand (oak vs pine) proved to be of greater significance than leaf type (pine, oak, or dogwood) in determining the type of arthropod community which developed. the characteristics of leaf-litter communities is the diversity of arthropod species which occur there. The inclusion of three leaf types in the experimental design was to test the hypothesis that some of the species of arthropods have a marked preference for particular types of leaves. Thus the diversity of arthropod species found in litter of pine stands might partially be due to the presence of species which function primarily in the breakdown of other leaf types. However, similar arthropod communities developed in pine, oak, and dogwood litter within each forest type. At any one of the later sampling intervals, some differences in arthropod population sizes in different leaf types were demonstrable, but these could be explained by differences in stage of litter breakdown between leaf types. Species tended to appear first in rapidly decaying dogwood leaves and last in slowly decaying pine needles.

Some of the diversity of species in arthropod communities can be related to time if not to differences in food preferences. Communities

in litter bags can be separated into at least three general stages: (1) early invaders which are primarily fungus eaters; (2) a middle group consisting of litter and fungus ingesters; and (3) a later group which attacks the more decayresistant fraction of the litter. Ordinary core samples of the forest floor include members of all three of these groups, but litter-bag sampling permits them to be separated. Thus it becomes possible to place importance values on many of the species of litter-inhabiting arthropods. Further evaluation of the relative importance of the various arthropod species to leaf-litter breakdown requires that the population data be transformed into biomass estimates and that metabolic rates and feeding rates be estimated for these species.

### Radioactive Tracer Studies with Millipedes

D. A. Crossley, Jr. C. L. Corley

Of the larger forest floor arthropods, millipedes (Dixidesmus erasus) are the most abundant ones in mixed mesophytic forests which occur in limestone sinks in the Oak Ridge area. Numbers of millipedes may exceed  $100/m^2$ . These animals undoubtedly contribute to the rapid rate of breakdown of leaf litter in the limestone sink forest stands. A series of laboratory and field experiments has been initiated with objectives of estimating the feeding rates for the millipedes (by

use of radioactive tracer techniques) and measuring the amounts of radioisotopes which pass through this trophic level of reducer organisms in contaminated areas.

Whole-body burdens of millipedes feeding on contaminated leaf litter were measured in the laboratory for a 40-day period. Figure 2.7 shows the accumulation of Co<sup>60</sup>, Sr<sup>85</sup>, and Cs<sup>134</sup> by millipedes in these experiments. The pattern of accumulation of Co<sup>60</sup> indicates that concentrations in millipedes equilibrated with concentrations in food; this conclusion is supported by laboratory estimates of a biological half-life of about 7 days for Co<sup>60</sup> in this millipede species. By contrast, Sr<sup>85</sup> accumulation resulted in increasing body burdens over the 40-day period; the biological half-life was estimated to exceed 15 days. Unlike most arthropods, millipedes have a calcareous matrix in the exoskeleton; therefore, strontium accumulation by these animals might be expected. Cesium-134 concentrations in milli-

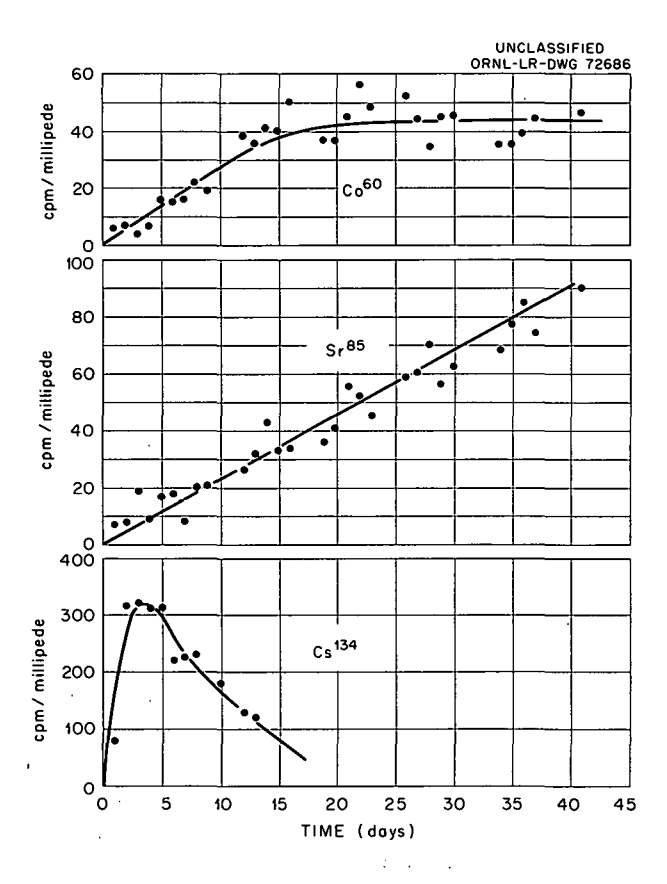


Fig. 2.7. Accumulation of Radioisotopes by Millipedes (*Dixidesmus erasus*) in Laboratory Experiments. Points are averages for 3-7 millipedes.

pedes reached a peak after 3 days of feeding and then declined, since Cs<sup>134</sup> was being leached from the leaf litter which served as food for the millipedes. The biological half-life for Cs<sup>134</sup> was estimated to be approximately 2 days; the half-time for loss of Cs<sup>134</sup> from leaf litter was about 6 days under these laboratory conditions. Iron-59 and zinc-65 were fed to millipedes, but only low activity was obtained, presumably because concentrations used were too low.

These laboratory results led to field studies involving similar experimentation under natural conditions. Millipedes were confined in Plexiglas pens, 0.5 m square. Recapture of marked millipedes released into the pens indicated no movement into or out of the pens during the period of study, but movements of millipedes down into the soil still prevented complete recaptures. Accumulation of Cs<sup>134</sup>, Co<sup>60</sup>, and Sr<sup>85</sup> by millipedes in these pens produced results similar to those found in laboratory experiments; however, data were less conclusive due to incomplete recaptures and longer elimination rates for the radioisotopes. The biological half-life for Co<sup>60</sup> was estimated at 17 days in the field vs 8 days in the laboratory; for Cs134, 5 days vs 2 days. Also, field data suggested that periods of low temperature may have a pronounced effect on elimination rates and thus on accumulation rates.

Additional field experimentation, with proven techniques of containing and counting millipedes in the field, will attempt to relate radioisotope concentrations in millipedes to those in food materials.

### Gross Effects of Arthropods and Microflora on Rates of Leaf Litter Breakdown

D. A. Crossley, Jr. C. L. Corley M. Witkamp G. Dodson

The processes of breakdown and decay of leaf litter are the result of interactions between microflora and soil animals. While the microflora is responsible for decay per se, arthropods fragment leaf material and mix it intimately with soil. The importance of the contribution of the soil fauna is obvious in some situations, but in forest floors of the mor type the effects of arthropods are not readily discernible. In the experiments reported here, an insecticide was used to suppress invertebrate animal populations, and weight loss

by leaf litter was then used as a criterion for evaluation of gross effects on breakdown.

In a preliminary experiment the influence of four insecticides on microbial respiration, fungal colony counts, development of fungal mycelium, and arthropod population sizes in oak litter was evaluated. p-Dichlorobenzene, dieldrin, and chlordane increased soil plus litter respiration and colony counts and decreased mycelium growth more than did naphthalene. p-Dichlorobenzene and naphthalene decreased arthropod numbers by 2 orders of magnitude; dieldrin and chlordane produced reductions of 1 order of magnitude. Naphthalene was chosen over p-dichlorobenzene for further experimentation on the basis of these findings and also because of its slower rate of evaporation.

In the subsequent experiment, twelve 1-m<sup>2</sup> plots of leaf litter in an oak forest stand received levels of 100, 35, 10, or 0 g of naphthalene (three replicates each). Weekly measurements on litter bags provided data on weight loss and Cs<sup>134</sup> loss by leaf litter as well as numbers of arthropods. Biweekly measurements were made of soil plus litter respiration and microflora.

Figure 2.8 shows contrasts of weight retention by litter in plots which received 100 g of naph-

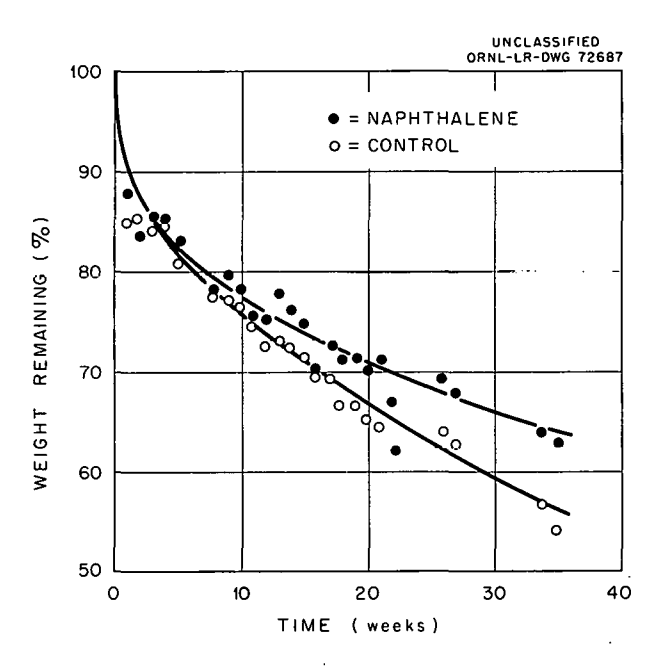


Fig. 2.8. Retention of Weight by Bagged Leaf Litter in Plots Receiving 100 g Naphthalene per  $\mathrm{m}^2$  and in Control Plots.

thalene with control plots (without naphthalene). After the initial period of rapid weight loss, the litter weight in the naphthalene-treated plots decreased at a slower rate than did the controls. By the 35th week (midsummer) there was 15% more litter in the treated plot than in the untreated one. Plots receiving 35 g of naphthalene were intermediate; those receiving 10 g were no different from controls. Cesium-134 loss was less rapid from treated than from control plots. After correction to specific activity (dis/min per g of litter), midsummer samples receiving 100 g of naphthalene had twice as much Cs<sup>134</sup> as did untreated litter.

Arthropods were not completely excluded from the treated plots so that the reduction in weight loss is no more than relative. Numbers in the plots with 100 g of insecticide were reduced approximately 2 orders of magnitude, to about 1000 per m<sup>2</sup>. Most of the arthropods found in treated plots were those capable of either flying or running rapidly. During winter, numbers of arthropods in the latter plots began to increase after about 6 weeks; therefore an additional application of naphthalene was necessary. Continued applications were made at 6-week intervals during winter and spring, but by summer biweekly or weekly applications were necessary to exclude arthropods from the 100-g plots to offset loss by evaporation.

No significant effect of naphthalene was observed on direct microbial counts in the soil and on litter plus soil respiration. Bacterial and fungal colony counts from litter tended to increase with increasing amounts of naphthalene and were two to three times as high in plots with 100 g of naphthalene per m<sup>2</sup> as in control plots. Increased fungal growth on oak leaves in the absence of arthropods was also observed in a parallel *in vitro* experiment in the laboratory.

These results indicate that the absence of arthropods decreases loss of weight by litter. The simultaneously observed increase in microflora is insufficient to counteract effects produced by the absence of arthropods. The failure of respiration measurements to detect reduced litter breakdown in the treated plots results from the fact that respiratory activity in soil was measured along with the activity in the litter, thus masking any effect on litter respiration only. Reduced loss of Cs<sup>134</sup> in litter without arthropods is assumed to be the result of increased cesium release from

comminuted leaf tissue in plots with arthropods and of increased microbial growth and subsequent microbial immobilization of cesium in plots without arthropods. Whereas trends in the experiment are clear, final results will not be obtained until the end of the annual cycle, when additional litter fall occurs.

### Microbiology of Forest Litter

Martin Witkamp G. J. Dodson

Measurement of microbial densities of forest litter is important, since (1) the forest floor is the environment with the most extensive organic matter decomposition, (2) the microflora is the main agent in litter breakdown, and (3) perpetuation of nutrient supply in forests depends on litter decay and subsequent remineralization. Integrated knowledge of microbial masses and of their ability to accumulate and cycle minerals will enable prediction of microbial uptake, accumulation, and release of radioisotopes and fertilizer minerals.

Microbial densities were measured by serial dilution plate techniques on the assumption that the counts will parallel microbial masses. The influences of leaf species, type of forest stand (coniferous vs hardwood), altitude (1600, 1000, and 250 m), exposure (north and south slopes), and season were evaluated. Bacterial as well as fungal counts differed significantly for leaf species, altitude, and season. Bacterial counts were significantly higher in hardwood than in coniferous stands. Bacteria dominated on mulberry leaves and fungi dominated on oak leaves. Microbial numbers increased from high to low altitudes and were highest in spring and lowest in winter. The chief factors controlling microbial population and the rates of breakdown of the various litter species were initial substrate, stage of decomposition, and moisture content. Stand differences of the microflora were assumed to be controlled by soluble inhibitors or pH. Microbial populations at the different altitudes and in the different seasons were influenced by temperature, moisture, and stage of decomposition. nificant interaction was found between microbial counts of different leaf species and seasons, primarily as a result of sharp decline of microbial densities on mulberry leaves that rapidly reached completion of decomposition. Bacterial counts showed a significant interaction between stand and exposure, presumably as a result of the insolation and subsequent low moisture content of litter on south slopes in hardwood stands.

In perhumid East Tennessee the influence of temperature on microbial populations dominates over the influence of moisture. The results show that a one-time measurement is inadequate to characterize the microflora, but that four microbial counts in different seasons already produce consistent and interpretable results. Future work will be aimed at obtaining factors to convert present microbial colony counts into microbial masses.

### Microbial Immobilization of Radionuclides in Forest Litter

Martin Witkamp G. J. Dodson

The rapid microbial uptake of radionuclides and their slow leaching from living microbial tissue as reported last year results in microbial immobilization of minerals in forest floors with profuse microbial growth. In vitro cultures of a Penicillium species growing on pulverized tulip poplar (Liriodendron tulipifera L.) leaves immobilized 45% of the Cs<sup>134</sup> and 20% of the Co<sup>60</sup> present, thus reducing leaching of both elements by more than 50% in two weeks. Rates of leaching equaled average precipitation at Oak Ridge. Leaching and microbial immobilization from pulverized tulip poplar leaves decreased in the order  $Cs^{134} > Zn^{65} > Co^{60} > Ca^{45} > Sr^{85} > Fe^{59}$ . Mineral immobilization was observed in whole leaves as well as ground leaves of dogwood, redbud, tulip poplar, white oak, and white ash and on pine needles with monocultures or mixed microflora. On whole leaves with mixed microflora, leaching as well as immobilization was two to four times lower and averaged about 10% of the minerals present in all leaf species. Release of radionuclides from microbial tissue that has been damaged by freezing or drying is partly masked by subsequent absorption of the remineralized isotopes by the litter. The microbial immobilization of minerals is positively correlated with microbial development measured as respiration, depends on the mineral and leaf species used, and is independent of the mineral concen-Rapidly decomposing mulberry leaves tration.

showed a mobilization of minerals as a result of microbial decay. This mobilization was observed on both ground and whole leaves with one fungal species as well as with natural microflora. The thick leachate from decomposing mulberry leaves lost only 31% of its Cs<sup>134</sup> after a 24-hr dialysis against distilled water, whereas leachate from white oak lost 96% of its Cs<sup>134</sup>. The mobilized Cs<sup>134</sup> may be leached out with amino acids resulting from the breakdown of protein-rich mulberry leaf tissue or by part of the abundant bacterial flora washed from these leaves.

In pot experiments with Cs<sup>134</sup>-tagged white oak leaves with and without microflora, soil, and leaf-eating millipedes, it was found that the microflora decreased the amount of Cs<sup>134</sup> leaching from the litter layer by 30 to 50%. The millipedes increased leaching by 15 to 20%; presumably by comminution of the leaves. The presence of soil increased loss of Cs<sup>134</sup> from the overlying leaves by 17 to 20% of the initial amount, possibly by diffusion and adsorption and by increased moisture content of the leaves. The soil adsorbed all but 1 to 2% of the Cs<sup>134</sup> leaching from the leaves.

These results indicate that under favorable conditions, such as exist on fresh moist leaves in the fall when temperatures are still adequate for microbial development, a larger percentage of nutrients in the leaves may be immobilized. However, unfavorable weather conditions, such as prolonged rain and low temperatures, will cause rapid loss of minerals from the litter layer. High arthropod activity will increase nutrient mineralization. Future work will be concerned with microbial immobilization in soil and testing of the above-mentioned laboratory results in the field.

### Cycling of Cs 134 in White Oak Trees

J. P. Witherspoon, Jr.

A 2-yr study of natural cycling of Cs<sup>134</sup> inoculated into 12 white oak trees was concluded in the spring of 1962. This study showed some of the major pathways and rates of movement of an individual isotope in a forest ecosystem. The ecological significance of this information lies in the basic knowledge gained on the biogeochemistry and physiology of alkali metal elements and in the practical implications concerning the

behavior of radiocesium which may enter a forest system as fallout or as a waste product.

Gains, losses, and transfer rates in various forest system compartments were reported last year. 33,34 This year a similar pattern was seen, with radiocesium moving into tree foilage early in the growing season, reaching a maximum accumulation in June, and decreasing during the remainder of the growing season. 35 Rapid movement of this isotope from trees to understory vegetation, litter, and soil was effected by the leaching action of rain. Rapid movement from 1960 litter to soil to plants was also demonstrated.

The radiocesium cycle in white oak trees is illustrated in Fig. 2.9. In addition to tree-to-soil transfers via rain, over half the Cs<sup>134</sup> contained in the annual litter fall was transferred into the mineral soil over the winter months. In both years the total annual loss from trees was estimated at 19% of the original 2 mc inoculated in tree trunks. With only small quantities being taken up by vegetation (recycled), it is estimated that in 5 to 6 yr the soil will contain most of the radiocesium in the system.

Abrupt horizontal gradients of soil radiocesium, presumably related to rain leaching and stem flow, were found under inoculated trees. Eighty percent of the total soil burden was confined to the area within crown perimeters, and 19% was concentrated in a small area around the trunks. Vertical distribution studies showed that soils on moist sites (bottomlands) had a significantly greater percentage of radiocesium at depths down to 12 in. than soils on drier (upland) sites. However, 92% of the total soil burden remained in the top 4 in. for 1 yr and 7 months after tree inoculations.

Approximately  $2 \times 10^3$  times more naturally occurring stable cesium (determined by activation analyses) than tracer  $Cs^{134}$  was involved in tree gains and losses. The amount of stable cesium

<sup>33</sup> J. S. Olson et al., Health Phys. Div. Ann. Progr. Rept. July 31, 1961, ORNL-3189, pp 113-15.

<sup>34</sup> J. P. Witherspoon, "Cycling of Cs<sup>134</sup> in White Oak Trees on Sites of Contrasting Soil Type and Moisture. I. 1960 Growing Season," Radioecology. Proceedings of the First National Symposium on Radioecology, in press.

<sup>&</sup>lt;sup>35</sup>J. P. Witherspoon, S. I. Auerbach, and J. S. Olson, Cycling of Cs<sup>134</sup> in White Oak Trees on Sites of Contrasting Soil Type and Moisture, ORNL-3328, in press.

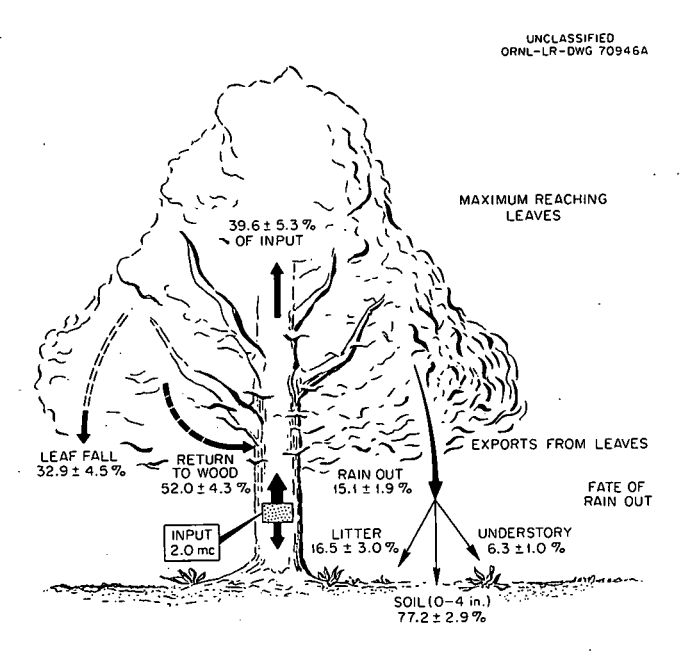


Fig. 2.9. Cycle of Cs<sup>134</sup> in White Oak During Growing Season. Average of 12 trees for 1960 and 1961 growing seasons; fate of rainout figures are for 1960 growing season only.

in the top inch of mineral soil was  $5 \times 10^6$  to  $6 \times 10^6$  times greater than the annual addition of radiocesium from trees. Thus, whereas tracer quantities used in this study (2.0 mc per tree) were adequate for following cyclic behavior of this element, they were small compared with natural levels occurring in a forest ecosystem.

# Mobility of Cs <sup>137</sup> Tracer in a Forest of Tulip Poplar

J. S. Olson H. D. Waller
D. A. Crossley W. C. Cate
M. Witkamp C. L. Corley
W. L. Tietjen

One objective of tracer studies in several Oak Ridge forests is to help predict the movement of radionuclides in ecosystems having a large biological capacity for storing contamination. A second objective is to understand the processes which maintain these systems and which explain the movement of nuclides in natural environments. Experiments have dealt with progressively larger areas: 1 dm square, 1 to 2 m square, and currently a 20 × 25 m ( $\frac{1}{8}$  acre) plot in a productive forest of tulip poplar (Liriodendron tulipifera).

Methodology and early results of experiments starting with decimeter bags of tagged litter have been reported. Further studies of breakdown rates with bagged and unbagged litter are being sampled or analyzed. The new large plot was mapped and tagged in May 1962. Cesium-137 was introduced into the trunks through chisel cuts through the bark. Application per tree was made approximately proportional to tree biomass, as estimated from previous weighing of harvested trees in the same vicinity. 37

Almost all tagging was completed in a 4-day period at the end of a prolonged spring drought. The first tree showed relatively slow upward movement of  $Cs^{137}$ , suggesting that limited water reserves and transpiration rates were impeding upward translocation of inorganic ions in the xylem. This tree and others tagged within 1 day prior to drought-breaking rain showed rapid subsequent movement throughout the crown. Within 2 to 4 weeks, foliage radioactivity averaged almost 1  $\mu$ c per g of dry weight.

As in earlier studies of white oak, leaching from rainfall proceeded promptly, but distribution on litter and soil varied greatly from centimeter to centimeter. In one plot area after 6 weeks, 52% of the leachate was retained in litter, 40% in 1.5 cm of mull  $A_1$  horizon, but only 8% had leached through the 1.5-cm soil.

Mushrooms collected 2 weeks after tagging contained  $\frac{1}{40}$  as much Cs<sup>137</sup> as the litter on a volume basis. After 6 weeks, Cs<sup>137</sup> in wood and litter-decaying fungi had increased to 2 to 3 times as high as that in the substrate. Absolute activities for *Clavaria* increased to 63,000, 85,000, and 100,000 dis/min per g of dry weight after 5, 7, and 8 weeks, respectively. Large variations in insect radioactivity seemed related to food chain relations. Higher concentrations of Cs<sup>137</sup> were found in caterpillars feeding directly on foliage and in predators which feed on these caterpillars than were found in litter-feeding insects and their predators.

<sup>&</sup>lt;sup>36</sup>J. S. Olson and D. A. Crossley, "Tracer Experiments on the Breakdown of Forest Litter," Radioecology, Proceedings of the First National Symposium on Radioecology, in press.

<sup>&</sup>lt;sup>37</sup>J. S. Olson et al., Health Phys. Ann. Progr. Rept. July 31, 1961, ORNL-3189, p 110.

### **CLINCH RIVER STUDIES**

D. J. Nelson R. E. Martin<sup>38</sup>
B. G. Blaylock<sup>38</sup> R. C. Early
N. A. Griffith

# Strontium in White Crappie (Pomoxis annularis) Flesh and Bone

D. J. Nelson

N. A. Griffith

When the distribution of strontium between fish and water is known, it should be possible to predict the levels of Sr<sup>90</sup> to be found in fish living in river water receiving a constant release of Sr<sup>90</sup>. Therefore, the relation

$$\frac{\text{Sr in fish tissue}}{\text{Sr in water}} = \frac{\text{Sr}^{90} \text{ in fish tissue}}{\text{Sr}^{90} \text{ in water}}$$

or

$$Sr^{90}$$
 in fish =  $\frac{Sr \text{ in fish tissue} \times Sr^{90} \text{ in water}}{Sr \text{ in water}}$ 

may be used to calculate the expected burden for a continuous release of  $Sr^{90}$ . The flesh and bone of white crappies (*Pomoxis annularis*) from the Clinch River are being analyzed for strontium and  $Sr^{90}$  in order to test the validity of the above relation.

The average strontium content of the flesh of nine white crappies analyzed was  $6.6 \times 10^{-8}$  g per g of wet weight. This strontium content in flesh represents a concentration factor of 1.12 times over that in Clinch River water. Preliminary data on the strontium and  $Sr^{90}$  content of white crappie bone indicate a good agreement between the value expected on the basis of  $Sr^{90}$  releases and the analytical results. Strontium is concentrated in bone by a factor of  $3.85 \times 10^3$  times that of river water. The average  $Sr^{90}$  concentration in bone was  $1.2 \times 10^{-10}$  curie/g. This  $Sr^{90}$  concentration in bone is equal to 31% of the MPC for  $Sr^{90}$  in water in the neighborhood of an atomic installation. Laboratory releases of  $Sr^{90}$  to the river vary from 10 to 30% of the MPC.

Stable strontium concentrations in bone were much less variable than were Sr<sup>90</sup> concentrations

in the same samples (Table 2.7). Since a long biological half-life is expected for strontium in fish bone, the variability of  $Sr^{90}$  values may be associated with the movement of fish into and out of White Oak Creek, where there is a higher concentration of  $Sr^{90}$ . The series of stable strontium and  $Sr^{90}$  analyses is being continued.

Table 2.7. Strontium and Strontium-90 in White Crappie Bone

Strontium (µg per g of bone)	Strontium-90 (μμο per g of bone)
217	36.7
250	24.5
218	10.0
204	277.0
189	12.6
234	295.0
251	3.0
230	9.4
244	297.0
233	232.0
Av 227	120.0

# Biological Half-Life of Strontium and Cesium in Fish

D. J. Nelson

R. C. Early

The biological half-life of fission-product elements in fish is being measured, since this parameter affects the dispersal of radionuclides by fish as they move from contaminated to uncontaminated areas of the river. Also, knowledge of the uptake rates is an important consideration in the event of acute environmental contamination.

Preliminary experiments with Cs<sup>134</sup> in bluegills (*Lepomis macrochirus*) suggest a biological half-life (whole-body) of about 40 days. Scott<sup>39</sup> found a biological half-life of 47.2 days in the brook

<sup>38</sup>ORINS Fellow.

<sup>&</sup>lt;sup>39</sup>D. P. Scott, "Radioactive Caesium as a Fish and Lamprey Mark," J. Fisheries Res. Board Can. 19, 149 (1962).

trout (Salvelinus fontinalis). Radiocesium concentrations in the bluegill were highest in the soft tissues (gonad, muscle, digestive tract, and skin) and lowest in hard tissues (bone, scales, and fins).

The biological half-life of Sr<sup>85</sup> in soft tissues of the white crappie (*Pomoxis annularis*) appears to be approximately one day. On the other hand, there has been no detectable loss of this isotope from bone.

### Fish Marking and Population Studies

R. E. Martin

D. J. Nelson

Scales of fish taken from White Oak Lake, White Oak Creek, and the Clinch River have shown the possibility of accumulation of radionuclides in definite patterns of concentric circles. Autoradiographic analysis has shown that all the normal scales from an individual have the same pattern (Fig. 2.10). Low-level radioanalyses of fish scales have shown the presence of Co<sup>60</sup> and Ru<sup>106</sup>, although analyses of fish bones have shown the presence of Zn<sup>65</sup>, Zr<sup>95</sup>-Ni<sup>95</sup>, and Cs<sup>137</sup> in addition to Co<sup>60</sup> and Ru<sup>106</sup>. Strontium-90 may be expected to accumulate in bones and scales also, because of its affinity for bony tissues.

Fish from the contaminated areas are being sampled regularly, and scales from these specimens are being autoradiographed to evaluate the correlation of radionuclide accumulation with growth and movement of the individuals as part of a broader goal of developing a radioisotope tagging method for population studies. numbers of smallmouth buffalo (Ictiobus bubalus), a commercially important fish, are being collected from Watts Bar Lake for the determination of instantaneous growth rates and for radiometric analysis to determine movement in and out of the Clinch River. The relation between radionuclide accumulation in scales and environmental contamination is also being tested in the laboratory with Cs134, as well as the possibility of translocation of radionuclides from other tissues into the scales.

### Radiation Effects on Chironomus tentans

B. G. Blaylock

S. I. Auerbach

D. J. Nelson

N. A. Griffith

The larvae of *Chironomus tentans* live in the radioactive bottom sediments of White Oak Creek and the Clinch River. The larvae are exposed to ionizing radiation which is 20 to 1000 times that of natural background. 40,41 The frequency of chromosomal aberrations in salivary gland chromosomes is being compared in irradiated and nonirradiated populations to determine whether there is an effect of increased radiation levels on the genetic constitution of the natural population.

Photographs of the chromosomes from a nonirradiated population were taken, to construct cytological maps. Besides facilitating the scoring of chromosomes, these maps are to be compared with the cytological maps of *C. tentans* from Europe and used to establish the standard chromosomal arrangement for this area.

Permanent slides are prepared of salivary glands of larvae collected from each population, observed microscopically, and scored for aberrations. Thirty-three larvae collected in October 1961 from White Oak Creek had a total of 43 aberrations of 12 different types, and 29 larvae from a control area had a total of 4 aberrations of 3 different types. These differences were significant (P < 0.01).

From a total of 141 permanent slides of material collected in the contaminated area from August to December 1961, the mean chromosomal aberration per individual was 0.86. The mean chromosomal aberration per individual per month was computed for testing for a change in frequency of chromosomal polymorphism. An analysis of variance among these monthly means, which were 0.59, 0.77, 1.22, 0.95, and 0.95 (August through December) showed no significant difference among them.

<sup>40</sup>S. I. Auerbach et al., Health Phys. Div. Ann. Progr. Rept. July 31, 1961, ORNL-3189, p 129.

<sup>&</sup>lt;sup>41</sup>Clinch River Study Steering Committee, Status Report No. 2 on Clinch River Study, ORNL-3202, p 71 (Mar. 30, 1962).



Fig. 2.10. Autoradiogram of Scales from a Smallmouth Buffalo. Rings are apparent except in regenerated scales such as the one in lower left corner.

### Strontium in Fresh-Water Clam Shells

D. J. Nelson R. C. Early

A comparison of strontium concentration in contemporary and prehistoric mollusk shells has been used as a basis for interpreting paleoecological conditions and for determining the biogeochemical cycle of strontium. Current work shows that there is a nonhomogeneous distribution of strontium within fresh-water mollusk shells and that this distribution is associated with growth and structure of the shell.

Previously published descriptions of the structure of fresh-water clam shells were found to be inadequate; consequently, a new structural analysis was developed. Shells of the clams (Unionidae), when viewed in cross section, consist of three calcareous layers. The external prismatic layer is relatively thin, covers the whole of the shell under the periostracum, and contributes little to the total shell. The remaining two layers, both nacreous, comprise the bulk of the shell, and the relative contribution which each makes to the total shell differs with the species. The medially located peripheral nacreous layer consists of imbricate lamellae deposited by that portion of the mantle which is peripheral to the The inner laminar nacre is also pallial line. composed of lamellae and is deposited within the area bounded by the pallial line. When a clam grows, the shell increases in size at the circumferences by the addition of peripheral layers and increases in thickness by the addition of laminar layers.

Cross sections were cut from the shells of eight species of Unionidae and ashed, after which it was possible to separate the annual growth in the respective shell layers. The annual increment of growth from each layer was analyzed for strontium by emission spectroscopy. Barium, sodium, magnesium, and manganese were obtained simultaneously from some of these same layers.

Strontium concentrations in the laminar layers increase noticeably, beginning with the shell deposited in the 6th year (Table 2.8). The analysis of this clam is typical of the average for most clams analyzed. Strontium concentrations in the laminar layers are relatively constant during the first five years; in the 6th-year layer and older layers, strontium is approximately 25% greater (Table 2.9). Exceptions to this generali-

Table 2.8. Strontium Concentrations in Laminar and Peripheral Layers of One Elliptio crassidens Shell

Age Class of	Strontium ( $\mu g$ per g of shell)		
Layer	Laminar Layers	Peripheral Layers	
1	240	210	
2	230	210	
3	220	210	
4	250	210	
5	240	190	
6	300	180	
7	300	190	
8	350	200	

zation include two shells from *Elliptio dilatatus* and one from *Lasmigona complanata* in which the strontium content of the laminar layers decreased with age. Strontium concentrations in the peripheral layers were relatively constant, and no change with age was suggested by the data (Tables 2.8, 2.9). However, there was less strontium in the peripheral layers than in the laminar layers. Strontium concentrations in the peripheral annual layers ranged from equal amounts to 46% of that in the corresponding laminar layers, averaging 77%.

The correlation of the occurrence of barium, manganese, magnesium, and sodium with strontium was studied with the Olmstead and Tukey corners test (Table 2.10). Of these elements only the distribution of barium was correlated consistently with strontium. This correlation may be expected because of the chemical relationship of barium and strontium. Manganese appears to be correlated with strontium in most clams, but the few correlations of magnesium and sodium with strontium may be by chance.

### Related Activities

The section chief served as chairman of the Radioecology Committee of the Ecological Society of America. Under his direction this committee sponsored the first institute for the teaching and application of radioisotope techniques in ecological research. This institute, which was held

Table 2.9. Normalized<sup>a</sup> Data on the Change in Strontium Concentration with Age in Laminar and Peripheral Layers of Clam Shells

Age Class of	La	minar Layers <sup>b</sup>	Peri	pheral Layers <sup>C</sup>
Layer	Number	Normalized Value <sup>d</sup>	Number	Normalized Value
1 .	5	1.02 ± 0.045	3	1.10 ± 0.10
2	8	1.00 ± 0.013	6	$1.06 \pm 0.071$
3	10	1.00	. 8	1.00
4	10	$1.00 \pm 0.044$	8	$1.00 \pm 0.020$
5	9	1.05 ±0.030	8	0.99 ± 0.045
6	10	1.22 ± 0.098	8	$1.08 \pm 0.10$
7	10	1.26 ± 0.062	8	$1.06 \pm 0.061$
8	8	$1.20 \pm 0.074$	7	$1.05 \pm 0.084$
9+	15	1.26 ± 0.057	9+	$1.09 \pm 0.18$

<sup>&</sup>lt;sup>a</sup>Data were normalized to 3d year layer because layers from years 1 and 2 were not always recovered, that is, 3d year layer = 1.00.

Table 2.10. Correlation  $^{\alpha}$  of Barium, Manganese, Magnesium, and Sodium with Strontium in the Shells of Eight Species of Clams

	Probability $^b$ if Correlation Is Observed			
Species 	Ba	Mn	Mg	Na
Plagiola lineolata	<0.001	<0.003	· c	<0.02
Elliptio dilatatus	<0.005	no	no	no
E. crassidens	<0.0002	<0.0002	•	no
Actinonaias carinata gibba	<0.0002	<0.0002	<0.0002	<0.05 (neg) <sup>d</sup>
Anodonta corpulenta	<0.01	no	<0.05	<0.002
Lasmigona complanata	<0.0002	<0.0002	no	no-
Cyclonaias tuberculata	<0.0002	<0.1		<0.02 (neg)
Quadrula pustulosa	<0.07	<0.005	no	

<sup>&</sup>lt;sup>a</sup>Correlation determined by the method of Olmstead and Tukey, Ann. Math. Stat. 18, 496 (1947).

<sup>&</sup>lt;sup>b</sup>Clams include four Elliptio crassidens, two Anodonta corpulenta, one Actinonaias carinata gibba, one Cyclonaias tuberculata, one Quadrula pustulosa, and one Plagiola lineolata.

<sup>&</sup>lt;sup>c</sup>Clams include three E. crassidens, two A. corpulenta, one A. c. gibba, one C. tuberculata, and one P. lineolata.

<sup>d</sup>All normalized values ± one standard error.

<sup>&</sup>lt;sup>b</sup>The probability that the arrangement of plotted points in a sample will have a quadrant sum equal to or greater than Olmstead and Tukey's indicated absolute values.

<sup>&</sup>lt;sup>c</sup>No data.

dNegative correlation.

in Oak Ridge, was attended by 20 college and university teachers and researchers of ecology.

The section chief also served as chairman of the Aquatic Biology Subcommittee of the Clinch River project.

One person served as a member of a USAEC scientific team that reviewed the University of Pittsburgh project "Radioecology of Fossorial Rodents."

Three staff members lectured and gave guided field tours to two classes of radiological health

trainees from the R. A. Taft Sanitary Engineering Center, Cincinnati, Ohio.

One staff member prepared materials for evaluating the possible ecological implications of a nuclear attack, following a request of the National Academy of Sciences — National Research Council Committee on Civil Defense.

One staff member was chairman of a subcommittee on Chemical Cycles in Ecological Systems and submitted a report to the Ecology Study Committee of the Ecological Society of America.

### 3. Radiation Physics and Dosimetry

### THEORETICAL PHYSICS OF DOSIMETRY

### J. Neufeld

J. C. Ashley 1 W. D. Moon 1,4
P. R. J. Burch 2 R. H. Ritchie
J. L. Feuerbacher 3 W. S. Snyder
G. S. Hurst J. E. Turner
H. A. Wright

### Electromagnetic Properties of a Plasma-Beam System

There are two electromagnetic modes in a plasma-beam system: the unstable "hybrid" mode characterized by the occurrence of a longitudinal component of the electric intensity E, and the traverse mode which does not show an instability and is characterized by the occurrence of a longitudinal component of the magnetic induction B. The behavior of this system has been described in terms of macroscopic quantities such as the electric displacement D and the magnetic intensity H. 5 The unstable hybrid mode in a plasma-beam medium is compared to related hybrid instabilities produced by a beam in a medium comprising harmonic oscillators. It is thus shown that the hybrid instability produced in a plasma is of type "l." Applying the appropriate criterion, it is found that the hybrid instability and the associated longitudinal instability are convective for  $\theta \neq 0$ , where  $\theta$  is the angle formed by the direction of the beam and the direction of the growing waves resulting from these instabilities. For  $\theta$  approaching  $\pi/2$  the instability produced by the beam becomes aperiodic. The plasma-beam system is electromagnetically anisotropic, and its anisotropy has

been investigated with reference to transverse For transverse waves the and hybrid waves. anisotropy is described in terms of a dependence between  $\phi$  and  $\theta$ , where  $\phi$  is the angle formed by the vectors H and B. For hybrid waves the anisotropy has been investigated in the "region of transparency" and in the "region of instability." In the region of transparency there is a dependence between  $\psi$  and  $\theta$ , where  $\psi$  is the angle formed by the vectors D and E. In the region of instability there is a similar angular dependence and also a phase difference between the longitudinal and transverse components of the electric intensity E. Some of the effects produced by a beam in a thermal plasma have been investigated in hydrodynamic representation. A formal analogy has been established between the Vavilov-Cherenkov effect produced by a single particle passing through a thermal plasma and the longitudinal instability produced by a beam having the same velocity as the particle. This analogy does not apply to hybrid waves.

# Vavilov-Cherenkov Effect and "Bohr Radiation" Produced by a Beam of Charged Particles in a Dispersive Medium

An electron beam interacting with a dispersive (atomic or molecular) medium produces two intense sources of instability that are represented by a growing longitudinal wave and a growing transverse wave. The longitudinal wave has frequencies that are equal to the atomic binding frequencies of the surrounding medium and is designated as the "Bohr wave." The transverse wave has frequencies determined by the Vavilov-Cherenkov criterion and is similar to the Vavilov-Cherenkov wave produced by a single particle interacting with the medium. These sources of instability are "continued" into lower frequency ranges in which they produce growing waves of a "hybrid" type that are characterized by an

<sup>&</sup>lt;sup>1</sup>Summer employee.

<sup>&</sup>lt;sup>2</sup>Visiting professor from University of Leeds.

<sup>&</sup>lt;sup>3</sup>Summer employee.

<sup>1</sup>Consultant

<sup>&</sup>lt;sup>5</sup>J. Neufeld, "Electromagnetic Properties of a Plasma-Beam System," to be published in *Phys. Rev.* 

electric vector having both longitudinal and transverse components. The longitudinal and transverse waves represent the "fundamental modes" that exist in the medium in the absence of the beam. The perturbation produced by the beam is responsible for the instability of the fundamental modes and for the occurrence of the coupling between these modes. The coupling produces electromagnetic waves in which the electric field has a longitudinal component. The conditions for coupling and the character of the instabilities have been investigated.

# "Distant Ionization" Produced by Heavy Ions in Tissue

The current estimate of RBE for ions of various energies is based on linear energy transfer and is therefore related to the rate of energy absorbed longitudinally per unit length of particle track. A possible biological significance may be attributed to the character of the "lateral" distribution of the energy losses, that is, in the direction perpendicular to the particle track. In accordance with the customary representation based on the theory of Bohr, the lateral distribution comprises the region of "close collisions" and "distant collisions." In the region of "close collisions" the dominant process is ionization, and in the region of "distant collisions" the corresponding process is the excitation of tissue atoms. In accordance with this mechanism, there is no energy transfer from the moving ion to the surrounding tissue beyond a maximum distance designated as the adiabatic limit, and consequently the initial "width" of the particle track does not extend beyond this limit. It is the purpose of this investigation to point out and to evaluate qualitatively an additional mechanism that produces ionization at distances exceeding the adiabatic limit. This additional contribution shall be designated as "distant ionization" and thus differentiated from "close ionization" which is accounted for by Bohr's theory. The "distant ionization" has been discussed by W. E. Lamb in connection with energy losses of fission In accordance with this process an approaching ion lowers the Coulomb barrier of orbital electrons in the tissue atoms and allows some electrons to escape, thus leaving the atom

in an ionized state. Investigations have been carried out dealing with the qualitative features of distant ionization and indicating the distances from the particle track for which this ionizing mechanism is dominant. These distances have been determined for various ions and ionic velocities of biological interest.

### Dosimetry of High-Energy Radiations 7

A calculation of the dose due to high-energy radiations was begun. The Neutron Physics Division at ORNL is developing machine codes to provide tapes with the histories of particles arising in shielding materials or tissue phantoms from bombardment with protons and neutrons of energies up to several billion electron volts. These codes may be used to generate the following information for any number of protons or neutrons of a given energy incident on a specified target:

- 1. type and number of particles arising from interactions of incident and secondary particles,
- 2. the positions of these particles in the target at birth,
- 3. the energies at birth,
- 4. direct cosines of the velocities at birth,
- 5. ultimate fate of the particles, that is, capture, escape, stopping, etc.

The Health Physics Division is writing a code for the calculation of the rad and rem dose in a tissue slab, with the particle histories mentioned above as the input. This is now essentially complete for incident nucleon energies up to 400 Mev, and is written to provide for an arbitrary choice of RBE. The rad dose results from assigning an RBE of 1 to all absorbed energy.

The handling of RBE values in the calculation of rem dose in this flexible way is done in order to avoid repetition of the entire calculation for each particular choice of RBE. In this way RBE values can be adjusted over a considerable range so that additional information can be relatively easily incorporated as it becomes available. The procedure is based on a polynomial expansion of expressions for rem dose in powers of particle energies. The sums of powers of particle energies can be printed out and weighted

<sup>&</sup>lt;sup>6</sup>J. Neufeld and H. Wright, Phys. Rev. 124, 1 (1961).

<sup>&</sup>lt;sup>7</sup>These studies are supported by the National Aeronautics and Space Administration.

with various coefficients (corresponding to particular choices of RBE) to obtain rem dose.

Above 400 Mev the contribution of  $\pi$ -mesons to dose will be included in a code of similar design. A systematic study of the dosimetric importance of interactions involving elementary particles is being made.

# Role of Physical Quantities in Radiation Dosimetry<sup>8</sup>

The dependence of RBE on the purely physical characteristics of radiation is being investigated. In particular, ways are being sought to use physical quantities in addition to energy absorbed per unit mass in the basic definition of radiation dose in a way which will describe the observed dependence of RBE on the purely physical parameters governing the interaction of radiation with tissue. For example, it has been found that if radiation dose is defined as a new quantity,  $\omega$ , which includes a term proportional to the magnitude of momentum absorbed per unit mass in addition to the usual rad dose, then  $\omega$  has a fixed value for a given rem dose of neutrons and gamma photons in any relative amounts and with any energy spectra in the range 0.4 to 10 Mev. This work is being combined with the generalized principle of dosimetry 10 in undertaking a broad investigation of the fundamental principles and concepts which are the basis for radiation dose and radiation dosimetry.

# Model for Spontaneous and Radiation Carcinogenesis

Conventionally, it has been assumed that a knowledge of the dose-response relationship in human radiation carcinogenesis would enable the etiology of cancer induction to be derived. Thus, a linear relationship would be interpreted as being indicative of a "one-hit" mechanism. Unfortunately, the numerous uncertainties in the available human data — statistical, dosimetric, clinical,

and interpretational — preclude the unambiguous estimation of dose-response patterns. It is proposed that in order to understand the phenomenon of radiation carcinogenesis, a prior knowledge of certain aspects of spontaneous carcinogenesis is necessary.

A study of this latter problem was begun in the University of Leeds and continued in the Health Physics Division. Attention has been concentrated on the leukemias, partly because they have been intensively investigated and partly because they are rather readily induced by ionizing radiation. The carcinogenic (in which is included the leukemogenic) process can be divided into two principal stages — "initiation" and "promotion" or "development". The latter "promotion" or "development" stage occurs during the latent period — the interval elapsing, for example, between a single acute irradiation and the onset of a malignancy.

Various alternative models of the initiation stage of spontaneous carcinogenesis have been reviewed, but these have been based upon mortality statistics for cancers in adults, and the phenomenon of childhood and adolescent tumors has been previously disregarded. By exploiting a wide range of epidemiological and clinical evidence, by considering growth from the zygote to the mature organism, and by adopting some plausible biological principles and criteria, a new mathematical model has been constructed to be drawn. The complexity of the problem defies brief description, but, broadly, it appears that most spontaneous malignancies in adult humans arise from one or more cells containing four specific mutant genes, one of which is generally, though not necessarily, inherited. Most malignancies of childhood and adolescence arise from one or more cells containing three specific mutant genes, one of which is normally inherited, though occasionally two are. When only one mutant gene is inherited, a "stress factor," such as a bacterial or viral infection, or a hormonal stimulus, is needed to complete the malignant transformation of a cell containing three specific mutant genes. In certain environments, it is probable that viral or bacterial agents sometimes complete the malignant transformation of a pre-leukemic cell in adult nongenetic carriers. The popular view current among oncologists that all human malignancies are exclusively of viral origin only survives critical quantitative examination when

<sup>&</sup>lt;sup>8</sup>Supported in part by the National Aeronautics and Space Administration.

<sup>&</sup>lt;sup>9</sup>J. E. Turner and Hal Hollister, "The Possible Role of Momentum in Radiation Dosimetry," to be published in Health Phys.

 <sup>10</sup>G. S. Hurst and R. H. Ritchie, Health Phys. 8, 117 (1962); G. S. Hurst et al., Health Phys. Div. Ann. Progr. Rept. July 31, 1961, ORNL-3189, pp 149-54.

extremely implausible postulates are adopted. A summary of the initiating requirements for spontaneous human leukemias is given in Table 3.1.

The application of the theory of the initiation stage to radiation carcinogenesis has been con-It is assumed that radiation is able to simulate the spontaneous somatic mutation A highly consistent interpretation is obtained of the dose-response and the age-dependence aspects of leukemia and cancer induction at Hiroshima. The great differences between the characteristics of leukemia and cancer induction are all a consequence of the value of a (the radiation mutation coefficient - mutations per gene at risk, per cell at risk per rem) which is about 10 times larger for leukemias than for nonleukemic malignancies. Excellent agreement is obtained between theory and the observations of leukemia induction in x-irradiated ankylosing spondylitis patients. The leukemogenic (and also cancerogenic) effect of small doses of pelvimetric x rays to the fetus is correctly predicted.

A hypothesis of the promotion or development stage has been evolved in conformity with the theory of the initiation stage, and clinical, and experimental evidence. The bearing of the overall argument on the problems of cancer therapy and prophylaxis has been considered.

In view of the quantitative applicability of the theory of the initiation stage to extensive evidence from both spontaneous and radiation carcinogenesis, it is considered that the essential features of the initiation stage have been correctly analyzed.

### Positron Annihilation in a Free Electron Gas

The experimental work of Bell and Jørgensen<sup>11</sup> has established an approximate total annihilation rate of positrons in a free electron gas at various electronic densities. Their work has been compared with the theory of Kahana<sup>12</sup> who solved, by approximate means, a Bethe-Goldstone equation for the relative wave function of an electron-positron pair in the free electron gas.

Table 3.1. Initiating Requirements for Spontaneous Human Leukemias

Character of leukemic cell

Childhood and Adolescent Acute	Adult <sup>a</sup> Acute Lymphatic and Lymphosarcoma	Adult <sup>a</sup> Chronic Lymphatic	Adult <sup>a</sup> Chronic Myeloid
One inherited mutant geneb	One inherited mutant gene	One inherited mutant gene	One inherited mutant gene
Somatic mutation of two genes	Somatic mutation of three genes	Somatic mutation of three genes; hyperplasia of cells containing three of four mutant genes	Somatic mutation of two genes and Ph <sup>b</sup> chromosome; or somatic mutation of three genes
Plus stress (growth and pyogenic infection, especially pneumonia) or oncogenic virus	$m_s \stackrel{\sim}{=} 5 \times 10^{-6}$ $m_g \stackrel{\sim}{=} 5 \times 10^{-6}$	$m_s \approx 2 \times 10^{-6}$	$m_s \stackrel{\sim}{=} 2 \times 10^{-6}$
$m_s \stackrel{\sim}{=} 3 \times 10^{-6}$ $m_g \stackrel{\sim}{=} 5 \times 10^{-6}$	•	$m_g \stackrel{\sim}{=} (3 \text{ to } 4) \times 10^{-6}$	$m_g \approx (3 \text{ to } 4) \times 10^{-6}$

<sup>&</sup>lt;sup>a</sup>Some adult leukemias involve no inheritance factor, and normally four somatic mutations are then required.

<sup>&</sup>lt;sup>11</sup>R. E. Bell and M. H. Jørgensen, Can. J. Phys. 38, 652 (1960).

<sup>&</sup>lt;sup>12</sup>S. Kahana, Phys. Rev. 117, 123 (1960).

<sup>&</sup>lt;sup>b</sup>Given one inherited mutant gene, the probability of death from acute stem cell or lymphatic leukemia in the age range 0 to 9 yr is about 2 to 3%. Occasionally two mutations will be inherited. The change of leukemia development during growth is then virtually 100%. No stress or infection factor is required for this inheritance.

The term  $m_s$  is the somatic mutation frequency;  $m_g$  is the germ cell mutation frequency, both in terms of mutatations per gene at risk per cell at risk per year. The terms  $m_s$  and  $m_g$  are calculated independently.

The experiment and theory differ by a factor of 2 for the annihilation rate.

An alternate theoretical approach has been made in which one assumes a static screened interaction between a given electron pair and expresses the annihilation rate in terms of ladder Feynman diagrams. Thus, the annihilation amplitude is represented as a sum of amplitudes corresponding to: (1) annihilation between a zero energy positron and an undisturbed electron in the Fermi sea plus (2) an interaction between the positron and an electron, resulting in the excitation of the electron outside the Fermi sphere, followed by annihilation with the positron plus (3) two successive excitations of an electron, which must remain outside the occupied region in momentum space, followed by annihilation plus (4) the sum of all possible higher-order successive excitations of this sort, followed by annihilation.

It is found that the annihilation rate  $\Gamma(s)$  at the momentum  $\overline{s}$  due to these interactions is given by

$$\Gamma(s) = \pi r_0^2 c |f(\overline{s}, \overline{x})|^2,$$

where  $f(\vec{s}, \vec{x})$  is the solution of the integral equation,

$$f(\overline{s}, \overline{x}) = 1 + \beta \int d\overline{y} \ v(|\overline{x} - \overline{y}|) \times f(\overline{s}, \overline{y})/(y^2 + \overline{y} \cdot \overline{s}),$$

and when the integration over  $\overline{y}$  does not include the occupied region in momentum space. The total annihilation rate  $\Gamma=(2\pi)^{-2}r_0^2\,c\,\int\,d\overline{s}\,\,\Gamma(s)$ , where the integral covers only the interior of the Fermi sphere. Here  $r_0$  is the classical electron radius,  $\beta=(16\pi^2\ a_0)^{-1}$ , and  $a_0$  is the Bohr radius. The term  $\nu(|k|)$  is the Fourier transform of the static interaction potential between an electron and a positron in the electron gas. A numerical solution of this integral equation and the associated annihilation rate is in progress.

### Absorption of Photons in Metals Due to Electron-Electron Collisions

Until about a decade ago, absorption of photons in metals was interpreted chiefly in terms of the Drude theory of the optical constants of metals and was thought to involve the same mechanisms giving rise to dc resistivity. It was recognized at an early stage that optical absorptivity in the alkali metals is considerably larger than would

be predicted on this basis. Among the possible explanations advanced for this discrepancy are: (1) additive absorption due to interband transitions, and (2) anomalously large absorptivity in a thin surface layer having properties different from the bulk metal. The possible importance of electron-electron collisions in the photon absorption process has been suggested, 13 but a quantitative study of this phenomenon has been made only recently, 14 by use of a many-body theory of the high-density electron gas.

We have considered the contribution of electronelectron collisions to photon absorption in detail and have shown that the absorption cross section in a free electron gas may be derived on a simple semiclassical basis. We find that  $\Sigma_a$ , the inverse mean free path for absorption, may be written

$$\begin{split} \Sigma_a &= \left(\frac{2^{14} \alpha}{9\pi^3 a_0 x^3 x_p^2}\right) \quad \int_0^x dx' \int_0^\infty z^4 dz \\ &\times Im \left[\frac{1}{\epsilon(z, x - x')}\right] Im \left[\epsilon(z, x')\right] \,, \end{split}$$

where  $\alpha=e^2/\hbar c$ ,  $a_0$  is the Bohr radius,  $x=\hbar\omega/E_F$ ,  $x_p=\hbar\omega_p/E_F$ ,  $\omega$  is the photon angular frequency,  $\omega_p$  is the plasma frequency of the free electron gas, and  $E_F$  is the Fermi energy. The term  $\epsilon(z,x)$  is the longitudinal dielectric constant of the electron gas for disturbances having wavelength  $\pi/zk_F$  and frequency  $xE_F/\hbar$ , in which  $\hbar^2k_F^2/2m=E_F$ .

Calculations of the reflectivity of a metal surface in the range of frequencies  $\omega < \omega_p$  have been made from this theory for electronic densities corresponding to those of the conduction band in the alkali metals. Reflectivity measurements for some of the alkali metals are available in the literature and show good agreement with these results for sodium and potassium and somewhat less satisfactory agreement in the case of rubidium and cesium. In all cases the present approach shows great improvement over the predictions of the Drude theory. Contributions from absorption due to the anomalous skin effect and due to mechanisms contributing to dc resistivity

<sup>&</sup>lt;sup>13</sup>C. W. Bentham and R. Kronig, *Physica* **20**, 293 (1954).

<sup>&</sup>lt;sup>14</sup>N. Tzoar and A. Klein, Phys. Rev. 124, 1297 (1961).

have been taken into account in making these comparisons. The results will be discussed in detail elsewhere.

### Surface Absorption of Photons in Metals

When a transverse electromagnetic wave impinges normally upon an ideal metal surface, real intra-band excitation of conduction electrons cannot occur in the first order. An allowed second-order process, which is important in the infrared region, is virtual excitation of an electron by the incident wave and de-excitation through interaction with the surface.

The metal surface plays an even more explicit role in the case of nonnormal incidence. Induced currents may assume a nontransverse character due to the constraint imposed upon electronic motion by the surface. This constraint results in a coupling of the incident transverse wave with the longitudinal field inside the metal.

The problem of photon absorption in an ideal semi-infinite free electron gas may be solved readily if one assumes that electrons are reflected internally in a specular mode when they strike the surface and if one restricts attention to photon frequencies  $\omega >> \omega_p \, v_F/c$ , where  $\omega_p$  is the plasma frequency of the free electron gas and  $v_F$  is its Fermi velocity. One finds that  $A_1$ , the surface absorptivity for photons incident at angle  $\theta$  with respect to the surface normal and with the polarization vector perpendicular to the plane of incidence, may be written as

$$A_{\perp} = 1 - \left| \frac{\cos \theta - i/S_{\perp}(\omega, \theta)}{\cos \theta + i/S_{\parallel}(\omega, \theta)} \right|^{2},$$

where

$$S_{\perp} = \frac{\omega}{\pi c} \int_{-\infty}^{\infty} \frac{dk_z}{k^2 - E_{\perp}(k,\omega)\omega^2/c^2},$$

while photons polarized parallel with the plane of incidence are characterized by absorptivity  $A_{11}$ , where

$$A_{||} = 1 - \left| \frac{\cos \theta - iS_{||}(\omega, \theta)}{\cos \theta + iS_{||}(\omega, \theta)} \right|^2,$$

$$S_{||} = \frac{\omega}{\pi c} \int_{-\infty}^{\infty} \frac{dk_z}{k^2} \left[ \frac{\sin^2 \theta}{\epsilon_{||}(k, \omega)} \right]$$

$$-\frac{k_z^2}{k^2-\omega^2\epsilon_1(k,\omega)/c^2}\bigg],$$

where  $k^2 = k_z^2 + \omega^2 \sin^2 \theta/c^2$ . In these equations,  $\epsilon_{||}(k,\omega)$  and  $\epsilon_{||}(k,\omega)$  are the longitudinal and transverse dielectric constants of the electron gas, respectively.

The antithetical case of diffuse electron reflection at the boundary may also be solved with a classical perturbation-theoretic approach. One finds by assuming  $\omega_p \, v_p << \omega < \omega_p$ , that

$$A_{\perp} = 3v_F \cos \theta/4c ,$$

$$A_{\parallel} = A_{\perp} / \left[ \cos^2 \theta + \frac{\sin^2 \theta}{(\omega_p / \omega)^2 - 1} \right].$$

The result for  $A_{||}$  shows clearly the strong effect of coupling between incident transverse and internal longitudinal fields for  $\theta$  close to  $\pi/2$ .

Experimental measurements of absorptivity for  $\theta << \pi/2$  have been made. <sup>15,16</sup> Measurements of this sort at grazing angles would test the predictions of the present theory and would allow one to decide which of the two conditions for surface reflection of electrons is more nearly correct.

### Optical Bremsstrahlung in a Dielectric Medium

There has recently been much interest in transition radiation from dielectric media irradiated by charged particles. Bremsstrahlung from charged-particle scattering on ion cores in a dielectric is an unavoidable concomitant of transition radiation. Bremsstrahlung from isolated scattering centers has been thoroughly investigated, but very little attention has been given to the influence of the

<sup>&</sup>lt;sup>15</sup>M. Biondi, Phys. Rev. 102, 964 (1956).

<sup>&</sup>lt;sup>16</sup>L. G. Schulz, Advan. Phys. 6, 102 (1957).

medium on these photons. They may be refracted at the surface of the medium or absorbed in its interior; coherency effects between equivalent currents generated in the scattering process must also be taken into account.

A general treatment has been carried out for the bremsstrahlung distribution from a foil of thickness a with dielectric permittivity  $\epsilon(\omega) = \epsilon_1(\omega) + i\epsilon_2(\omega)$  bombarded normally by charged particles with velocity  $\overline{v}(v^2/c^2 << 1)$  and charge Ze. The foil is assumed to contain n scattering centers per unit volume, each with effective charge  $Z_a e$ .

The number of bremsstrahlung photons per incident particle per unit solid angle in a direction making an angle  $\theta$  with the foil normal and per unit frequency range  $\omega$  may be written

$$\frac{d^2N}{d\omega~d\Omega} = \frac{\alpha\beta^2z^2}{2\pi^2\omega} \left\langle \Theta^2 \right\rangle ~G(\theta\,,\omega)~,$$

where  $\alpha = e^2/\hbar e$ ,  $\beta = v/c$ , and  $\langle \Theta^2 \rangle$  is the mean square angle for ionic scattering per unit length in the foil. If one divides the distribution into photons with electric vector parallel with (11) and perpendicular to (1) the plane containing the foil normal and the photon propagation vector, the components of G are:

$$G_{\perp} = \frac{1}{2Re\left[\left(i\omega/c\right)\sqrt{\epsilon - \sin^2\theta}\right]} \times \frac{\cos^2\theta}{\left|\cos\theta + \sqrt{\epsilon - \sin^2\theta}\right|^2},$$

$$G_{\parallel} = G_{\perp} \left|\cos\theta + \frac{(\epsilon - 1)\sin^2\theta}{\epsilon\cos\theta + \sqrt{\epsilon - \sin^2\theta}}\right|^2,$$

if  $a\omega/c >> 1$  and

$$G_{\perp} = a/4 (1 + \epsilon_2 a\omega/c \cos \theta)$$
,

$$G_{||} = \cos \theta (\cos \theta + \epsilon_2 a\omega/c \sin^2 \theta)G_{\perp}$$
,

if  $a\omega/c \ll 1$ . This result shows that the medium may have a very strong effect upon bremsstrahlung in condensed media in the region of optical frequencies. The formulas for the case of a foil of arbitrary thickness are very long and will be published elsewhere.

#### EXPERIMENTAL PHYSICS OF DOSIMETRY

#### R. D. Birkhoff

E. T. Arakawa	L. B. O'Kelly
T. E. Bortner <sup>17</sup>	J. E. Parks <sup>19</sup>
M. Edmunson <sup>18</sup>	J. A. Sivinski <sup>19</sup>
L. C. Emerson <sup>18</sup>	J. L. Stanford <sup>19</sup>
D. C. Hammer <sup>18</sup>	T. D. Strickler <sup>19</sup>
H. H. Hubbell, Jr.	J. A. Stockdale <sup>20</sup>
G. S. Hurst	W. H. Wilkie, Jr. 18

### Ionization of Gas Mixtures

Studies of alpha-particle ionization of binary mixtures of gases containing argon have continued. If one assumes that two excited states in argon may transfer energy to the added gas, provided that the ionization potential,  $I_x$ , is less than the metastable levels in argon,  $E_2$  (11.5 ev), and that energy may be transferred to ionization of x from only one level  $E_1$ , where  $E_1 > E_2$  if  $E_1 > I_x > E_2$ , then a semiempirical equation for the W of a mixture  $W_m$  may be shown to be

$$\frac{1}{W_m} = \left[ \left( \frac{1}{W_x} - \frac{1}{W_{Ar}} \right) Z + \frac{1}{W_{Ar}} \right] + \alpha_1 \frac{f_x}{f_x + c_1 f_{Ar}} (1 - Z) + \frac{\alpha_2 f_x}{f_x + c_2 f_{Ar}} (1 - Z) ,$$

where

$$Z = \frac{f_x}{f_x + af_{Ar}}$$

and where  $f_x$  and  $f_{Ar}$  are the mole fractions of gas x and argon, respectively. In this equation a,  $\alpha_1$ ,  $\alpha_2$ ,  $c_1$ , and  $c_2$  may be regarded as empirical parameters (see Table 3.2). Experimental data of  $W_m$  as a function of  $f_x$  were fitted to the equation, and values of the parameters shown in the table were obtained. The generalized least-square code

<sup>&</sup>lt;sup>17</sup>Consultant.

<sup>&</sup>lt;sup>18</sup>AEC Health Physics Fellow,

<sup>&</sup>lt;sup>19</sup>Summer employee.

<sup>&</sup>lt;sup>20</sup>Alien guest from Australian Atomic Energy Research Establishment, Lucas Heights, Sydney, Australia.

Table 3.2.	Parameters Appearing in the Equation Which Expresses ${\it W}$
	for Binary Mixtures Containing Argon

Gas, x	$l_{_{m{x}}}$	а	$c_1$	$a_1$	c <sub>2</sub>	$a_2$
Krypton	13.9	0.412	0.0617	0.00456		-
Carbon Dioxide (CO <sub>2</sub> )	14.4	0.637	0.351	0.00209		
Methane (CH <sub>4</sub> )	12.8	0.487	0.016	0.00114		
Nitrous Oxide (N <sub>2</sub> O)	12.3	0.521	0.00656	0.00193		
Ethane (C <sub>2</sub> H <sub>6</sub> )	11.6	0.167	0.000138	0.000804	0.0122	0.00401
Acetylene (C <sub>2</sub> H <sub>2</sub> )	11.25	0.256	0.0000101	0.00185	0.000117	0.00924
Propane (C <sub>3</sub> H <sub>8</sub> )	11.2	0.158	0.0000611	0.00324	0.00556	0.00255
n-Butane (C <sub>4</sub> H <sub>10</sub> )	10.8	0.210	0.0000296	0.00373	0.000852	0.00234
Ethylene (C <sub>2</sub> H <sub>4</sub> )	10.56	0.255	0.0000552	0.00254	0.00143	0.00193
Isobutane (C <sub>4</sub> H <sub>10</sub> )	10.34	0.195	0.000108	0.00469	0.00437	0.00129
Cyclopropane (C <sub>3</sub> H <sub>6</sub> )	10.23	0.197	0.0000584	0.00429	0.00351	0.00213
Propylene (C <sub>3</sub> H <sub>6</sub> )	9.8	0.262	0.0000137	0.00242	0.000645	0.00206
Butene-1 (C <sub>4</sub> H <sub>8</sub> )	9.72	0.203	0.0000197	0.00329	0.00209	0.00248

written for the IBM  $7090^{21}$  gave rapidly converging results for most of the mixtures. For cases where  $I_x > 11.5$  v, the three-parameter equation (i.e., dropping the third term) did not give a good fit to the experimental data, which indicates that at least two excited levels must be taken into account in these cases.

# Interaction of Low-Energy Electrons with Binary Gas Mixtures Containing a Polar Component

Experimental studies of low-energy (less than 1 ev) electron capture and drift velocity in mixtures of H<sub>2</sub>O with N<sub>2</sub>, CO<sub>2</sub>, C<sub>2</sub>H<sub>4</sub>, and CH<sub>4</sub> show

that: (1) electron capture takes place only in the  $\rm H_2O\text{-}CO_2$  mixture; thus permanent electron capture to form a negative ion of water does not take place; (2) the drift velocity in mixtures of  $\rm H_2O\text{-}CO_2$ ,  $\rm H_2O\text{-}C_2H_4$ , and  $\rm H_2O\text{-}CH_4$  decreases appreciably due to the addition of a few percent of  $\rm H_2O$  to the nonpolar molecular gases when the total pressure ranges between 100 to 400 mm Hg. In fact, the transport time per centimeter,  $w^{-1}$ , can be represented by

$$w^{-1} = w_0^{-1} + S(E/P) f_1 / f_2 , \qquad (1)$$

 $<sup>^{2\,</sup>l}\mbox{We}$  are grateful for computation assistance given by D. Bagwell, Central Data Processing, Oak Ridge Gaseous Diffusion Plant.

where  $w_0^{-1}$  is the drift time per centimeter in the pure nonpolar gas,  $f_1/f_2$  is the ratio of pressures for water and the nonpolar gases, and S(E/P) is a function of E/P only. When water is replaced with other polar molecules (e.g., acetone, D<sub>2</sub>O, methyl alcohol, dimethyl ether, H2S, toluene, and nitrous oxide) in mixtures with ethylene, Eq. (1) also fits the experimental data for these mixtures.

The results quoted above for the water-vapor mixtures combined with the Bradbury-Tatel<sup>22</sup> data for pure water vapor suggested<sup>23</sup> the interesting idea that electrons make collision of long duration in H<sub>2</sub>O, and successive collision of the quasinegative ion leads to a state in which the electron is trapped in a potential well supported by collective interaction with many water molecules, that is, the polaron.<sup>24</sup> Recent unpublished results<sup>25</sup> do not confirm the Bradbury-Tatel data<sup>22</sup> for pure H2O, and this may require revision of the mechanism suggested above.

### Electron Swarm Measurements with a Time-of-Flight Method

A new method has been developed which permits the study of the motion of individual electrons in a swarm. The one-dimensional differential equation describing the motion of electrons is

$$\frac{\partial n(x,t)}{\partial t} = \frac{D \ \partial^2 n(x,t)}{\partial x^2} - \frac{W \ \partial n(x,t)}{\partial x} - \beta W n(x,t),$$

where n(x,t) is the number density of free electrons, D is the diffusion coefficient, W is the drift velocity, and  $\beta$  is the probability of capture in moving 1 cm in the field direction. The timedependent solution of the differential equation, neglecting boundary effects, is

$$n(x,t) = \frac{N}{\sqrt{4\pi D}} t^{-1/2} e^{-(x-Wt)^2/4Dt} e^{-\beta Wt},$$

where N is the number of free electrons per square centimeter on the plane x = 0 at time t = 0.

Experimental measurement of the time-of-arrival of electrons at a point on a plane x = L is achieved by means of a Geiger-Mueller counter operating with a low efficiency so that the number of electrons detected by it is a small fraction of the number of ultraviolet light pulses releasing electrons at t = 0 on the plane x = 0. In this way it may be shown that the distribution of time intervals between the ultraviolet pulse and the registration of a pulse in the Geiger-Mueller detector provides the distribution function n(L,t). A measurement of n(L,t) with a multichannel pulse-height analyzer provides simultaneously the parameters D, W, and  $\beta$ . Preliminary results with C2H4 appear to be in agreement with Forester and Cochran<sup>26</sup> for the quantities D and W.

### Measurement of Light Emission from Irradiated Metal Foils

The investigation of visible and ultraviolet light emitted by thin metallic foils irradiated by highenergy electrons as reported in the last annual report (ORNL-3189, p 162) has been continued. Typical results are shown in Figs. 3.1 and 3.2

<sup>&</sup>lt;sup>26</sup>D. W. Forester and L. W. Cochran, Diffusion of Slow Electrons in Gases, ORNL-3091 (Sept. 29, 1961).

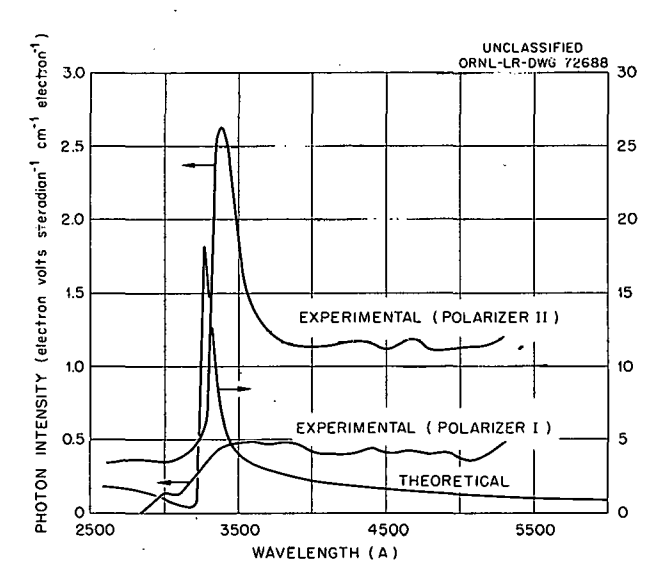


Fig. 3.1. Spectral Distributions for Silver Foil at 30° from Foil Normal. Experimental: t = 570 A, E = 25 kev;theoretical; t = 600 A, E = 30 kev.

<sup>&</sup>lt;sup>22</sup>N. E. Bradbury and H. E. Tatel, J. Chem. Phys. 2, 835 (1934).

<sup>&</sup>lt;sup>23</sup>G. S. Hurst, L. B. O'Kelly, and J. A. Stockdale, Nature 195, 66 (1962).

<sup>&</sup>lt;sup>24</sup>S. Pekar, J. Phys. U.S.S.R. X(4), 341 (1946).

<sup>25</sup> J. L. Pack, R. E. Voshall, and A. V. Phelps, Drift Velocities of Slow Electrons in Krypton, Xenon, Deuterium Carbon Monoxide, Carbon Dioxide, Water Vapor, Nitrous Oxide, and Ammonia, Westinghouse Technical Report No. 11 (Mar. 19, 1962).

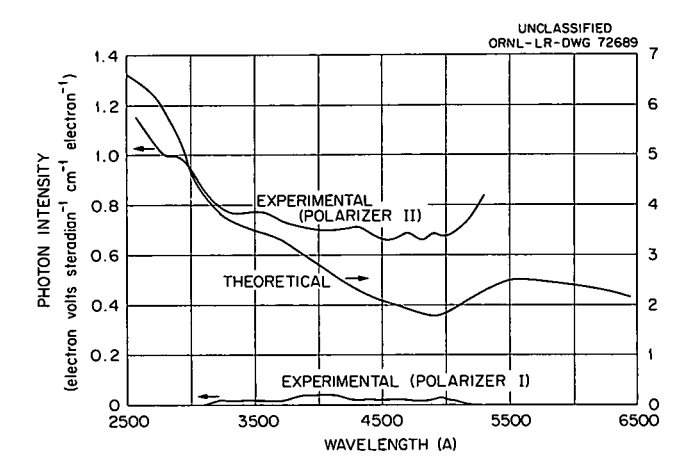


Fig. 3.2. Spectral Distribution for Gold Foil at  $30^{\circ}$  from Foil Normal. Experimental: t = 340 A, E = 100 key; theoretical: t = 500 A, E = 100 key.

for silver and gold foils, respectively, the silver foil showing the sharp emission peak as predicted theoretically <sup>27</sup> from optical reflectivity data.

A brief period was also spent in the investigation of radiation from foils bombarded by lowenergy (50-100 ev) electrons as suggested by Silin and Fetisov. 28 They report that the sharp emission line expected from the plasma oscillation of free electrons in metals can only be observed if the incident electron energy is of the order of the Fermi energy. No sharp line was observed experimentally. However, the results were not considered completely conclusive due to the large amount of background light from the electron-emitting filament and the fact that the lowest-energy electrons used were substantially above the Fermi energy (~10 ev).

A grating calibrator has been designed, constructed, and used extensively during this period to determine the absolute transmission of the optical spectrometer in the visible and into the far ultraviolet. An accurate knowledge of the grating and spectrometer efficiency has made possible a much more precise analysis of the spectra distribution of the light emitted by the foils. The results for two gratings are shown in

Fig. 3.3. This study shows that large differences may exist in the absolute efficiencies of various gratings and also that the efficiency does not vary smoothly with wavelength but shows distinct peaks at several wavelengths. Spectral data taken with these gratings will show similar peaks which may be misinterpreted as representing true emission peaks from the material investigated if grating efficiency is not known accurately.

For the coming year a detailed investigation will be made of the angular distribution of radiation emitted by various foils under high-vacuum conditions ( $10^{-8}$  to  $10^{-9}$  torr). An irradiation chamber has been designed and constructed which makes possible a continuous rotation of the spectrometer from 0 to  $153^{\circ}$  with reference to the electron beam direction and which will operate at the vacua mentioned above.

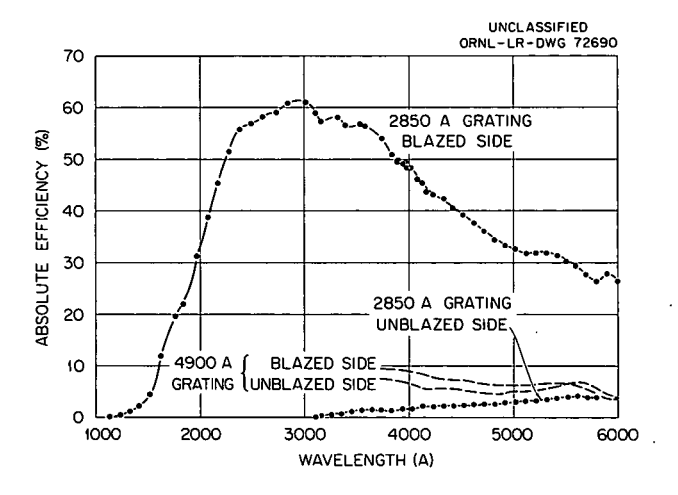


Fig. 3.3. Efficiency of Two Concave Diffraction Gratings as a Function of Wavelength. Solid line: Bausch and Lomb 50-cm grating blazed at 2850 A; dashed line: Jarrell-Ash 50-cm grating blazed at 4900 A.

### Spherical Electrostatic Analyzer

The spherical electrostatic beta-ray analyzer (the Keplertron) described in the last progress report has undergone extensive tests and development. The Keplertron consists of two concentric spheres with the source spread on the inner sphere in an area around the axis of symmetry as shown in Fig. 3.4. The electron spectrum is analyzed by

<sup>&</sup>lt;sup>27</sup>R. H. Ritchie and H. B. Eldridge, Phys. Rev. 126, 1935 (1962); A. L. Frank, E. T. Arakawa, and R. D. Birkhoff, Phys. Rev. 126, 1947 (1962); A. L. Frank et al., Optical Emission from Irradiated Thin Metallic Foils, ORNL-3114 (July 2, 1962).

<sup>&</sup>lt;sup>28</sup>V. P. Silin and E. P. Fetisov, *Phys. Rev. Letters* 7, 374 (1961).

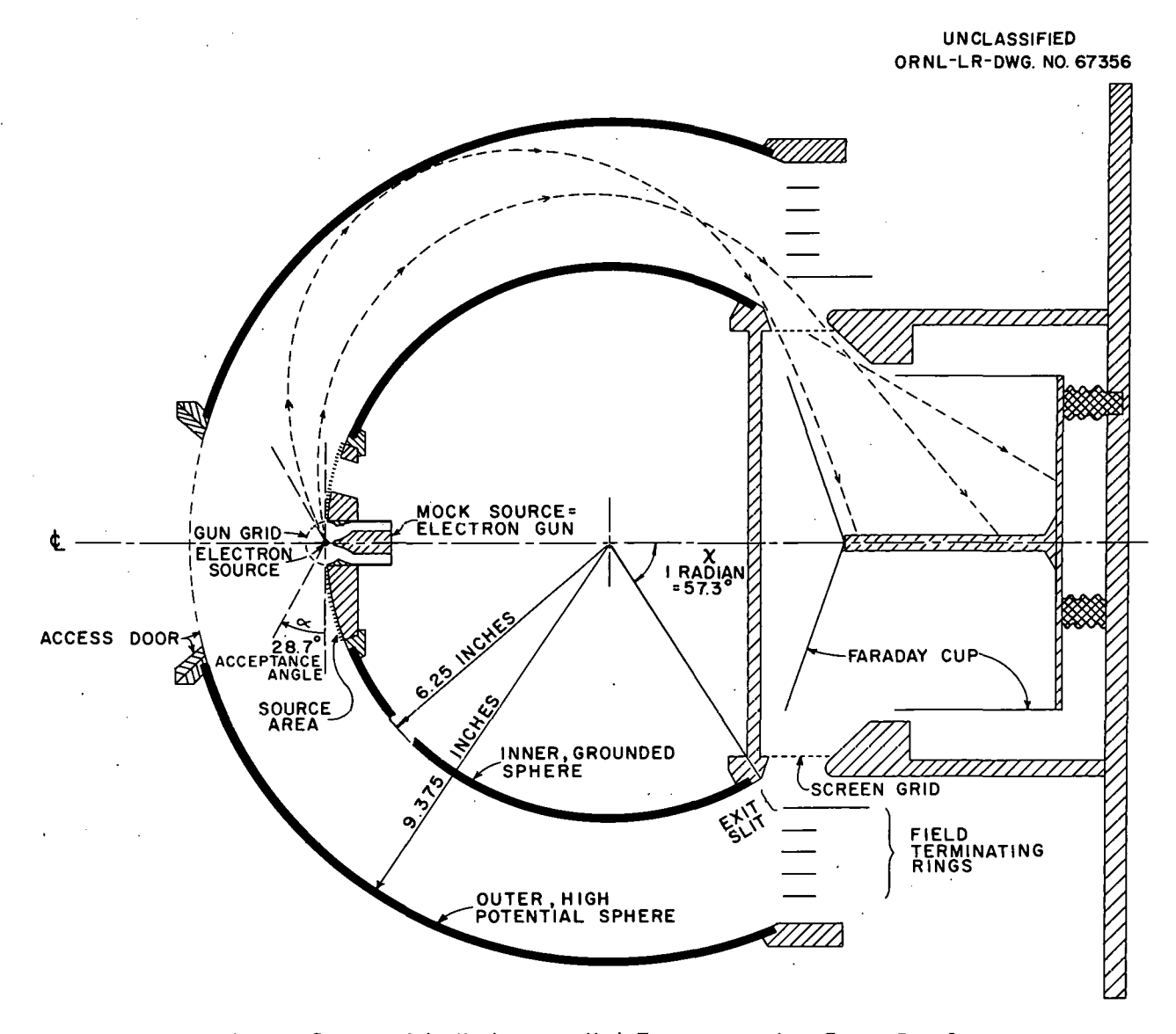


Fig. 3.4. Schematic Diagram of the Keplertron, a High-Transmission, Low-Energy Beta Spectrometer.

varying the voltage on the outer sphere. The instrument is to be used for making absolute intensity measurements on electron slowing-down spectra over the energy range 1 ev to 40 kev. Therefore a precise knowledge is required of the transmission of the instrument as a function of electron source energy and the resolution as determined from spectral line shape for monoenergetic electrons.

An electron gun was used to simulate a radioactive source giving monoenergetic electrons of known energy and intensity, since sufficiently intense line sources of accurately known intensity are not available in the region of interest below 40 kev. It was extremely difficult to build a gun simulating the isotropic emission expected of a beta-ray source and postulated in the theoretical analysis of the Keplertron. Also, in spite of the large overall size of the instrument, the gun structure had to be very tiny to avoid distorting the electric field on which the Keplertron operation depends. Two completely different gun structures and about a dozen different cathode and filament designs were tried. The most satisfactory design consisted of a tungsten ball 0.2 in. in diameter heated internally by a double-wound

tungsten helical filament. The ball is at the center of a 0.7-in.-diam hemispherical grid of gold wires.

A typical calibration curve is shown in Fig. 3.5. The line shape closely resembled the theoretical shape; and the energy resolution, defined as the width of the line at half maximum intensity. is 7% compared with a calculated value of 6.25%. The transmission of the instrument is 25% as calculated after correction for the transmission of the screen grid used to reduce the capacity between the Faraday cup and the outer sphere to 10-16 f. Similar line shapes were observed from 40 to 2000 v, and the transmission and resolution remained constant over this range. At lower electron energies, the energy spread of the electrons from the gun affected the natural line shape, but the instrument operated satisfactorily down to about 2 ev.

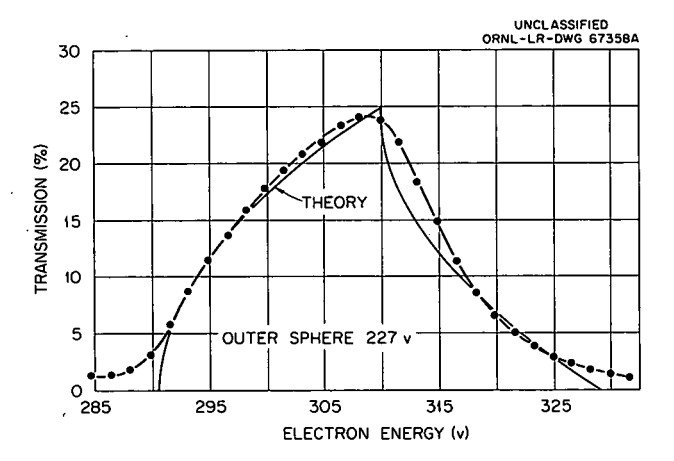


Fig. 3.5. Transmission of the Keplertron as a Function of Electron Energy.

A preliminary measurement of the negatron spectrum from a thick plane Cu<sup>64</sup> source over the energy range 14 ev to 41 kev is shown in Fig. 3.6. The flux may be seen to go through a minimum at about 20 kev and to double each time the energy below this value is halved. No comparison with the Spencer-Fano theory is possible because a flat source was used. Further measurements will use cavity sources where such comparison is valid.

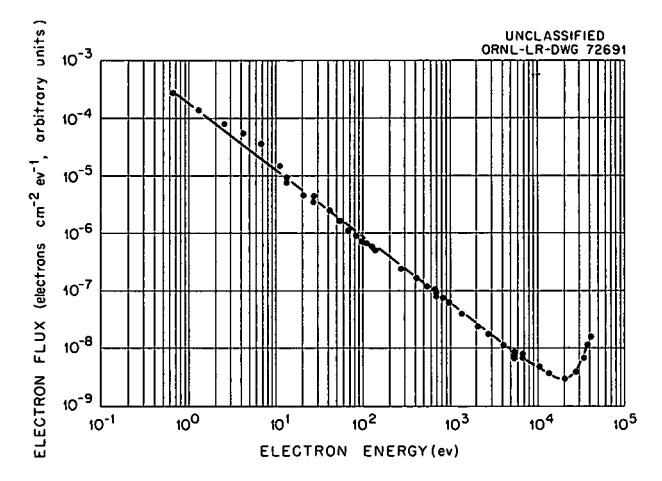


Fig. 3.6. Electron Flux from Plane Source of Cu<sup>64</sup>.

### Slowing-Down Spectrum of Positrons in Copper

A previous measurement<sup>29</sup> of the slowing-down electron flux in an infinite beta radioactive (P<sup>32</sup>) medium (bakelite) revealed close agreement with a simplified version of the continuous slowingdown theory of Spencer and Fano<sup>30</sup> above 350 kev; between this energy and 50 kev, the experiment fell below theory by as much as 20%. In order to determine whether this disagreement was due to experimental uncertainty in spectrometer transmission or was a consequence of the use of the simplified slowing-down model, a similar study has been made of positrons in a pile-irradiated copper medium. Because the positrons may be distinguished experimentally from the secondary electrons they generate, this experimental arrangement permits an observation of the primary slowing-down flux.

An anthracene button 2 ml thick on a 6199 photomultiplier and a 256-channel analyzer served as a scintillation spectrometer. Deviations from linearity in a Fermi plot of Pm<sup>147</sup> were found to be explainable by a theory of the scintillation process by Birks, and positron data were corrected accordingly. An NaI(Th) spectrometer, adjusted to count annihilation photons from positrons dying in the anthracene, served to gate a coincidence arrangement which rejected all positron pulses not accompanied by an annihilation photon. Thus, the negatron and secondary electron spectrum from Cu<sup>64</sup>

 <sup>&</sup>lt;sup>29</sup>R. D. Birkhoff et al., Health Phys. 1, 27 (1958).
 <sup>30</sup>L. V. Spencer and U. Fano, Phys. Rev. 93, 1172 (1954).

did not contribute to the anthracene spectrum. Plane and cavity sources were used, and corrected spectra are shown in Figs. 3.7 and 3.8 along with the theoretical spectrum for an infinitely thick source. The data in the former case fall below the theoretical curves at low energies as expected, because the absence of source material adjacent to the emitting surface results in a loss of backscattered positrons of degraded energy from the spectrum. For the cavity source the agreement is very good, substantiating the recent Monte Carlo calculations of electron slowing down by Schneider and Cormack. 31

### <sup>31</sup>D. O. Schneider and D. V. Cormack, *Radiation Res.* 11, 418 (1959).

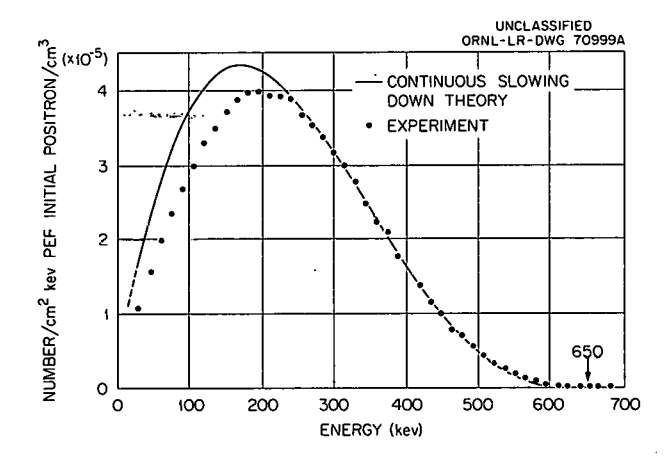


Fig. 3.7. Positron Flux Emitted to a Flat Copper Disk Containing  $\mathrm{Cu}^{64}$ .

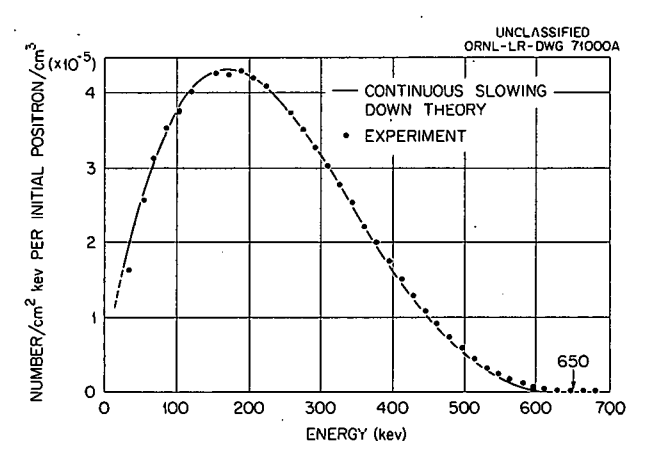


Fig. 3.8. Positron Flux Emitted from a Cavity Source of Copper Containing Cu<sup>64</sup>.

### DOSIMETRY METHODS AND APPLICATIONS

J. A. Auxier	F. J. Davis
A. E. Carter	D. Pittman <sup>35</sup>
J. S. Cheka	P. W. Reinhardt
L. W. Gilley <sup>32</sup>	F. W. Sanders
J. A. Harter	W. H. Shinpaugh, Jr.
F. F. Haywood <sup>33</sup>	R. M. Simmons
E. T. Loy <sup>34</sup>	J. H. Thorngate
E. B.	₩agner

# Radiation Measurements over Simulated Plane Sources

Preliminary mockup and circuitry to be used with the  $9 \times 9$  in. NaI crystal in the BREN program 2 (Bare Reactor Experiment in Nevada) experiments have been made. These experiments will entail spectral measurements of gamma rays scattered from the air and ground from various configurations of sources including point and distributed sources of various energies. 9 x 9 in. crystal will be supported 100 ft to one side of the 1500-ft tower by cables, thus allowing measurements to be made from ground level to Measurements will include the effect 1200 ft. of ground roughness on the ratio of ground readings to those taken in aircraft. Such scattering experiments will lead to a better understanding of the measurement of dose due to fallout from weapons and reactor incidents.

### Energy Response of G-M Tubes

During numerous experiments involving both pure gamma radiation and mixed component field radiation with the G-M gamma-ray dosimeter, <sup>36,37</sup> the need for further development of this type of dosimeter was suggested. The original dosimeter has been improved by designing a new energy

<sup>&</sup>lt;sup>32</sup>Neutron Physics Division.

<sup>&</sup>lt;sup>33</sup>Applied Health Physics Section, Health Physics Division.

 $<sup>^{34}</sup>$ Engineering and Maintenance Group, Health Physics Division.

<sup>35</sup> Engineering and Mechanical Division.

<sup>&</sup>lt;sup>36</sup>F. J. Davis et al., Health Phys. Ann. Progr. Rept. July 31, 1960, ORNL-2994, p 226.

<sup>&</sup>lt;sup>37</sup>E. B. Wagner and G. S. Hurst, *Health Phys.* 5, 20-26 (1961).

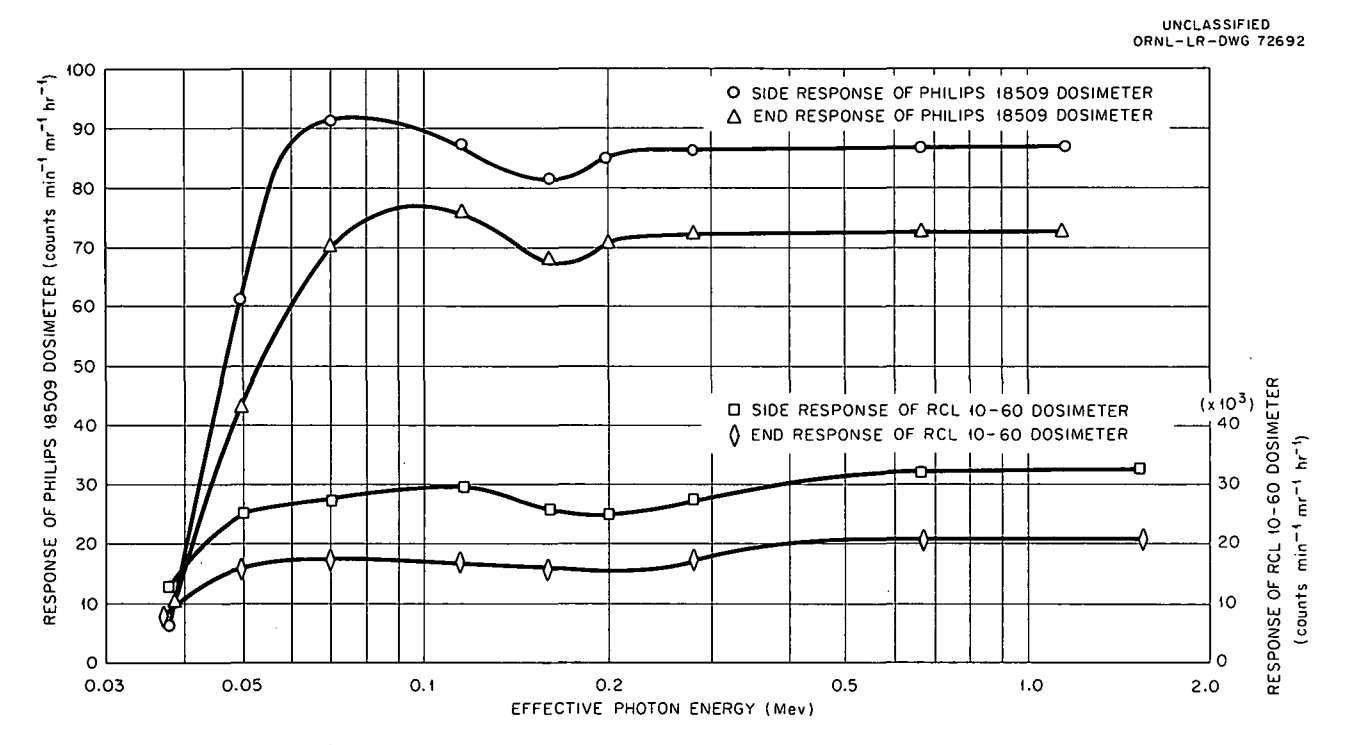


Fig. 3.9. Response of Philips 18509 and RCL 10-60 Shielded Counters as a Function of Gamma-Ray Energy.

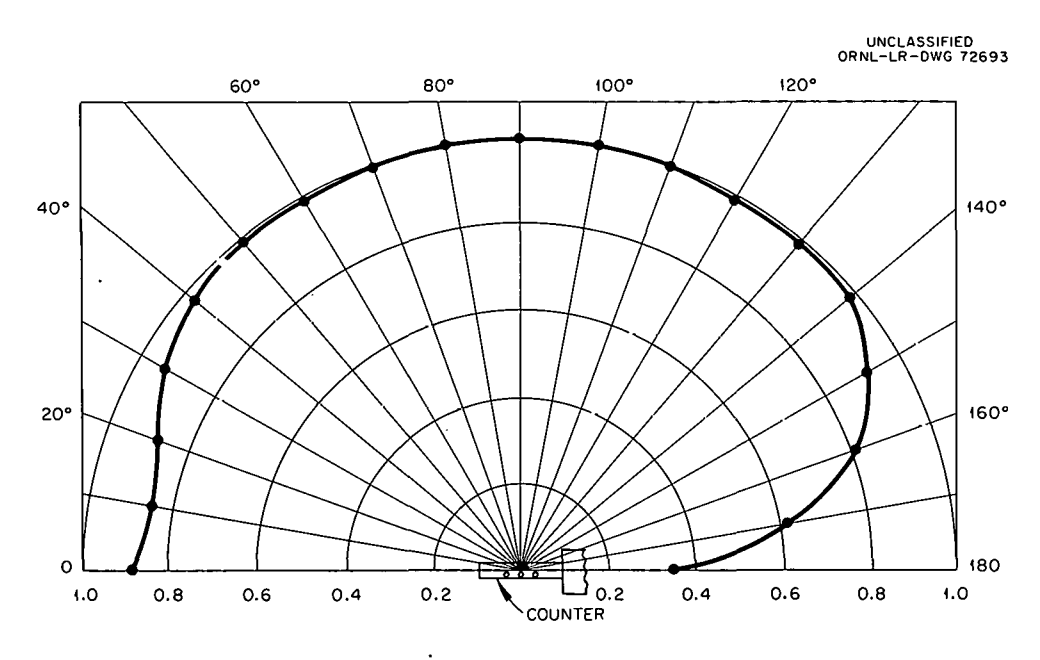


Fig. 3.10. Relative Angular Response of Philips 18509 Small Counter, with a Perforated Shield for  $Co^{60}$  Gamma Rays.

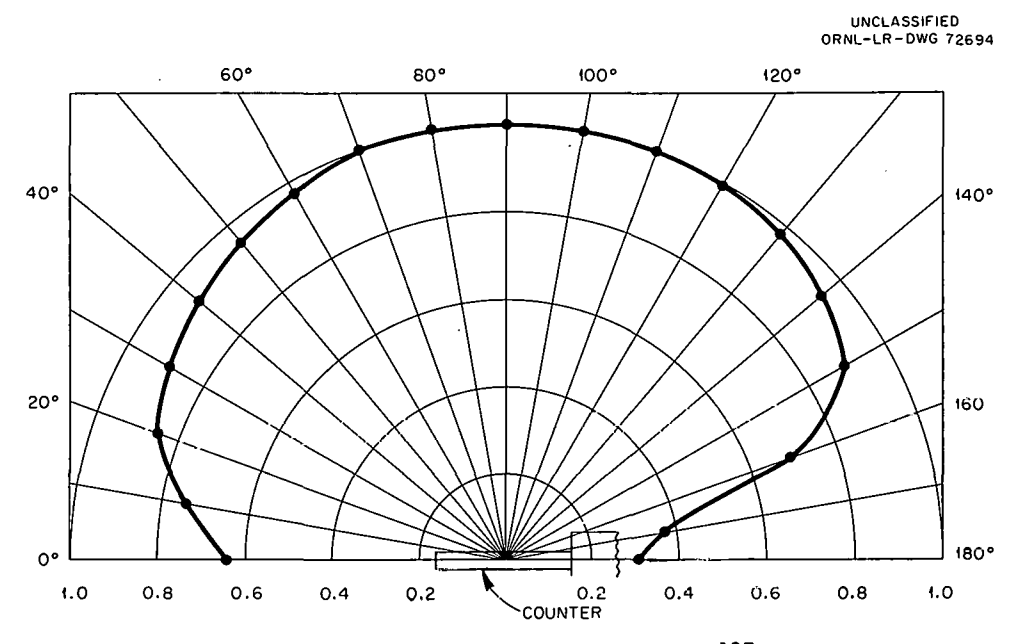


Fig. 3.11. Relative Angular Response of RCL 10-60 G-M Counter for Cs 137 with Energy Correction Shield.

correction shield which extends its response down to 55 kev. To fill the need for a more sensitive gamma dosimeter for low-level gamma dose measurements, an energy correction shield has been designed for an RCL 10-60 halogen-filled G-M counter which is 37 times more sensitive than the Philips 18509 counter.

The new energy correction shield for the Philips 18509 counter is similar to the original shield with the three following changes:

- Thirty holes, 0.081 in. in diameter, were drilled in the wall of the shield along the axial direction.
- An additional 0.003 in. of lead was used around the outside walls of the shield covering all of the shield, including the 30 holes but not covering the end of the shield.
- 3. Eight holes, 0.040 in. in diameter, were drilled in the end of the shield.

As shown in Fig. 3.9, the response of the dosimeter with the new perforated shield is independent of gamma-ray energies down to 55 kev within  $\pm 6\%$ . The polar response obtained with the same counter and shield is shown in Fig. 3.10.

The energy correction shield for the RCL 10-60 G-M counter consists of 0.040 in. of tin around the walls of the counter with 20 holes, 0.156 in. in diameter, and 24 holes, 0.186 in. in diameter. The end of the shield is also 0.040 in. of tin

with 5 holes, 0.106 in. in diameter, and 4 holes, 0.095 in. in diameter. From Fig. 3.9 it can be seen that the response of the RCL 10-60 dosimeter is independent for gamma energies down to 50 kev  $\pm$  12%. The polar response of the larger G-M dosimeter is shown in Fig. 3.11.

### Fast-Neutron Spectrometer

The dual-crystal scintillation proton recoil fastneutron spectrometer described in the preceding annual report<sup>38</sup> has been in use at the Nevada Test Site for Operation BREN (Bare Reactor Experiment in Nevada).

In Nevada the device was used to measure the fast neutron spectrum from the HPRR (Health Physics Research Reactor) as a function of distance and angle.

Several improvements in the electronics were made in the field; the major improvements were in the coincidence circuits. A tunnel diode circuit was designed, which allowed a coincidence timing of less than 0.1  $\mu$ sec. This resulted in improved gamma-ray rejection. Further monoenergetic neutron studies with the neutron spectrometer and a computer program to allow machine reduction to the BREN data are contemplated.

<sup>&</sup>lt;sup>38</sup>J. A. Auxier et al., Health Phys. Ann. Progr. Rept. July 31, 1961, ORNL-3189, p 177.

### Gamma-Ray Spectrometer

The gamma spectrometer described previously <sup>39</sup> proved to have too low a sensitivity to allow truly significant measurements to be made in the low-radiation fields at large distances from the BREN tower. However, it should be satisfactory for use closer to the HPRR (Health Physics Research Reactor), for example, 100 ft or less.

Additional work on the spectrometer is planned. The gamma spectrometer will be redesigned, and measurements of the gamma spectrum will be attempted after the HPRR is in operation at the DOSAR (Dosimetry Applications Research) facility.

### Health Physics Research Reactor (HPRR)

The HPRR was completed and tested and was used in experiments at the Nevada Test Site (Operation BREN). Operation has included steady-state runs of up to 1250 w for periods of several hours and bursts of approximately 10<sup>17</sup> fissions. Figure 3.12 shows the reactor mechanism without the core but with the safety plate installed in an aluminum hoist car on the 1527-ft-high BREN tower at NTS. Figure 3.13 shows the preamplifier cabinet mounted on a second (higher) level of the same car. A view of the aluminum car with doors removed is shown in Fig. 3.14. The control console and weather recording instruments located in an underground bunker are shown in Fig. 3.15.

A histogram showing neutron flux and percent of total dose as a function of neutron energy is shown in Fig. 3.16. The threshold detector station was located 44 in. from the center of the core, on a line perpendicular to the central axis of the core. The exposure was 15 min at a power level of 1250 w; the total dose was 822 tissue rads of fast neutrons. At 1 m from the core, operated in this configuration, the dose rate should be approximately 3200 tissue mrads hr<sup>-1</sup> w<sup>-1</sup>. The gammaradiation dose was about 15% of the neutron dose; the neutron-gamma ratio should increase when the reactor is operated at the DOSAR facility.

Nuclear characteristics of the reactor and the results of criticality studies have been reported elsewhere.  $^{40-42}$ 

Gamma-Radiation Source. — A nominal 1200-curie Co<sup>60</sup> source was fabricated for use at the DOSAR

facility and for BREN. Figure 3.17 shows the capsule designed to be operated pneumatically at the DOSAR and to provide for low "self-absorption" in the source capsule.

Other DOSAR Facilities. — A plot plan of the DOSAR structures is shown in Fig. 3.18. A plan view of the control and reactor buildings is shown in Figs. 3.19 and 3.20, respectively. The major facilities have been completed and are shown in Figs. 3.21-3.23. The reactor positioning device, Fig. 3.24, will be completed by early August 1962.

### Bare Reactor Experiment in Nevada (BREN)

Operation BREN 43,44 was the major effort in the Ichiban Program. During BREN the radiation fields from nuclear weapons were simulated by means of an unshielded nuclear reactor, the ORNL Health Physics Research Reactor (HPRR), 45 suspended at several elevations on a 1500-ft tower located at the Nevada Test Site. The reactor-tower facility provided a good simulation of the neutron field due to a nuclear weapon, because in both devices the leakage neutrons escaped from the assembled fissile material and were moderated by air. At distances from the source greater than a few hundred yards, equilibrium obtains in the neutron-energy distribution, and energy and angular distributions are not strongly influenced by the design of the neutron source. Use of a reactor operated in the steady-power mode permitted use of sensitive "in-laboratory" type instruments that could not be used for brief intervals at high dose rates or with blast conditions present.

Several components of the gamma-ray field of a nuclear device are well simulated by means of a bare reactor. Because the neutron field so

<sup>&</sup>lt;sup>39</sup>J. A. Auxier et al., Health Phys. Ann. Progr. Rept. July 31, 1961, ORNL-3189, p 176.

<sup>&</sup>lt;sup>40</sup>W. E. Kinney and J. T. Mihalczo, ORNL Fast Burst Reactor: Critical Experiments and Calculations, ORNL CF-61-8-71 (Aug. 24, 1961).

<sup>41</sup> J. T. Mihalczo, Reactivity Calibrations and Fission Rate Distributions in an Unmoderated, Unreflected Uranium-Molybdenum Alloy Research Reactor, ORNL TM-189 (May 10, 1962).

<sup>&</sup>lt;sup>42</sup>J. T. Mihalczo, Superprompt Critical Behavior of an Unreflected Unmoderated, Unreflected Uranium-Molybdenum Alloy Assembly, ORNL TM-230 (May 10, 1962).

<sup>&</sup>lt;sup>43</sup>J. A. Auxier et al., Technical Concept - Operation BREN, CEX-62.01 (January 1962).

<sup>&</sup>lt;sup>44</sup>F. W. Sanders et al., Operation Plan and Hazards Report - Operation BREN, CEX-62.02 (April 1962).

<sup>&</sup>lt;sup>45</sup>M. I. Lundin, Health Physics Research Reactor Hazards Summary, ORNL-3248 (June 27, 1962).

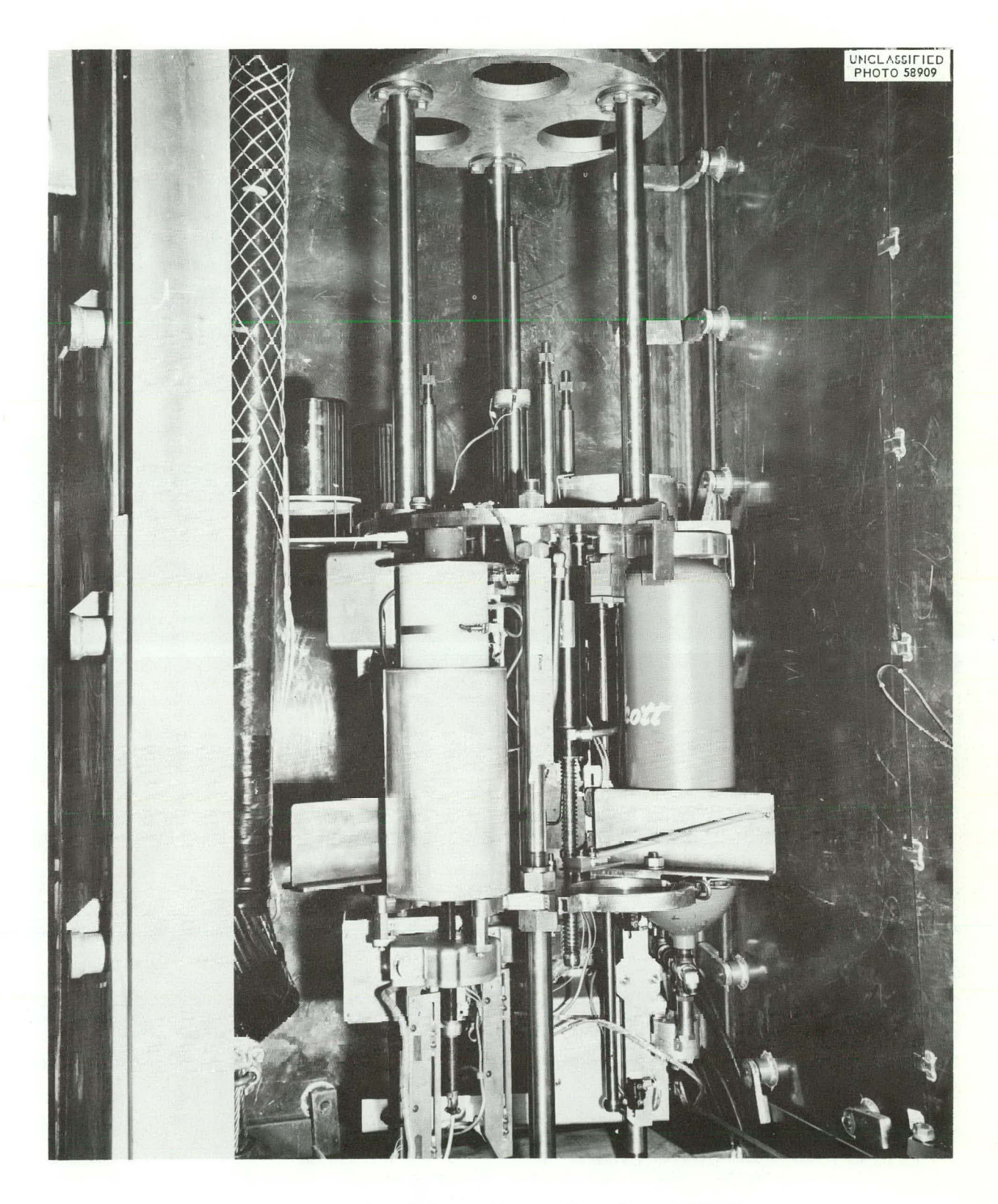


Fig. 3.12. HPRR Installed in an Aluminum Hoist Car on BREN Tower.

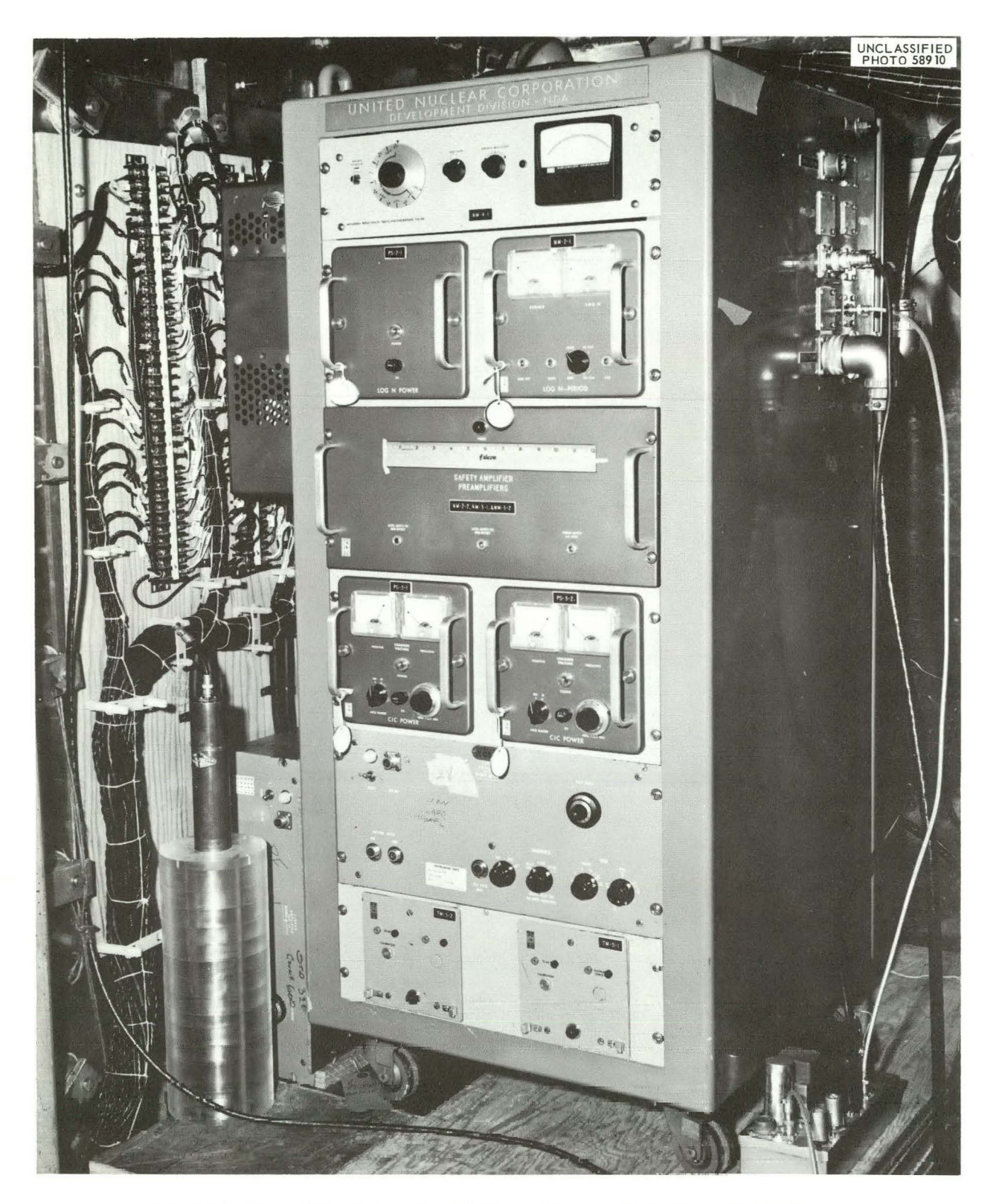


Fig. 3.13. Preamplifier Cabinet Installed in an Aluminum Hoist Car on BREN Tower.



Fig. 3.14. Aluminum Hoist Car Containing HPRR and Preamplifier Cabinet Installed on BREN Tower.

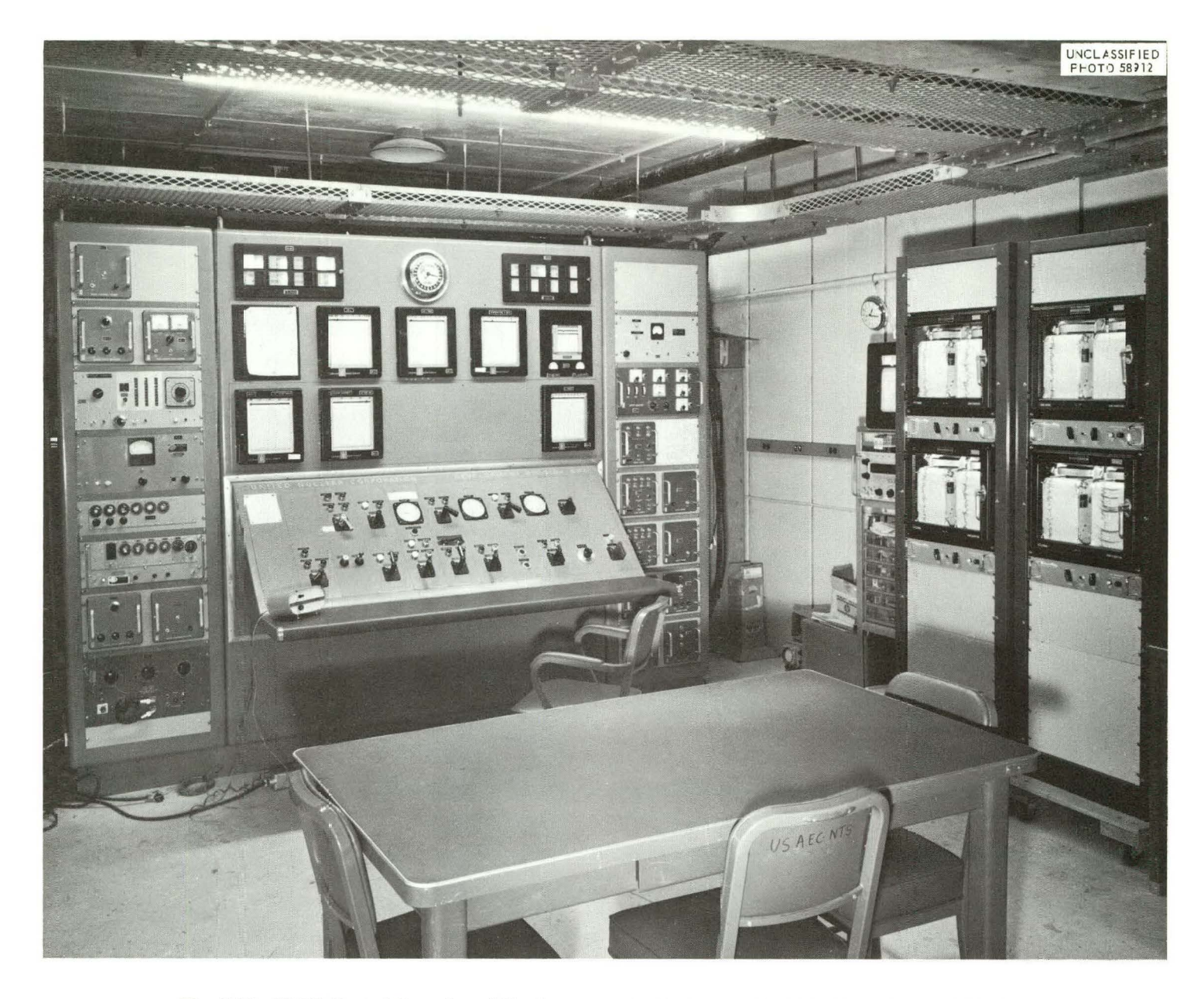


Fig. 3.15. HPRR Control Console and Weather Recording Instruments Installed in Underground Bunker.

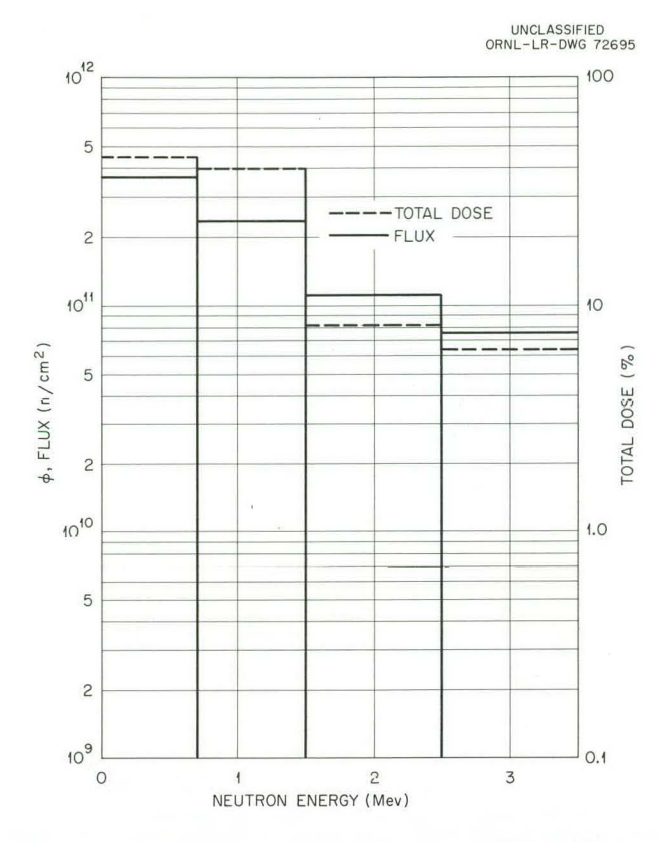


Fig. 3.16. Neutron Flux and Percent of Total Dose as a Function of Neutron Energy.

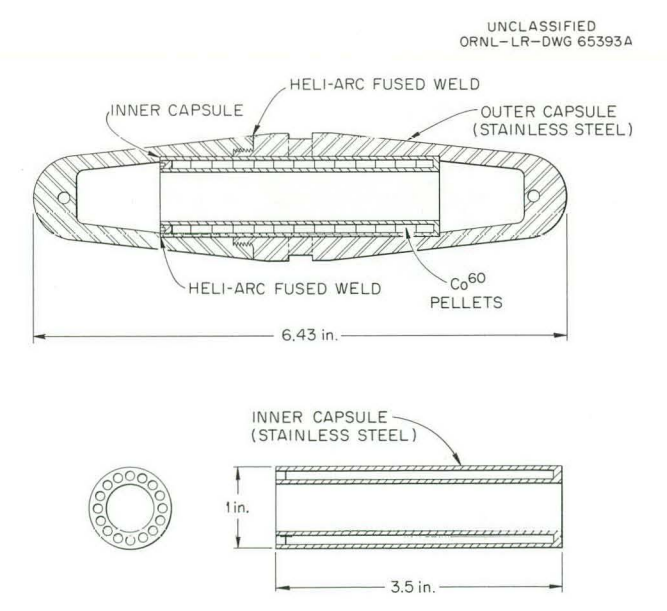


Fig. 3.17. Cobalt-60 Source Container.

closely approximates that from a weapon, neglecting hydrodynamic effects, the gamma rays originating in neutron-air interactions will have the same energy and angular distributions as the corresponding weapons gamma rays. Prompt gamma rays from fission leak through the assembled fissile material as do those from fission in weapons. The gamma rays from fission products in a reactor, however, leak from the assembled fissile material, whereas fission products from a weapon detonation are distributed in an expanding and rising cloud.

To separate, at least semiquantitatively, the components of the gamma-ray field, dose measurements (as a function of angle of incidence and distance from the reactor) were made during steady-power-level operation of the HPRR. Measurements were also made of the energy distributions as a function of time after the reactor was operated in the burst mode. A 1200-curie Co<sup>60</sup> point gamma-ray source was then substituted for the HPRR, and energy and dose distributions (as functions of angle of incidence) were measured at distances of 750 and 1000 yd from the tower.

Although most of the data are being processed at present, some typical angular distribution curves are shown in Figs. 3.25–27. Figure 3.25 shows the neutron distribution at 750 yd from the tower for a reactor operating height of 1125 ft, and Fig. 3.26 shows the gamma-dose distribution for the same configuration. The gamma-ray curve is subject to some modification, since the response of the detector to the high-energy gamma rays from neutron interactions with nitrogen must yet be determined. Figure 3.27 shows the angular distribution of gamma radiation from the 1200-curie Co<sup>60</sup> source for the same configuration.

#### Metaphosphate Glass Microdosimeters

Experimental evaluation on the additivity of small doses noted in the previous annual report (ORNL-3189, p 175) is continuing with the additional exposure of 500 mr of radium gamma exposure per working day. The weekly readings have been suspended due to the demands of the Ichiban and BREN projects. Meanwhile, partial results on dose integration and fading have been obtained. In July 1960, an experiment was initiated wherein a group of badges were exposed to 10 mr of radium gamma per working day for 1 yr, another group was stored in a lead pig to serve

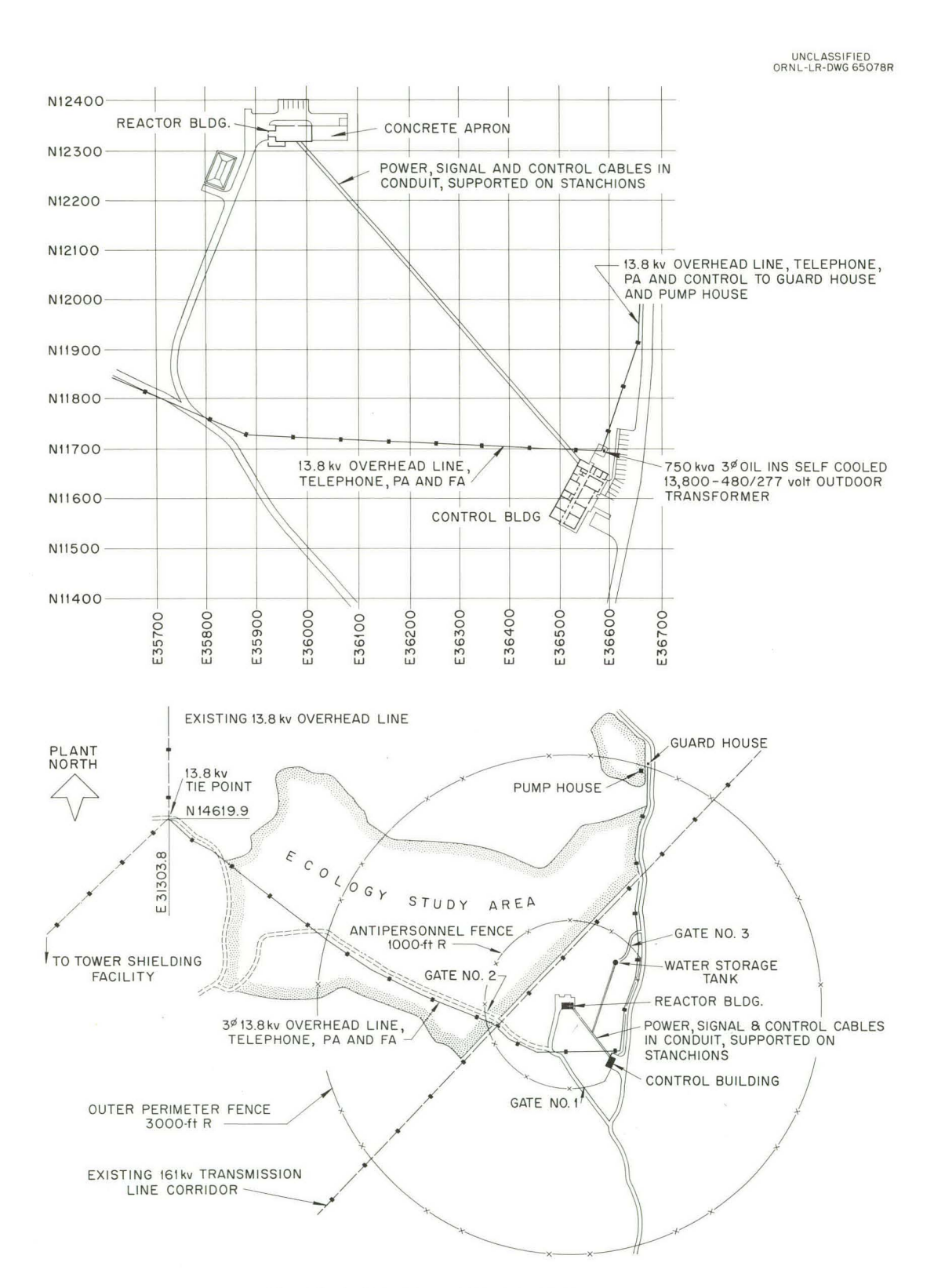


Fig. 3.18. Plot Plan of the DOSAR Structures.

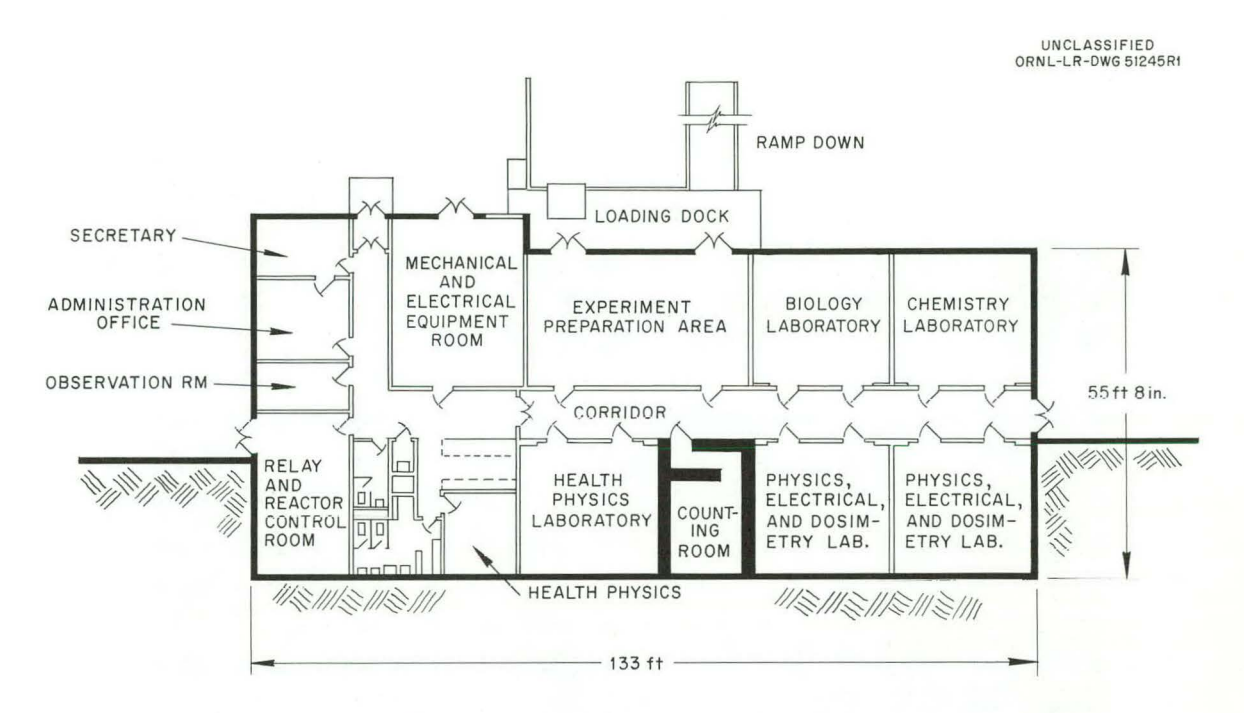


Fig. 3.19. Plan View of Control Building.

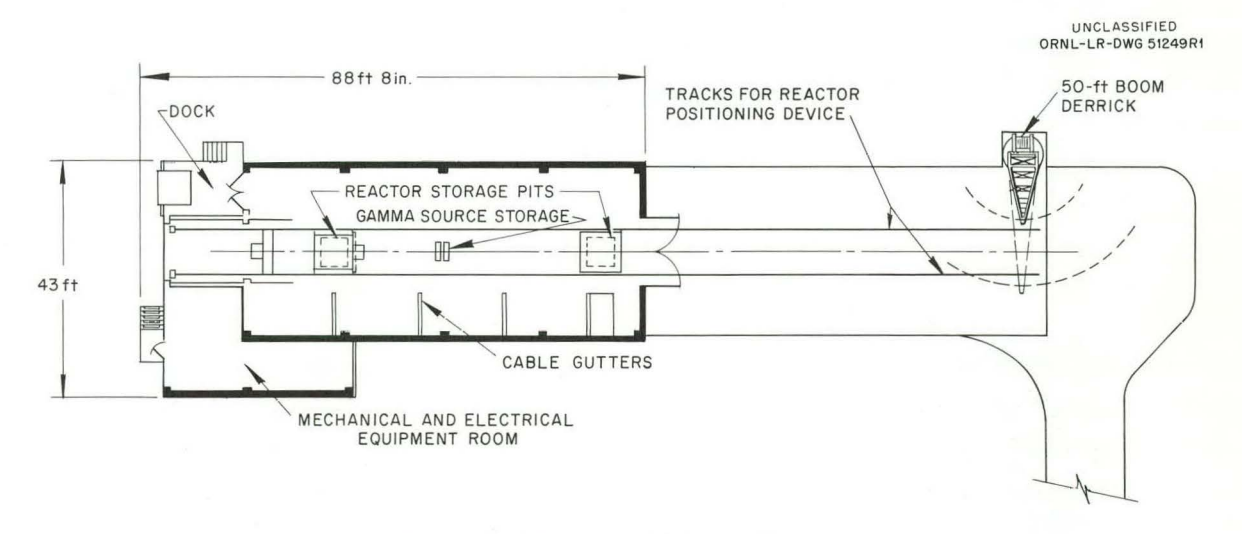


Fig. 3.20. Plan View of Reactor Building.

as controls, and others were exposed to single doses of 2.5 r in July 1960, January 1961, and July 1961, respectively. The net readings and standard deviations as of July 1961 are shown in Table 3.3.

Exposures are also being made periodically over a wide range of doses to three kinds of glass to get a better determination of effects of dose on regression (i.e., decrease of fluorescence with time) rate and the comparison of regression rates after single exposures to the three types of glass. In this experiment the fluorods are exposed at different times to the same doses and will be read at one time. Previously, one exposure was made, and the fluorods were read repeatedly thereafter. In many cases the rods became chipped and the results were consequently erroneous.



Fig. 3.21. Exterior View of Control Building.

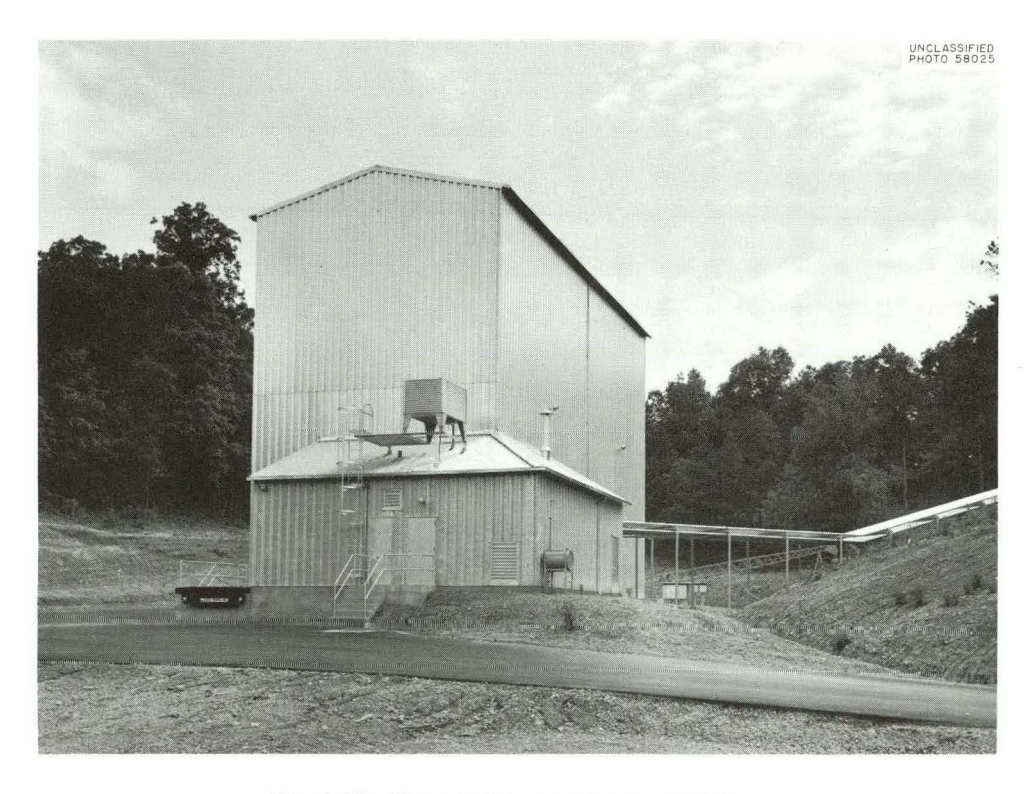


Fig. 3.22. Exterior View of Reactor Building.

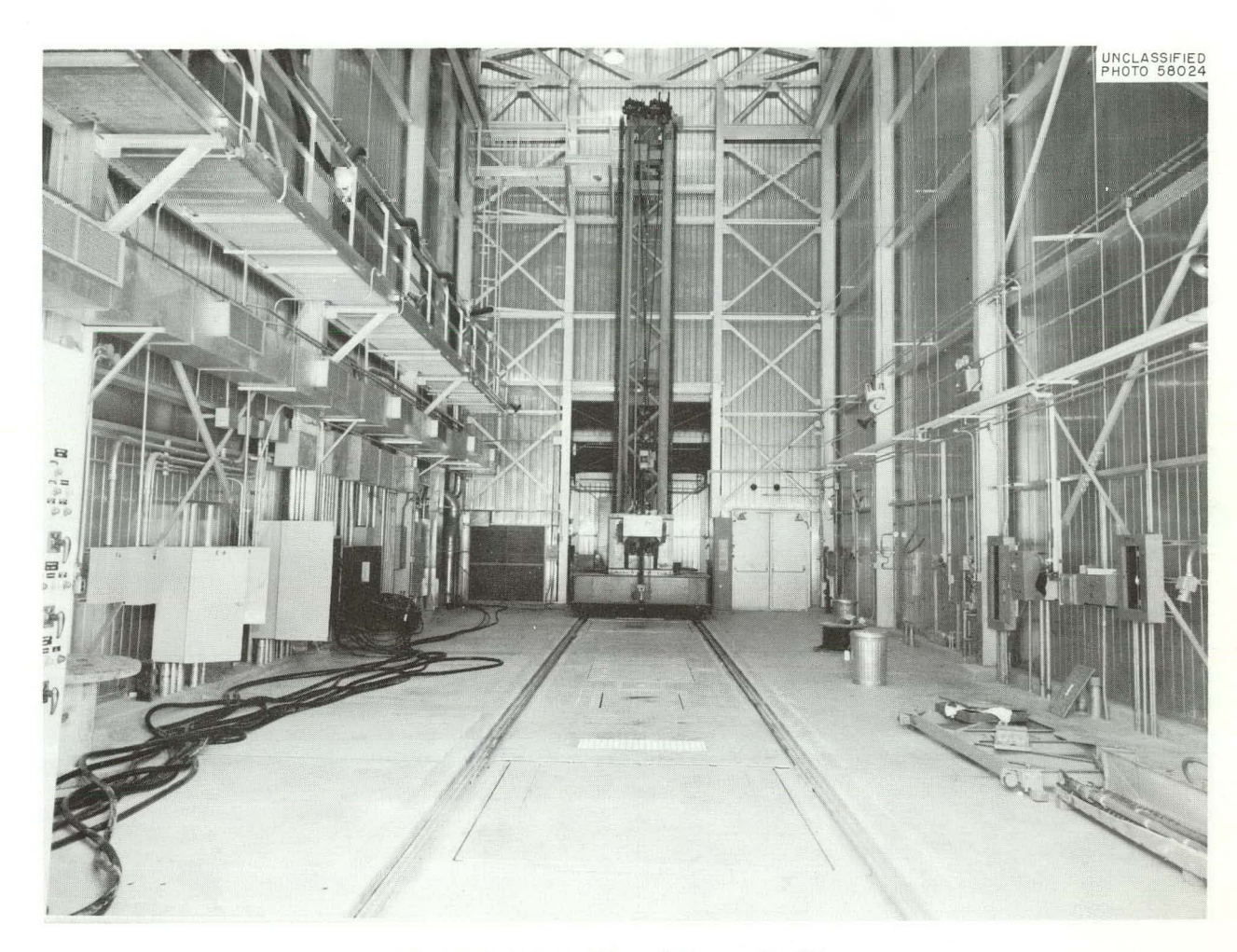


Fig. 3.23. Interior View of Reactor Building.

Table 3.3. Time-Dependence of Low-Dose Response of Fluorods

Exposure	Number of Rods	Av Predose	Av July 1961	Av Difference
10 mr per working day, ~2.5 r	24	8.46 ±0.33	10.07 ±0.72	1.61 ±0.79
2.5 r, July 1960	6	$8.58 \pm 0.27$	$9.50 \pm 0.23$	$0.92 \pm 0.35$
2.5 r, January 1961	6	$8.68 \pm 0.41$	$10.40 \pm 1.23$	$1.72 \pm 1.30$
2.5 r, July 1961	6	$8.60 \pm 0.53$	$10.44 \pm 0.91$	$1.84 \pm 1.05$

UNCLASSIFIED ORNL-LR-DWG 56287A

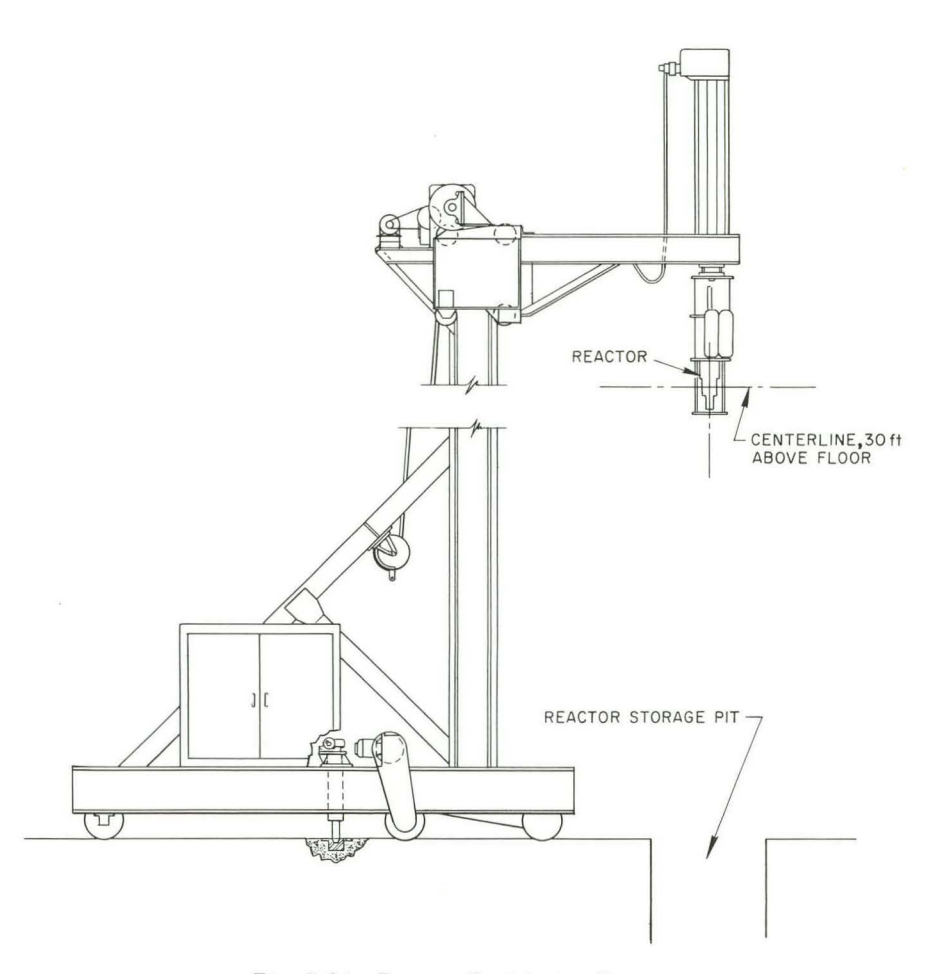


Fig. 3.24. Reactor Positioning Device.

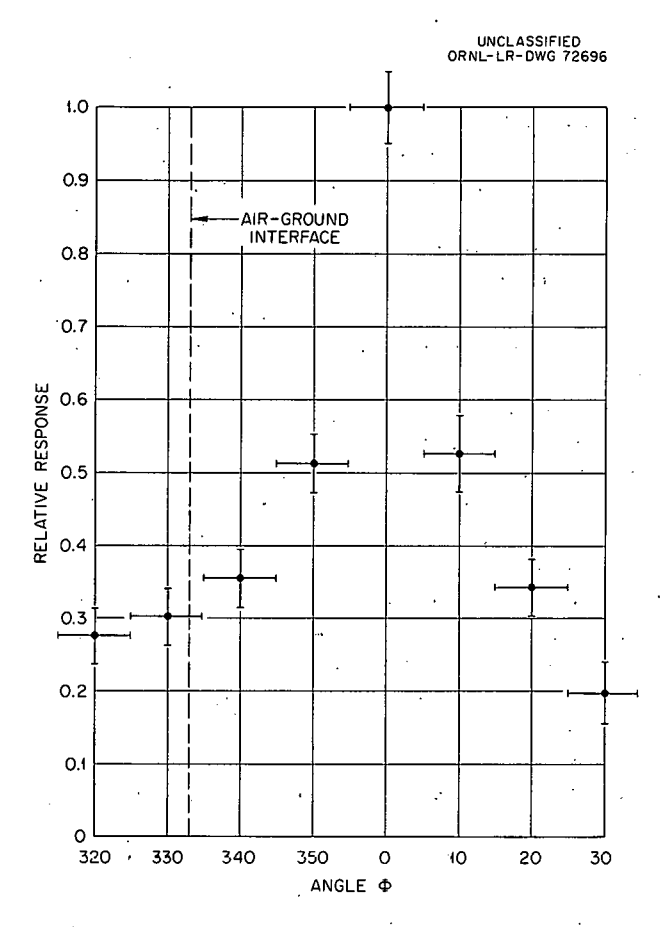


Fig. 3.25. Relative Angular Neutron Dose Distribution at 750 yd. Reactor at 1125 ft. 10° Cone.

#### PHYSICS OF TISSUE DAMAGE

R. D. Birkhoff

J. G. Carter

D. R. Nelson

# Emission Spectra of the Low-Temperature Thermoluminescence from X-Irradiated Biochemicals

The Physics of Tissue Damage Program has continued the study of the disposition of energy (in biological materials) absorbed from ionizing radiation. The interference filter spectrograph, described in the previous annual report (ORNL-3189, p 160), was calibrated absolutely with a NBS standard light source in order to determine

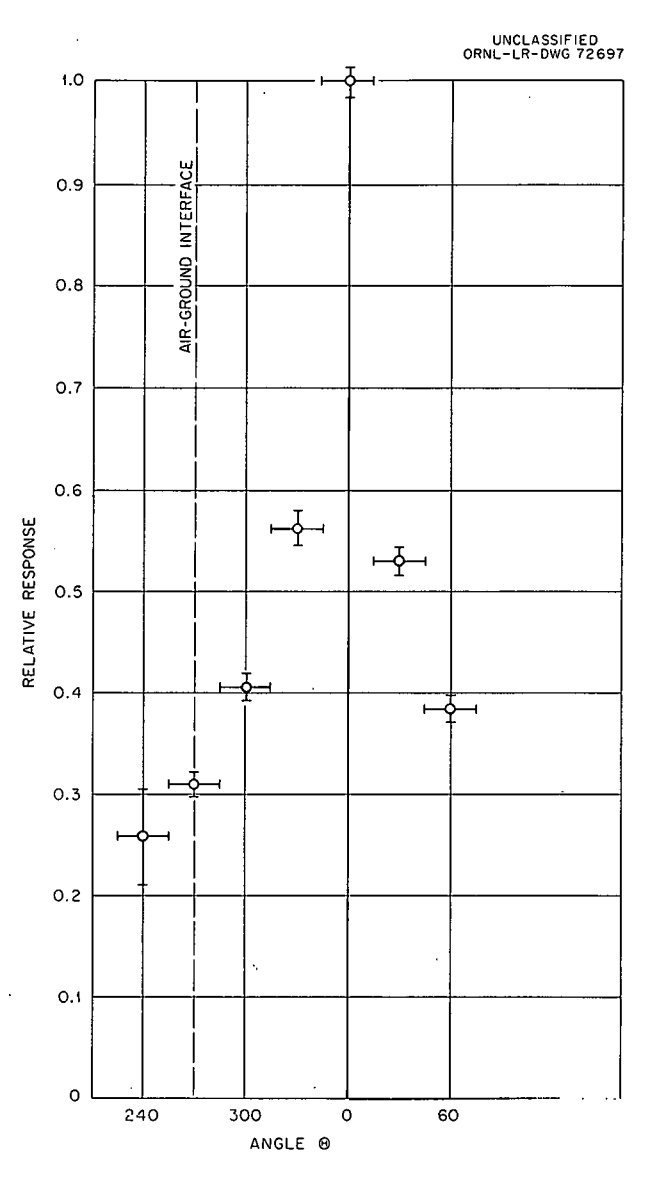


Fig. 3.26. Relative Angular Gamma Dose Distribution at 750 yd. Reactor at 1125 ft.  $30^{\circ}$  Cone.

the absolute light yields from the materials. In addition, the associated experimental apparatus was modified so as to permit a better measure of the effects produced when the samples are placed in different gas atmospheres.

Thin layers of powdered trypsin, tyrosine, phenylalanine, and tryptophan were irradiated under an atmosphere of helium with 230 kvp x rays at 77°K. The intensities of the immediate luminescence (IL) emitted during the irradiation and the thermoluminescence (TL) emitted upon subsequent heating were recorded through a series

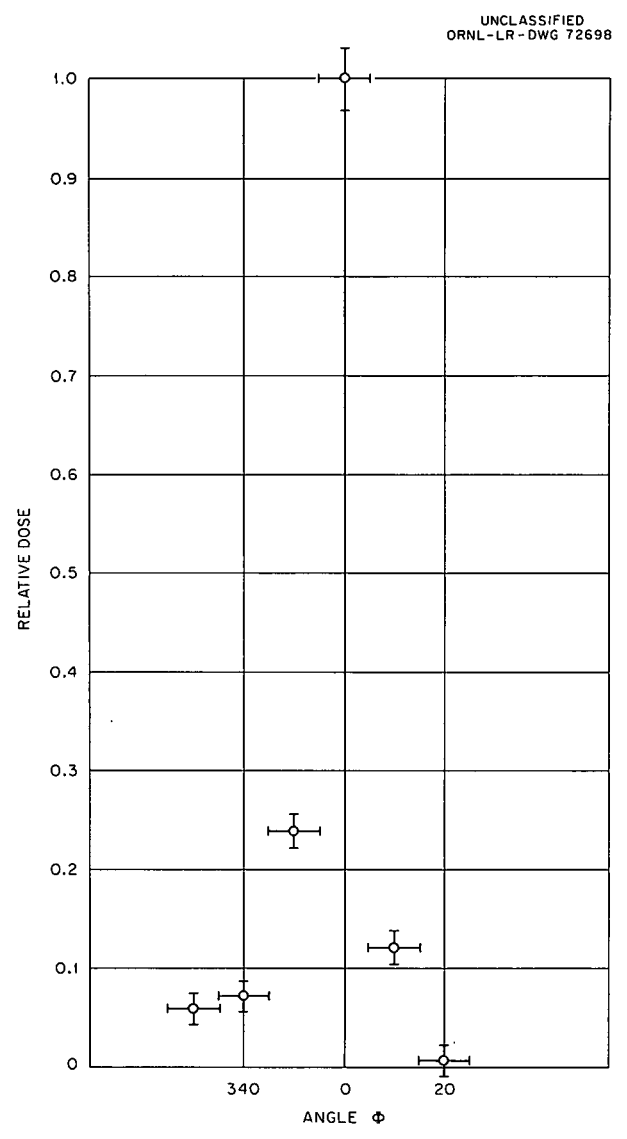


Fig. 3.27. Cobalt-60 Angular Distribution at 750 yd.  $10^{\circ}$  Cone.

of interference filters spanning the spectral region 2500 to 7500 A. From these values it is estimated that of the total energy absorbed by these biochemicals at 77°K, the amount reemitted as visible or near-ultraviolet light in IL and TL varies from about 0.1% for trypsin to about 3.8% for tryptophan. This compares with an IL of 12.6% for anthracene at room temperature under the same conditions. For the IL, a quantum is emitted for about each 80.4 ev (for tryptophan) to 3145 ev (for trypsin) absorbed. The ratio of energy emitted in TL to energy emitted in IL varies from 0.0004 to 0.008 for the four compounds studied.

In contrast to the intensity of IL, the intensity of TL is dependent upon the pressure of gas present during the irradiation and heating. That is, the better the vacuum, the lower the TL in-Furthermore, if the gas was present tensity. during irradiation at low temperature and then pumped off before the sample was warmed, light was emitted during this pumpoff. The amount of light emitted was approximately the same as would have been given off if the sample had been warmed at the normal rate. With vacua of the order of 10<sup>-5</sup> mm Hg, the TL from the various samples was reduced by at least a factor of 50. Furthermore, upon adding gases (helium, argon, oxygen), it was found that there was no difference in the resulting spectrum. Each amino acidior protein had a characteristic spectrum which was independent of the type of gas present but was dependent on gas pressure. A series of experiments were made on the effect of surface area of the sample. Since it was not possible to obtain our biochemicals in various crystalline size's, another substance (NaCl) was chosen which was easily obtainable in various crystalline size's. At a given gas pressure of 500  $\mu$  of O<sub>2</sub>, there was a linear increase in the total amount of TL as a function of sample surface area. Similar results were obtained with helium, H2O vapor, and argon.

These results with NaCl point out the importance of surface effects on the phenomenon of TL. Similar measurements of a qualitative nature on the amino acids showed a similar dependence on crystalline size.

The dependence of TL on surface gas absorption indicates that this phenomena may be quite indirectly related to radiation effects in biological systems. Although some additional study is necessary to confirm and evaluate the above observations, it is possible that future experimental effort may better be devoted to a more direct study of the interactions of electrons and biological mole-As examples, an electron time-of-flight energy analyzer is being developed which may make possible measurement of the cross section for exchange of energy of as little as 0.01 ev between fast electrons and molecules. Or, the application of the new electron tunneling techniques to the measurement of electronic mean free paths in biological materials for electrons of energies between 1 and 20 ev may be attempted.

## 4. Internal Dosimetry

#### **ESTIMATION OF INTERNAL DOSE**

### Estimation of the Intake of Pu<sup>239</sup> to Blood

W. S. Snyder

Two computer codes for estimation of the body burden (exclusive of lung burden) of  $Pu^{239}$  from urinalysis data were reported previously. These codes are basically similar, both depending upon the metabolic model developed by Langham. Langham found that urinary excretion and total excretion of  $Pu^{239}$  on day t following a single intravenous injection of a unit amount were approximately expressed by the equations

$$Y_{u}(t) = at^{-\alpha}, (1)$$

$$Y_{u+t}(t) = bt^{-\beta} , \qquad (2)$$

with a = 0.0023,  $\alpha = 0.77$ , b = 0.0079, and  $\beta = 0.94$ .

If  $l(\tau)$   $d\tau$  designates the amount of Pu<sup>239</sup> entering the blood in time interval  $d\tau$  about  $\tau$ ; then the urinary excretion resulting from total exposure up to time t days is given by

$$U(t) = a \int_0^t d\tau \ I(\tau) (t - \tau)^{-\alpha}. \tag{3}$$

Equation (3) can be inverted to obtain

$$\begin{split} &\int_0^t d\tau \ I(\tau) \\ &= \frac{1}{a\Gamma(\alpha)\Gamma(1-\alpha)} \ \int_0^t d\tau \ U(\tau)(t-\tau)^{\alpha-1}, \ (4) \end{split}$$

where  $\Gamma(x)$  is the well-known gamma function. Thus, the total intake of  $Pu^{239}$  to blood before time t can be obtained from Eq. (4) if the urinary excretion data symbolized by  $U(\tau)$  are known. In practice the function U is only partially known since only occasional urine specimens will be analyzed. However, even an approximate estimate of intake is desirable since it is very difficult to obtain a reliable estimate of exposure to  $Pu^{239}$  by other means.

To test the accuracy of Eq. (4), the data of the hospital patients studied by Langham<sup>2</sup> have been used in Eq. (4). The amount of  $Pu^{239}$  excreted in the urine by a given patient was used to establish the values of U(t) on the sampling days, and excretion rates at intermediate times were obtained by linear interpolation. A code for the IBM 7090 was prepared which evaluated Eq. (4) for the function U(t) obtained. Table 4.1 shows the results for ten patients studied, giving the amounts injected and the percent of error of the estimate.

To determine the major sources of error contributing to the inaccuracy of the method, the urine data of each patient were approximated by a power function. The power function  $at^{-\alpha}$  was fitted to the data in three ways:

- 1. a least-squares fit to the daily exerction values,
- 2. a fit by minimizing

$$\sum_{i=1}^{n-1} \left| S_i - a \frac{i^{1-\alpha} - (i-1)^{1-\alpha}}{1-\alpha} \right|,$$

3. a fit minimizing

$$\sum_{i=1}^{n-1} \left| S_i - a \frac{i^{1-\alpha} - (i-1)^{1-\alpha}}{1-\alpha} \right|^2.$$

<sup>&</sup>lt;sup>1</sup>W. S. Snyder, Health Phys. Div. Ann. Progr. Rept. July 31, 1961, ORNL-3189, p 191.

<sup>&</sup>lt;sup>2</sup>W. H. Langham et al., Distribution and Excretion of Plutonium Administered Intravenously to Man, LA-1151 (1950).

Table 4.1.	Estimation of	Plutonium	Intake
------------	---------------	-----------	--------

	(Average	curve <sup>a</sup> )			
Case	Plutonium Injected (μc)	Estimated Injection (μc)	Percent o Error		
—————— Нр 1	0.283	0.173	39		
Hp 2	0.314	0.239	24		
Нр 3	0.302	0.198	34		
Нр 4	0.302	0.292	3		
Hp 5	0.314	0.140	55		
Hp 7	0.388	0.186	52		
Нр 8	0.401	0.344	14		
Нр 9	0.388	0.249	36		
Hp 10	0.376	0.310	18		
Hp 12	0.289	0.241	17		

 $<sup>^{</sup>a}$ LA-1151, 0.0023 $t^{-0.77}$ .

The expression

$$a \frac{i^{1-\alpha} - (i-1)^{1-\alpha}}{1-\alpha} = \int_{i-1}^{i} dt \ at^{-\alpha}$$

represents the amount excreted on the  $i^{th}$  day if the excretion rate is  $at^{-\alpha}$ , and methods (2) and (3) minimize the sum of the deviations and the sum of squares of the deviations of this quantity from the sample value. Methods (2) and (3) seem more appropriate for the use of the function  $at^{-\alpha}$ in the code reported here since this code uses the function to describe a continuous excretion rate and does not use it to define a discrete set of amounts excreted on each day. Figure 4.1 illustrates the difference in principle involved here. By method (1) the daily values  $S_i$  are compared with the height of the curve, while in methods (2) and (3) the areas under the curve for each day are compared with the daily excretion values. Table 4.2 shows the values of a and  $\alpha$  obtained by each of these methods. It is clear that whichever method is used, there is considerable difference in the values of a and  $\alpha$  obtained for different individuals, indicating that there are significant individual differences and that no "average curve" or single set of values of a and  $\alpha$  can be expected to represent any individual's data with great precision.

The values of a and  $\alpha$  obtained by the above methods were used in the code, and the individual's

intake to blood was then estimated at various times postinjection. Table 4.3 shows the results obtained with all the urine data of each patient and with the parameters a and  $\alpha$  as determined by fitting the data to the area under the curve by methods (2) and (3). Comparison with Table 4.1 shows that these methods significantly improve the accuracy

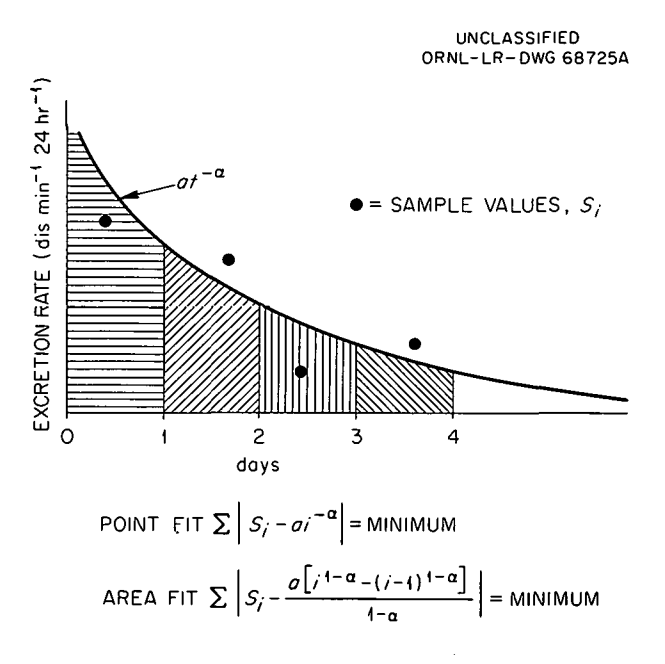


Fig. 4.1. Point Fit and Area Fit of Excretion Data.

Table 4.2. Individual Retention Functions

Average excretion (Langham),  $0.23t^{-0.77}$ 

Case	Least S (poin	-	Least De (area		Least Squares (area fit)			
	a	а	a	α	a	а		
Hp 1 0.2603		0.811	0.1050	0.422	0.1188	0.416		
Hp 2	0.6843	1.224	0.1733	0.633	0.2090	0.581		
Hp 3	0.4799	1.171	0.1645	0.711	0.2069	0.645		
Нр 4	0.6871	0.6871 1.081		0.500	0.2281	0.508		
Hp 5	0.1898	0.844	0.1110	0.625	0.1218	0.599		
Нр 7	0.3926	1.201	0.0797	0.633				
Нр 8	0.3352	0.832	0.1561	0.586	0.1780	0.556		
Нр 9	0.1137	<b>0.45</b> 5	0.0950	0.406	0.0960	0.402		
Hp 10	0.6009	1.137	0.1650	0.602	0.2119	0.535		
Hp 12	0.1192	0.470	0.0844	0.383	0.0851	0.333		

Table 4.3. Individual Retention Functions and Estimates of Intake

Case I	Injection	Least S (area	-	Estimated	Error (%)	Least De (area		Estimated Intake	Error (%)	
	(μc)	а	α	Intake		а	<u>a</u>	Intake		
Hp 1	0.283	0.1188	0.416	0.224	-26.3	0.1050	0.422	0.256	- 9.5	
Hp 2	0.314	0.2090	0.581	0.219	-43.4	0.1733	0.633	0.293	- 6.7	
Hp 3	0.302	0.2069	0.645	0.217	-39.1	0.1645	0.711	0.284	- 6.0	
Hp 4	0.302	0.2281	0.508	0.222	-36.0	0.2200	0.500	0.225	-25.4	
Hp 5	0.314	0.1218	0.599	0.265	-18.5	0.1110	0.625	0.295	- 6.0	
Hp 7	0.388					0.0797	0.633	0.487	+25.4	
Hp8	0.401	0.1780	0.556	0.320	-25.3	0.1561	0.586	0.394	- 1.8	
Нр 9	0.388	0.0960	0.402	0.382	- 1.6	0.0950	0.406	0.393	+ 1.4	
Hp 10	0.376	0.2119	0.535	0.265	-29.5	0.1650	0.602	0.388	+ 3.1	
Hp 12	0.289	0.0851	0.333	0.326	+11.3	0.0844	0.383	0.383	+32.5	

of the estimate, so that individual variation and the method of fitting the curve to the data seem to be significant sources of inaccuracy. The results obtained when the intake was estimated at earlier times were essentially comparable.

In using the code with data from employees, there will be rather large intervals between the dates at which urine specimens are collected. This may be expected to introduce further inaccuracies in the estimate. Table 4.4 shows the results obtained when only the sample values for alternate days (every third day) are used. There is no very marked effect on the estimate in these cases. It is not feasible to use gaps of 20 to 30 days in these data since they do not extend far in time, so the practical question is not resolved by this study.

Table 4.4	Effect of Sample	Spacing on Estimated	Intaka
1 abie 4,4.	Ettect of Jampie	Spacing on Estimated	intake

Least Deviations (area fit)		Daily Sa	amples	Alterna	te Day	Every Third Day			
Case (arca no)		a	Estimated	Error (%)	Estimated	Error (%)	Estimated	Error (%)	
Hp <sup>·</sup> 1	0.1050	0.422	0.256	- 9.5	0.259	- 8.5	0.249	-12.0	
Hp 2	0.1733	0.633	0.293	- 6.7	0.310	- 1.3	0.309	- 1.6	
Hp 3	0.1645	0.711	0.284	- 6.0	0.298	- 1.2	0.347	+14.9	
Hp 4	0.2200	0.500	0.225	-25.4	0.247	-18.1	0.249	-17.5	
Hp 5	0.1110	0.625	0.295	- 6.0	0.301	- 4.1	0.334	+ 6.4	
Нр 7	0.0797	0.633	0.487	+25.4	0.476	+22.7	0.486	+25.3	
Нр 8	0.1561	0.586	0.394	- 1.8	0.393	- 2.0	0.426	+ 6.2	
Нр 9	0.0950	0.406	0.393	+ 1.4	0.398	+ 2.6	0.412	+ 6.2	
Hp 10	0.1650	0.602	0.388	+ 3.1	0.393	+ 4.5	0.417	+10.9	
Hp 12	0.0844	0.383	0.383	+32.5	0.344	+19.0	0.420	+45.3	

It is concluded that the model and programming methods developed here for estimating intake of Pu<sup>239</sup> to blood from urinalysis data are sound in principle. It is clear that the estimate will not be highly accurate if one must use an excretion curve representing an "average" individual or if sampling is infrequent. Perhaps accuracy within a factor of 2 might be a measure of the average error to expect, although it seems highly probable there will be cases where the error is greater than this. With more adequate data the error can be reduced substantially, particularly if individual variation can be taken into account in some way. The optimum type of program to use with this model is being explored, particularly with respect to the first few days following intake.

#### STABLE-ELEMENT METABOLISM BY MAN

Statistical Evaluation of Dose Resulting from a Constant Level of Contamination in the Environment

W. S. Snyder M. J. Cook

Because recommended limits on intake of ingested radionuclides are frequently based upon a "standard man," individual variations correlated with age, sex, weight, individual habits, etc., are not taken into account. These various individual characteristics might plausibly be considered as producing differences in dose among a chronically exposed population. In an attempt to delineate as objectively as possible the extent of this dose variation, two statistical treatments have been applied to the data of Tipton et al., Kulp et al., and Bryant et al. If the exposure is chronic, the distribution of doses should be, within a factor of

<sup>&</sup>lt;sup>3</sup>I. H. Tipton and M. J. Cook, "Trace Elements in Human Tissue. Part II. Adult Subjects from the United States," submitted to Health Physics J.; I. H. Tipton, "Work Book: Raw Data for Spectrographic Analysis of Human Tissue. One Hundred and Fifty Subjects from the United States," unpublished data (August 1961); I. H. Tipton and M. J. Cook, "Inorganic Analysis of Human Tissue," Health Phys. Div. Ann. Progr. Repts.: July 31, 1958, ORNL-2590, p 149-55; July 31, 1959, ORNL-2806, p 194-200; July 31, 1960, ORNL-2994, p 256-64; and July 31, 1961, ORNL-3189, p 203-6; I. H. Tipton, "The Distribution of Trace Metals in the Human Body," Metal-Binding in Medicine (ed. by M. J. Seven and L. A. Johnson), p 27-42, Lippincott, Philadelphia, 1960.

<sup>&</sup>lt;sup>4</sup>J. L. Kulp and A. R. Schulart, Sr<sup>90</sup> in Man and His Environment, Vol. II: Analytical Data, NYO-9934 (September 1961).

<sup>&</sup>lt;sup>5</sup>F. J. Bryant et al., Radioactive and Natural Strontium in Human Bone, United Kingdom Results for Mid and Late 1958, AERE-R-2988 (1959); F. J. Bryant et al., Radioactive and Natural Strontium in Human Bone, United Kingdom Results for 1957, AERE-C/R-2583 (1958); J. W. Arden et al., Radioactive and Natural Strontium in Human Bone, United Kingdom Results for 1959. Part I, AERE-R-3246 (1960).

proportionality, that of the concentration of a corresponding stable isotope present in the environment.

The distribution of a real-valued, random variable in a population, for example, average concentration of Ra<sup>226</sup> in the skeleton of an individual, is usually characterized by the cumulative probability function f of the distribution. This function may be defined by  $f(x_0) = \text{probability that an individual}$ selected randomly in the population will have a value (concentration) less than  $x_0$ . Thus,  $f(x_0)$  is the fraction of the population whose value for the characteristic in question is less than  $x_0$ . It is clear that in the case of a concentration in a tissue, f(0) = 0 and f(x) = 1 for very large values of x. The function is nondecreasing within these extreme values. In most cases of practical interest, the function / for a given statistic is unknown, and inferences concerning it must be based on sampling of the population.

Suppose a sample of n individuals is selected randomly from a given population. Let  $x_i$ , i =1, 2, ..., n, be the values of the random variable being sampled; for example, 100 individuals may be selected randomly and their body burdens of Cs 137 may be determined. We may suppose the values are ranked, that is,  $x_1 \le x_2 \le x_3 \le \dots \le$  $x_n$ , although this is not intended to imply that  $x_1$ was the value determined for the first individual sampled,  $x_2$  for the second, etc. The sample cumulative will be denoted by  $f_s$  and is defined as follows:  $f_{c}(x)$  = the fraction of the sample with values less than x. Thus, if a value x lies between  $x_i$  and  $x_{i+1}$  of the sample, then  $f_{x}(x) = i/n$ . It would be expected that a second sample of nindividuals selected randomly from the same population would show a somewhat different sample cumulative. However, if the sample size is large and the sampling sufficiently unbiased, one would expect that f would approximate f in some sense. The statistical methods used here permit one to infer objectively certain conclusions about f from the study of  $f_s$ . In particular, a band about the graph of  $f_s$  will be indicated within which the graph of / may be expected to lie with rather high probability.

Brunk<sup>6</sup> has given a method of determining a confidence interval in which a given percentile of

the population must lie. By a slight modification of the argument, one can determine confidence bounds on the cumulative distribution function at a given value  $x_0$ . That is, given an arbitrary but fixed value  $x_0$ , one wishes to determine a value  $P_0$  such that the statement  $f(x_0) > P_0$  can be asserted with 95% confidence. The statement " $f(x_0) > P_0$ " is equivalent to asserting that the  $P_0$  th percentile of the distribution is less than  $x_0$ . If  $x_{k+1}$  is the ranked sample value immediately above  $x_0$ , then it follows that the  $P_0$ th percentile is less than  $x_{k+1}$ . The probability for this to occur is easily seen to be

$$\sum_{j=0}^{k} {}_{n}C_{j}P_{0}^{j}(1-P_{0})^{n-j}.$$

If  $P_0$  is selected to make this sum equal to 0.05, then the statement  $f(x_0) > P_0$  implies that an event of probability 0.05 has occurred, that is, one has 95% confidence that the statement  $f(x_0) > P_0$  is wrong. Thus, if  $x_{k+1}$  is the observed sample value immediately greater than  $x_0$  and if  $P_0$  is selected so that

$$\sum_{j=0}^{k} {}_{n}C_{j}P_{0}^{j}(1-P_{0})^{n-j} = 0.05,$$

then the statement  $f(x_0) \stackrel{\leq}{=} P_0$  can be asserted with 95% confidence.

By a similar argument, if  $x_k$  is the sample value immediately less than  $x_0$  and if  $p_0$  is determined so that

$$\sum_{j=k}^{n} {}_{n}C_{j}p_{0}^{j}(1-p_{0})^{n-j} = 0.05,$$

then the statement  $f(x_0) \stackrel{\leq}{=} p_0$  can be asserted with 95% confidence. It will be noted that while  $p_0$  and  $P_0$  as defined above depend on the choice of  $x_0$ , they are constant for any choice of  $x_0$  such that  $x_k < x_0 < x_{k+1}$ . Moreover, if  $x_0$  is selected to exceed  $x_n$ , the method does not determine a corresponding  $P_0$ , and one has only the trivially correct bound  $f(x_0) \stackrel{\leq}{=} 1$ . Likewise, if  $x_0$  is less than  $x_1$ , then one can only assert the trivially correct  $f(x_0) \stackrel{\geq}{=} 0$ . It is clear that this type of analysis can be applied for other degrees of confidence, but if the sample size n is small,  $P_0$  and  $p_0$  may differ greatly and thus not give a good indication of the position of the value of the

<sup>&</sup>lt;sup>6</sup>H. D. Brunk, An Introduction to Mathematical Statistics, Finn, New York, 1960.

cumulative distribution function at  $x_0$ . This has been discussed somewhat in ref 1.

The band obtained by Brunk's method is not a confidence band for the entire distribution curve but rather gives an upper (lower) bound for the distribution at each point of the range with 95% confidence. Massey has defined a somewhat wider band for which the statement 'the cumulative of the distribution lies within the band' can be asserted with 95% confidence. The band is of width  $2d_{\alpha}$ , where  $d_{\alpha}$  is a function of the confidence  $1-\alpha$  that is desired and also of the sample size. For sample size N greater than 50,  $d_{0.05}$  is approximately  $1.36/\sqrt{N}$ , and for sample size below 50,  $d_{\alpha}$  is tabulated by Massey.

Figures 4.2 - 4.4 show the sample cumulative, the 95% confidence band for the population cumulative distribution as given by Massey, and the 95%

confidence bounds at each concentration as obtained by the method of Brunk for the tissues and isotopes analyzed in this report. The median and the mean of the sample also are shown.

The concentration of aluminum in lungs as measured by Tipton in 123 adults from U.S. urban population is shown in Fig. 4.2. Because the sample mean is greater than the sample median, it is likely that the distribution is skewed toward the high values and therefore is not a normal distribution. The shape of the confidence bands gives further confirmation of this skewed distribution.

Aluminum is considered to be a nonessential element, that is, there is no known metabolic function. Such nonessential elements generally are found to show a greater degree of variability in the population than the elements which are known to have a metabolic function or which are chemically similar to an essential element. Thus, the 80% range of aluminum, defined as the difference  $P_{90} - P_{10}$  of the 90th and the 10th percentile of the sample distribution, is 40.5  $\mu$ g/g, and the ratio of this 80% range to the sample median is

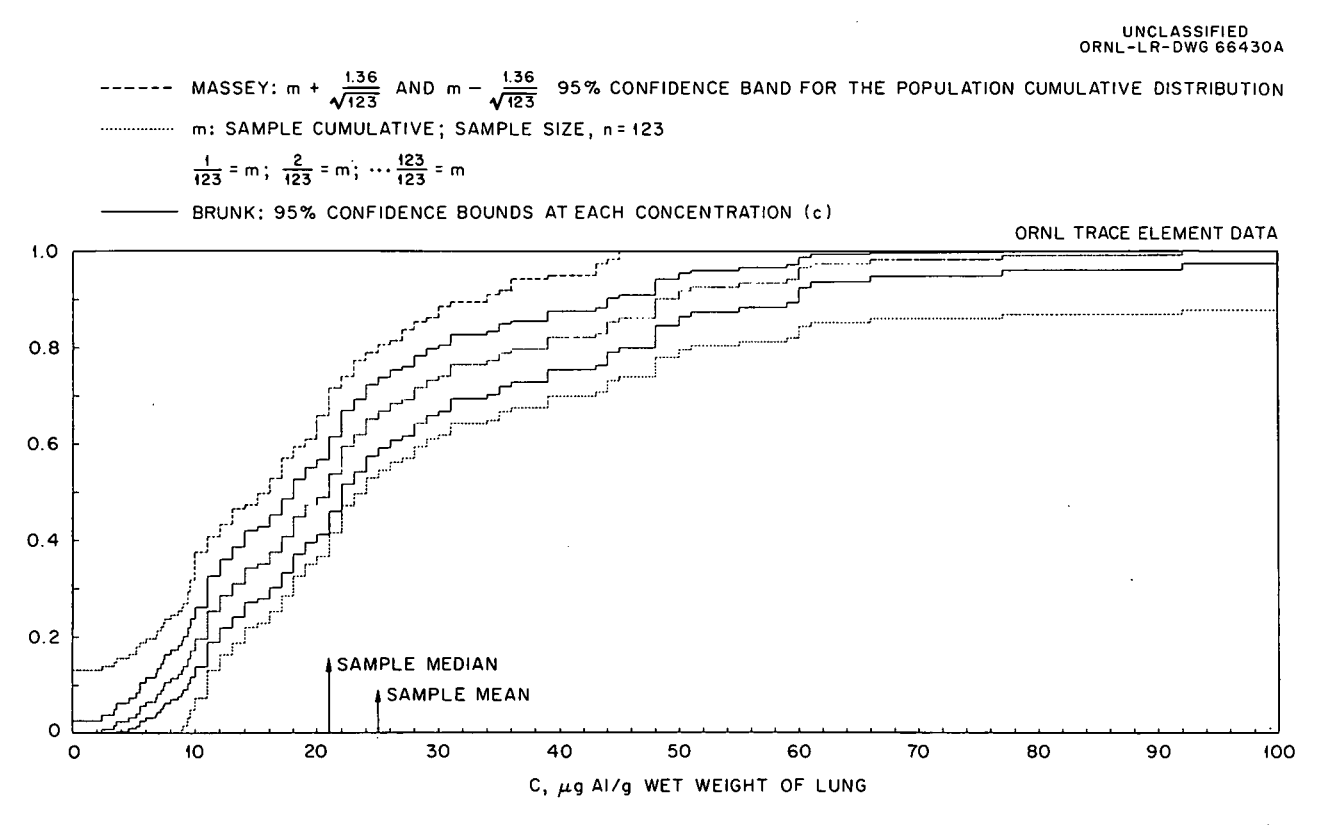


Fig. 4.2. 95% Confidence Bands for the Distribution of Aluminum in Lungs of Adults in U.S. Urban Populations (Ages: 20-59).

<sup>&</sup>lt;sup>7</sup>W. J. Dixon and F. J. Massey, Jr., Introduction to Statistical Analysis, 2d ed., McGraw-Hill, New York, 1957.

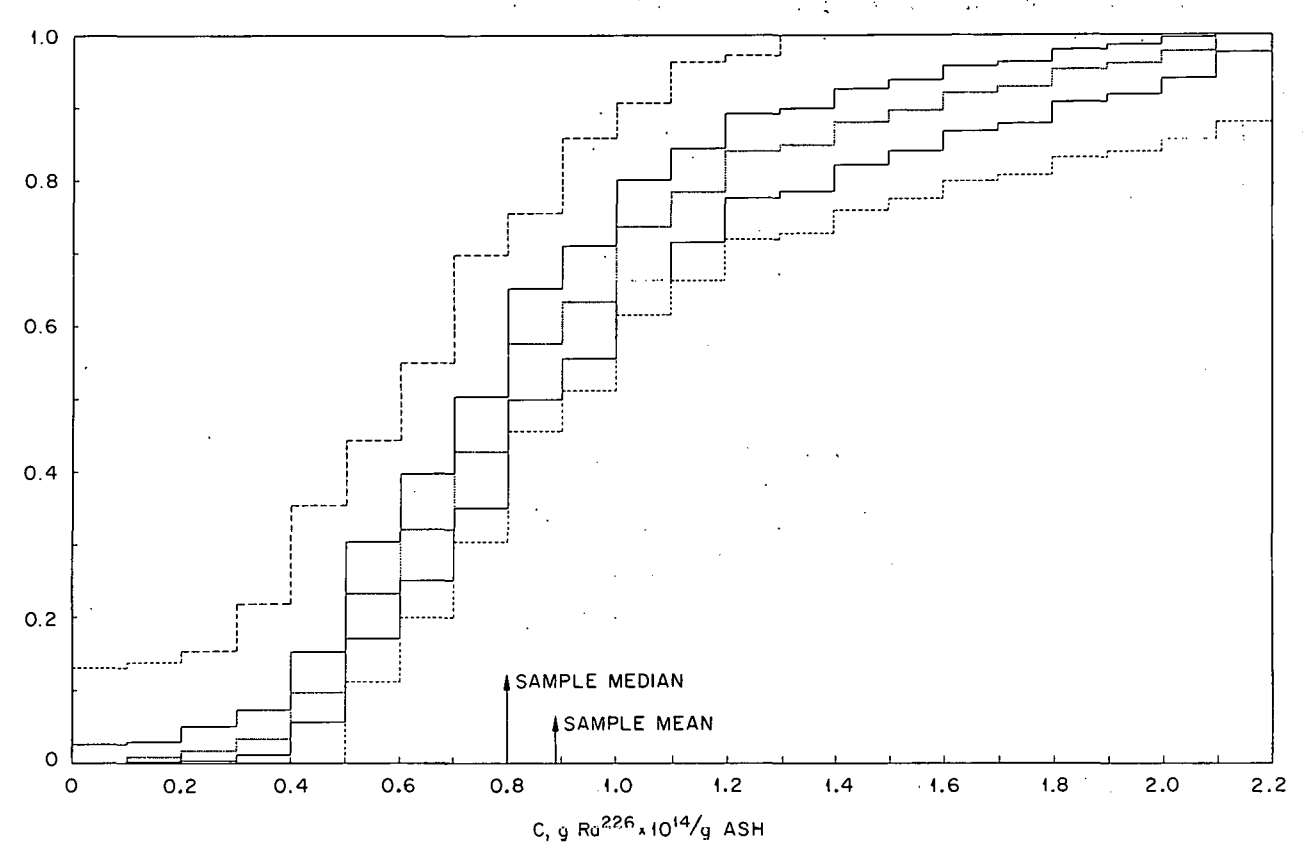


Fig. 4.3. 95% Confidence Bands for the Distribution of Ra<sup>226</sup> in Total Skeletal Ash of Cadavers from New York City (Ages: 20-91).

found to be 1.93. This statistic is invariant under a change of scale and may be considered as one measure of variability of the distribution.

As an illustration of the use of these curves, the percent of the adult urban population with concentration of aluminum in the lungs exceeding three times the sample median may be estimated. This amounts to estimating the percentage of the U.S. adult urban population with concentration values in excess of  $63 \mu g/g$ . Using the Massey test, one can assert with 95% confidence that the population cumulative at  $63 \mu g/g$  is greater than

86%, and thus one can assert with 95% confidence that the percent of the population with concentration values about 63  $\mu$ g/g does not exceed 14%. However, the Brunk method can also be used and is always more efficient in making a test at a single value of the concentration. Thus, the method of Brunk indicates with 95% confidence that the population cumulative at 63  $\mu$ g/g is above 95% and thus with 95% confidence that the adult urban population with concentration values above 63  $\mu$ g/g is no more than 5%. While the Brunk test is more efficient for such estimates, the band

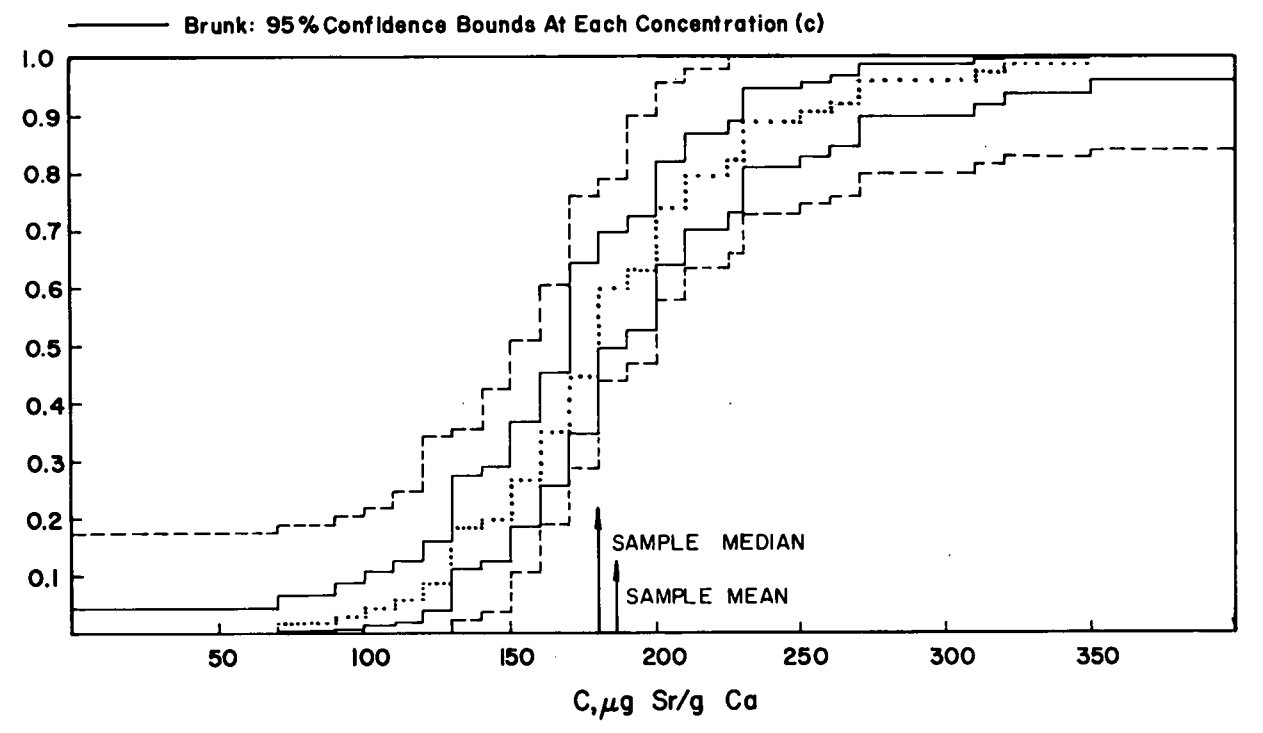


Fig. 4.4. 95% Confidence Bands for the Distribution of Sr/Ca Ratios in British Stillbirths.

given by the Massey method must be used for assertions concerning the behavior of the curve as a whole.

The distribution of Ra<sup>226</sup> in the total skeletal ash of 125 cadavers of adults from New York City as reported by Kulp and Schulert<sup>4</sup> has been analyzed similarly, and the results are shown in Fig. 4.3. Again the distribution seems skewed to the right and thus is not a normal distribution. The 80% range divided by the sample median is 1.38; thus, this variability seems somewhat smaller than in the case of aluminum in lungs.

Three times the median of the sample is  $2.4 \times 10^{14}$  g of Ra<sup>226</sup> per g of ash, which exceeds all 125 values of this sample. By the use of Brunk's test, one may assert with 95% confidence that the

population cumulative at 2.4 is above 97.5% and that the adult urban populations with concentration values above 2.4 is not more than 2.5%.

The distribution of strontium-calcium ratios in 72 British stillbirths as reported by Bryant et al. 8 is analyzed in Fig. 4.4. The distribution appears more nearly symmetrical. It is found, however, that the distribution is not normal. There are

<sup>&</sup>lt;sup>8</sup>F. J. Bryant et al., Radioactive and Natural Strontium in Human Bone, United Kingdom Results for Mid and Late 1958, AERE-R-2988 (1959); F. J. Bryant et al., Radioactive and Natural Strontium in Human Bone, United Kingdom Results for 1957, AERE-C/R-2583 (1958); J. W. Arden et al., Radioactive and Natural Strontium in Human Bone, United Kingdom Results for 1959. Part I, AERE-R-3246 (1960).

various tests that may be applied to show this. Perhaps the simplest is to estimate the mean and standard deviation and to compare these with the 80% range of the distribution. It is found that the mean is 184 and that  $\sigma = 511$ . From standard tables the 80% range is 2.56,  $\sigma = 1308$ . However, Fig. 4.4 indicates that the 90th percentile  $P_{00}$  lies between 230 and 310. Similarly, with 95% confidence  $P_{10}$  lies between 100 and 130. Thus, the 80% range is between 100 and 310. Thus, the variance is too large for the assumption of normality to be valid. The ratio of the 80% sample range to the sample median is found to be 120/180 =0.67, indicating rather less variability in these data than in the case of aluminum in the lungs and Ra<sup>226</sup> in the skeleton.

These three examples have been chosen to illustrate two types of statistical analysis. A slight modification of the test by Brunk determines confidence bounds on the cumulative distribution function at a given value. The method of data analysis by Massey defines a confidence band within which the cumulative distribution of the population lies. From such tests it is possible to estimate the extent of the dose variation in the case of certain nuclides and tissues for the case of chronic, low-level exposure.

#### Tissue Analysis Laboratory Progress Report

S. R. Koirtyohann

C. Feldman

**Sample Analyses.** – Spectrographic analysis of all the samples from San Francisco and about one-half of the soft tissues from Atlanta and New York was completed. This is a total of 967 samples (27 types of tissues) that were analyzed for 23 elements. Averages of the values obtained for each tissue are given in Tables 4.5-4.7. The analytical method was reported previously. The only significant change is that  $K_2S_2O_7$  was substituted for NaBr in the arcing mixture.

Several samples of tissue ash which were previously analyzed at the University of Tennessee were received. These were run, and the agreement was found to be generally good. In 59 of 96 com-

parisons, the UT-ORNL agreement was 20% or better and was 50% or better in 91 of the 96 cases. These comparisons were made on 11 samples, representing 4 different tissues, and include most of the commonly detected elements.

Wet chemical checks on the spectrographic analysis were made in a few cases. These comparisons are given in Table 4.8. Other attempts to get wet chemical analyses were hampered by the low concentrations of the elements of interest and by the small samples that are available.

Previous estimates of the precision of the spectrometric analyses were based on replicate exposures made during a short time (~1 hr). A measure of the long-term stability of the method was needed. Composite samples were made for each of four different tissues by mixing equal portions of ash from each San Francisco sample of that tissue. These were run on the Quantometer, in duplicate, on five different days covering a five-month period. Standard deviations were calculated from the ten Quantometer values in the cases where the data were sufficiently complete. They are summarized below:

Standard Deviation (%)	No. of Values
2.5 - 10	12
10 - 15	10
15 - 21	6

The results obtained from these "physically averaged" composite samples should agree with the mean of the individual values for the tissue samples used to make the composite. These values were compared, and the results are summarized below:

Difference Between Analytical Result for Composite Sample and Mean of Individual Results for Component Samples (%)	No. of Cases
0 — 5	. 11
5 — 10	7
10 - 20	5
>20	7

In most cases the larger differences were obtained for elements that were near their detection limits.

Analysis of Bone. — Bone samples have been collected and ashed throughout the program, but very few have been analyzed. These samples are now being analyzed for the elements of interest

<sup>9</sup>S. R. Koirtyohann and C. Feldman, "The Spectrographic Determination of Trace Elements in Human Tissue," Analytical Chemistry in Nuclear Reactor Technology, Fourth Conference, Gatlinburg, Tennessee, October 12-14, 1960, TID-7606, p 56.

Table 4.5. Average Values for San Francisco Tissues  $(\mu g \text{ per } g \text{ of ash})$ 

Tissue	Dry (%)	Ash (%)	Со	Cu	Ni	Cr	v	РЬ	Al	Mn	Мо	Sn	Ti	Sr	Ва	Ag	Zn	Cd	Fe	Mg	Zr	Ga
————— Adrenal			<u>.                                    </u>		<del></del>					<u> </u>						-	-					
Glands	50.9	0.72		237	20	8.8		39	140	58	18	88	29	14	6.9		2300	77				
Aorta	28.8	2.3		87	19			220	65	18		54	8	110	19		2150	33				
Bone	68	27		4.3				51	19	2.3				130			180		490	4800		
Brain	27.1	1.5		460	5.7			70	17	21	2.0		5.4	4.2		1.1	1140	12				
Cartilage	41.8	2.7		38	19			34	24	8.3		22	6.3	42	4.1		700	5.8				
Diaphragm	29.2	0.72		170	16	6.1		33	60	18	3.0	59	66	11			5000	33				
Esophagus	21.1	0.78		150	13	8.5		240	88	16	1.9	82	12	12	9.4		2300	20				
Fat	83.9	0.11	6.6	240	48	29		54	430	37	6.1	100	41	36	26	4.9	1800	39			6.3	
Gall																						
Bladder	38.3	0.67	10	350	32	16		44	100	51	9.7	68	22	27	11	1.8	1800	76				
Heart	26.0	0.91	5.1	370	44	2.3		8.8	33	24	3.7	28	10	7.5			3300	7.9				
Intestine																						
Jejunum	19.6	0.79		250		3.2		35	72	60	5.4	240		23	5.1	6.3	3100	77				
Rectum	28.0	0.86		88	8.0	13		20	86	10	2.0	34	11	9.4	3.9		6200	17				
Sigmoid																						
Colon	27.8	0.61		200	18	10		25	280	47		280	10	58	11		3800	35				
Kidney	23.3	1.1		220	34	3.9		56	26	68	16	74	6.7	7.6			3500	2500				
Liver	31.5	1.2	8.2	660	21	2.2		160	65	150	55	130	5.7	5.0		3.0	5100	160				
Lung	19.8	1.0	3.4	100	24	17	5.7	5.6	2400	18	2.7	100	279	11	16		1200	33			10.2	3.4
Muscle	26.0	0.89	1.6	110	7.3	3.4		13	58	7.4		7.4		6.9	6.4	0.76	6000	15				
Omentum	85.7	11	12	340	28	22		92	240	73	12	100	25	62	15	4.0	2900	65				
Pancreas	42.9	1.0		150	2.5	2.4		65	45	130	3.3	52		8,7	4.5	2.3	4100	120				
Prostate	22.2	1.1		110	29	6.2		22	39	17	3.9	0.36		30	4.0	4.3	10000	28				
Skin	35.4	0.48	3.9	94	24	11		17	170	13	2.0	47	21	14	8.4	1.0	600	13				
Spleen	25.2	1.3		100	1.7			50	57	12	4.1	24	5.6	4.0			1800	11	-			
Stomach	25.9	0.66	1.8	220	17	5.3		24	81	47	3.1	93	32	20	9.6	2.2	3100	4.7				
Testes	19.9	1.0		100	6.2	3.0		19	33	18	3.2	41		7.8			1700	29				
Trachea	34.7	1.3	1.5	59	15	9		80	42	23		69	7	64	16		950	22				
Thyroid	27.1	1.1		85	20	5.5		25	47	28	3.2	120		20	14		3700	140				
Urinary								-														
Bladder	31.8	0.68		140	11	11		43	110	22		49	9	20	7.4		2900	27.				
Uterus	22.6	1.6		120	16	1.3		17	125	13		55	18	30	10		1600	38				

111

Table 4.6. Average Values for Atlanta, Georgia, Tissues  $(\mu g \ per \ g \ of \ ash)$ 

									APO I - C	•	,								
Tissue	Dry (%)	Ash (%)	Со	Cu	Ni	Ct	V	РЬ	Al	Mn	Мо	Sn	Ti	Sr	Ва	Ag	Zn	Cq	Zr
Adrenal	·					_										,			
Glands	50.2	0.74		230	20	25		34	310	58	14	37	86	6.2	14		2300	51	
Appendix	56.8	0.90		230	32	5	4	20	1000	500	14	180	70	100	100	2	3100·	54	10
Aorta	33.3	1.5		91	9			99	96	12		14		36	12 ·		1700	16	
Brain	25.4	1.4		460	3			14	. 22	24			5.6	2.1			960		
Breast	69.2	0.37		125	7	14		.23	150	14			11	5.3	5.0		880	27	
Cartilage	48.8	.9.1		. 27	4			38	17	11				54	6.3		790	5 <b>.</b> 8	
Diaphragm	27.1	0.94		160	9	11		11	64	17	. 4	14	8.5	3.2			4500	16	
Esophagus	27.0	0.87		140	13	10		20	260	23	2	18	29	6.5	6.5		2400	16	
Fat	84.7	0.23		150	20	28		27	280	18	4.2	14	41	9.3	8.5		1000	18	
Gall Bladder		0.89		620	8	14		43	110	59		12				1.0	1100	30	
		•	,					-			8.5		11	9.7	4.4	1.0		_	
Heart	23.6	1.0	4	400	23	10		10	56	22	6.2	16	5	1.7			3300	8	
ntestine Cecum	22 6	0.60		270	20.	10		40	420	120	<i>5</i> 2	220	110	40	20	1.0	2000	20	
Ileum	33.6 28.0	0.60 0.72			32	18 18		40 29	420 330	130 110	5.3 8.0	220 170	1 <sub>.</sub> 10 95	48 · 27	39 32	1.0	2900 3400	29 38	
Jejunum	24.8	0.72		340	10	11		16	160	100	7.6	140	23	12	12		3800	52	
Rectum	39.7	0.76		190	10	17		42	330	52	4.3	59	32	20	14		3500	20	
Sigmoid	37.1	0.70		1,70		1,		42	))0	72	4.7	"	72	20	14		3,00	20	
	35.4	0.66		230	14	10		16	280	55	5.4	130	12	20	11		2800	23	
Kidney	23.5	1.1		320	14	2.7		140	40	97	19	13	12	4.2			4300	29	
Lung	20.9	1.1		110	8	28	4.4	56	3800	24	3.9	33	610	9.8	29		1500	47	8

Table 4.7. Average Values for New York Tissues  $(\mu g \text{ per } g \text{ of ash})$ 

Tissue	Dry (%)	Ash (%)	Со	Cu	Ni	Cr	V	Pb	Al ·	Mn	Мо	Sn	Ti	Sr	Ва	Ag	Zn	Cd	Zr
Adrenal Glands	56.0	0.55	6.5	440	310	12	9.9	60	390	78	13	45	43	13	12		3100	140	
Aorta	32.1	2.1		120	58	5.0		160	84	15		19	10	72	8.9		1500	37	
Brain	23.0	1.4		480	16			20	18	25				2.8			1200		
Breast	84.6	0.18		140	51	18		20	140	14	2.3	19	15	12	3.6		2100	23	
Diaphragm	29.2	0.94		170	44	4.3		11.4	120	23	2.0	16	10	8.5	4.6		3300	16	
Esophagus	23.9	0.86		180	65	10		29	330	25	4.6	26	81	12	7.7		2600	27	
Fat	88.3	0.11		440	260	30		25	230	29	5.6	20	21	9.6	6.7	1.7	980	8.	5
Gall Bladder	36.2	0.85		480	65	5.8		29	81	84	6.4	7.6	11	21	4.9	0.9	830	30	
Heart	21.9	1.1	5.2	370	44	3.5		14	65	28	6.3	13	9.4	4.9			2900	8.	8
Intestines	32.0	0.66		550	88	8.7	6.6	42	150	130	8.3	100	25	35	14		3100	43	
Kidney	21.9	1.1		260	30			91	47	88	43	32	6.4	8.9	2.2		4200	3000	
Lungs	19.3	1.2		130	39	29	17	58	1700	46	1.3	55	520	14	15		1100	30	28

Table 4.8.	Comparison of Wet Chemical and Spectrographic Results
	(μg per g of ash)

•		Copper			Cadmium	
Sample	Colorimetric	ORNL Spectrographic	U.T. Spectrographic	Polarographic	ORNL Spectrographic	U.T. Spectrographic
160 H	270	280	370			
C-78 L	590	690	700			
250 L	800	780	960			
276 K	240	200	. 240	1310	1300	1850

in the internal dose program. The complete analysis will require several separate procedures.

First, the samples are being examined for general trace element content by an arc method quite similar to that used for soft tissues. Standards are prepared by fusing a trace element mix with  $K_2S_2O_7$  and mixing this fusion cake with purified  $Ca_3(PO_4)_2$  (ref 10) to give the desired trace element concentrations. The samples are exposed on the Quantometer and photographically by the same methods as for the soft tissues. The elements sought by this method and their detection limits are given in Table 4.9. The elements Fe, Cu, Pd, Al, Mn, Mg, Sr, and Zn are detected in almost all samples; Co, Cr, Mo, Cd, and Au are seldom observed, while Ni, Sn, and Ba are detected occasionally.

The next step planned in the analysis of bone is to determine the major constituent concentrations (Ca, P, Na, K). This will be done on the Quantometer with either a flame source or porous-cup exposures.

Methods for the chemical concentration of specific elements or groups of elements (Cesium, rare earths) are being considered.

Ashing Loss Experiments. - Experiments were run to test if any of the trace elements of interest are lost during dry ashing of the tissues. The apparatus used for this work is shown schematically in Fig. 4.5. Exhaust gases from the furnace, along with about 0.8 liter/min of air, are drawn

Table 4.9. Detection Limits in Bone (μg per g of ash)

Element	Detection Limit	Element	Detection Limit
Со	2	Мо	2
Cu	2	Sn	5
Fe	20	Mg	
Ni	2	Sr	1
Cr	2	Ва	10
РЬ	5	Zn	50
Al	5	Cq	5
Mn	. 2	Au	2

UNCLASSIFIED ORNL-LR-DWG 70724A

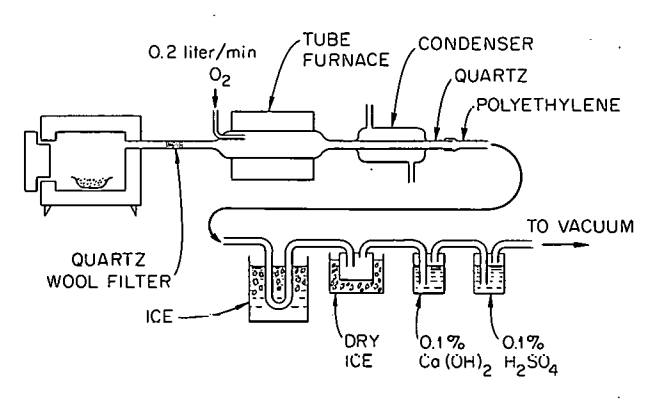


Fig. 4.5. Apparatus for Ashing Loss Experiments.

<sup>10</sup> R. L. Mitchell, "The Spectrographic Analysis of Soils, Plants, and Related Materials," Commonwealth Bur. Soil Sci. (Gt. Brit.), Tech. Commun. No. 4, p 129.

through a heated quartz tube (~700°C) where the vapors undergo complete combustion. The burned gases are then cooled, passed through a trap packed in dry ice, bubbled through a 0.1% solution of Ca(OH)<sub>2</sub>, and then through 0.1% H<sub>2</sub>SO<sub>4</sub>. All parts are made of quartz or polyethylene. A quartz wool filter is used to avoid "fly ash" contamination in the tube. Furnace operation is not affected by the trapping system. All ashings are started in a cold furnace. The temperature is raised slowly to 450°C and held there until ashing is complete. The tube is then cooled, and the inside is rinsed into the dry-ice trap. The trap solutions are concentrated and analyzed for the trace elements of interest.

This system collects and analyzes the material which is actually volatilized from the sample. It correctly reflects any volatilization characteristics of a given element which may be affected by the element's state of chemical combination in the sample. It thus avoids the ambiguities which are possible in the interpretation of experiments in which the recovery of added inorganic material is measured. It also allows the use of large samples with corresponding high sensitivity.

The efficiency of the trapping system was tested by heating a sample of H<sub>3</sub>BO<sub>3</sub> along with a sample of plant ash in separate dishes. The recovered boron (nearly all from the dry-ice trap) indicated a minimum trapping efficiently of 50%. The actual efficiency may be considerably higher, because part of the boron was undoubtedly absorbed by the basic plant ash.

Samples of kidney and liver have been run with this system. Liver ashes very slowly at 450°C. For this reason the ashing was divided into two parts. The temperature was raised slowly (~18 hr) to 450°C and held there for 24 hr. The trap solutions were then changed, and a separate run was made for the rest of the ashing (~48 hr).

The results from these experiments are given in Table 4.10. In cases where the elements were not detected in the trap solutions, the detection limit and corresponding percent loss figures are given. In most cases where positive results were obtained, the losses were very small. The apparent loss of aluminum from both tissues and of nickel from the liver is somewhat surprising, especially since it occurred to an equal or greater extent during the second phase of the liver ashing when the sample was completely carbonized. These experiments will be repeated to verify the findings.

A special effort will be made to avoid nickel and aluminum contamination.

Conclusions. — The analysis of both soft tissue and bone is being carried out on a routine basis. About two man-hours per sample is required for the ashing and analysis. The agreement between ORNL and UT spectrographic data is generally good. Wet chemical and spectrographic results agree in the cases that were tested. The precision of the method, tested over a five-month period, is satisfactory.

Most of the trace elements of interest are not lost during dry ashing. Apparent losses of small amounts of nickel and somewhat larger amounts of aluminum were found. More experiments are needed to verify these findings. If they are accepted as true, however, they are not large enough to seriously affect the data that have been collected.

#### Further Statistical Interpretations of Trace Element Concentration in Human Tissue

I. H. Tipton M. J. Cook Jane Shafer Fred Roberts

Various statistical operations on the IBM 1620 and 7090 data processing machines have been performed on the data from a group of 150 adults (age > 20) who died suddenly and whose tissues showed no gross pathologies. The data from this group will serve as a base line in future studies of other groups.

In a study such as this, where the occurrence of possible causes contributing to the variation of the concentration of an element in an organ can be observed but cannot be controlled, the correlation coefficient is an important, descriptive, observational feature of the population. Granted it does not measure the influence of one element on another, but it does measure, on a conventional scale, the importance of factors which (on a balance of like and unlike action) act alike on both elements as against the remaining factors which affect the two independently. The interaction is proportional to the square of the correlation coefficient.

To determine the similarities of action among elements in a tissue, the rank correlation coefficient was calculated by Kendall's method and the significance of its difference from zero was determined for 24 elements taken two at a time. This calculation was made for each tissue. To assess the similarity of action of the various tissues with

Table 4.10. Ashing Loss Results

								Ele	ment					•	
	Со	Cu	Ni	∠ Cr	-Pb	ΆΊ	Mn	Mo	√ Sn	~ Sr ·	~ Ba	Ag	-Zn	_Cq	Fe
		•					Kidney	(2 g of a	sh)						
μg in ash		2000	20	4	100	170	260	80	1500	20	120	2	4000	70	20,000
μg trapped	•	8	< 3	<1	<12	20	1	<1.2	< 5	<0.1	<5	<0.4	40	< 4	25
% trapped		0.4	<15	<25	<12	12	0.4	<1.5	<0.3	<0.5	<4	< 20	1	<6	0.1
	•						Liver (	6 g of as	h)						
μg in ash	90	8000	200	30	1000	610	1200	580	90	8		15	50,000 -	1200	60,000
μg trapped Run No. 1	<6	8 .	3	<1	<12	40	2	<1.2	< 5	<0.1		<0.4	< 10	< 4	200
μg trapped Run No. 2	<6	8	3	<1	<12	60	. 2	<1.2	<5	<0.1		<0.4	20	<4	50
μg trapped total	<12	16	6	< 2	< 24	100	4	<2.4	< 10	<0.2		<0.8	20	<8	250
% trapped	< 14	0.2	3	< 7	< 2.4	16	0.3	<0.4	<11	< 2.5		< 5	0.04	<0.7	0.3%

regard to a specific element, the same kind of study was made for each element, taking the tissues two at a time.

In addition to the strong correlations between certain pairs of essential elements such as copper and iron, strong correlations, some positive, some negative, between certain nonessential elements and essential elements were observed. This report includes the correlations for five nonessential elements, aluminum, barium, chromium, lead, and tin which were observed in over 80% of all samples of all tissues, and one, cadmium, which occurred in every sample of kidney and over 90% of the samples of liver and pancreas. Included, in addition, is one essential element, manganese, which is highly correlated with essential elements in brain, with nonessential elements in lung, and with both in the other tissues.

Although aluminum (Table 4.11) was observed above the limit of detection (4  $\mu$ g per g of ash) in

every sample of every tissue, the concentration in the lung was 10 to 100 times as great as in other tissues. The concentration in the lung was also observed to increase with age, although this was not observed for other tissues. In the lung this element was highly correlated with other non-essential elements, some of which are contaminants from the inhalation of dusty air. In fact, in every organ aluminum was found to be more highly correlated with nonessential than essential elements. There was no significant correlation, however, between the concentration of aluminum in the lung and that in the other organs (Table 4.23), although the correlations among most other organs were significant (Tables 4.18-4.22, 4.24).

Barium (Table 4.12) was observed above the detection limit (0.2  $\mu$ g per g of ash) in about 90% of all samples. This element showed high correlations in most tissues with all essential elements, except cobalt and molybdenum, and with

Table 4.11. Aluminum Rank Correlation Coefficients Significantly Different from Zero at a Confidence Level > 99%

Tissue				Esser	tial							1	Nones	sentia	i			
lissue	Ca	Ço	Cu	Fe	Mg	Mn	Мо	Zn	Ag	Ва	Cq	Ct	Ni	Pb	Sn	Sr	Ti	V
Adrenal											-							
Aorta			0.43	0.40		0.29	9										0.27	
Brain																		
Heart					0.26					0.26								
Intestine	0.44		0.29	0.42	0.46	0.4	3		0.44	0.45			0.30		0.29	0.38	0.43	
Kidney						-0.2	7		0.25									
Liver										0.23	0.35							
Lung						0.4	3			0.68		0.49	0.35		0.28	0.37	0.65	0.59
Muscle	0.28					0.2	7		0.26	0.34						0.25		
Ovary																	0.67	
Pancreas			0.27	0.39						0.48		0.24				0.23	0.41	
Prostate																		
Skin			0.51			0.6	2			0.62							0.68	0.58
Spleen									0.26									
Stomach	0.28				0.32				0.23	0.40						0.26	0.33	0.22
Testis																		
Thyroid			0.63											0.52			0.58	
Uterus																		

Table 4.12 Barium Rank Correlation Coefficients Significantly Different from Zero at a Confidence Level > 99%

				Ess	ential								Nones	sential				
Tissue	Ca	√Co	Cu	/ Fe	Mg	Mn	∠ Mo	_Zn	Ag	Al	Çd	Ctr	Ni	РЪ	S'n	Sr	Ti	v .
Adrenal	0.74			•	=01													
Aorta					0.23		,							0.27		0.26		
Brain				0.38	0.35	0.44	0.24		0.24					.0.24				
Heart	•		0.34		0.34	0.41		0.38		0.26		0.21		0.34	0.24		0.23	
Intestine	0.44		0.42	0.32	0.54	0.67	•	,	0.31	0.45		0.37	0.43	0.39	0.32	0.48	0.34	
Kidney					0.24					•		0.31			0.21	0.24		
Liver	-0.33	0.21	0.21			0.39			•	0.23	0.23	0.30					0.26	
Lung						0.50				0.68		0.43.	0.30		0.40	0.39	0.64	0.58
Muscle			0.41	0.39	0.26	0.58		0.35	0.22	0.34		0.30		0.49	0.22	0.22	0.22	: :
Ovary	0.60							4			•							
Pancreas			0.34	0.52	0.26			0.33	0.27	0.48					0.31	0.36	0.33	
Prostate								0.38			0.40	,		0.33		0.54		
Skin				0.58		0.74				0.62				•			0.62	0.50
Spleen			0.22		0.25	0.52		0.26				0.35			0.25		0.38	
Stomach	0.28			0.26	0.28	0.23				0.40			0.24		0.26	0.27	0.32	
Testis	0.32					0.30		0.38				0.35		•		0.34	0.41	
Thyroid												-						
Uterus												0.47	0.47					

most nonessential elements. Although barium was positively correlated with calcium in many organs, in liver the two were negatively correlated. This fact plus the two occurrence of barium in liver (only 47% of the total number of samples had values above the detection limit) would indicate that calcium had an action antagonistic to barium in liver. In general, an elevated concentration of barium in one organ was accompanied by an increased concentration in most others (Tables 4.18-4.24). The physiological effects of barium need to be investigated.

Cadmium (Table 4.13) was observed above the detection limit of the method (50  $\mu$ g per g of ash) in every sample of adult kidney and liver and in about 90% of the samples of pancreas. It was highly correlated with zinc in all organs in which it was ordinarily observed. This supports the observations that the metabolism of these elements is similar. <sup>11,12</sup> The case for cadmium as an essential element has been weakened by the observation <sup>13</sup> that cadmium does not obey homeostatic control. Both Cotzias' and Gunn's observations imply that cadmium is an antimetabolite for zinc. The concentration of cadmium in kidney was highly correlated with that in the other organs in which it is observed (Table 4.21).

Chromium (Table 4.14) was observed above the detection limit (0.1 µg per g ash) in over 90% of all samples of all organs and in every sample of lung, ovary, and skin. The highest concentration occurred in the lung, for which the median value was some ten times that for most of the other tissues. Visek and his co-workers <sup>14</sup> observed that after intravenous injection of Cr <sup>51</sup>Cl 2 the lungs of sheep contained 2 to 20 times more Cr <sup>51</sup> than than any other organ, which would indicate that the high concentration of chromium in the lung which we observed was not due just to the inhalation of insoluble dust containing chromium. This element was highly correlated with nickel and, to a lesser extent, with barium and lead. The high

correlation of chromium with manganese and copper in liver and in other organs, while it gives no particular support to, is not at variance with the observation of a chromium-activated glucose tolerance factor in the liver. <sup>15</sup> Except for the aorta, there appeared to be a high correlation between the organs with respect to the concentration of chromium (Tables 4.18–4.24).

Lead (Table 4.15) was observed above the limit of detection in every sample of the adrenal, aorta, kidney, liver, lung, pancreas, and in over 90% of the samples of the other tissues except the brain (69%) and muscular tissues such as the heart, muscle, and uterus, where it occurred in only about one-half the samples. The highest concentrations of lead occurred in the aorta, liver, kidney, pancreas, and lung. In the aorta, lead was correlated with calcium, magnesium, strontium, and barium, whereas in the kidney it was correlated with copper, manganese, zinc, and cadmium. It was correlated with manganese in nine organs, but otherwise showed no consistent behavior. The concentration of lead in the lung was highly correlated with that in other organs (Table 4.23).

Tin (Table 4.16) was observed above the limit of detection (5  $\mu$ g per g of ash) in about 80% of all samples of all organs, though much less frequently in the brain (5%) and muscle (19%). The highest concentrations occurred in the sigmoid colon and lung. Tin was correlated with zinc and with barium in most organs. It is the only element of the group included in this paper that was not correlated with manganese in most tissues. With the exception of the brain, most other organs showed a high correlation with respect to tin (Tables 4.18–4.24).

Manganese (Table 4.17) was observed above the limit of detection (2  $\mu$ g per g of ash) in every sample of every tissue. The highest concentrations occurred in the liver and pancreas, intestine, and stomach. Manganese was very highly correlated with magnesium in most organs. A similarity in the behavior of these two elements has been observed in vitro, and this high correlation would indicate that there are some common factors affecting the distribution of these in vivo. In the brain, manganese was observed to be most highly correlated with the essential elements. This is

<sup>&</sup>lt;sup>11</sup>S. A. Gunn, T. C. Gould, and W. A. D. Anderson, Acta Endocrinologica. 37, 24-30 (1961).

<sup>&</sup>lt;sup>12</sup>G. C. Cotzias, D. C. Borg, and B. Selleck, Am. J. Physiol. 201, 63-66 (1961a).

<sup>&</sup>lt;sup>13</sup>G. C. Cotzias, D. C. Borg, and B. Selleck, Am. J. Physiol. **201**, 927-30 (1961b).

<sup>&</sup>lt;sup>14</sup>W. J. Visek et al., Proc. Soc. Exptl. Biol. Med. **84**, 610-15 (1953).

<sup>&</sup>lt;sup>15</sup>K. Schwarz and W. Mertz, Arch. Biochem. Biophys. **85**, 292 (1959).

Table 4.13. Cadmium Rank Correlation Coefficients Significantly Different from Zero at a Confidence Level >99%

<b>T</b> :				Esse	ential							No	onesse	ential				
Tissue	Са	Со	Cu	Fe	Mg	Mn	Мо	Zn	Ag	Al	Ba	Cr	Ni	Pb	Sn	Sr	Ti	V
Adrenal												0.82						
Aorta								0.32										
Brain (no cadmium observed)	)																	
Heart												•						
Intestine			0.29			0.25												
Kidney						0.23		0.70						0.40				
Liver		0.27					0.30	0.29	0.31	0.35	0.23				0.36			
Lung							0.23							0.26				
Muscle				0.25										0.22				
Ovary						•												
Pancreas							0.26	0.35				*						
Prostate											0.40			0.44				
Skin (no cadmium observed)																		
Spleen			0.23			0.33		0.26							0.30			
Stomach			0.28	0.26		0.36	0.23	0.31						0.50			0.33	
Testis								0.40									0.29	
Thyroid																		
Uterus .		0.44			•	٠								0.48				

12

Table 4.14. Chromium Rank Correlation Coefficients Significantly

Different from Zero at a Confidence Level > 99%

Essential

Ca Co Cu Fe Mg Mn Mo Zn Ag Al Ba Cd

<b>T</b> :				Esser	ntial							N	Vonessei	ntial				
Tissue	Ca	Со	Cu	Fe	Mg	Mn	Мо	Zn	Ag	Al	Ва	Cq	Ni	Pb	Sn	Sr	Ti	v
Adrenal												0.82						
Aorta													0.29					
Brain													0.23	0.24				
Heart		0.23	0.30		0.38	0.47		0.28			0.21		0.38	0.41			0.28 ·	
Intestine	0.27		0.27		0.29	0.34					0.37		0.49	0.29			0.24	
Kidney			0.24		0.25	0.42		0.27	-0.48		0.31		0.32	0.22				
Liver		0.33	0.35			0.31					0.30		0.41					
Lung						0.53				0.49	0.43		0.63	0.37	0.45		0.37	0.48
Muscle			0.31	0.39	0.29	0.43		0.32			0.30		0.44	0.34				
Ovary				0.62													•	
Pancreas			0.29	0.34						0.24			0.44					
Prostate								-									0.35	
Skin																		
Spleen						0.31					0.35		0.30	0.21			0.30	
Stomach			0.24			0.33			-0.30				0.34				0.27	
Testis					0.33	0.35					0.35							
Thyroid																		
Uterus						0.44					0.47		0.54	0.57				

Table 4.15. Lead Rank Correlation Coefficients Significantly Different from Zero at a Confidence Level > 99%

				Esse	ntial								Noness	ential				
Tissue	Са	Co	Cu	Fe	Mg	Mn	Мо	Zn	Ag	A1	Ba	Cq	Cr	Ni	Sn	Sr	Ti	V
Adrenal			•				<u>.</u> .			•								
Aorta	0.26				0.37						0.27					0.34		
Brain						0.27					0.24		0.24					
Heart			0.27	0.28	0.24	0.44		0.36			0.34		0.41		0.22			
Intestine		*	0.28	0.29		0.50					0.39		0.29			0.34	0.27	0.33
Kidney			0.22			0.36		0.36				0.40	0.22					
Liver																		
Lung				0.40								0.26	0.37					
Muscle			0.31	0.35	0.25	0.43	0.22	0.23	0.24		0.49	0.22	0.34	•			0.35	
Ovary																		
Pancreas																		
Prostate						0.44					0.33	0.44	•					
Skin																		
Spleen				0.40		0.23							0.21					
Stomach			0.27	0.43		0.44		0.34				0.50					0.28	
Testis						0.33		0.34										
Thyroid										0.52								
Uterus		0.43										0.48	0.57					

Table 4, 16. Tin Rank Correlation Coefficients Significantly Different from Zero at a Confidence Level > 99%

				Ess	ential								Nones	sential				
Tissue	Ca	Со	Cu	Fe	Mg	Mn	Мо	Zn	Ag	Al	Ва	Cq	Cr	Ni	Pb	Sr	Ti	V
Adrenal																		
Aorta				0.33				0.26										
Brain																	0.42	
Heart				0.24				0.27	0.26		0.24				0.22			
[ntestine					0.27	0.39	0.25	0.27	0.32	0.29	0.32			0.34		0.32	0.26	
Kidney											0.21							
Liver								0.35				0.36						
Lung						0.38				0.28	0.40		0.45	0.31			0.27	0.34
Muscle		•					0.29				0.22							
Ovary																		
Pancreas			0.25	0.29			0.26	0.25	0.27		0.31					0.25		
Prostate								0.41								0.37		
Skin									0.64									
Spleen			0.24			0.28		0.28			0.25	0.30					0.21	
Stomach											0.26							
Testis																		
Thyroid			0.55	0.67														
Uterus																		

. .

Table 4.17. Manganese Rank Correlation Coefficients Significantly Different from Zero at a Confidence Level > 99%

			E	ssential	•			<u> </u>				Nor	nessenti	al				
Tissue	Ca	Со	Cu	Fe	Mg	Мо	Zn	Ag	Al	Ba	Cq	Cr	Ni	РЪ	Sn	Sr	Ti	V
Adrenal						0.70				-	-						_	
Aorta			0.42				0.44		0.29									
Brain			0.54	0.61	0.61					0.44				0.27				
Heart		0.41	0.41	0.30	0.55		0.44			0.41		0.47	0.24	0.44			0.40	
Intestine	0.32		0.56	0.46	0.51			0.38	0.43	0.67	0.25	0.34	0.44	0.50	0.39	0.51	0.29	0.25
Kidney	•	0.25	0.46		0.44		0.40		-0.27		0.23	0.42	•	0.36				
Liver	-0.32	0.43			0.48					0.39		0.31						
Lung			0.40		0.28				0.43	0.50		0.53	0.55		0.38		0.42	0.53
Muscle			0.54	0.49	0.37		0.43		0.27	0.58		0.43		0.43		0.23	0.27	
Ovary												•						
Pancreas			0.23		0.52											-0.29		
Prostate			0.41	0.51									•	0.44				
Skin				0.61					0.62	0.74								0.56
Spleen			0.28		0.31		0.22			0.52	0.33	0.31		0.23	0.28		0.23	
Stomach		0.28	0.46	0.24	0.39	0.32	0.34			0.23	0.36	0.33		0.44				
Testis					0.69		0.42			0.30		0.35		0.33				
Thyroid					0.63		0.54						1			0.55	0.56	
Uterus					0.53		0.52					0.44						

consistent with the observation that chronic manganese poisoning results in a disturbance of the central nervous system similar to "Parkinsonism". If in the lung, manganese was correlated with the nonessential elements. Although the aorta showed no correlation with other organs so far as manganese was concerned, all other organs showed a high correlation (Tables 4.18–4.24).

In general, the correlations between the elements and percent ash and percent dry were not significantly different from zero; that is, the ashing method was not a factor in the correlations between two elements.

Table 4, 18. Aorta Rank Correlation Coefficients Significantly Different from Zero at a Confidence Level > 99%

Tissue			None	ssential			Essential
IIssue	Al	Ва	Cd	Cr	РЬ	Sn	Mn
Adrenal				None			None
Brain							
Heart						60	
Intestine					36	28	
Kidney	31	28	43		35	62	
Liver			39		35	56	
Lung		28			38	38	
Muscle	34		41				
Ovary					67		
Pancreas		25	33				
Prostate	59		51		40		
Skin					•		
Spleen							
Stomach			40		44	57	
Testis		44	54		33	49	
Thyroid		60 ·					
Uterus					61	55	

<sup>16</sup>G. C. Cotzias, Federation Proceedings Supplement No. 10, p 98-102 (1961c).

Table 4.19. Brain Rank Correlation Coefficients Significantly Different from Zero at a Confidence Level > 99%

<b></b>		Nonessential'							
Tissue	Al	Ва	Cq	Cr	Pb	- Sn	Mn		
Adrenal			None						
Aorta									
Heart	23	52		51	47		65		
Intestine				29	30				
Kidney	24	41		54	43		49		
Liver		55		54	23		57		
Lung		25		28	57	29	50		
Muscle	40	61		59	50	35	54		
Ovary									
Pancreas	32	37		47			42		
Prostate					50	41			
Skin				. •		i			
Spleen									
Stomach	24			52	43		35		
Testis		37		55	37				
Thyroid			•						
Uterus	55			51	46		61		

Table 4.20. Heart Rank Correlation Coefficients Significantly Different from Zero at a Confidence Level > 99%

· '			Nones	sential	•		Essential
Tissue	Al	Ва	Cd	Cr	Pd	Sn	Мп
Adrenal					71 .	·	71
Aorta						60	
Brain	23	52		51	47		65
Intestine					31	32	
Kidney	46	57		63	27	63	63
Liver		44		53		50	59
Lung		28		35	37	48	54
Muscle	37	48		58	· 60	49	56
Ovary			63	71		80	
Pancreas	35	53		51			50
Prostate	35	49		43	41	61	59
Skin							
Spleen							
Stomach	30	34		51	52	37	57
Testis		56		52	52	64	53
Thyroid		•					60
Uterus	48	42		50	51	75	69

Table 4.21. Kidney Rank Correlation Coefficients Significantly Different from Zero at a Confidence Level > 99%

Tissue		Essential					
lissue	Al	Ba	Cq	Cr	Pd	Sn	Mn
Adrenal	79	·			67	87	
Aorta	31	28	43		35	62	
Brain	24	41		54	43		49
Heart	46	57		63	27	63	63
Intestine			32	37	52	30	26
Liver		41	47	55	54	59	76
Lung		27	42	34	66	45	33
Muscle	43	45		47	30	33	38
Ovary				68		76	62
Pancreas	35	41	60	49			58
Prostate	38		51	39		53	
Skin							
Spleen							
Stomach	31		46	47	51	59	58
Testis	.33	52	49	66	43	59	32
Thyroid	69	71	53				
Uterus	44		50	63		61	52

Table 4.22. Liver Rank Correlation Coefficients Significantly Different from Zero at a Confidence Level > 99%

Tissue	Nonessential							
lissue	Al	Ва	Cd	Cr	РЬ	Sn	Mn	
Adrenal			-			78		
Aorta			39		35	56		
Brain		55		54	23		57	
Heart		44		53		50	59	
Intestine					37		25	
Kidney		41	47	55	54	59	76	
Lung			34	35	45	44	3.4	
Muscle		50	23	52		23	45	
Ovary				59			64	
Pancreas	22	49	52	42			51	
Prostate		36	41			51		
Skin								
Spleen	•							
Stomach	23		29	49	48	51	52	
Testis	43	29	38	63	39	56		
Thyroid								
Uterus	53			65		68	55	

Table 4.23. Lung Rank Correlation Coefficients Significantly Different from Zero at a Confidence Level > 99%

			Nones	sential			Essential
Tissue	A1	Ва	Cd	Cr	Pd	Sn	Mn
Adrenal	None				81		
Aorta		28			38	38	
Brain		25		28	57	29	50
Heart		28		35	37	48	54
Intestine					47		
Kidney		27	42	34	66 .	45	33
Liver			34	35	45	44	34
Muscle		27		26	42	38	56
Ovary						81	. 42
Pancreas			45 .	25			26
Prostate						50	
Skin		54					•
Spleen		•					
Stomach			33 .	25	40	42	33
Testis		33	41	53	31	39 ·	
Thyroid				•			63
Uterus						71	76

Table 4.24. Muscle Rank Correlation Coefficients Significantly Different from Zero at a Confidence Level > 99%

Tissue		Essential					
lissue .	Al	Ва	Cq	Cr	РЬ	Sn	Mn
Adrenal	67			81			
Aorta	34		41				
Brain	40	. 61.		59	50	35	54
Heart	37	48		58	60	49	56
Intestine					33	27	
Kidney	43	45		47	30	33	38
Liver		50	23	52		23	45
Lung		27	•	26	42	38	56
Ovary							69
Pancreas	33	35		49	,		31
Prostate			36	48	· 41	37	59
Skin							•
Spleen							
Stomach	23			52	. 33	. 39	42
Testis	32	49	41	34	30	30	30
Thyroid		59 .					61
Uterus				61	62	48	77

## MICROSCOPIC AND AUTORADIOGRAPHIC STUDIES OF URANIUM DISTRIBUTION IN THE RAT KIDNEY

## E. S. Jones

Studies by the autoradiographic method of the distribution of uranium in rat kidney have been carried forward to confirm previous studies on the phenomenon of prolonged retention of uranium by kidneys of animals given an intravenous injection of a large mass of uranium. This retention of uranium has been discussed in the last three annual reports.  $^{17,18,19}$  When the mass of uranium is varied, there is a greater fractional retention at the higher levels. This retention, however, is not always linear, for, in some cases, the retention of uranium from a  $100 \mu g/kg$  injection is higher than from a dose of  $1000 \mu g/kg$ .

A change in the concept of the factor used in converting counts to disintegrations per minute per gram, additional figures for the concentration ratio (previously called the nonuniform distribution factor), and a study of the comparison between the disintegrations as found by autoradiographic and by radiochemical methods are presented in this report. Also, studies of the location of uranium tracks in the histological units and of the pathological conditions observed in the tissues of rats given different dosages and sacrificed at different postinjection times are included.

#### Methods

The methods used are the same as previously reported <sup>17</sup> except that in calculating the conversion factor to change autoradiographic counts to disintegrations per minute per gram, the factor now used is 27.46. In the last paper, this factor was doubled to include tracks radiating from the lower part of the section. A study was made of this. Since the tracks were visible under low power, the slide could be reversed, making possible the counting of tracks in identical fields from both

upper and lower sides. The number of tracks observed from above and from below coincided. This led to the conclusion that the liquid photographic emulsion penetrates the tissue so that essentially all tracks are visible microscopically.

#### Concentration Ratio

The contrast between activities in cortex and medulla is illustrated by the photographs in Fig. 4.6. This shows tracks in the cortex and in the medulla of a rat injected with  $1000~\mu g$  of uranium per kg of body weight and sacrificed at 1 day postinjection.

The data of the distributions of the mean concentrations of uranium in the cortex and medulla are expressed in terms of the concentration ratio. This is defined as the ratio of the average counts in the fields in the cortex to the average number of tracks per unit area assuming the entire activity spread evenly over the whole kidney. In the previous papers this has been called a "nonuniform distribution factor" and has been estimated to be 1.3. The term  $R_k$  is now used for data from autoradiographic tissues and  $R_{k\,1}$  for that from radiochemical analysis. The method of calculations is the same as in the previous report. <sup>18</sup>

The average counts per field observed in autoradiograms from 32 injected half kidneys are shown in Table 4.25:  $R_k$  is 1.28 with a range of 1.11 to 1.41 and a probable error of 0.07. The factor  $R_{k1}$  from 24 half kidneys ashed (Table 4.24) was 1.22 with a range of 0.82 to 1.37 and a probable error of 0.10.

Larger amounts of activity in the medulla were observed in one animal injected with  $100~\mu g/kg$  and sacrificed at 4 days so that the concentration ratios were 1.03 and 1.07 in the autoradiographic material for the two half kidneys. A similar result was found in a rat injected with  $1000~\mu g/kg$  and sacrificed at 10 days postinjection, giving the ratios of 1.19 and 1.06. There was a reversal of activity from the cortex to the medulla in the two half kidneys of rats injected with  $100~\mu g/kg$  and sacrificed at 84 days, giving ratios of 0.79 and 0.56. The values from the last two half kidneys are excluded in estimating the concentration ratio which thus represents the situation only at earlier times, perhaps for as much as 60 days.

<sup>&</sup>lt;sup>17</sup>E. S. Jones, Health Physics Div. Ann. Progr. Rept. July 31, 1959, ORNL-2806, p 194.

<sup>&</sup>lt;sup>18</sup>E. S. Jones, *Health Phys. Div. Ann. Progr. Rept. July 31*, 1960, ORNL-2994, p 274.

<sup>&</sup>lt;sup>19</sup>E. S. Jones and S. R. Bernard, Health Phys. Div. Ann. Progr. Rept. July 31, 1961, ORNL-3189, p 210.

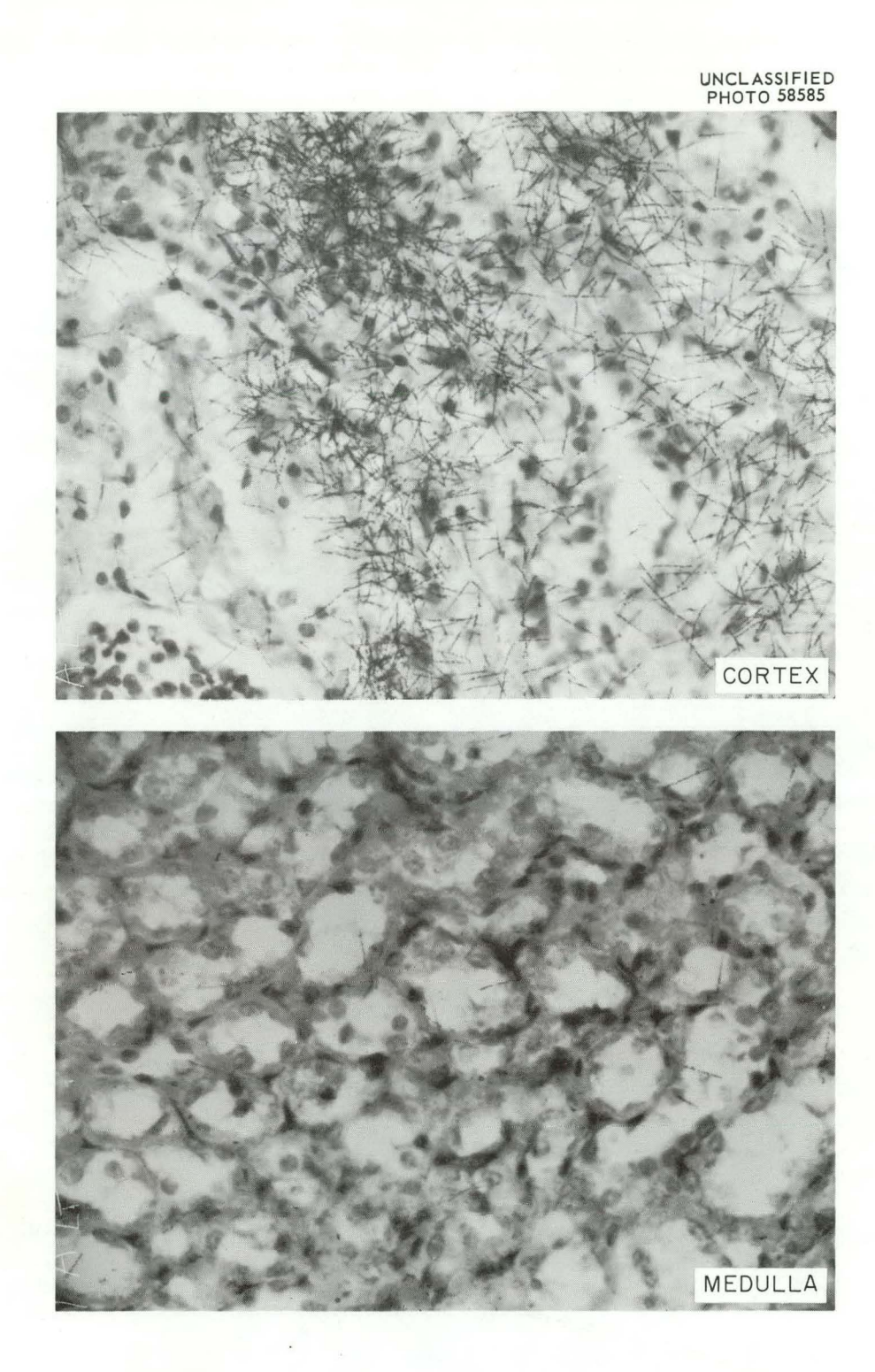


Fig. 4.6. Autoradiograms of Kidney Cortex and Medulla from a Rat Injected with 1000  $\mu \rm g/kg$  of Uranium and Sacrificed 1 Day Postinjection.

Table 4.25. Concentration Ratio Between Cortex and Medulla of Rat Kidney
Based on Autoradiographic Data and Radiochemical Analysis

Dosage (μg/kg)	Postinjection Time (days)	Autoradiographic Concentration Ratio $R_{\dot{k}}$	Radiochemical Concentration Ratio $R_{\pmb{k}}$
1000	1	1.37	1.34
1000	1	1.36	1.33
1000	1	1.36	,
1000	2	1.39	1.34
1000	2	1.38	1.16
1000	2	1.35	1.37
1000	4	1.26	1.31
1000	4	1.24	1.26
1000	7	1.30	
1000	10	1.06	0.8
1000	10	1.19	1.37
1000	28	1.36	1.19
1000	28	1.36	1.06
100	1	1.28	1.31
100	1	1.31	1.37
100	2	1.22	1.13
100	4	1.03	1.02
100	4	1.07	1.11
100	7	1.28	
100	10	1.20	1.20
100	10	1.24	0.97
100	28	1.16	1.24
100	56	1.33	
100	56	1.11	
10	1	1.35	1.37
10	1	1.39	1.10
10	1	1.38	
10	2	1.41	1.28
10	2	1.40	1.34
10	4	1.32	1.27
10	4	1.31	-1
10	7	1.38	
		Average 1.28	1.22

## Comparison Between Activity Counted in Autoradiograms and Activity Measured by Radiochemical Analysis

At the time of sacrifice the kidneys were bisected; <sup>17</sup> one half was used for autoradiograms and the other half was analyzed radiochemically. These values, when compared, gave a gross check, and the results appear in Table 4.26. Activities in the whole half kidneys observed in autoradiograms are calculated with the formula given in the earlier report,  $^{18}$  namely, 0.7c + 0.3m = K, where c = average counts per field in cortex, m = average counts per field in medulla, and K = calculated average counts per field over entire half kidney. Activity recorded for the ashed material was calculated with relation to the weights, that is, the

Table 4.26. Arithmetic Means in Half Kidneys Autoradiographic Method Compared with Radiochemical in dis min  $^{-1}$  g  $^{-1}$ 

Part I

Level (μg/kg)	Postinjection Time (days)	Autoradiographic Mean (dis $\min^{-1} g^{-1}$ )	Radiochemical Mean (dis min <sup>-1</sup> g <sup>-1</sup> )	Ratio Between the two Methods
1000	1	8,923	11,642	0.76
1000	1	10,579	6,209	1.7
1000	2	5,793	6,807	0.85
1000	2	7,807	4,841	1.6
1000	2	8,129	6,227	1.3
1000	4	2,032	2,983	0.7
1000	4	2,101	4,347	0.48
1000	10	1,337	614	2.17
1000	10	805	1,209	0.66
1000	28	1,065	1,115	0.96
1000	28	917	1,393	0.66
100	1	6,923	7,286	0.95
100	1	6,437	4,681	1.38
100	2	6,418	5,570	1.15
100	4	2,208	2,590	0.85
100	4	2,057	3,073	0.67
100	10	836	605	1.38
100	10	1,022	840	1.22
100	28	2,192	4,471	0.49
10	1	2,882	1,987	1.45
10	1	4,896	3,626	1.35
10	2	3,753	2,556	1.47
10	2	3,122	2,380	1.31
10	4	169	184	0.92
				Av 1.1

amount in the cortex plus that in the medulla divided by the weight of the total half kidney.

The methods were not as accurate as desired for detailed comparison due to the difficulties of rapidly separating the fresh medulla from the cortex 20 and weighing the proportionately very small amount of the medulla. In general, the radiochemical data showed greater variance than the autoradiographic data.

The ratio of mean activity per field by autoradiographic counting to the estimate of activity by

Table 4.26. Arithmetic Means in Cortex Autoradiographic Method Compared with Radiochemical in dis  $\min^{-1} g^{-1}$ 

Part II

Level (μg/kg)			Radiochemical Mean (dis min <sup>-1</sup> g <sup>-1</sup> )	Ratio Between the two Methods
1000	1	12,181	13,124	0.93
1000	1	14,447	6,740	2.14
1000	2	8,031	7,790	1.03
1000	2	10,736	5,482	1.96
1000	2	11,012	7,251	1.52
1000	4	2,546	3,218	0.79
1000	4	2,568	4,538	0.57
1000	10	956	1,509	0.63
1000	10	1,415	512	2.76
1000	28	1,458	1,275	1.14
1000	28	1,245	1,504	0.83
100	1	8,827	7,693	1.15
100	1	8,413	4,935	1.7
100	2	7,832	5,815	1.35
100	4	2,282	2,622	0.87
100	4	2,189	3,059	0.72
100	10	994	645	1.54
100	10	1,252	821	1.52
100	28	2,537	4,731	0.54
10	1	3,902	2,274	1.72
10	1	6,819	3,694	1.85
10	2	5,306	2,953	1.80
10	2	4,404	2,766	1.60
10	4	222	200	1.11
				Av 1.32

<sup>&</sup>lt;sup>20</sup>One experiment was performed to check on the accuracy of separating the cortex and medulla. The two types of tissue were separated and cut into serial sections. The separation appeared clean except for two small bits of cortex which had been included in the medulla. The amount of cortex was so slight that the separation of the cortex and medulla seemed a justifiable procedure.

radiochemical analysis was averaged. A mean ratio of 1.32 with a range of 0.57 to 2.76 was obtained for the cortex, a mean ratio of 0.87 with a range of 0.13 to 2.13 for the medulla, and a mean ratio of 1.1 with a range of 0.48 to 2.17 for the whole half kidney.

## Aggregates

An aggregate may be defined as a set of tracks which emerge in such proximity to each other that

light may not be observed through its central core when studied under a light microscope. With the method used in this study, the number of tracks counted cannot be considered to be highly accurate. The possible biological significance of such high local concentrations led to the counting of aggregates on all slides.

Aggregates estimated to contain 200-600 or 600-1000 tracks are recorded in Table 4.27. They are found mainly in the cortex and in tissues of

Table 4.26. Arithmetic Means in Medulla Autoradiographic Method Compared with Radiochemical in dis min  $^{-1}$  g  $^{-1}$ 

Level (μg/kg)	Postinjection Time (days)	Autoradiographic Mean (dis min <sup>-1</sup> $g^{-1}$ )	Radiochemical Mean (dis min <sup>-1</sup> g <sup>-1</sup> )	Ratio Between the two Methods
1000	1	1321	2015	0.65
1000	1	1552	1124	1.38
1000	2	569	1155	0.49
1000	2	973	2913	0.33
1000	2.	1401	782	1.79
1000	4	799	709	1.13
1000	4	969	1436	0.67
1000	10	1154	877	1.32
1000	28	147	591	0.25
1000	28	151	1203	0.13
100	1	2480	1701	1.46
100	1	1826	524	1.23
100	2	312	3527	0.88
100	4	2038	2452	0.83
100	4	1752	1743	1.00
100	10	467	290	1.61
100	10	483	904	0.53
100	28	1386	1705	0.81
10	1	503	236	2.13
10	1	410	2545	0.16
10	2	129	829	0.16
10	2	132	439	0.3
10	4	44	58	0.76
				Av 0.87

Table 4.27.	Number of Aggregates Observed on Every 40th and 41st Section
	in Rats Injected with 1000 $\mu\mathrm{g/kg}$

Postinjection Time (days)	Aggregates Containing 200 - 600 Tracks	Aggregates Containing 600 - 1000 Tracks	Autoradiographic Exposure Time (days)
1	390	55	28
1	592	164	28
2	159	20	28
2	219	16	28
4	77	0	28
4	155	3	28
10	3	0	35

animals sacrificed at 1, 2, 4, 7, and 10 days postinjection. None were observed in tissues sacrificed at longer postinjection times. An occasional aggregate was found in the medulla.

In tissues of animals injected with 100  $\mu$ g/kg, no aggregates were observed except one on a section from a rat sacrificed 2 days postinjection. None were found in rats injected with 10  $\mu$ g/kg.

## Fraction of Injected Dose to the Kidney

Figure 4.7 shows the kidney cortex of a rat injected with 1000  $\mu g/kg$  and contrasted with that of a rat injected with 10  $\mu g/kg$  and both sacrificed at 1 day. The fractions of injected dose to the kidney, as recorded by counting tracks in autoradiograms, are listed in Table 4.28. In animals sacrificed at 1, 2, and 10 days postinjection, the fractions are consistently higher with increasing dose levels. On the other hand, at 4 and 7 days the fractions found in the kidneys of animals injected with 1000  $\mu g/kg$  are slightly higher than in animals injected with 1000  $\mu g/kg$ . With the kidneys analyzed radiochemically (Table 4.29), the slightly higher fraction in rats injected with 100  $\mu g/kg$  is observable at 1 day and at 4 and 28 days.

## Retention as Shown By 95% Confidence Limits

Figure 4.8 shows the arithmetic means of the autoradiographic data obtained from cortices at the various dose levels and postinjection times. Figure

4.9 shows the arithmetic means of the data obtained from radiochemical analysis of the cortices. Although there is some overlapping of the 95% confidence limits, in general, greater retention at the high levels is evident.

## Location of Uranium Tracks in Histological Units

A study was made of the cells  $^{21}$  from which the uranium tracks seemed to originate. The data from four different animals, two injected with  $1000~\mu g/kg$  of uranium and two with  $100~\mu g/kg$ , are shown in Table 4.30. The postinjection times are 1, 28, 56, and 84 days, respectively. A high percent of the tracks was found in the proximal convoluted tubules, their epithelial cells, nuclei, and cellular debris in the autoradiograms from animals sacrificed at 1, 28, and 56 days and a low percent in the distal tubules. However, in those sacrificed at 84 days the high percent of tracks was found in the distal tubules. There was a trace of uranium found in the glomeruli at both dose levels and at all four injection times.

# Pathological Conditions<sup>22</sup>

Additional work has been done on the pathological conditions observed and recorded in Table

<sup>&</sup>lt;sup>21</sup>A. W. Ham, *Histology*, 2d ed., p 595, Lippincott, Philadelphia, 1953.

<sup>&</sup>lt;sup>22</sup>By Dr. A. C. Upton, Biology Division.

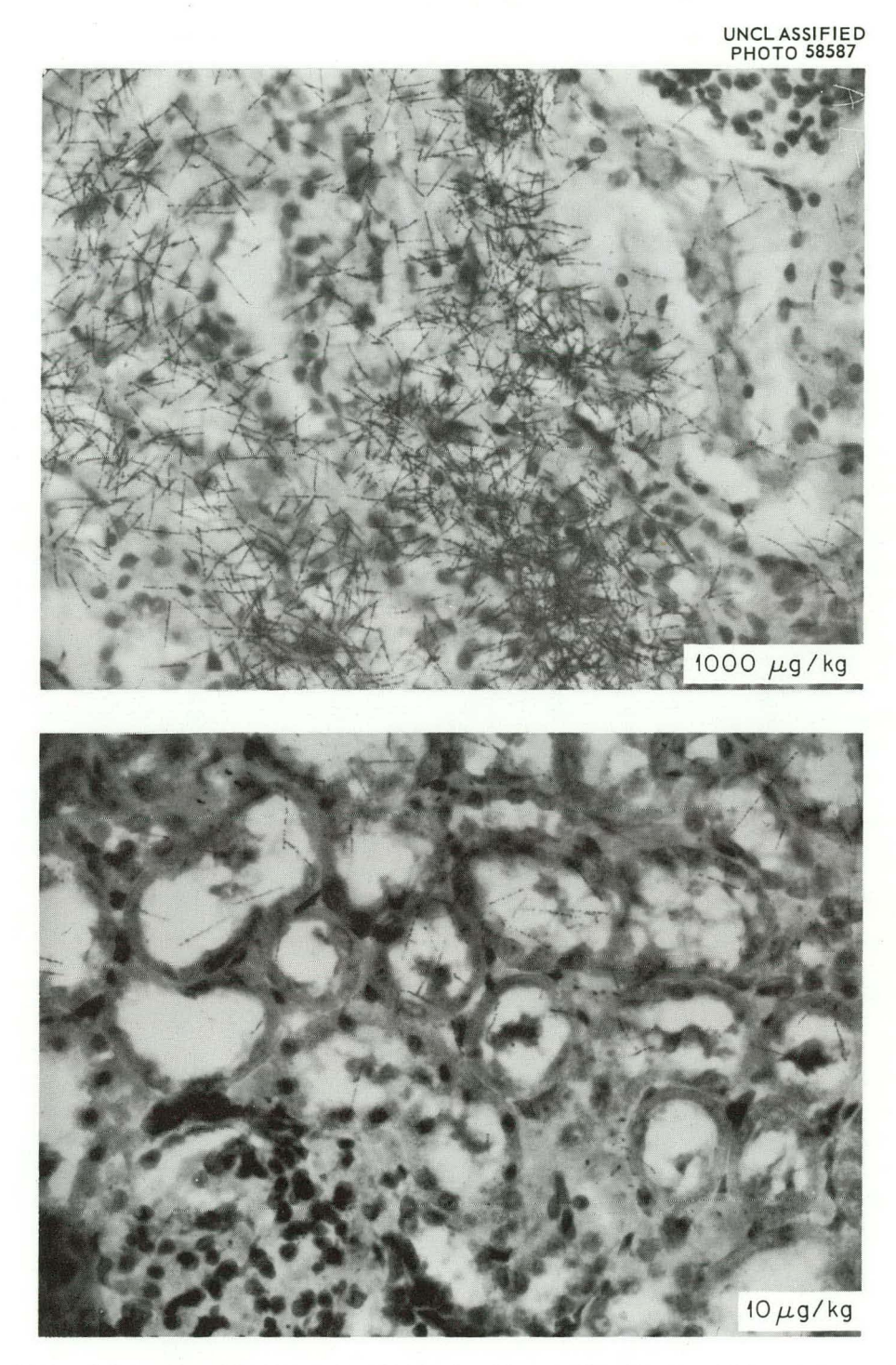


Fig. 4.7. Kidney Cortex from Rat Injected with 1000  $\mu g/kg$  and Sacrificed at 1 Day. Kidney Cortex from Rat Injected with 10  $\mu g/kg$  and Sacrificed at 1 Day.

Table 4.28. Fraction of Injected Dose in the Kidney
Based on Autoradiographic Counting

Dosage Level (μg/kg)	Postinjection Time (days)	Fraction of Injected Dose to Kidney	Standard Deviation	Number of Animals	Number of Half Kidneys
1000	1	0.209	0.015	2	3
100	1	0.146		1	2
10	1	0.087	0.008	2	3
1000	2	0.205	0.001	2	3
100	2	0.107		1	1
10	2	0.073		1	2
1000	4	0.047		1	2
100	4	0.053		1	2
10	4	0.004		1	1
1000	7	0.073		1	1
100	7	0.074		1	1
10	7	0.007		1	1
1000	10	0.034		1	2
100	10	0.023		1	2
1000	28	0.020		2	2
100	28	0.052		1	1
100	56	0.001		1	2
100	84	0.037		1	2

4.31 and Fig. 4.10. These conditions become apparent in tissues 2 days after injection. These are seen in the animals injected with 100 μg/kg and are striking in animals injected with 1000 μg/kg. The lumen and lining cells of scattered proximal, distal, and collecting tubules show mucoid or waxy material. Other tubules of the cortex, primarily in the junction of cortex and medulla, show hyaline droplet degeneration of epithelium. Four and seven days after injection these conditions are increased in the tissues with 1000 µg, indicating injured kidneys, and mildly nephrotic conditions are found in the tissues with 100  $\mu$ g. In the former there is extensive cellular degeneration of the hyaline droplet type in proximal convoluted tubules. Mucoid or waxy casts are found at all levels of the nephrons. At 10 days

the diffuse hyaline droplet degeneration in the proximal convoluted tubules is less severe than at 7 days, and regeneration is beginning. Focal calcification is seen occasionally at both the 1000- and the 100- $\mu$ g levels. Waxy change seems to show at the cortico-medullary junction. At 28 days the tissues from animals injected with 100  $\mu$ g/kg show no abnormalities, whereas those from animals injected with the higher amount of uranium are very abnormal. Atrophy and interstitial lymphoid infiltrations are present. Many tubules show regeneration, and there is associated hydropic change in the epithelium.

Kidneys of rats injected with 10 and 1 μg/kg show no easily recognizable pathological conditions.

Table 4.29. Fraction of Injected Dose in the Kidney Based on Radiochemical Analysis

Dosage Level (μg/kg)	Postinjection Time (days)	Fraction of Injected Dose to Kidney	Standard Deviation	Number of Animals	Number of Half Kidneys	
1000	1	0.152 <sup>a</sup>	0.024	4	8	
100	1	0.159 <sup>a</sup>	0.027	5	10	
10	1	0.11 <sup>a</sup>	0.016	5	10	
1000	2	0.228	0.035	3	6	
100	2	0.193		1	2	
10	2	0.074		1	2	
1000	4	0.115		1	2	
100	4	0.121		1	2	
10	4	0.006		1	1/2	
1000	7	0.134 <sup>a</sup>	0.056	3	6	
100	7	0.095 <sup>a</sup>	0.004	4	8	
10	7	0.04 <sup>a</sup>	0.045	4	8	
1000	10	0.052		1	2	
100	10	0.031		1	2	
1000	28	0.049		1	2	
100	28	0.147		1	1	
100	56	0.002		1	2	
100	84	0.035		1	2	

<sup>&</sup>quot;Contains unpublished data of S. R. Bernard.

#### Conclusions and Discussion

Although the number of animals used in these experiments is too small for firm general conclusions, several trends are suggested. These expand and corroborate earlier studies.

The concentration ratio of uranium in the rat kidney is usually 1.3 but tends to approximate 1 at the 10-day postinjection time at the 1000  $\mu g/kg$  level. At the 100  $\mu g/kg$  level and at 4 days postinjection, the concentration ratio also approximates 1, and this may indicate a time when active removal of uranium from the kidney takes place. The relatively greater concentration of uranium in the medulla of the kidney at these periods may be

indicative of the time at which the process of clearance of uranium occurs.

More data are needed to establish any possible relation between the injury to the kidney at the high dose which might have delayed clearance or to establish that at the lower level, where there is less injury, clearance takes place earlier.

The comparison between the autoradiographic and the radiochemical methods of measuring activity gave a gross check in spite of the experimental difficulties and large variance of some of the estimates.

The apparent greater retention at the higher levels is indicated by the data on the fractions of total injected dose found in the kidney at the 1

UNCLASSIFIED ORNL-LR-DWG 70721A

ARITHMETIC MEANS dis min-1 g-1

OBSERVED AT DIFFERENT LEVELS AND POSTINJECTION TIMES WITH 95% CONFIDENCE LIMITS AUTORADIOGRAPHIC DATA

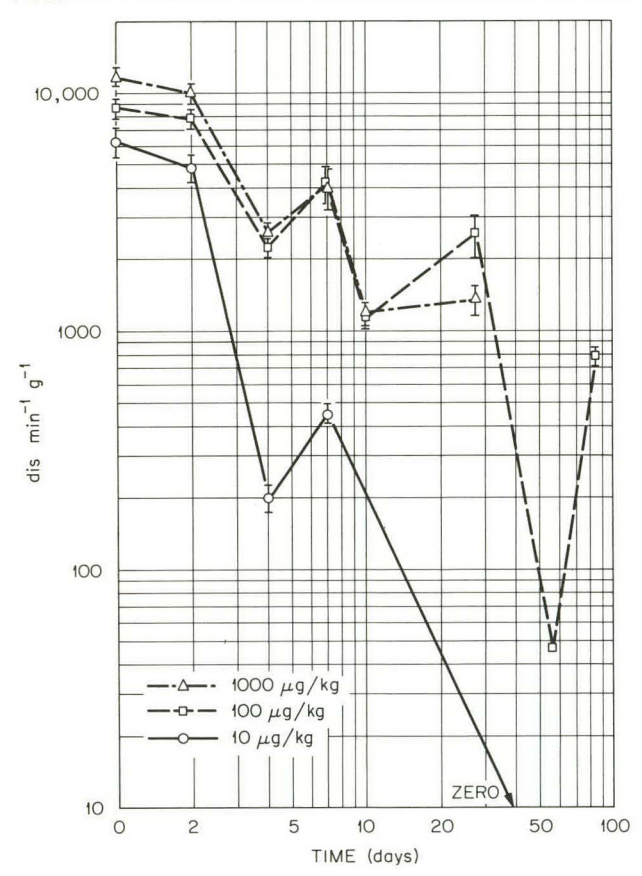


Fig. 4.8. Activity in the Cortex — Arithmetic Means in Autoradiographic Data.

various levels and postinjection times. Although these fractions do not differ greatly, the non-linearity of this retention with dose also appears at the 4-, 7-, and 28-day fractions found by autoradiographic counting and at the 1-, 4-, and 28-day fractions found by radiochemical analysis. However, they do corroborate the findings of Muir. <sup>23</sup>

UNCLASSIFIED ORNL-LR-DWG 70722A

ARITHMETIC MEANS dis min<sup>-1</sup> g<sup>-1</sup>
OBSERVED AT DIFFERENT LEVELS AND POSTINJECTION TIMES WITH 95% CONFIDENCE LIMITS

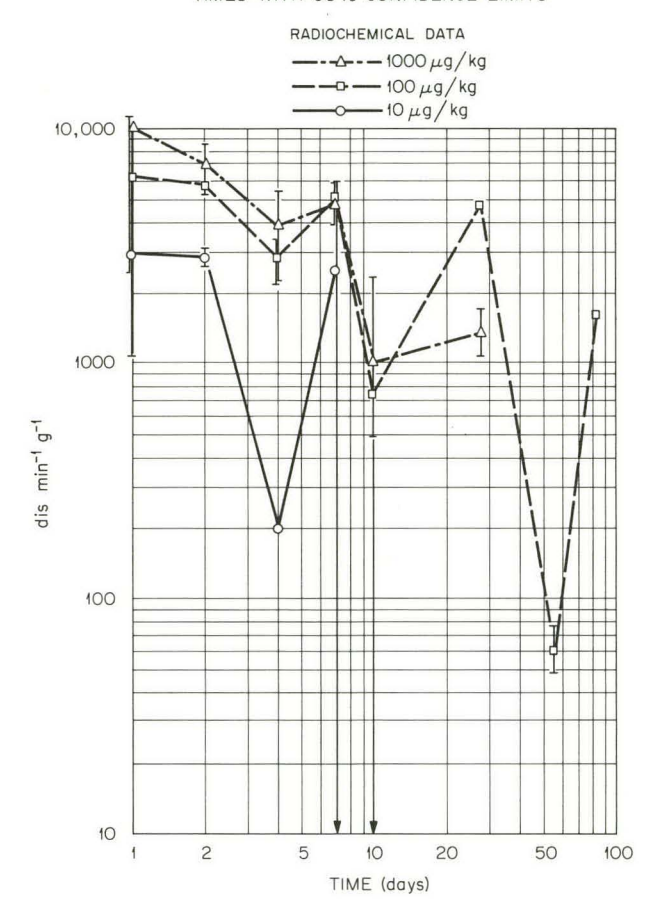


Fig. 4.9. Activity in the Cortex — Arithmetic Means in Radiochemical Data.

The retention pattern is shown in Figs. 4.8 and 4.9. There is some overlapping of 95% confidence limits, especially in the radiochemical material.

Whether there is a relationship between the pathological conditions caused by the mass of uranium and the retention with its nonlinearity is a matter for which more data are needed. Whether the destruction of cells will prevent the nephrons from functioning, causing the uranium to be retained in the kidney with high doses, needs to be

<sup>&</sup>lt;sup>23</sup>J. R. Muir, Health Phys. Div. Ann. Progr. Rept. July 31, 1960, ORNL-2994, p 272.

Table 4.30. Histologic Units in Cortex in Which Tracks Were Observed

Dose (μg/kg)	Postinjection Time of Sacrifice (days)	Total No. of Tracks Counted	No. of Tracks in Identified Cells	% of Tracks in Identified Cells	% of Tracks in Proximal Convoluted Tubules	% of Tracks in Distal Tubules	% of Tracks in Glomeruli	% of Tracks in Other Units
1000	1	43,969	40,458	92	96	1	1	2
1000	1	43,231	43,055	99.6	97	0.6	0.5	1.9
1000	28	2,403	1,279	53	72	7	3	18
1000	28	2,267	884	39	47	4.8	1.8	53.6
100	56	82	79	96	80	10	3.6	6.4
100	56	107	107	100	72	10	2.8	15.2
100	84	2,774	2,549	92	30	61	0.5	8.5
100	84	3,288	2,199	67	9.6	77	0.2	13.2

Table 4.31. Pathological Anatomy of Rat Kidney After Injection of Uranium-238 + Uranium-233

								Postinje	ction Time	and Animals Injected										
Level	Number of Animals	1 Day	Number of Animals	2 Days	Number of Animals	4 Days	Number of Animals	7 Days	Number of Animals	10 Days	Number of Animals	14 Days	Number of Animals	15 Days	Number of Animals	28 Days	Number of Animals	56 Days	Number of Animals	84 Days
990 µg U <sup>238</sup> + 10 µg U <sup>233</sup> per kg body weight	2	Occasional tubules show waxy casts; small foci of calcifi- cation are also noted sporadically	3	Scattered tubules with mucoid or waxy material in lumen as well as in lining cells including proximal, distal and collecting tubules; other tubules show hyaline droplet degeneration of epithelium; these are in the cortex, not in medulla, but primarily in junction of cortex and medulla	1	Shows extensive cellular degeneration of hyaline droplet type in proximal convoluted tubules; many tubules at all levels of nephrons show waxy casts. This is a sick kidney	1	Extensive degeneration; epithethial cells sloughed off; mucoid or waxy ma- terial in lumen; hyaline droplet degeneration	1	Diffuse hyaline drop- let degeneration in proximal convoluted tubules; less severe than at 7 days with beginning regeneration; occasional focal cal- cification	0		0		2	Atrophy and interstitial lymphoid infiltrations; many tubules show dilatation and contain precipitate in lumen; proximal convoluted tubules show regeneration but there is associated hydropic change in the epithelium	0		0	
90 μg U <sup>238</sup> + 10 μg U <sup>233</sup> per kg	2	Occasional waxy casts at all levels of nephron; focal calcification	1	Hyaline droplet change diffuse throughout proximal convoluted tubules	1	Hyaline droplet change diffuse throughout proximal convoluted tubules; mild; also waxy casts in many tubules	1	Slight degeneration; some waxy casts; similar but not so severe as high level	1	Focal calcification. Seems to show waxy change at cortico- medullary junction	0		0		1	Negative	1	Focal interstitial lymphoid infil- trations; other- wise negative	1	Negative
0 μg U <sup>238</sup> + 10 μg U <sup>233</sup> per kg	2	Negative	1	Negative	1	Negative	1	Negative	0		1	Focal calcifi- cation; other- wise negative	1	Negative	0		1	Negative		
$0~\mu g~{\rm U}^{~238} + 1~\mu g~{\rm U}^{~233}$	2	Negative; a few des- quamated epithelial cells in lumen of proximal and distal convoluted tubules; these were also found in controls	1	Negative	0		1	Negative	1	Negative	0		0		0		0		0	

investigated. The possibility that the greater amounts of uranium cause a malfunctioning at first which prevents clearance cannot be overlooked.

The observed location of the uranium tracks is consistent with the pathological conditions, and

the pathological conditions corroborate earlier findings on chemical injury. 24

<sup>&</sup>lt;sup>24</sup>T. B. Barnett and R. G. Metcalf, *Pharmacology and Toxicology of Uranium Compounds* (ed by Carl Voegtlin and H. C. Hodge), p 214, McGraw-Hill, New York, 1949.

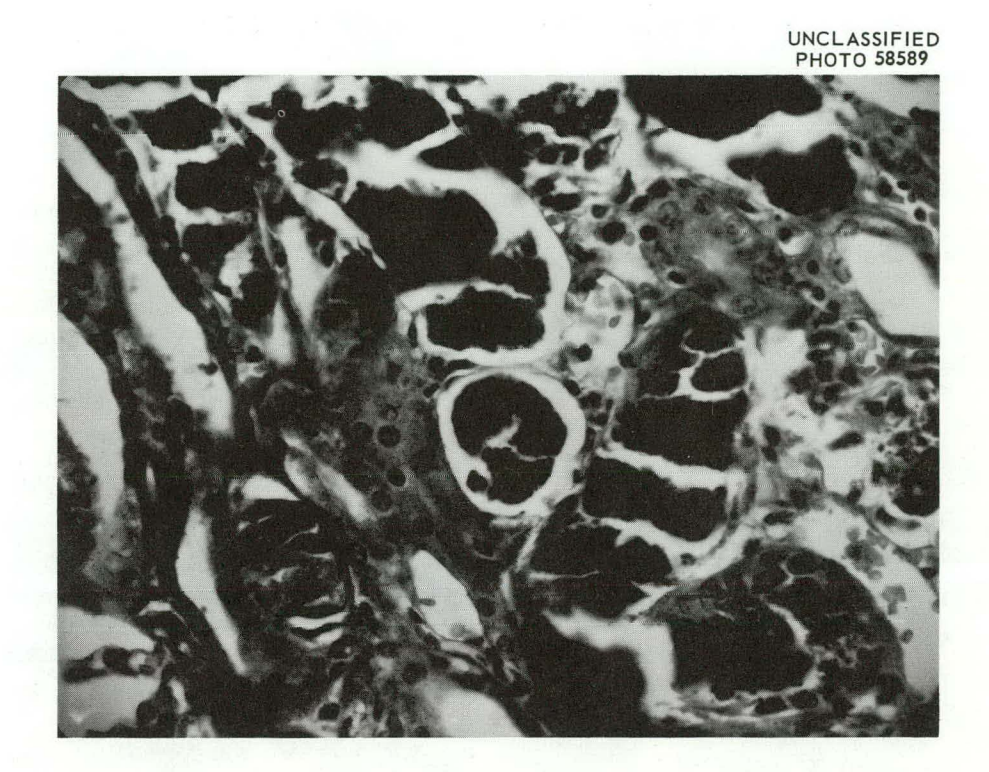


Fig. 4.10. Hyaline Droplet Degeneration of Tubules with Desquamation of Cells.

# 5. Health Physics Technology

B. R. Fish

#### **AEROSOL PROJECT**

G. W. Royster, Jr.

## Studies of Surface Contamination

Comparisons of methods of measurement of surface contamination have been reported. 1-3 Three methods of measurement have been investigated: (1) the smear or wipe technique; (2) the adhesive paper technique; and (3) a procedure which employs air impingement to remove loose contamination from a surface. The air impingement samples are referred to as "smair" samples. Table 5.1 shows the results of testing a number of common building materials that were uniformly contaminated with a solid particulate. There are no consistent correlations between these methods of measurement for the different test surfaces. The rougher surfaces, in general, showed a lower percentage of contamination removed by the smear technique, and a more detailed study was begun to investigate the influence of surface roughness on contamination measurements by these three methods.

The dust settling chamber used in this study is shown in Fig. 5.1. The sides of this chamber are removable and may be raised to permit insertion of the test surface. Thorium-dioxide dust is introduced into the chamber by means of a Wright dust feed, and a uniform suspension of the dust is obtained by operating a fan in the chamber. After the dust feed and fan are turned off, the chamber is left undisturbed for 5 min so that any large aggregrates may settle to the bottom. A test surface is inserted into the chamber, and the ThO2 particles are allowed to settle over-Total activity on the test surface is measured by using an alpha scintillation probe and by measuring deposited activity on thin metal disks which are spaced over the test surface. An indication of the uniformity of deposition for 18 different surfaces is shown in Fig. 5.2. The average dis min<sup>-1</sup> cm<sup>-2</sup> for 12 measurements on each surface is shown along with the standard deviation which is expressed as a percentage of the mean. Particle size of the deposited dust was approximately 1  $\mu$ , and the concentration was in the order of 106 particles per cm<sup>2</sup>.

The effect of surface roughness was examined for a series of Plexiglas sheets which were treated to produce a selection of surface finishes while keeping the surface composition constant (Fig. 5.3). A root-mean-square deviation of 100 μin. represents about the same finish as that of masonite; 1000 µin. is approximately the roughness of coarse sandpaper. The data indicate that the potential hazard associated with the redispersion of contamination by air blowing over the surface is essentially the same for a wide range of surface roughness. The relative hazard as indicated by the smear and adhesive paper measurements is a factor of 6 lower for the roughest surface than that for smooth finishes. At the other extreme, smooth surfaces that are covered with an oily film or grease (Table 5.1) show the same fractions removed by the smear

<sup>&</sup>lt;sup>1</sup>G. W. Royster, Jr., and B. R. Fish, ORNL CF-61-3-39 (1960).

<sup>&</sup>lt;sup>2</sup>G. W. Royster, Jr., and B. R. Fish, Studies of Surface Contamination. I. Intercomparison of Methods for Measuring "Removable" Contamination, presented at the Annual Health Physics Society Meeting, June 12-16, 1961, Las Vegas, Nev.

<sup>&</sup>lt;sup>3</sup>G. W. Royster, Jr., and B. R. Fish, Studies of Surface Contamination. II. Surface Characteristics Affecting the Measurement and Redispersion of Particulates, presented at the Annual Health Physics Society Meeting, June 11-16, 1962, Chicago, Ill.

and adhesive paper techniques as do clean surfaces of the same material, whereas it is very difficult to redisperse dust adhering to greasy surfaces. In this case the potential hazard re-

sulting from air currents blowing over an oily surface is small, whereas the apparent hazard measured by smears and adhesive paper is the same as that for a clean dry surface.

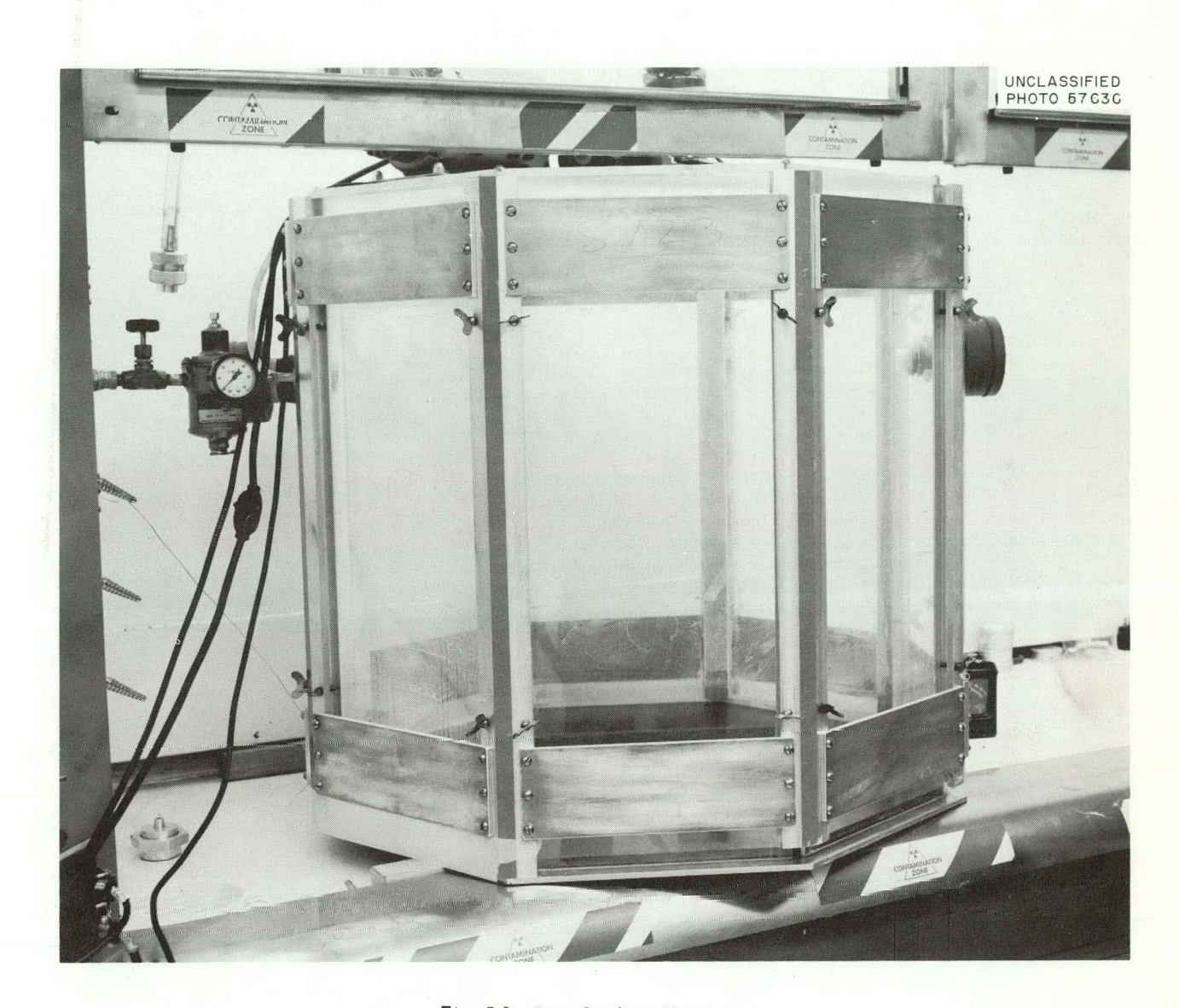


Fig. 5.1. Dust Settling Chamber.

Table 5.1. Percentage of Total Radioactivity on Surfaces Measured by Different Sampling Techniques

Composition of Surface	Radioacti	vity Removed (%)	
Composition of Surface	Adhesive Paper	Smear	Smain
Polyethylene	70.3	56.6	10.9
Glass	75.0	64.6	27.2
Plexiglas	78.0	71.3	15.8
Fiberboard treated with Polymer Ma	53.8	44.3	10.2
Fiberboard treated with Soil Retardant <sup>b</sup>	75.9	34.4	20.0
Fiberboard scrubbed <sup>c</sup>	56.9	23.5	9.0
Fiberboard untreated	73.4	23.5	6.6
Formica	73.4	70.6	26.5
Aluminum painted <sup>d</sup>	70.0	50.3	24.8
Aluminum painted, treated with Soil Retardant $^b$	86.0	67.1	33.0
Asphalt floor tile untreated	58.6	48.5	14.6
Asphalt floor tile waxed <sup>e</sup>	74.5	74.5	30.3
Concrete unsealed	55.5	39.5	22.0
Concrete sealed (Onex-Seal and wax)	62.2	59.5	24.0
Concrete sealed (Gellman and Du-Ev wax) <sup>g</sup>	54.8	47.7	27.2
Stainless steel	67.7	50.5	10.5
Concrete, greased <sup>b</sup>	43.5	37.5	1.32

<sup>&</sup>lt;sup>a</sup>Polymer M is a floor treatment manufactured by the Johnson Wax Company.

<sup>&</sup>lt;sup>b</sup>Greased lightly with stopcock grease.

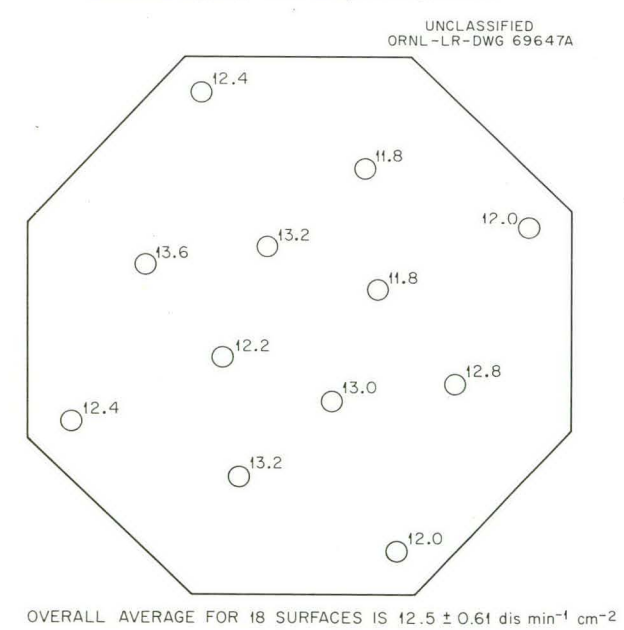


Fig. 5.2. Uniformity of Deposition for 18 Different Surfaces.

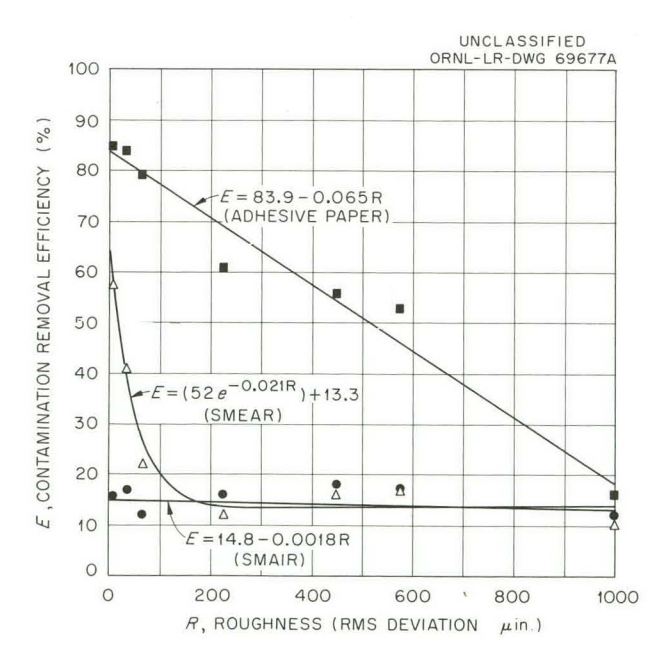


Fig. 5.3. Comparison Surface Contamination Removability as a Function of Surface Roughness (Plexiglas).

<sup>&</sup>lt;sup>b</sup>Soil Retardant Finish Concentrate (Eng. 8474, VM-5642), manufactured by E. I. du Pont de Nemours and Company.

<sup>&</sup>lt;sup>c</sup>Scrubbed for 10 min with Babbit's cleanser, a soft cloth, and water.

dAmercote No. 74.

<sup>&</sup>lt;sup>e</sup>Du-Ev Wax (Do everything Wax), Du-Ev Products Company, Inc.

fOnex-Seal, Hilliard Chemical Company, used with Polymer M.

<sup>&</sup>lt;sup>8</sup>Gellman Sealer, Gellman Paint and Varnish Company, used with Du-Ev wax.

## Production of Submicron Aerosols

F. G. Karioris<sup>4</sup> A. J. Moll<sup>4</sup>

The exploding wire aerosol generator  $^{5,6}$  has been used to produce aerosols from 18 different metals by wire explosions in air and in argon at barometric pressure. In this apparatus,  $^{7}$  the current surge from a 20- $\mu f$  capacitor bank charged to voltages up to 20 kv can be made to pass through small wires in an explosion chamber with controlled atmosphere. The sudden release of of energy explodes the wire and fills the chamber with smoke which can be sampled with a thermal precipitator, collected on a membrane filter, or

withdrawn and used for other studies. Table 5.2 shows that a large variety of aerosols can be produced and dispersed efficiently. These aerosols differ in chemical composition, crystal structure,

Table 5.2. Aerosols from Exploding Wires All explosions at 10 kv with 20  $\mu f$ ; aerosols collected on membrane filters

		Exploded in Air			Exploded in Argon		
Metal	Color of Deposit	Relative Yield <sup>a</sup> (%)	Composition by X-Ray Diffraction	Color of Deposit	Recovery from Aerosol <sup>a</sup> (%)		
Ag	Black	76 -	Ag, AgS <sup>b</sup>	Black	77		
A1	Gray	136	$Al_2O_3^c$	Dark gray	44		
Au	Chocolate	59	Au	Velvet black	72		
Cd	Yellow-brown	92		Dark gray.	80		
Cu	Brown	98	Cu, Cu <sub>2</sub> O, CuO	Velvet black	75		
Fe	Brown	111	Fe <sub>3</sub> O <sub>4</sub>	Velvet black	37		
In	Gray	91		Dark gray	68		
Mg	Gray	100	MgO	Gray	68		
Mo	Teal blue	98	MoO <sub>2</sub> , MoO <sub>3</sub>	Black	14		
Ni	Gray	73	Ni, NiO	Velvet black	26		
Pb	Cream	82	2PbCO3 • Pb(OH)2	Dark gray	73		
Pt	Black	40	Pt	Velvet black	35		
Sn	Pale tan	106	SnO <sub>2</sub>	Dark gray	73		
Ta	Gray	43	Ta, Ta <sub>2</sub> O <sub>5</sub>	Velvet black	26		
Th	Violet	103	ThO <sub>2</sub>	Black	86		
U	Gray	100	U <sub>3</sub> O <sub>8</sub> , UO <sub>2</sub>	Black	33		
W	Purple	55	w, wo <sub>3</sub> c	Dark brown	8		
Zr	Cream	110		Velvet black	34		

<sup>&</sup>lt;sup>a</sup>Weight of aerosol collected/weight of wire exploded times 100.

<sup>&</sup>lt;sup>4</sup>Temporary summer employees of Marquette University, Milwaukee, Wisconsin, and University of Washington, Seattle, Washington, respectively.

<sup>&</sup>lt;sup>5</sup>F. G. Karioris et al., Health Phys. Div. Ann. Progr. Rept. July 31, 1960, ORNL-2994, pp 266-69.

<sup>&</sup>lt;sup>6</sup>F. G. Karioris and J. W. Youngblood, Health Phys. Div. Ann. Progr. Rept. July 31, 1961, ORNL-3189, pp 227-29.

<sup>&</sup>lt;sup>7</sup>F. G. Karioris and B. R. Fish, *J. Colloid Sci.* 17, 155-61 (1962).

<sup>&</sup>lt;sup>b</sup>Probably formed after collection by exposure to laboratory air.

<sup>&</sup>lt;sup>c</sup>Several crystal forms.

density, electrical and thermal conductivity, dielectric permittivity, magnetic properties, melting point, boiling point, and other physical properties which may be related to the mechanisms of formation or other aerosol characteristics. Samples have been collected for the electron microscope with the oscillating thermal precipitator and membrane filter to explore any relationship between bulk properties of materials and the basic particle size and structure of aerosol particles.

Qualitative analyses by x-ray diffraction have been completed for aerosols produced previously, and yield studies have been done for uranium and copper as a function of mass of wire exploded and voltage on the capacitor bank used for explosion. It is found that the amount of aerosol produced varies with the voltage used for explosion and the mass of wire exploded. Recovery of metal in the aerosol approaches 100% for explosion of small wires with high voltages. The composition of aerosols from uranium and copper wires exploded in air also varies with the voltage used for explosion. For uranium wires the percentage of UO, decreases rapidly with increasing voltage, and the aerosol consists almost entirely, of U2O8 for explosions8 above 6 kv. The aerosol from copper wires exploded in air consists of the mixture Cu-Cu2O-CuO whose composition varies with the voltage used for the explosion. 9 A small percentage of copper is present, which decreases rapidly with increasing voltage. The CuO/Cu2O ratio tends to increase with increasing voltage but depends also on the inductance in the circuit. At 5 kv this aerosol is predominantly CuO.

There is evidence that the pressure of an indifferent gas influences the particle size of the condensate from metal vapors 10 as well as the electrical characteristics of the exploding wire phenomenon. 11 Copper wires have been exploded in air at pressures below barometric to determine

The primary particles formed by the generator are spheres having diameters ranging from 0.01 to 0.1  $\mu$ . These spheres agglomerate rather rapidly to form the chains and complex agglomerates which are typical of metallic smokes. <sup>7,8</sup> Polyhedral particles frequently present in some arc smokes <sup>12</sup> have not been observed in the exploded wire smoke.

Particulate material of the size range given above are of interest in health physics because:

(1) Such particles frequently are formed in process operations. 13 (2) Radioactive materials absorb readily on naturally occurring dust or smoke particles. 13,14 (3) Such particles are retained in the alveoli with relatively high efficiency. 13,15 (4) Such fine particles are difficult to filter. 13 Primary particles from the explosion of aluminum wire in argon with 5 kv on the capacitor bank are shown in Fig. 5.4. These were collected from the explosion chamber on a membrane filter and redispersed for the electron microscope. Primary particles of metallic aerosols are chosen for study because the bulk properties are well known and the composition is not complicated

whether the primary particle size varies significantly with the pressure in the explosion chamber. It is found that the aerosol yield tends to decrease with decreasing pressure. At low air pressures, wires which can sustain the electrical discharge at pressures of about  $100~\mu$  will explode when the pressure is reduced below  $0.5~\mu$ . Such explosions are studied by placing glass slides in the vicinity of the wire inside a vacuum chamber. With high vacuum it is found that only a small fraction of the exploded mass condenses on the slide from the vapor state and that the thin film formed is subsequently struck by large, very hot droplets which splatter and form small spheres which are visible under low magnification (0 to 40X).

<sup>&</sup>lt;sup>8</sup>F. G. Karioris, B. R. Fish, and G. W. Royster, "Aerosols from Exploding Wires," to be published in the Proceedings of the Second Conference on the Exploding Wire Phenomenon, Boston, Nov. 13-15, 1961.

<sup>&</sup>lt;sup>9</sup>A. G. Barkow, F. G. Karioris, and J. J. Stoffels, "X-Ray Diffraction Analysis of Aerosols from Exploding Wires," to be presented at the Eleventh Annual Conference on Applications of X-ray Analysis, Denver, Aug. 8-10, 1962.

 $<sup>^{10}\</sup>mathrm{W}.$  E. Gibbs, Clouds and Smokes, p 33, J. S. Churchill, London, 1924.

<sup>&</sup>lt;sup>11</sup>T. Korneff, J. L. Bohn, and F. H. Nadig, Exploding Wires (ed. by W. G. Chace and H. K. Moore), pp 104— 107, Plenum Press, New York, 1959.

<sup>&</sup>lt;sup>12</sup>J. H. Harvey, H. I. Mathews, and H. Wilman, Discussions Faraday Soc. 30, 113-23 (1960).

<sup>&</sup>lt;sup>13</sup>J. J. Fitzgerald and C. G. Detwiler, A.I.H.A. Quart. 18(1), 47-58 (1957).

<sup>&</sup>lt;sup>14</sup>A. C. Chamberlain, Aspects of the Deposition of Radioactive and Other Gases and Particles in Aerodynamic Capture of Particles (ed. by E. G. Richardson), Pergamon Press, London, 1960.

<sup>&</sup>lt;sup>15</sup>P. E. Morrow, Health Phys. 2, 366-78 (1960).

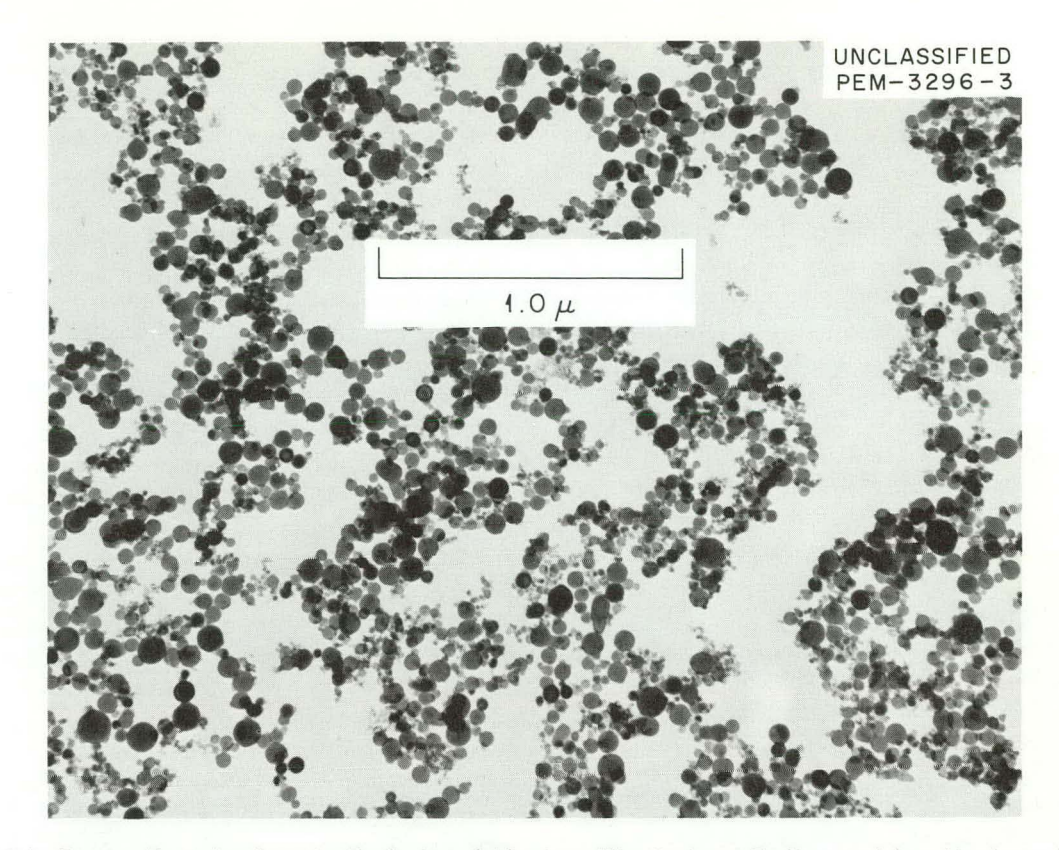


Fig. 5.4. Primary Particles from the Explosion of Aluminum Wire in Argon Redispersed from Membrane Filter.

by the products of simple combustion. The distribution of aluminum particles produced by a wire explosion in argon with 5 kv on the capacitor bank is shown in Fig. 5.5. The mass median particle diameter is about 0.06  $\mu$ , and approximately one-half the mass is accounted for by particles 0.05 to 0.08  $\mu$  in diameter.

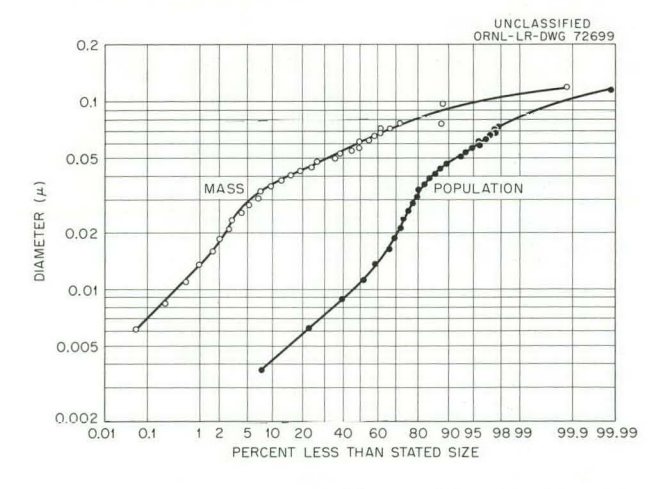


Fig. 5.5. Distribution of Primary Particles from the Explosion of Aluminum Wire in Argon.

#### APPLIED INTERNAL DOSIMETRY

## ORNL In Vivo Gamma-Ray Spectrometry Facility

P. E. Brown	D. L. Mason 16
L. B. Farabee	J. L. Thompson
S. A. Helf <sup>17</sup>	W. H. Wilkie, Jr.
S. W	$00d^{18}$

Introduction. — During the second year of operation of the IVGS Facility, several improvements have been made in the counting equipment. Two new 8 × 4 in. NaI(Tl) crystals have been put into use for IV counting and a Nuclear Data 512-channel analyzer-computer has been installed. Use of the larger crystals has made it possible to reduce the necessary counting time, and the new analyzer enables the facility to record data and to make rough estimates of internal contamination more

<sup>&</sup>lt;sup>16</sup>ORINS undergraduate trainee, Austin Peay State College, Clarksville, Tenn.

<sup>&</sup>lt;sup>17</sup>Picatinny Arsenal, Dover, N. J.

<sup>&</sup>lt;sup>18</sup>ORINS research participant, Austin Peay State College, Clarksville, Tenn.

rapidly by automatic stripping operations. A computer program is being prepared for rapid and accurate processing of large volumes of spectrometer data by locally available high-speed computers. Formerly, all human gamma-ray spectra were obtained with a 200-channel analyzer, and the punch paper tapes from those examinations are presently being converted to new tapes in a format compatible with the paper tape input system of the new 512-channel analyzer.

**Operation.** – Pending completion and testing of the computer program, now under development, the scheduling of whole-body counter examinations has been directed primarily toward investigating known or suspected contamination exposures. A total of 142 whole-body counts have been made on 102 people. Of these, 12 have shown measurable amounts of activity other than the normal  $K^{40}$  and  $Cs^{137}$  (Table 5.3).

Table 5.3. Measurable Activity Found in Suspected Exposures

Isotope	Number of People	Highest Activity (μc)
Cs 137	3	0.36
Zr <sup>95</sup> -Nb <sup>95</sup>	1	0.011
Sb 125	5	0.162
Ru 106-Rh 106	3	0.131
Co <sup>60</sup>	4	0.013
Ce <sup>144</sup> (+ Pr <sup>144</sup> )	1	0.03
Co 58	3	0.02
Fe <sup>59</sup>	3	0.04
Cr 51	.3	0.32
I 131	4	0.20
Zn <sup>65</sup>	1	0.04
Hg <sup>203</sup>	1	$0.5 \times 10^{-6}$

Three employees were exposed to radioactive corrosion products while working on an in-pile loop. Figure 5.6 shows the gamma spectrum of one employee approximately one day after exposure. This was the first of a series of chest counts made on two of the exposed persons. Extrapolation to zero time of the values obtained

in this series of counts produced estimates of lung burdens at the time of the exposure (Table 5.4).

Physical Equipment. - One of the major problems in applied internal dosimetry is the detection and measurement of low-energy photons. At present the only available method that may be used for routine personnel monitoring for low-energy gamma emitters is the analysis of This approach is limited by the difficulty in obtaining unequivocal estimates of internal deposits. Two approaches to in vivo counting of low-energy photons, attempted by various groups, have included the use of thinwindow proportional counters and the application of thin NaI crystal spectrometers. Three thin NaI(Tl) crystals, each 1/16 in. thick and 5 in. in diameter, have been obtained and are being installed in the iron room. These crystals have a 0.005-in. beryllium window and are expected to be about 100% efficient for 90-kev gammas. This installation is about 75% completed.

Colibrations. — Basic calibrations have been completed for most of the gamma-emitting isotopes encountered at ORNL. Rapid calibration for other isotopes and source geometries can be done, as necessary, with the available phantoms and mannikins. Table 5.5 summarizes calibration data for some of the isotopes encountered at ORNL and gives an indication of the relative sensitivity by use of 4 × 4 and 8 × 4 in. NaI(Tl) crystals.

Additional calibrations are being performed with an arc geometry. The arc position is expected to result in less variation in counting efficiency than is experienced with the "standard" chair geometry for persons of differing size, shape, and location of internal deposit. Present studies are directed toward the selection of the best geometry for utilizing the available spectrometry equipment in an expanded routine program.

Some work has been done toward detecting and measuring  $Cf^{252}$  and  $Cf^{254}$  in the lung, utilizing the thick crystals to detect the spontaneous fission gamma spectrum produced by these two isotopes. With these crystals approximately 75% of the maximum permissible lung burden for insoluble  $Cf^{252}$  particles can be detected.

1<sup>131</sup> in Milk and In Cattle Thyroids. – During the summer of 1960, a study was begun in which cattle thyroids were collected and analyzed for I<sup>131</sup>. The purpose of this study, initially, was

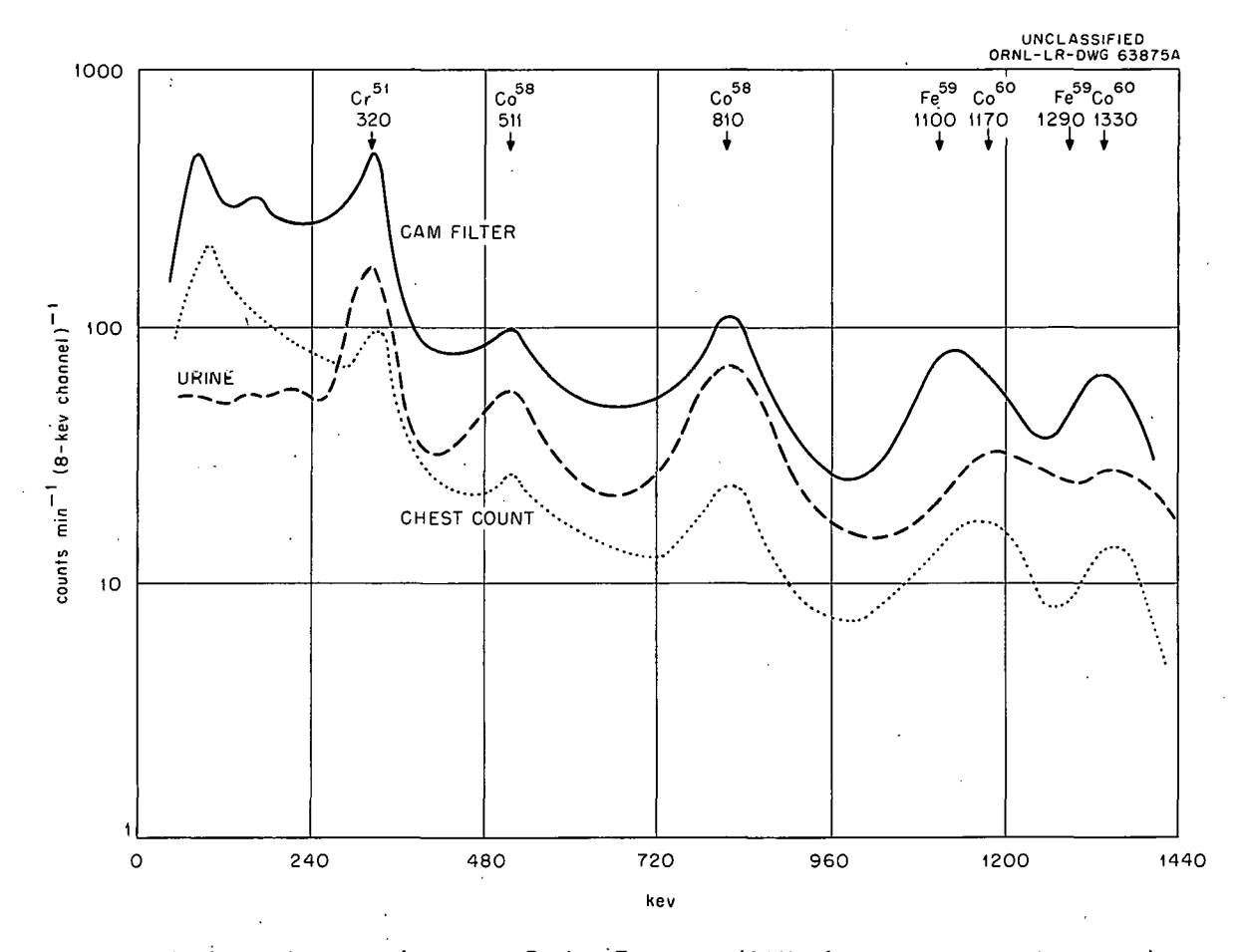


Fig. 5.6. Gamma Spectrum of Corrosion Product Exposure. (CAM refers to continuous air monitor.)

Tuble 5.4. Estimates of Lung Burden Following an Accidental Exposure ( $\mu$ c)

Isotope	Case A-5644	Case A-5414		
Co <sup>60</sup>	0.008	0.008		
Fe <sup>59</sup>	0.042	0.041		
Co <sup>58</sup>	0.021	0.021		
Cr 51	0.28	0.32		

to improve the sensitivity of available environmental monitoring procedures. In this connection a correlation was sought between ORNL stack releases, meteorological data, and I<sup>131</sup> content in the cattle thyroids.

As a result of the Soviet weapons tests in September 1961, a sizable increase in the amount of  $I^{131}$  was observed in cattle thyroids. Milk

samples collected in the same general area from which some of the thyroids were obtained provide a rough indication of the relative concentrations of I<sup>131</sup> in these materials. Figure 5.7 illustrates the changes in I<sup>131</sup> levels and the correlations observed between average pc (picocuries) of I<sup>131</sup> per gram of thyroid and the observed pc of I<sup>131</sup> per liter of milk.

# Analysis of Milk for I 131 by Anion Exchange Resin: The Effect of Protein-Bound I 131

## L. B. Farabee

The high fission yield and the volatility of I<sup>131</sup> make it one of the most probable and in many cases the controlling radiocontaminant in gaseous wastes from nuclear installations. Radioactive iodine is strongly adsorbed on pasture grasses; thus, cattle grazing on such grasses may secrete

Table 5.5. Summary of Calibration Data

Isotope	Photopeak Used	Band Width	Background in Band (counts/min)		Net counts/min per MPBBa	
isotope	(Mev)	(Mev)	$4 \times 4$ in.	8 × 4 in.	$4 \times 4$ in.	$8 \times 4$ in.
K <sup>40</sup>	1.46	0.184	9	50		
Cs <sup>13 7</sup>	0.662	0.152	15	95	$1.02 \times 10^{5}$	$2.7 \times 10^5$
Na <sup>24</sup>	2.76	0.300	9	21	$0.963 \times 10^{4}$	$3.4 \times 10^4$
$Zn^{65}$	1.11	0.136	10	41	$0.642 \times 10^{5}$	$2.07 \times 10^{5}$
Zr <sup>95</sup> -Nb <sup>95</sup>	0.75	0.136	16	70		$1.39 \times 10^{5}$
I 13 I	0.364	0.096	20	136	1280	
Pa <sup>233</sup>	0.310	0.080	20	135	5.16 × 10 <sup>5</sup>	
Hg <sup>203</sup>	0.28	0.056	61	110	$1.87\times10^{4}$	$5.53 \times 10^4$
Ce <sup>144</sup> -Pr <sup>144</sup>	0.134	0.096	59	397		$2.47 \times 10^{4}$
Sb <sup>125</sup>	0.427	0.080	50	120		$1.135 \times 10^{5}$
Cf <sup>252</sup> (+ 4% Cf <sup>254</sup> )	Fission Gamma Spectrum	2.7		80		12 <sup>b</sup>

<sup>&</sup>lt;sup>a</sup>Maximum Permissible Body Burden in critical organ.

quantities of I 131 in milk such as to be hazardous to human beings, particularly infants. In experiments to simulate conditions of prolonged exposure to continuous feeding of dairy cows with grass contaminated with I 131, it has been found 19 that 5 to 10% of the daily dose appeared in milk each day. The measurement of I131 in milk from cows grazing in the vicinity of a nuclear facility gives a reliable reflection of the contamination of the cow's diet consumed within the past few Such a measurement can be used to determine the fitness of milk for human consumption. The Federal Radiation Council<sup>20</sup> has suggested a graded series of contamination levels as criteria for guidance on intake of I131 in exposed population groups; thus, in order to comply with Range I (0 to 10 pc intake per day), it is necessary that the I<sup>131</sup> analysis procedure be sufficiently sensitive to detect less than 10 pc/liter of milk.

A procedure has been developed for the analysis of a large volume of milk for I<sup>131</sup>, which is sensitive to less than 10 pc/liter. It is based on the removal of I 131 from liquid milk onto a strong-base anion resin column. Measurement of the I 131 which is collected on the resin is made by summing the counts within the 0.364-Mev gamma photopeak using a 4 × 2 in. NaI(Tl) crystal with a gamma spectrometer. Boni<sup>21</sup> has described a method for the determination of I<sup>131</sup> in milk by the use of an anion exchange resin. However, no indication has been given of the inadequacy of this technique whereby losses of the I<sup>131</sup> may be incurred by failure of the resin to remove that portion of the I<sup>131</sup> in milk which is chemically bound to the protein.

The efficiency of the anion exchange procedure for the recovery of I<sup>131</sup> from liquid milk was tested by analyzing the milk from cows that had been given single intravenous doses of I<sup>131</sup> in a study being performed at the UT-AEC Agricultural

bLung burden.

<sup>&</sup>lt;sup>19</sup>F. W. Legemann and E. W. Swanson, "A Study of the Secretion of Iodine in Milk of Dairy Cows, using Daily Oral Doses of I<sup>131</sup>," J. Dairy Sci. XL(3), 216–24 (1957).

<sup>&</sup>lt;sup>20</sup>Radiation Protection Standards, Report No. 2, Federal Radiation Council, September 1961.

<sup>&</sup>lt;sup>21</sup>A. L. Boni, Rapid Determination of I<sup>131</sup> in Milk, paper No. 37, presented at the Seventh Annual Health Physics Society Meeting, June 11-16, 1962, Chicago, III.

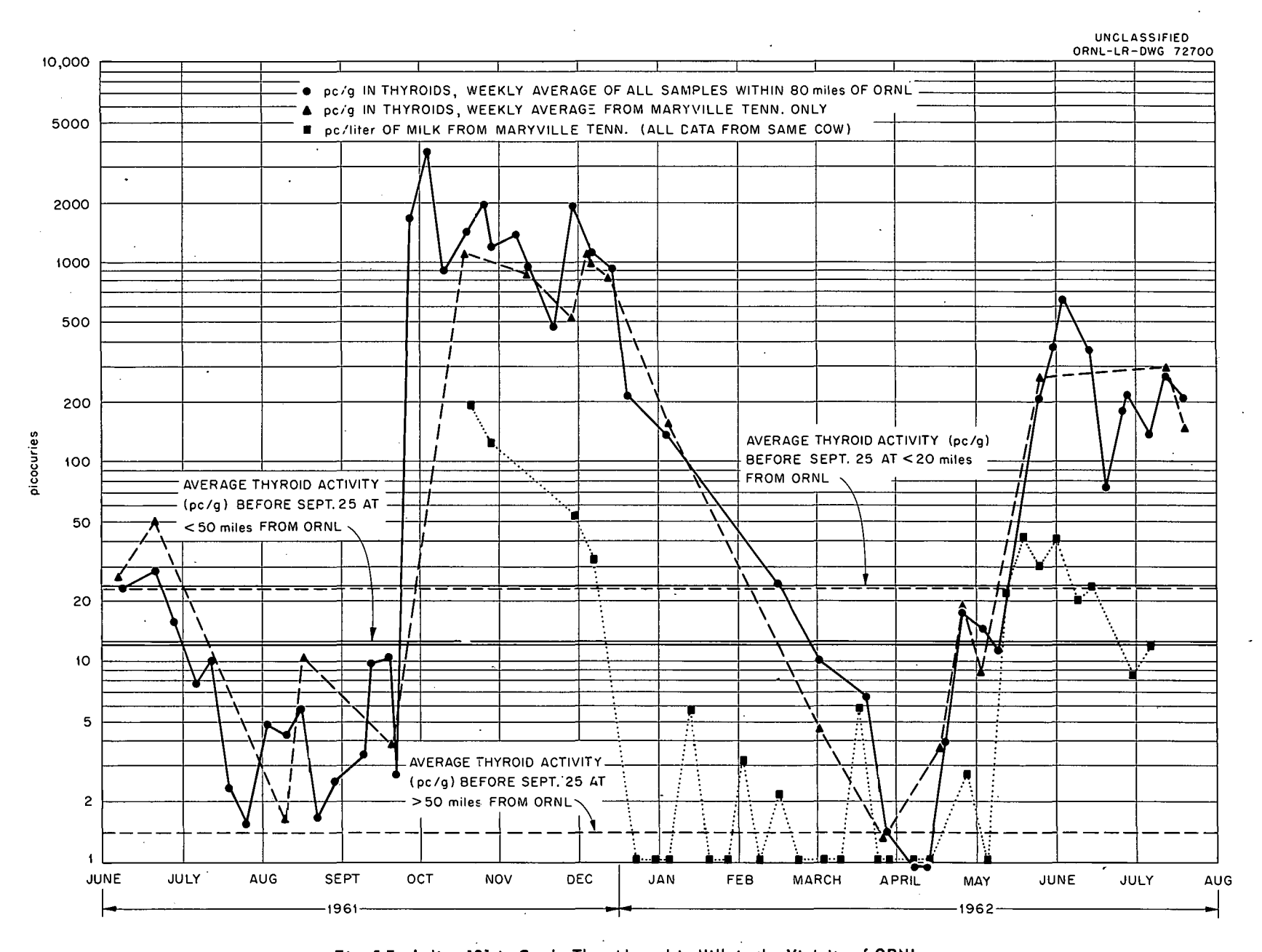


Fig. 5.7. Iodine-131 in Cattle Thyroids and in Milk in the Vicinity of ORNL.

Research Laboratory. Three liters of this milk was passed over a resin column (2.5 cm ID containing 25 ml of Dowex 1-X8, 50-100 mesh, in the Cl<sup>-</sup> form), at a flow rate of 20 ml/min. The loss was checked by counting the I<sup>131</sup> in the effluent milk and was found to average about 10% as shown in Table 5.6.

Table 5.6. Loss of 1<sup>131</sup> in Effluent from Resin Column
Alternate 200-ml aliquots analyzed

Volume Put	Loss (%)						
Through (ml)	Cow No. 1	Cow No. 1 Repeat	Cow No. 2				
0-200	9.7	7.9	8.1				
400-600	10.2	8.6	8.9				
800-1000	11.1	9.3	9.5				
1200-1400	11.2	9.5	9.8				
1600-1800	11.2	9.7	10.3				
2000-2200	11.6	10.1	10.4				
2400-2600	11.6	10.8	10.9				
2800-3000	12:0	11.6	11.3				
. А	v 11.0	9.5	9.8				

Essentially all the I<sup>131</sup> in the column effluent was shown to be protein-bound by the following tests:

- 1. Precipitation of the protein from the effluent showed that 94% of the lost I<sup>131</sup> is present in a protein-bound form.
- 2. Milk was equilibrated with Dowex 1-X8 resin in order to study the distribution coefficient. After separation of the resin and milk, new resin was added to the milk, and the process was repeated until no further I<sup>131</sup> could be removed from the milk. In general, this nonextractable I<sup>131</sup> was about equal to the effluent losses when this milk was passed over a resin column.
- 3. The effluent milk was recycled over a new resin column. In seven recycle runs an average of only 0.6% of the original I<sup>131</sup> was retained on the second resin column.

This procedure can be used to analyze milk for  $I^{131}$  at levels of less than 10 pc/liter. The simplicity of the method makes it easily adaptable for routine use. The chief limitation to this procedure is that protein-bound  $I^{131}$  will not be

removed from the milk. Since it has been demonstrated that this loss is about 10%, an overall recovery of about 90% can be expected.

## NS "Savannah" Bioassay Development Program

G. W. Royster, Jr.

In support of the NS "Savannah" Medical Department, a study was initiated in June 1961 to establish shipboard bioassay procedures. It was desired to develop a minimum program adequate for detecting significant exposures to internal radioactive contamination, for estimating radionuclide deposition in body organs, and for determining Na<sup>24</sup> levels in the blood following neutron exposures. As a result of space and equipment restrictions aboard ship, all procedures were necessarily simplified so as to entail a minimum of processing. Equipment that was already purchased and aboard ship consisted of a 128-channel analyzer with a 2 x 2 in. NaI(Tl) crystal. A 3 × 3 in. NaI(T1) crystal was purchased later to provide more sensitivity.

Initial efforts were directed toward establishing a screening procedure with which significant internal exposures may be recognized. gamma-ray spectrometry of raw urine samples was found to provide adequate sensitivity for detecting significant chronic or acute internal exposures to gross mixtures of radioactive corrosion products or fission products. Since not all the corrosion products nor all the fission products are excreted via the urine, it was decided to concentrate on representative nuclides that could be expected to be present in urine following exposure. Cobalt-60 was chosen as a representative corrosion product, and cesium-137 was chosen as a representative fission product. Thus, if either of these nuclides (or others) is detected in a urine sample, an exposure is assumed, and a more comprehensive investigation is undertaken to estimate the quantities deposited in body organs.

The  $3 \times 3$  in. NaI(Tl) crystal is housed in a 3-in.-thick, 6-in. ID, steel cylindrical shield. With the top removed, the shield becomes a collimator which is used to scan selected portions of the body of a subject lying on a cot positioned over the shield. This procedure is sufficiently sensitive to provide estimates of internal deposits. Organ burdens of 5% of the maximum permissible levels for individual major corrosion or fission

products may be detected easily. The sensitivity of this approach was emphasized in October 1961 by an incident involving the accidental exposure of two ORNL employees to a mixture of radioactive corrosion products. The potential exposure was detected by means of a constant air monitor (CAM) and confirmed by counting the men with a collimated 4 × 4 in. NaI(Tl) crystal in the ORNL whole-body counter (IVGS). The gamma spectra of the CAM filter of the collimated chest count and of a 24-hr urine sample are shown in Fig. 5.6. The two highest energy peaks for the filter and chest count are assumed to be a mixture of Co<sup>60</sup> and Fe<sup>59</sup> since the peaks fall in the energy range of both. These peaks in the urine spectrum, however, more nearly approximate Co<sup>60</sup> energy and probably result from a lower fractional excretion of iron than of cobalt in the urine. The total dose that these men received was estimated to be in the order of 4% of a maximum permissible lung burden.

## Excretion of Sr<sup>90</sup> by Man

L. B. Farabee B. R. Fish

In a previous study<sup>22</sup> the urinary excretion pattern of Sr<sup>90</sup> in man was described. At that time the fecal excretion data were incomplete because initially only a small aliquot of each daily fecal sample was taken for Sr<sup>90</sup> analysis; thus, the activity level of some of the samples was too low to be valid. All the fecal samples were reanalyzed by use of a large aliquot of the sample, and corrections were applied to account for the daily ingestion of Sr<sup>90</sup> in foods. The excretion during the first 22 days in both urine and feces is summarized in Table 5.7.

Total excretion rate data (urine + feces) for the first 115 postexposure days have been fitted with a variety of functions (Table 5.8). Many authors report their strontium retention and excretion data in terms of the power function  $At^{-B}$  or as a linear combination of exponentials. <sup>23,24</sup> In discussing the power function, most writers concede that the data at early times do not seem to fall on such a curve and so they arbitrarily drop the first few data points and fit the remainder. There are at least two difficulties imposed by this procedure. First, there is no unanimity concerning the number of data points to be ignored; current practice ranges from dropping the first day to dropping the

first 20 days. Secondly, it is probably rare to find a case in which the author does not make the tacit assumption that the errors in the logarithms of the observations are distributed homogeneously. This assumption is implicit in fitting a straight line to the logarithms of the observed values

Table 5.7. Daily Urine and Fecal Excretions of Sr<sup>90</sup>

During the First 22 Days After Exposure

Days	Sr <sup>90</sup> Dose <sup>a</sup>	Sr <sup>90</sup> Dose a		
After	Excreted in Urine	Excreted in Feces		
Injection	Per Day (%)	Per Day (%)		
1	16.5	2.48		
2	8.8	2.48		
3	4.7	1.12		
4	7.7	1.12		
5	3.8	1.12		
6	2.8	2.35		
7	2.5	1.40		
8	1.43	0.74		
9	0.65	0.41		
10	0.92	0.22		
11	0.92	0.37		
12	0.64	0.19		
13	0.64	0.19		
14	0.65	0.29		
15	0.51	0.24		
16	0.47	0.31		
17	0.62	0.31		
18	0.43	0.11		
19	0.24	0.07		
- 20	0.27	0.08		
21	0.18	0.27		
22	0.21	0.13		
	Total ' 55.6	16.0		

<sup>&</sup>lt;sup>a</sup>Based on an estimated initial injection of 17,790 dis/min.

<sup>&</sup>lt;sup>22</sup>L. B. Farabee, *Health Phys. Div. Ann. Progr. Rept. July* 31, 1961, ORNL-3189, pp 224-26.

<sup>&</sup>lt;sup>23</sup>Margaret Bishop et al., Intem. J. Radiation Biol. 2, 125-42 (1960).

<sup>&</sup>lt;sup>24</sup>P. W. Durbin et al., Metabolism of Sr<sup>90</sup> in the Monkey, p 13, presented at the meeting of Bio-Medical Program Directors of the United States Atomic Energy Commission, Feb. 6-7, 1961.

unless proper adjustment is made in the relative weights assigned to the data points. Failure to make appropriate changes in the weights is equivalent to assigning weights inversely proportional to the square of the observed value; that is, the lowest values are given the highest weights. The parameter estimates given in Table 5.8 illustrate the disparity that can arise in presenting the same set of data in reference to different models and to arbitrary rules for the rejection of data.

Table 5.8. Parameter Estimates for Functions Fitted to  $Sr^{90}$  Total Excretion Rate Data a

	Data	Parameters			Integrated Excretion		
Function	Points	Wt	<sup>c</sup> = 1	$Wt = 1/E^2$		$(t \to \infty)$	
	Dropped $^{b}$	· A	В	Α	В	Wt = 1	$Wt = 1/E^2$
$E = At^{-B}$	0	5,303	1.440	12,697	1.723	(15,436)	(20,937)
	. 1	7,294	1.526	12,698	1.723	17,266	20,937
	2	8,726	1.577	12,699	1.724	15,539	16,022
	3	10,071	1.615	12,701	1.724	14,766	14,359
	4	9,734	1.606	12,701	1.724	14,933	14,435
	. 5	9,714	1.605	12,701	1.724	14,932	14,353
•	6	8,938	1.584	12,701	1.724	15,180	14,600
•	. 7	8,125	1.559	12,699	1.724	15,404	14,802
•	8	7,902	1.552	12,699	1.724	15,449	14,804
	9	8,594	1.573	12,723	1.724	15,356	14,686
	11	8,692	1.576	12,728	1.724	15,341	14,651
	13	9,188	1.590	12,744	1.724	15,292	14,610
	14	8,748	1.578	12,734	1.724	15,335	14,642
·	15	8,580	1.573	12,727	1.724	15,350	14,654
	16	8,020	1.556	12,708	1.724	15,407	14,686
	<b>17</b> .	6,998	1.523	12,682	1.723	15,531	14,748
·	18	6,671	1.511	12,665	1.723	15,573	14,761
•	19	7,288	1.533	12,779	1.725	15,504	14,740
	20	7,612	1.543	12,817	1.726	15,473	14,731
$E = A/(1+Ct)^B$		4,314	1.988	5,739	1.792	15,297	13,717
		(C =	0.2856)	(C=0)	.5282)		
$E = ae^{-\alpha t} + be^{-\beta t} + ce^{-\gamma t} + de^{-\delta t}$		a = 3,264 b = 490 c = 35 d = 4.75	$\alpha = 0.42$ $\beta = 0.10$ $\gamma = 0.021$ $\delta = 0.0013$			17,992	
Observed integrated excretion $0 \rightarrow t =$	115				•	14	,561
In vivo counting [beta-absorption and of bremsstrahlung (Y90)]	thin crystal	measureme	nt			~17	,800
Comparison with Sr <sup>85</sup> excretion data (average total excretion, 81.3% for		Margaret Bi	shop et al.			17	<b>,</b> 790

aORNL Case A-12167.

<sup>&</sup>lt;sup>b</sup>Day through which all data dropped.

cWeight.

# 6. Education, Training, and Information

Twenty-one students completed the course in Applied Radiation Physics at Vanderbilt University in May 1962. Sixteen of these were AEC Fellows, three were from the Nuclear Engineering Department of the University, one was an Air Force officer, and one was a citizen of Japan. Sixteen AEC Fellows, one Air Force officer, and one citizen of India reported to the Health Physics Division in June for Applied Health Physics training.

Fourteen of the AEC Fellows were granted extensions to the Fellowship to complete the requirements for the MS degree. Thirteen AEC Fellows for the 1962-63 program were selected in March 1962 and will enroll at Vanderbilt University in September 1962.

Two 60-hr courses in Health Physics were presented by the Division for ORSORT. These were combined lecture and laboratory courses covering various aspects of Health Physics. Two 5-hr lecture series were given to NSF-AEC Institutes in Radiation Biology for high school teachers. One was at Florida State University and the other at the University of Wyoming.

Lectures and tours were given for:

- 1. U.S. Public Health Service, Cincinnati, Ohio
- 2. ORNL Orientation Program
- 3. ORINS Radioisotope Techniques Course
- 4. ORINS Medical Division (Courses in Clinical Techniques)
- 5. ORNL-Radiation Safety and Control Course
- 6. American Industrial Hygiene Association
- Oak Ridge, Clinton, and Norris Policemen and Firemen
- 8. University of North Carolina, School of Public Health

One member of the Section conducted the Health Physics Division Seminar Program and was responsible for all visitors to the Division.

Samuel Helf, Picatinny Arsenal, New Jersey, has completed a 1-yr training program which was co-ordinated by this section.

# **Publications**

- W. T. Atyeo and D. A. Crossley, Jr., "The Labidostommidae of New Zealand (Acarina)," Rec. Dominion Museum (Wellington, N.Z.) 4, 29-48 (1961).
- S. I. Auerbach, "Analytical Requirements for Environmental Surveys," Nucl. Safety 3(3), 51-54 (March 1962).
- S. I. Auerbach, "Summary of Session, First National Symposium on Radioecology 1961, Cycling in the Terrestrial Environment," in *Proceedings of the Conference on Radioactive Fallout from Nuclear Weapons*, 1962.
- J. A. Auxier, "Dosimetric Considerations in Criticality Exposures," pp 141-50 in Diagnosis and Treatment of Acute Radiation Injury, World Health Organization, Geneva, Switzerland, 1961.
- J. A. Auxier, F. W. Sanders, F. F. Haywood, J. H. Thorngate, and J. S. Cheka, Technical Concept Operation BREN, CEX-62.01 (January 1962).
- R. E. Blanco and E. G. Struxness, Waste Treatment and Disposal Progress Report for June and July 1961, ORNL TM-15 (Oct. 24, 1961).
- R. E. Blanco and E. G. Struxness, Waste Treatment and Disposal Progress Report for August and September 1961, ORNL TM-49 (Nov. 29, 1961).
- R. E. Blanco and E. G. Struxness, Waste Treatment and Disposal Progress Report for October and November 1961, ORNL TM-133 (Mar. 13, 1962).
- R. E. Blanco and E. G. Struxness, Waste Treatment and Disposal Progress Report for December 1961 and January 1962, ORNL TM-169 (June 15, 1962).
- R. L. Bradshaw, W. J. Boegly, Jr., F. M. Empson, H. Kubota, and E. G. Struxness, "Storage of High Level Packaged Solid Waste in Rock Salt," pp 477-90 in Ground Disposal of Radioactive Wastes, Second Conference Proceedings, TID-7628 (March 1962).
- R. L. Bradshaw, J. J. Perona, J. T. Roberts, and J. O. Blomeke, Evaluation of Ultimate Disposal Methods for Liquid and Solid Radioactive Wastes: I. Interim Liquid Storage, ORNL-3128 (Aug. 7, 1961).
- L. W. Cochran and D. W. Forester, "Diffusion of Slow Electrons in Gases," Phys. Rev. 126, 1785-88 (1962).
- K. E. Cowser, "Movement of Ruthenium in the ORNL Waste-Pit System," pp 513-31 in Ground Disposal of Radioactive Wastes, Second Conference Proceedings, TID-7628 (March 1962).
- K. E. Cowser, T. F. Lomenick, and W. M. McMaster, Status Report on Evaluation of Solid Waste Disposal at ORNL: 1, ORNL-3035 (Feb. 8, 1961).
- F. J. Davis and P. W. Reinhardt, "Radiation Measurements over Simulated Plane Sources," *Health Phys.* 8, 233-43 (1962).
- P. B. Dunaway and S. V. Kaye, "Effects of Industrial Oil Disposal on Wild Mammals," J. Mammalogy 42, 554-56 (1961).
- P. B. Dunaway and S. V. Kaye, "Studies of Small-Mammal Populations on the Radioactive White Oak Lake Bed," Trans. 26th N. Am. Wildl. Natl. Res. Conf., pp 167-85, 1961.

- H. B. Eldridge, P. Flusser, and R. H. Ritchie, Proton Recoil Energy Loss Distributions in Plane Geometry, ORNL-3089 (June 25, 1962).
- F. M. Empson, "Incineration," Nucl. Safety 3(3), 54 (1962).
- F. M. Empson, "Storage of Low Level Packaged Solids in a Salt Mine," pp 469-76 in Ground Disposal of Radioactive Wastes, Second Conference Proceedings," TID-7628 (March 1962).
- F. M. Empson, W. J. Boegly, Jr., R. L. Bradshaw, H. Kubota, F. L. Parker, and E. G. Struxness, Status Report on Waste Disposal in Natural Salt Formations: III, ORNL-3053 (July 11, 1961).
- A. L. Frank, E. T. Arakawa, and R. D. Birkhoff, "Optical Emission from Irradiated Foils II," Phys. Rev. 126, 1935-47 (1962).
- A. L. Frank, E. T. Arakawa, R. D. Birkhoff, R. H. Ritchie, and H. B. Eldridge, Optical Emission from Irradiated Thin Metallic Foils, ORNL-3114 (July 2, 1962).
- E. L. Grove, Rose Ann Jones, and Weldon Mathews, "The Loss of Sodium and Potassium During the Dry Ashing of Animal Tissue," Anal. Biochem. 2, 221-30 (1961).
- G. S. Hurst, L. B. O'Kelly, and T. E. Bortner, 'Dissociative Electron Capture in Water Vapor,' Phys. Rev. 123, 1715-18 (1961).
- G. S. Hurst, L. B. O'Kelly, and J. A. Stockdale, "Quasi-Trapping of Low Energy Electrons in Water Vapor," Nature 195, 66-67 (1962).
- G. S. Hurst and R. H. Ritchie, "A Generalized Concept for Radiation Dosimetry," Health Phys. 8, 117-29 (1962).
- D. G. Jacobs, "Cesium Exchange by Vermiculite," pp 282-91 in Ground Disposal of Radioactive Wastes, Second Conference Proceedings, TID-7628 (March 1962).
- D. G. Jacobs, Cesium Exchange by Vermiculite, ORNL CF-61-9-31 (Sept. 12, 1961).
- D. G. Jacobs, "Cesium Exchange Properties of Vermiculite," Nucl. Sci. Eng. 12(2), 285 (1962).
- F. G. Karioris and B. R. Fish, "An Exploding Wire Aerosol Generator," J. Colloid Sci. 17, 155-61 (1962).
- S. V. Kaye, "Laboratory Life History of the Eastern Harvest Mouse," Am. Midland Naturalist 66, 439-51 (1961).
- S. V. Kaye, "Movements of Harvest Micc Tagged with Gold-198," J. Mammalogy 42, 323-37 (1961).
- S. V. Kaye and P. B. Dunaway, "Bioaccumulation of Radioactive Isotopes by Herbivorous Small Mammals," Health Phys. 7, 205-17 (1962).
- W. J. Lacy, O. M. Sealand, D. G. Jacobs, and E. G. Struxness, Laboratory Progress on the Disposal of High-Level Radioactive Wastes by Deep-Well Injection, ORNL TM-127 (Mar. 7, 1962).
- W. de Laguna, "Engineering Geology of Radioactive Waste Disposal," Reviews in Engineering Geology 1, 129-60 (1962).
- T. F. Lomenick and K. E. Cowser, "Land Burial of Solid Waste at Oak Ridge National Laboratory," pp 437-55 in Ground Disposal of Radioactive Wastes, Second Conference Proceedings, TID-7628 (March 1962).
- T. F. Lomenick and K. E. Cowser, Status Report on Evaluation of Solid Waste Disposal at ORNL: II, ORNL-3182 (Dec. 29, 1961).
- R. J. Morton (ed.) et al., Status Report No. 2 on Clinch River Study, ORNL-3202 (Mar. 30, 1962).
- R. B. Neel and J. S. Olson, "Use of Analog Computers for Simulating the Movement of Isotopes in Ecological Systems," ORNL-3172 (Jan. 10, 1962).
- D. J. Nelson, "Clams as Indicators of Strontium-90," Science 137, 38-39 (1962).

- D. J. Nelson, "Strontium, Strontium-90, and Calcium Analyses of Clinch and Tennessee River Clams," ORNL TM-270 (June 20, 1962).
- Jacob Neufeld, "Space Dispersive Properties of Plasma," Phys. Rev. 123, 1-10 (1962).
- J. Neufeld, "Electromagnetic Properties of a Plasma-Beam System," to be published in Phys. Rev.
- J. Neufeld and H. Wright, "Vavilov-Cherenkov Effect and Bohr Radiation' Produced by a Beam of Charged Particles in a Dispersive Medium," Phys. Rev. 124, 1-16 (1961).
- J. S. Olson, "Ecological Sampling and Meteorological Calculation of Fallout on Forests Near Oak Ridge," ORNL-3181 (Sept. 6, 1961).
- F. L. Parker, "Eddy Diffusion in Reservoirs and Pipelines," J. Hydraulics Div., Am. Soc. Civil Engrs. 87, 151-71 (1961).
- F. L. Parker, G. D. Schmidt, W. B. Cottrell, and L. A. Mann, "Dispersion of Radiocontaminants in an Estuary," Health Phys. 6, 66-85 (1961).
- J. J. Perona, R. L. Bradshaw, J. T. Roberts, and J. O. Blomeke, Evaluation of Ultimate Disposal Methods for Liquid and Solid Radioactive Wastes: II. Conversion to Solid by Pot Calcination, ORNL-3192 (Sept. 27, 1961).
- H. Mitchell Perry, Jr., Isabel H. Tipton, Henry A. Schroeder, Robert L. Steiner, and Mary Jane Cook, "Variation in the Concentration of Cadmium in Human Kidney as a Function of Age and Geographic Origin," J. Chronic Diseases 14(2), 259 (1961).
- R. H. Ritchie, V. E. Anderson, and H. B. Eldridge, ORNL-3116 (July 12, 1962) (classified).
- R. H. Ritchie and G. R. Dalton, "Thermal Neutron Flux Depression by Absorbing Foils and Flux Perturbations by Thermal Neutron Detectors," Nucl. Sci. Eng. 11, 451-52 (1961).
- R. H. Ritchie and H. B. Eldridge, "Optical Emission from Irradiated Foils I," Phys. Rev. 126, 1947-52 (1962).
- F. W. Sanders, F. F. Haywood, M. I. Lundin, L. W. Gilley, J. S. Cheka, and D. R. Ward, Operation Plan and Hazards Report Operation BREN, CEX-62.02 (April 1962).
- H. A. Schroeder, J. J. Balassa, and I. H. Tipton, "Abnormal Trace Elements in Man Nickel," J. Chronic Diseases 15, 51-65 (1962).
- R. W. Strandtmann and D. A. Crossley, Jr., "A New Species of Soil-Inhabiting Mite, Hypoaspis marksi (Acarina, Laelaptidae)," Proc. Kansas Ent. Soc. 35, 180-85 (1962).
- E. G. Struxness, Atomic Energy Waste: Its Nature, Use, and Disposal (ed. by E. Glueckauf), Interscience, New York, 1961; Butterworth & Co., London, 1961; submitted to Nucl. Safety for publication.
- E. G. Struxness, Radioactive Wastes: Their Treatment and Disposal (ed. by J. C. Collins), John Wiley & Sons, New York, 1960; E. & F. N. Spon Ltd., London, 1960; Nucl. Sci. Eng. 12(4), 551 (April 1962).
- T. Tamura, "Strontium Reactions with Minerals," pp 187-95 in Ground Disposal of Radioactive Wastes, Second Conference Proceedings, TID-7628 (March 1962).
- C. J. Weinberg, D. R. Nelson, and J. G. Carter, "Thermoluminescence from Gamma-Irradiated Biochemicals. Investigation of Emission Spectra," J. Chem. Phys. 36, 2869 (1962).
- Martin Witkamp, "Influence of Radiation from an Unshielded Reactor on a Natural Microflora," ORNL TM-29 (Oct. 19, 1961).
- Martin Witkamp, Abstract, "Microbial Populations of Leaf Litter Related to Litter Breakdown Under Various Conditions," Bact. Proc., 25 (1962).
- Martin Witkamp and J. van der Drift, "Breakdown of Forest Litter in Relation to Environmental Factors," Plant and Soil 15(4), 295-311 (December 1961).

# **Papers**

#### E. T. Arakawa

Emission from Thin Metal Foils Irradiated by Electron Beams, University of Kentucky, February 16, 1962, Lexington, Kentucky.

Interaction of Accelerated Electrons with Electrons in Thin Foils, University of Southern California, July 21, 1961, Los Angeles, California.

#### S. I. Auerbach

Ecology and Radioactive Waste Area Studies, First National Symposium on Radioecology (AIBS), September 11, 1961, Fort Collins, Colorado.

Summary of Session, First National Symposium on Radioecology 1961, Cycling in the Terrestrial Environment, Radioactive Fallout from Nuclear Weapons Conference, November 13-17, United States Atomic Energy Commission Headquarters, Washington, D.C.

## S. I. Auerbach and J. S. Olson

Biological and Environmental Behavior of Ruthenium and Rhodium, First National Symposium on Radioecology (AIBS), September 12, 1961, Fort Collins, Colorado.

#### I. A. Auxier

Neutron Dosimetry, St. Louis University School of Medicine, July 20, 1961, St. Louis, Missouri.

#### S. R. Bernard

Mathematical Biological Approach to the Problem of Radiation-Induced Carcinogenesis, Annual Health Physics Society Meeting, June 11-14, 1962, Chicago, Illinois.

#### R. D. Birkhoff

Electron Spectroscopy, Health Physics Society, Seventh Annual Meeting, June 10-15, 1962, Chicago, Illinois.

On Recent Experiments on the Interaction of Radiation with Solids, Vanderbilt University, November 8, 1961, Nashville, Tennessee.

## W. J. Boegly, Jr.

Plastic Flow Studies, Meeting of the Waste Disposal Committee, Division of Earth Sciences, National Academy of Sciences-National Research Council, December 8, 1961, Savannah River Plant.

#### R. L. Bradshaw

Disposal of High-Level Radioactive Wastes in Rock Salt: Heat Studies, Meeting of the Committee on Waste Disposal, Earth Sciences Division, National Academy of Sciences-National Research Council, December 8, 1961, Savannah River Plant.

## P. E. Brown

Application of Whole Body Counting Techniques to the Estimation of Transuranic Contaminants in Man, Symposium on the Biology of the Transuranic Elements, May 28-30, 1962, Richland, Washington.

## P. R. J. Burch

Carcinogenesis with Respect to Somatic Mutation and Immunological Factors, University of Chicago, March 28, 1962, Chicago, Illinois.

Human Carcinogenesis, Donner Laboratory, April 2, 1962, Berkeley, California.

Human Carcinogenesis, Los Alamos Scientific Laboratory, April 10, 1962, Los Alamos, New Mexico.

Human Carcinogenesis, University of Tennessee, March 20, 1962, Knoxville, Tennessee.

## P. R. J. Burch

Human Leukaemogenesis, California Institute of Technology, April 6, 1962, Pasadena, California.

Human Leukaemogenesis, Memorial Sloan-Kettering Cancer Center, June 21, 1962, New York, New York.

Human Leukaemogenesis, Stanford University, April 3, 1962, Stanford, California.

Human Leukaemogenesis, University of California, April 5, 1962, Los Angeles, California.

The Interpretation of Radiogenic Mammary Carcinogenesis in Rats, Brookhaven National Laboratory, November 3, 1961, Upton, Long Island, New York.

Natural and Radiation Carcinogenesis, M.D. Anderson Hospital and Tumour Inst., Texas Medical Center, October 17, 1961, Houston, Texas.

Radiation and Carcinogenesis, Case Institute of Technology, February 15, 1962, Cleveland, Ohio.

Radiation and Carcinogenesis, Medical College of Virginia, January 15, 1962, Richmond, Virginia.

Radiation Carcinogenesis in Man, University of Pittsburgh, Graduate School of Public Health, February 14, 1962, Pittsburgh, Pennsylvania.

The Relationship of Existing Radiation Levels to Carcinogenesis, American Association for the Advancement of Science, December 28, 1961, Denver, Colorado.

## D. A. Crossley, Jr.

Consumption of Vegetation by Insects, First National Symposium on Radioecology (AIBS), September 14, 1961, Fort Collins, Colorado.

Insect-Vegetation Relations in a Radioactive Waste Area, 26th Annual Meeting of the Georgia Entomological Society, March 21, 1962, Radium Springs, Georgia.

Movement and Accumulation of Radiocesium and Radiostrontium in Insects, First National Symposium on Radioecology (AIBS), September 11, 1961, Fort Collins, Colorado.

## P. B. Dunaway and S. V. Kaye

Effects of Ionizing Radiation on Mammal Populations on the White Oak Lake Bed, First National Symposium on Radioecology (AIBS), September 10-15, Fort Collins, Colorado.

Effects of Radiation on Mammalian Population Dynamics, First International Conference on Wildlife Disease, June 24-28, 1962, High View, New York.

## F. M. Empson

Status Report on Completion of Liquid Waste Experiments, Meeting of the Waste Disposal Committee, Division of Earth Sciences, National Academy of Sciences-National Research Council, December 8, 1961, Savannah River Plant.

#### L. B. Farabee

Excretion of Sr<sup>90</sup> and Ca<sup>45</sup> by Man Following an Accidental Puncture Wound, Health Physics Society, Seventh Annual Meeting, June 11-14, 1962, Chicago, Illinois.

## D. C. Hammer, E. T. Arakawa, and R. D. Birkhoff

A Calibrator for Concave Diffraction Gratings, American Physical Society, Southeastern Section, April 5-7, 1962, Tallahassee, Florida.

#### H. H. Hubbell

The Radiation Dose to Japanese Atomic Bomb Survivors, an Example of Health Physics Research, Berea College, March 23, 1962, Berea, Kentucky.

## H. H. Hubbell, Jr., R. M. Johnson, and R. D. Birkhoff

Performance of the Keplertron, a Spherical Electrostatic Analyzer, American Physical Society, Southeastern Section, April 5-7, 1962, Tallahassee, Florida.

#### G. S. Hurst

Dosimetric Considerations in Criticality Exposures, U.S. Public Health Service, June 4, 1962, Montgomery, Alabama.

Measurement of Electron Capture Cross Sections Using Swarm Methods, ASTM Meeting on Mass Spectrometry, June 3-8, 1962, New Orleans, Louisiana.

The Radiation Physics and Dosimetry Program at ORNL and Studies of the Interaction of Radiation with Gases, Vanderbilt University, October 11, 1961, Nashville, Tennessee

#### G. S. Hurst, L. B. O'Kelly, and J. A. Stockdale

Interaction of Subexcitation Electrons with Water Vapor, Institute of Molecular Biophysics, Florida State University, March 14, 1962, Tallahassee, Florida.

Interaction of Subexcitation Electrons with Water Vapor, University of Kentucky, March 2, 1962, Lexington, Kentucky.

#### D. G. Jacobs

Ion Exchange in the Deep-Well Injection of Radioactive Wastes, Joint Meeting of the Waste Disposal Committee of the American Association of Petroleum Geologists and the AEC Advisory Committee on Deep Well Disposal of Radioactive Wastes, April 1, 1962, San Francisco, California.

#### S. V. Kaye and P. B. Dunaway

Estimation of Dose Rate and Equilibrium State from Bioaccumulation of Radionuclides by Mammals, First National Symposium on Radioecology (AIBS), September 10-15, 1961, Fort Collins, Colorado.

## R. A. McRae, J. G. Carter, D. R. Nelson, E. T. Arakawa, and R. D. Birkhoff

An Interference Filter Spectrometer for Solid State Spectroscopy, American Physical Society, Southeastern Section, April 5-7, 1962, Tallahassee, Florida.

## K. Z. Morgan

Dental X-Ray Exposures, Medical College of Virginia School of Dentistry, January 29-30, 1962, Richmond, Virginia.

Future Advances in Radiation Effects on the Human Body, Health Physics Symposium, March 30-31, 1962, Augusta, Georgia.

Radiation Protection Criteria and Standards-Their Basis and Use, Second Annual Nuclear Applications Research Symposium, September 19-22, 1961, Reno, Nevada.

Relative Hazards of the Various Radioactive Materials, Annual Health Physics Society Meeting, June 11-14, 1962, Chicago, Illinois.

Safety in Health Physics, Conference on Subcritical Assemblies, August 28-30, 1961, Gatlinburg, Tennessee.

Types of Data Needed for the Establishment of Adequate Standards, International Biophysics Congress, July 30-August 4, 1961, Stockholm, Sweden.

## D. J. Nelson

The Strontium and Calcium Relationships in Clinch and Tennessee River Mollusks, First National Symposium on Radioecology (AIBS), September 11-15, 1961, Fort Collins, Colorado.

## D. J. Nelson and B. G. Blaylock

The Preliminary Investigation of Salivary Gland Chromosomes of Chironomus tentans Fabr. from the Clinch River, First National Symposium on Radioecology (AIBS), September 10-15, 1961, Fort Collins, Colorado.

## J. Neufeld

The Calculations of Maximum Permissible Dose for High Energy Neutrons and Protons, Colloquium on the Protection Around High Energy Accelerators, January 18-20, 1962, Orsay, France.

#### L. B. O'Kelly, G. S. Hurst, and T. E. Bortner

Electron Capture in Gas Mixtures Containing Water Vapor, Fourteenth Annual Gaseous Electronics Conference, October 11-13, 1961, Schenectady, New York.

#### J. S. Olson

Analog Computer Models for Movement of Nuclides Through Ecosystems, First National Symposium on Radioecology (AIBS), September 11-15, 1961, Fort Collins, Colorado.

Tracer Experiments and Theory of Chemical Cycling in Terrestrial Ecosystems, Symposium on Chemical Cycles of Biologically Important Elements, Purdue University, August 30, 1961, Lafayette, Indiana.

Tracer Studies of Forest Litter, First National Symposium on Radioecology (AIBS), September 11-15, 1961, Fort Collins, Colorado.

#### F. L. Parker

Environmental Consequences of Radioactive Waste Disposal, Ninth Session, United Nations Scientific Committee on the Effects of Atomic Radiation, March 20, 1961, Geneva, Switzerland.

#### G. W. Royster and B. R. Fish

Studies of Surface Contamination. II. Surface Characteristics Affecting the Measurement and Redispersion of Particulates, Health Physics Society, Seventh Annual Meeting, June 11-14, 1962, Chicago, Illinois.

#### W. S. Snyder

Major Sources of Error in Interpreting Urinalysis Data to Estimate the Body Burden of  $Pu^{239}$ : A Preliminary Study, Symposium on the Biology of the Transuranic Elements, May 28-30, 1962, Hanford, Washington.

Some Computer Codes for Estimating the Body Burden of Pu<sup>239</sup>, Seventh Annual Bioassay and Analytical Chemistry Meeting, October 12-13, 1961, Argonne, Illinois.

## W. S. Snyder and Mary Jane Cook

The Distribution of Dose Resulting from a Constant Level of Contamination of the Environment by  $Sr^{90}$  and Various Other Radionuclides, Annual Health Physics Society Meeting, June 11-14, 1962, Chicago, Illinois.

## W. S. Snyder, J. Neufeld, J. E. Turner, W. E. Kinney, and C. D. Zerby

Calculation of Dose Due to High Energy Particles, Annual Health Physics Society Meeting, June 11-14, 1962, Chicago, Illinois.

Calculation of Dose Due to High Energy Particles, Health Physics Society, Seventh Annual Meeting, June 10-15, 1962, Chicago, Illinois.

#### E. G. Struxness

Storage of Radioactive Waste in Mine Cavities, Northern Ohio Geology Society Symposium on Salt, May 3-5, 1962, Cleveland, Ohio.

Waste Disposal Research at ORNL, Second Annual Nuclear Applications Research Symposium, September 19-22, 1961, Reno Metallurgy Research Center, Reno, Nevada.

#### T. Tamura

Cesium Sorption Reactions as Indicator of Clay Mineral Structures, Tenth Annual Clay Mineral Conference, October 18, 1961, Austin, Texas.

#### I. H. Tipton

Spectrographic Analysis of Human Tissues, Spectroscopy Society of Pittsburgh, September 1961, Pittsburgh, Pennsylvania.

## J. P. Witherspoon, Jr.

Cycling of Cesium-134 in White Oak Trees on Sites of Contrasting Soil Type and Moisture, First National Symposium on Radioecology (AIBS), September 11-15, 1961, Fort Collins, Colorado.

## Martin Witkamp

Microbial Populations of Leaf Litter Related to Litter Breakdown Under Various Conditions, Sixty-second Annual Meeting of the American Society for Microbiology, May 8, 1962, Kansas City, Missouri.

# Lectures

#### S. I. Auerbach

Radioecology, Naval Research Reserve, 12th Annual Nuclear Sciences Seminar, June 12, 1962, Oak Ridge, Tennessee.

Effects of Fallout on Natural Effects of Populations, First International Conference on Wildlife Disease, June 25-29, 1962, High View, New York.

Some Aspects of Radiation Ecology, Kansas Chapter of Sigma XI, March 15, 1962, Lawrence, Kansas.

## J. A. Auxier

Blast Effects of Atomic Weapons, Advanced Technology Seminar No. 17 on Civil Defense Problems and Technology (J. A. Auxier, K. Z. Morgan, F. C. Maienschein, W. de Laguna, and F. R. Bruce), ORNL, October 30, 1961, Oak Ridge, Tennessee.

#### W. J. Boegly, Jr.

Disposal of Radioactive Wastes, Naval Research Reserve Company 6-3, September 20, 1961, Oak Ridge, Tennessee.

Field Experiments on the Disposal of Radioactive Wastes in Salt Formations, Oak Ridge Section of the American Society of Civil Engineers, January 10, 1962, Oak Ridge, Tennessee.

#### R. L. Bradshaw

Radioactive Waste Disposal, Oak Ridge School of Reactor Technology, January 12, 1962, Oak Ridge, Tennessee.

## P. R. J. Burch

Certain Aspects of Radiation Physics, Radiation Chemistry, and Radiobiology, ORNL, August 10, 11, 14-18, 21-25, Oak Ridge, Tennessee.

A Theory of Natural Carcinogenesis with Reference to Cytogenetic, Immunological, and Deletion Factors, ORNL, December 21, 1961, Oak Ridge, Tennessee.

The Relation of Radiation to Natural Carcinogenesis, ORNL, December 21, 1961, Oak Ridge, Tennessee.

Human Carcinogenesis, ORNL, July 2, 3, 5, 1962, Oak Ridge, Tennessee.

## K. E. Cowser

Selection of Sites for Waste Burial at ORNL, Atomic Energy Advisory Board for the State of Kentucky, July 20-21, 1961, Oak Ridge National Laboratory, Oak Ridge, Tennessee.

## D. A. Crossley, Jr.

The Biological Half-Life of Radioisotopes as an Ecological Research Tool, and Relationships of the Soil Mites (Acarina) to Leaf Litter Breakdown, Department of Biology, Texas Technological College, April 12, 1962, Lubbock, Texas.

The Biological Half-Life of Radioisotopes as an Ecological Research Tool, Department of Biology, North Texas State University, April 13, 1962, Denton, Texas.

Insect-Vegetation Relationships in a Radioactive Waste Area, and The Biological Half-Life of Radioisotopes as an Ecological Research Tool, Department of Biology, Texas Woman's University, April 14, 1962, Denton, Texas.

The Biological Half-Life of Radioisotopes as an Ecological Research Tool, Department of Biology, Wabash College, April 23, 1962, Crawfordsville, Indiana.

The Biological Half-Life of Radioisotopes as an Ecological Research Tool, Department of Biology, Purdue University, April 24, 1962, West Lafayette, Indiana.

The Biological Half-Life of Radioisotopes as an Ecological Research Tool, Department of Entomology, the University of Kansas, May 14, 1962, Lawrence, Kansas.

Insect-Vegetation Relationships in a Radioactive Waste Area, and The Biological Half-Life of Radioisotopes as an Ecological Research Tool, Summer Institute in Radiochemistry, Texas Woman's University, August 4, 1961, Denton, Texas.

Radioecology, Institute in Radiation Biology, Oak Ridge Institute of Nuclear Studies, August 30, 1961, Oak Ridge, Tennessee.

Relationships of the Soil Mites (Acarina) to Leaf Litter Breakdown, Department of Entomology, the University of Georgia, October 17, 1961, Athens, Georgia.

Relationships of the Soil Mites (Acarina) to Leaf Litter Breakdown, Department of Entomology, North Carolina State College, December 7, 1961, Raleigh, North Carolina.

Relationships of the Soil Mites (Acarina) to Leaf Litter Breakdown, Department of Zoology, the University of Tennessee, February 6, 1962, Knoxville, Tennessee.

Relationships of the Soil Mites (Acarina) to Leaf Litter Breakdown, Department of Entomology, the University of Kansas, May 12, 1962, Lawrence, Kansas.

## F. M. Empson

Nature and Composition of Radioactive Wastes, U.S. Public Health Service Course in Reactor Environmental Health Problems, Oak Ridge National Laboratory, September 5, 1961, and May 15, 1962, Oak Ridge, Tennessee.

Safety Problems in a Nuclear Facility, Meeting of the Wichita Chapter of the American Society of Safety Engineers, June 4, 1962, Hutchinson, Kansas.

#### G. S. Hurst

General Remarks on Radiation Dosimetry, ORNL, September 21, 1961, Oak Ridge, Tennessee.

Electron Interactions in Molecular Gases, ORNL, February 8, 1962, Oak Ridge, Tennessee.

Interaction of Electrons with Water Molecules, ORNL, May 24, 1962, Oak Ridge, Tennessee.

### D. G. Jacobs

Movement of Radionuclides Relative to the Movement of Water in Nuclear Waste Disposal, Seminar at Department of Geology, University of Arizona, March 28, 1962, Tucson, Arizona.

Chemistry of Ruthenium of Interest in the Ground Disposal of Radioactive Wastes, Seminar at Department of Sanitary Engineering, University of California, April 2, 1962, Berkeley, California.

#### S. V. Kaye

Studies of Wild Mammals in Areas Contaminated by Radioactive Wastes, Department of Zoology, University of Tennessee, November 21, 1961, Knoxville, Tennessee.

Use of Radioisotopes as Tags for Studying Animal Populations, Radiation Biology-Ecology Institute, Oak Ridge Institute of Nuclear Studies, June 18, 1962, Oak Ridge, Tennessee.

#### T. F. Lomenick

Ground Disposal of Solids and Liquids at ORNL, Short Course in Health Physics, April 18, 1961; ORSORT, January 4, 1961, Oak Ridge National Laboratory, Oak Ridge, Tennessee.

Environmental Monitoring at ORNL Burial Grounds, Atomic Energy Advisory Board for the State of Kentucky, at Oak Ridge National Laboratory, July 21, 1961, Oak Ridge, Tennessee.

Handling, Treatment, and Disposal of ORNL Wastes, U.S. Public Health Service Course on Environmental Health Aspects of Nuclear Reactor Operations, May 15, 1962 (lecture and field tour), September 5, 1961 (lecture and field tour); and August 11, 1961 (lecture and field tour), ASEE-AEC Summer Institute at Oak Ridge National Laboratory, Oak Ridge, Tennessee.

#### K. Z. Morgan

The Control of Radiation by the Health Physicist, Lecture to Church Group, July 24-29, 1961, Massanetta, Virginia; Kingsport Safety Council, March 13, 1962, Kingsport, Tennessee; Oak Ridge Municipal Building, September 5, 1961, Oak Ridge, Tennessee.

Permissible Exposure to Ionizing Radiation, October 10, 1961, Carrollton, Georgia.

Radiation Fallout Problems, Advanced Technology Seminar, ORNL, October 30, 1961, Oak Ridge, Tennessee.

Civil Defense, DAR Program, November 4, 1961, Knoxville, Tennessee.

Dosimetry of Internal Radioactive Isotopes, ORSORT Lecture, ORNL, December 18, 20, and 22, 1961, Oak Ridge, Tennessee.

Health Physics, Medical College of Virginia, March 29, 1962, Richmond, Virginia; Florida Section, American Industrial Health Association, April 3, 1962, Jacksonville, Florida; Radiation Safety Training Program, ORNL, April 17-19, 1962, Oak Ridge, Tennessee; ORSORT lecture, April 25-27, 1962, Oak Ridge, Tennessee; AEC Fellowship Students, Vanderbilt University, April 30-May 1, 1962, Nashville, Tennessee; Navy Seminar, ORINS, June 7, 1962, Oak Ridge, Tennessee.

The Nature of Nuclear Attack, Civil Defense Program, Jefferson Junior High School, April 25, 1962, Oak Ridge, Tennessee.

## R. J. Morton

The Civil and Sanitary Engineer in the Development of Nuclear Energy, Meeting of Vanderbilt Student Chapter, American Society of Civil Engineers, Vanderbilt University, March 6, 1962, Nashville, Tennessee.

## D. J. Nelson

Ecological Studies at Oak Ridge National Laboratory, Department of Physics, Vanderbilt University, December 6, 1961, Nashville, Tennessee.

Aquatic Radioecology Studies at Oak Ridge National Laboratory, Radiation Biology-Ecology Institute, Oak Ridge Institute of Nuclear Studies, June 27, 1962, Oak Ridge, Tennessee.

#### J. S. Olson

Fallout of Leaves, Seeds, Spores, and Isotopes, Department of Botany, University of Tennessee, November 30, 1961, Knoxville, Tennessee.

Forest Ecology Studies at Oak Ridge National Laboratory, Radiation Biology-Ecology Institute, Oak Ridge Institute of Nuclear Studies, June 22, 1962, Oak Ridge, Tennessee.

#### J. S. Olson

Ecological Implications of Nuclear War, Radiation Biology-Ecology Institute, Oak Ridge Institute of Nuclear Studies, July 17, 1962, Oak Ridge, Tennessee.

Use of Activation Analysis in Ecology, Radiation Biology-Ecology Institute, Oak Ridge Institute of Nuclear Studies, July 27, 1962, Oak Ridge, Tennessee.

#### W. S. Snyder

Internal Exposures, Maximum Permissible Concentrations, and Interpretation of Handbook 69, Summer Postgraduates, St. Louis University School of Medicine, July 25, 1961, St. Louis, Missouri.

Single Exposure Dose, Neutron Dose, Federal Radiation Council, National Committee on Radiation Protection, and International Commission on Radiological Protection, ORSORT Lectures, ORNL, January 3 and 5, 1962, Oak Ridge, Tennessee.

A Method of Producing Bounds for the Solution of Certain Fredholm Integral Equations on a Digital Computer, Sharp Forms of Lebesgue's Theorems on Differentiation of Set Functions or Functions of a Real Variable, The Use of Steiner Symmetrization in the Study of the Fundamental Eigenvalue of a Region or Solid, and Using Digital Computers to Obtain Bounds for the Solution of Certain Problems, Society for Industrial and Applied Mathematics (SIAM) Lectureship Program, Virginia Polytechnic Institute, February 1-2, 1962, Blacksburg, Virginia.

Monte Carlo Calculations of Dose from Neutron Irradiation, Some Mathematical Models Used to Estimate Dose from Ingested Radionuclides, and Using Digital Computers to Obtain Bounds for the Solution of Certain Problems, SIAM Lecture, North Georgia College, March 5-6, 1962, Dahlonega, Georgia.

The Use of Steiner Symmetrization in the Study of the Fundamental Eigenvalue of a Region or Solid, and Sharp Forms of Lebesgue's Theorems on Differentiation of Set Functions or Functions of a Real Variable, SIAM Lecture, University of Kentucky, March 19-20, 1962, Lexington, Kentucky.

Trends in Internal Dose Estimation, Japanese Delegation, Lecture, ORNL, April 18, 1962, Oak Ridge, Tennessee.

#### T. Tamura

Mechanisms That Impede Movement of Radionuclides into the Environment, Short Course in Health Physics for ORSORT, Oak Ridge National Laboratory, January 17, 1962, Oak Ridge, Tennessee.

Selective Reactions for Radio-Strontium and Radio-Cesium by Minerals, University of Tennessee, Department of Geology, May 24, 1962, Knoxville, Tennessee.

Use of Radiochemical Methods for Soil Studies, Summer Institute in Radiobiology (ORINS-ORNL), July 23, 1962, Oak Ridge, Tennessee.

## I. H. Tipton

Health Physics, WUOT Faculty Forum, November 1961, Knoxville, Tennessee.

Trace Element Program at UT, Teacher's Institute, December 1961, Martin, Tennessee.

Trace Elements in Human Tissue, Sigma Pi Sigma Banquet, February 1962, Knoxville, Tennessee.

Atomic Spectroscopy, Physics Department Seminar, University of Tennessee, March 1962, Knoxville, Tennessee.

#### J. E. Turner

The Possible Role of Momentum in Radiation Dosimetry, ORNL, May 31, 1962, Oak Ridge, Tennessee.

## J. P. Witherspoon, Jr.

Cycling of Cesium-134 in White Oak Trees on Sites of Contrasting Soil Type and Moisture, Department of Botany, University of Tennessee, March 1962, Knoxville, Tennessee.

## ORNL-3347 UC-41 — Health and Safety TID-4500 (18th ed.)

## INTERNAL DISTRIBUTION

1.	C. E. Larson		87.	G. S. Hurst
2.	Biology Library		88.	S. R. Bernard
3-5.	Central Research Library		89.	J. A. Lane
6.	Laboratory Shift Supervisor		90.	W. S. Snyder
	Reactor Division			L. B. Holland
8-9.	ORNL - Y-12 Technical Library,		92.	J. L. Gabbard
	Document Reference Section		93.	A. C. Upton
10-59.	Laboratory Records Department	)		D. M. Davis
	Laboratory Records, ORNL R.C.		95.	R. L. Clark
	J. P. Murray (K-25)		96.	L. C. Johnson
	R. F. Hibb's (Y-12)			O. D. Teague
	A. M. Weinberg			E. J. Kuna
	J. A. Swartout			A. D. Warden
65.	K. Z. Morgan			J. A. Auxier
	M. L. Nelson		101.	S. I. Auerbach
67.	S. C. Lind		102.	F. C. Maienschein
	A. S. Householder			B. Fish
	C. S. Harrill		104.	C. E. Breckinridge
	F. L. Parker			R. D. Birkhoff
71.	E. H. Taylor		106.	J. A. Harter
	W. H. Jordan		107.	R. W. Peelle
73.	T. A. Lincoln		108.	R. M. Richardson
74.	A. Hollaender		109.	J. S. Olson
75.	F. L. Culler		110.	R. J. Morton (consultant)
76.	H. E. Seagren		111.	T. E. Bortner (consultant)
77,	M. T. Kelley		112.	P. H. Doyle (consultant)
	R. S. Livingston			U. Fano (consultant)
79.	C. D. Susano		114.	T. D. Strickler (consultant)
80.	W. J. Boegly		115.	J. C. Frye (consultant)
81.	E. G. Struxness			W. H. Langham (consultant)
82.	W. E. Cohn			G. M. Fair (consultant)
83.	M. L. Randolph		118.	R. E. Zirkle (consultant)
	M. J. Skinner	•		L. S. Taylor (consultant)
85.	J. C. Hart			R. S. Platzman (consultant)
86.	T. H. J. Burnett			N. Wald (consultant)
				•

## EXTERNAL DISTRIBUTION

- 122. R. W. McNamee, Union Carbide Corporation, New York
- 123. Physics and Engineering Group, Balcones Research Center, RFD 4, Box 189, Austin, Texas
- 124. G. E. Thoma, St. Louis University Hospital, 135 South Grand Boulevard, St. Louis, Missouri
- 125. Vanderbilt University (Physics Library)
- 126. Paul Jones, U.S. Geological Survey, Washington, D.C.
- 127. Lola Lyons, Librarian, Olin Industries, Inc., East Alton, Illinois
- 128. Jack Story, Health Physicist, North Carolina State College, Raleigh, North Carolina

- 129. J. H. Ebersole, USS Nautilus, c/o Fleet Post Office, New York, New York
- 130. David S. Smith, Health and Safety Division, U.S. Atomic Energy Commission, Chicago Operations Office, P.O. Box 59, Lemont, Illinois
- 131. Research and Development Division, AEC, ORO
- 132. S. C. Sigoloff, Edgerton, Germeshausen and Grier, Inc., P.O. Box 98, GoLeta, California
- 133. Robert Wood, Department of Physics, Memorial Center, 444 E. 68th St., New York 21, New York
- 134. John Wolfe, Division of Biology and Medicine, U.S. Atomic Energy Commission, Washington, D.C.
- 135. Orlando Park, Department of Biology, Northwestern University, Evanston, Illinois
- 136. Eugene Odum, Department of Zoology, University of Georgia, Athens, Georgia
- 137. W. T. Ham, Medical College of Virginia, Richmond, Virginia
- 138. F. H. W. Noll, Department of Physics, Berea College, Berea, Kentucky
- 139. Herbert E. Stokinger, Bureau of State Service, Department of Health, Education and Welfare, Penn 14 Broadway, Cincinnati 2, Ohio
- 140. J. B. Lackey, University of Florida, Gainesville, Florida
- 141. J. J. Davis, Biology Operation, Hanford Atomic Power Operations, Seattle, Washington
- 142. Robert B. Platt, Department of Biology, Emory University, Atlanta, Georgia
- 143. C. H. Bernard, Physics Department, Texas A&M, College Station, Texas
- 144. C. E. Dady, Watertown Arsenal, Ordinance Material Research Office, Watertown, Massachusetts
- 145. John I. Hopkins, Davidson College, Department of Physics, P.O. Box 327, Davidson, North Carolina
- 146. W. J. Lacy, Office of Civil Defense Mobilization, Battle Creek, Michigan
- 147. G. A. Andrews, Oak Ridge Institute of Nuclear Studies, Oak Ridge, Tennessee
- 148. E. P. Resner, States Marine Lines, c/o New York Shipbuilding Corp., Camden, New Jersey
- 149-153. Walter Belter, Division of Reactor Development, AEC, Washington, D.C.
  - 154. H. J. Carey, Jr., The Carey Salt Company, Hutchinson, Kansas
  - 155. C. Orr, Georgia Institute of Technology, Atlanta, Georgia
  - 156. E. F. Gloyna, Department of Civil Engineering, University of Texas, Austin 12, Texas
  - 157. J. S. Cragwall, Jr., U.S. Geological Survey, Surface Water Branch, 823 Edney Building, Chattanooga, Tennessee
  - 158. H. H. Waesche, AEC Liaison Officer, Geochemical and Petrology Branch, U.S. Geological Survey, Naval Gun Factory, Building 213, Washington 25, D.C.
  - 159. S. Leary Jones, Tennessee Department of Public Health, Cordell Hull Building, Nashville, Tennessee
  - 160. H. C. Thomas, Chemistry Department, University of North Carolina, Chapel Hill, North Carolina
  - 161. Glenn Gentry, Fish Management Division, Game and Fish Commission, Cordell Hull Building, Nashville, Tennessee
  - 162. Vincent Schultz, Environmental Sciences Branch, Division of Biology and Medicine, U.S. Atomic Energy Commission, Washington 25, D.C.
  - 163. O. W. Kochtitzky, Tennessee Valley Authority, 717 Edney Building, Chattanooga, Tennessee
  - 164. Leslie Silverman, Industrial Engineering, Department of Industrial Hygiene School of Public Health, Harvard University, 55 Shattuck Street, Boston 15, Massachusetts
  - 165. J. Wade Watkins, U.S. Bureau of Mines, Washington, D.C.
  - 166. Kansas State Board of Health, Topeka, Kansas (Dwight F. Metzler)
  - 167. Kansas State Geological Survey, Lawrence, Kansas (Frank C. Foley)
  - 168. W. R. Thurston, Executive Secretary, Division of Earth Sciences, National Academy of Sciences National Research Council, Washington, D.C.
  - 169. C. S. Shoup, Biology Division, U.S. Atomic Energy Commission, Oak Ridge, Tennessee
  - 170. L. Garcia, Naval Research Laboratory, Washington, D.C.
  - 171. J. A. Lieberman, Division of Reactor Development, AEC, Washington, D.C.
  - 172. Conrad Straub, Robert A. Taft Sanitary Engineering Center, Cincinnati, Ohio
- 173—852. Given distribution as shown in TID-4500 (18th ed.) under Health and Safety category (100 copies OTS)